ASSESSING AND MAPPING OF CARBON IN BIOMASS AND SOIL OF MANGROVE FOREST AND COMPETING LAND USES IN THE PHILIPPINES

A Thesis submitted by

Jose Alan A. Castillo
B.Sc. Forestry, *University of the Philippines*
M. Env & Nat Res Mgmt, *University of the Philippines*

For the award of

DOCTOR OF PHILOSOPHY

2017

Abstract

Mangrove forests provide many ecosystem goods and services, and are important carbon (C) sinks in the tropics. Yet, land use conversions in mangroves still continue, especially in Southeast Asia. Carbon stocks in biomass and soil as well as the soil emissions of greenhouse gases (GHG) are important parameters to quantify, monitor and map in mangrove area, and are vital inputs for assessing the impact of mangrove conversion on C budget. This study was conducted in a section of tropical intertidal zone in Honda Bay, Philippines, with the following objectives: 1) evaluate the biomass C stocks in mangrove forests and land uses that replaced mangroves, 2) examine the potential of Sentinel satellite radar and multispectral imagery for mapping the aboveground biomass in mangrove area, 3) investigate the soil C stocks and the potential of GIS-based Ordinary Kriging for mapping the C stocks in mangrove soil, and 4) assess the soil fluxes of greenhouse gases and the potential of Ordinary Kriging for mapping the soil GHG fluxes. I used intensive field assessments, combined with laboratory analysis, remote sensing and GIS methods, to achieve the above objectives.

To address the first objective, the biomass C stocks of the study land uses were quantified. Their relationships with selected canopy variables were also evaluated. Results reveal that for mangrove forests, the mean biomass was 22.4 to 178.1 Mg ha^{-1}, which store 10 to 80 MgC ha^{-1} or 47.9 MgC ha^{-1}, on average. Leaf Area Index significantly correlated with mangrove biomass C. In contrast, the biomass C stock of the land uses that replaced mangroves was, on average, 97% less than that in mangrove forests, ranging from zero in salt pond and cleared mangrove, 0.04 Mg C ha^{-1} in abandoned aquaculture ponds, to 5.7 Mg C ha^{-1} in the coconut plantation. C losses in biomass from conversion were estimated at 46.5 Mg C ha^{-1}, on average.

For the second objective, the potential of Sentinel imagery for the retrieval and predictive mapping of aboveground biomass in mangrove area was evaluated. I used both Sentinel SAR and multispectral imagery. Biomass prediction models were developed through linear regression and Machine Learning algorithms, each from SAR backscatter data, multispectral bands, vegetation indices, and canopy biophysical variables. The results show that the model based on biophysical variable

Leaf Area Index (LAI) derived from Sentinel-2 was more accurate in predicting the overall aboveground biomass. However, the SAR-based model was more accurate in predicting the biomass in the usually deficient-to-low vegetation cover replacement land uses. These models had 0.82 to 0.83 correlation/agreement of observed and predicted value. Overall, Sentinel-1 SAR and Sentinel-2 multispectral imagery can provide satisfactory results in the retrieval and predictive mapping of aboveground biomass in mangrove area.

In the third objective, the soil C stocks of the study land uses were quantified to estimate C losses in soil owing to conversion. I also evaluated the potential of GIS-based Ordinary Kriging for predictive mapping of the soil C stock distribution in the entire study site. On average, the soil C stock of mangrove forests was 851.9 MgC ha^{-1} while that of their non-forest competing land uses was less than half at 365.15 MgC ha^{-1}. Aquaculture, salt pond and cleared mangrove had comparable C stocks (453.6, 401, 413 MgC ha^{-1}, respectively) and coconut plantation had the least (42.2 MgC ha^{-1}). Overall, C losses in soil owing to land use conversion in mangrove ranged from 398 to 809 MgC ha^{-1} (mean: 486.8 MgC ha^{-1}) or a decline of 57% in soil C stock, on average. It was possible to map the site-scale spatial distribution of soil C stock and predict their values with 85% overall certainty using Ordinary Kriging approach.

To achieve the fourth objective, the soil fluxes of CO_2, CH_4 and N_2O in the study land uses were investigated using static chamber method. I also evaluated the potential of GIS-based Ordinary Kriging for predictive mapping of the soil GHG fluxes in the entire study site. Results show that the emissions of CO_2 and CH_4 were higher in mangrove forests by 2.6 and 6.6 times, respectively, while N_2O emissions were lower by 34 times compared to the average of non-forest land uses. CH_4 and N_2O emissions accounted for 0.59% and 0.04% of the total emissions in mangrove forest as compared to 0.23% and 3.07% for non-forest land uses, respectively. Site-scale soil GHG flux distribution could be mapped with 75% to 83% accuracy using Ordinary Kriging.

This study has shown that C losses in biomass and soil arising from mangrove conversion are substantial (63%; 571 MgC ha^{-1}). Moreover, mangrove conversion heavily altered the soil-atmosphere fluxes of GHG, increasing the N_2O fluxes by 34 times. The use of Sentinel imagery for biomass mapping, as well as the application of Ordinary Kriging for soil mapping of C stocks and GHG fluxes, offer good potentials for mangrove area monitoring. This study advances current knowledge on the C stocks and soil GHG fluxes in mangrove area and the C emissions owing to mangrove conversion. The mapping techniques presented here contribute to advancing the knowledge for mapping the biomass and soil attributes in mangrove ecosystem.

Certification of Thesis

This thesis is entirely the work of Jose Alan A. Castillo except where otherwise acknowledged. The work is original and has not previously been submitted for any other award, except where acknowledged.

Student and supervisors signatures of endorsement are held at USQ.

Prof. Armando A. Apan
Principal Supervisor

Dr. Tek N. Maraseni
Associate Supervisor

Publications during the PhD Study Period

Journal Papers

Castillo, JAA, Apan, AA, Maraseni, TN & Salmo III, SG 2017, 'Soil C quantities of mangrove forests, their competing land uses, and their spatial distribution in the coast of Honda Bay, Philippines', *Geoderma*, vol. 293, pp. 82-90.

Apan, A, Suarez, LA, Maraseni, T & Castillo, JA 2017, 'The rate, extent and spatial predictors of forest loss (2000–2012) in the terrestrial protected areas of the Philippines', *Applied Geography*, vol. 81, pp. 32-42.

Castillo, JAA, Apan, AA, Maraseni, TN & Salmo, SG 2017, 'Soil greenhouse gas fluxes in tropical mangrove forests and in land uses on deforested mangrove lands', *CATENA*, vol. 159, pp. 60-69.

Castillo, JAA, Apan, AA, Maraseni, TN & Salmo III, SG 2017, 'Estimation and mapping of above-ground biomass of mangrove forests and their replacement land uses in the Philippines using Sentinel imagery', *ISPRS Journal of Photogrammetry and Remote Sensing*, vol. 134, pp. 70-85.

Castillo, JAA, Apan, AA, Maraseni, TN & Salmo III, SG, 'Biomass, carbon storage and correlates of tropical mangrove forests and their replacement land uses', submitted for publication to *Global Journal of Environmental Science and Management*

Conference Presentation

Castillo, JAA, Apan, AA, Maraseni, TN & Salmo III, SG 2016, 'Using Sentinel imagery in modelling the aboveground biomass of mangrove forest and their competing land uses' *Proceedings of the Pacific Islands GIS/RS User Conference 2016*, 28 November – 1 December 2016, Suva, Fiji, 12 p. (Conference proceedings in website: http://gisconference.gsd.spc.int/index.php/agenda-2015/presentations-2016/day-2-presentations)

Castillo, JAA, Apan, AA, Maraseni, TN & Salmo III, SG 2017, 'Simulation of future Carbon storage of mangrove forest in Honda Bay, Philippines under land use change scenarios' *Proceedings of the 2nd ASEAN Congress on Mangrove R&D*, 04 - 07 September 2017, Manila, Philippines.

Acknowledgements

I would like to acknowledge that God has willed the completion of this work. To Him, I give back all the honour and glory that come with this humble piece of work.

I also would like to extend my great appreciation to my PhD Supervisory/Advisory Team for their scientific guidance, valuable advise, and for generously sharing their expertise, without whose support and encouragement I would not have been able to complete the study. To my Principal Supervisor, Professor Armando Apan, for his motivation and guidance, and for patiently guiding me while I learn the ropes of Satellite Remote Sensing, Spatial Modelling, and publishing in high-quality journals. To my Associate Supervisor, Dr. Tek Maraseni, for his scientific guidance and expertise in Forest Carbon assessment. To Dr. Severino Salmo III, my external mangrove expert from Ateneo de Manila University, Philippines, for his valuable insights and expertise in mangrove ecology.

I would like to thank the Government of Australia through the Australia Awards Scholarships for giving me full scholarship to pursue my PhD program in Australia.

Special thanks are also extended to the following persons and institutions who have become a great part of this undertaking:

- The University of Southern Queensland for providing all the support I needed for my research: USQ Australia Awards team Lorraine Juliana, Damien Zekants and staff; The School of Civil Engineering and Surveying of Faculty of Health, Engineering and Sciences for providing my work station and space, and for contributing additional research funds.

- The Ecosystems Research and Development Bureau (ERDB) management and staff in the Philippines under the subsequent leaderships of Dr. Portia Lapitan and Dr. Henry Adornado for allowing me to go on study leave and for providing the logistical support during my fieldwork in Honda Bay, Palawan. Special thanks to Boss Poits Palis, Boss Lito Exconde and staff, Assistant Director Tony Daño, Boss Lita Villamor and staff, the mangrove research section, for all the support and prayers

- Dr. Rudolf Espada for proofreading the manuscript, and for his valuable suggestions to help improve the paper's readability

- The help and company of Elmer Caliwagan, Leoncio Piolo Baguhin, Digno Garcia, Perfecto Melo, Artemio Ortega, Benjo Salvatierra and Donald Apan during the fieldwork are highly appreciated

- The European Space Agency for providing the Sentinel SAR and Multispectral data, and the open-source SNAP software for image processing; The United States NASA for the SRTM digital elevation model data that I used for biomass modelling. The University of Waikato for their open-source WEKA that I used for machine learning and linear regression modelling

- The village officials and residents of San Jose, Tagburos, Santa Lourdes, Bacungan, Santa Cruz and Salvacion, for providing access and assistance in the field and for giving information on land use history of the area, are also highly appreciated

- My co-students under Dr. Apan's GIS and Remote Sensing PhD research group for the support, encouragement, friendships and prayers: Sis Ning, Brod Rudolf, Zana, Ernest, Irvin, Angelica and Rani

- Our Toowoomba family and friends for all the friendships, prayers and support, for making us feel at home in Australia even though we are miles away from

Philippines: Brod Rudolf, Sis Malou and Trish; Kuya Jun and Ate Zenny; Nice, Melvin and kids; Sis Ning, Brod Jun and kids; Brod Arman, Ate Hope and kids; Kuya Orlie, Ate Pinky and kids; Ging, Nemo and Eric; Ethel and Irvin; and Sis Myra and Michael; To Sis Ning and family for accommodating me during my first two months in Australia

- My parents and siblings for all the support and prayers. To my mother who had gone to the great forest up there during this study without seeing the completion of this Australia PhD Scholarship

- My in-laws for all the support and prayers. Special thanks to Inay Ising and Papin for staying with the family while I was away doing field works in Philippines

- To those whom I failed to mention but have been an important part of this study and our Australian journey

My deep appreciation also goes to the taxpayers of Australia and the Philippines, through your taxes I was able to achieve this life-long dream and reach this far.

And finally, I would like to extend my sincerest thanks to my wife, **Judith** and daughters, **Mary** and **Maedy**, for all the love, support and understanding.

To all of you, I will forever be indebted.

Thank you very much. Maraming Salamat po.

Alan Castillo
July 2017, Toowoomba, Qld

To my wife, Judith,

for the ultimate sacrifice
you had to make
for this Australian journey

and

to the Filipino people,

our struggles, hopes and aspirations

Table of Contents

List of Figures

List of Tables

Abbreviations

AGB	Aboveground Biomass
ALOS	Advanced Land Observing Satellite
ASAR	Advanced Synthetic Aperture Radar
B	Band
BD	Bulk Density
BGB	Belowground Biomass
C	Carbon
dB	Decibel
DEM	Digital Elevation Model
DWB	Downed Woody debris Biomass
Envisat	Environmental Satellite
ESA	European Space Agency
FAO	Food and Agriculture Organisation
fCover	Fraction of Vegetation Cover
FMB	Forest Management Bureau
fPAR	Fraction of Absorbed Photosynthetically Active Radiation
GHG	Greenhouse Gas
GIS	Geographic Information System
GPS	Global Positioning System
GRD	Ground Range Detected
HH	Horizontal transmit and Horizontal receive
HR	High Resolution
HV	Horizontal transmit and Vertical receive
IPCC	Intergovernmental Panel on Climate Change
IRECI	Inverted Red-Edge Chlorophyll Index
IUCN	International Union for Conservation of Nature
IW	Interferometric Wide Swath
LAI	Leaf Area Index
LOO	Leave-One-Out
ME	Mean Error
Mg	Megagram

ML	Machine Learning
MSL	Meters above Sea Level
NAMRIA	National Mapping and Resource Information Authority
NASA	National Aeronautics and Space Administration
NDI45	Normalised Difference Index using bands 4 (Red) and 5 (Red Edge)
NDVI	Normalised Difference Vegetation Index
NIR	Near Infrared
NSO	National Statistics Office
PAGASA	Philippine Atmospheric Geophysical and Astronomical Services Administration
PALSAR	Phased Array type L-band Synthetic Aperture Radar
pH	Potential of Hydrogen
PPC	Puerto Princesa City
PSA	Philippine Statistics Authority
QQ	Quantile-Quantile
RADAR	Radio Detection And Ranging
REDD+	Reducing Emissions from Deforestation and Forest Degradation and other activities that increase C stocks
Redox	Reduction-oxidation
RGB	Red Green Blue
RMSE	Root Mean Square Error
SAR	Synthetic Aperture Radar
SNAP	Sentinel Application Platform
SPOT	Le Systeme pour l'Observation de la Terre
SRTM	Shuttle Radar Topography Mission
SWIR	Short Wave Infrared
TNDVI	Transformed Normalised Difference Vegetation Index
VH	Vertical transmit and Horizontal receive
VNIR	Visible and Near Infrared
VV	Vertical transmit and Vertical receive
WEKA	Waikato Environment for Knowledge Analysis

Chapter 1

INTRODUCTION

1.1 Background

Mangrove forests are a type of forest vegetation that can be found along sheltered coastlines of tropical and subtropical countries that are regularly inundated with tides, extending inland along the streams where water is brackish. They are distributed in the coasts of at least 124 countries and areas in Asia, America, Oceania, and Africa (FAO 2007). The global mangrove area as of year 2000 has been estimated at 137,760 km^2 (Giri et al. 2011) to 152,361 km^2 (Spalding et al. 2010), or less than 1.4% of the global forest area, with over 30 % found in Southeast Asian countries. There is a total of 73 true mangrove plant species and hybrids; however, only 38 of which are considered as "core species" being the dominant species in many localities (Spalding et al. 2010).

Mangroves provide timber and other construction materials, fuelwood, storm protection, fishery products, sediment regulation and many other ecosystems services to coastal residents (Alongi 2002). Over the last few years, mangroves are increasingly recognised as among the most carbon (C) dense tropical forests. Estimate of global mangrove C stock is reported as high as 20 PgC (Murdiyarso et al. 2013). As mangroves store a very high mean global whole-ecosystem C stock of 956 MgC ha^{-1} (Alongi 2014) with soil storing up to 98% (global mean average of 75%) of the total C (Donato et al. 2011; Kauffman et al. 2013; Murdiyarso et al. 2013), conserving and expanding mangrove forest is important for C emissions mitigation (Lovelock & McAllister 2013).

However, despite the numerous goods and services provided by mangroves, they are being depleted at alarming rates probably because until a few decades ago, mangroves were considered as "marginal wasteland better used for other purposes" (Clough 2013 p. 2). There have been significant reductions in the area of mangrove

forests over the years (FAO 2007; Giri et al. 2010; Long et al. 2013). Mangroves have declined in global area by 30-50% in the last 50 years (Murdiyarso et al. 2013). During the 1980s, the rate of mangrove deforestation is 185,000 ha per year. Overexploitation, conversion of mangroves to aquaculture, agriculture, urban, tourism and industrial developments in the coastal area are considered to be among the drivers of global mangrove loss (Richards & Friess 2016). In the Philippines, for instance, a country that belongs to the top 15 most mangrove-rich countries in the world that make up 75% of the world's mangrove cover (Giri et al. 2011), mangroves have been deforested and reduced by half (51.8 %) in just < 100 years, from around 450,000 hectares (Brown & Fischer 1920) in 1918 to 240,824 ha (Long et al. 2013) in 2010. Conversion of mangroves to aquaculture ponds (by at least 70 %) is considered the main cause of mangrove deforestation and the main land use that replaced mangroves in the country. However, overexploitation and conversion to other non-forest land uses such as agriculture, salt ponds and settlements are also among the causes of mangrove cover reduction in the country (Primavera & Esteban 2008).

Global concerns about deforestation, forest clearing, change in land use from forest to non-forest, and forest degradation have been unprecedented in recent decades. Mostly from tropical countries, deforestation and forest degradation are considered significant sources of global C emissions and consequently linked to the issues of global warming and climate change (Kanninen et al. 2007; IPCC 2013, 2014b). In fact, deforestation has been the second largest source of total global CO_2 emissions after fossil fuel burning and cement production, contributing 32 % of the total anthropogenic CO_2 emission from 1750 to 2011 and about 10 % during 2002-2011 (IPCC 2013).

Despite the awareness on the importance of mangroves and policies that restrict mangrove losses, for instance the IUCN Protected Area network, Philippines' Republic Act 8550 (Fisheries Code of the Philippines), RA 7161, Presidential Decree 705 as amended (Revised Forestry Code), massive mangrove deforestation and land use conversion are still happening until today (Hamilton & Casey 2016; Richards & Friess 2016). Forest clearing could result in the loss of stored C in the biomass and from the oxidation of C in the soil. In a high-carbon forest ecosystem like mangrove,

forest clearing releases CO_2 and other greenhouse gases (GHGs) to the atmosphere (Lovelock et al. 2011). It is important, therefore, to monitor the mangroves and evaluate the associated impacts of this on-going land use change to mangrove's C budget particularly the associated changes in the sequestered soil and biomass C and the soil-borne fluxes of GHGs. Availability of such information will contribute to help refining emission estimates of the carbon footprint of mangrove conversion and provide scientific input for decision-making as to whether conserve them as forest against the alternative uses. This thesis will be valuable in the assessment, monitoring, and refinement of policies on C stocks and GHGs in mangrove ecosystem.

1.2 Statement of the Problem

Over the years, land use/land cover change in mangrove has been studied in terms of the number of hectares converted to other land uses (Giri et al. 2011, Long et al. 2013). However, one equally important aspect that has been overlooked in the past was the impact of the prevailing land use/land cover change on mangrove's C budget (Richards & Friess 2016). The C stocks in mangrove have been found to be high (~950 MgC ha^{-1}), apparently three to five times higher than its terrestrial forest counterparts because the former has high C storage capacity in the soil (Donato et al. 2011; Kauffman et al. 2011). Concerns have been raised regarding the magnitude of the stored C that may be released back into the atmosphere due to the continuing land use/land cover change in mangrove (Pendleton et al. 2012; Murdiyarso et al. 2013; Alongi 2014). While these concerns are not well understood (Donato et al., 2011), particular interests to investigate include the quantification of changes in soil and biomass C stocks and the changes in soil surface GHG (CO_2, CH_4 and N_2O) fluxes/emissions resulting from land use/land cover change.

Previous studies on C budget of mangrove ecosystem were done through a piecemeal approach (i.e. aboveground biomass C stock, belowground biomass C stock, soil C stock and soil GHG emissions were not studied simultaneously), dealt mostly on plot-scale C stocks of different types of mangroves, and did not consider all of the three land sector-based GHGs such as CO_2, CH_4 and N_2O (e.g. Allen et al. 2011; Donato et al. 2011; Lovelock et al. 2011; Adame et al. 2013; Kauffman et al.

2013; Sidik & Lovelock 2013). Evaluating the impact of mangrove land use/land cover change on C budget requires the investigation of C stocks from various C pools of the original mangrove vegetation and the land uses that replaced them. The evaluation also entails the quantification of possible changes in the fluxes/emissions of soil surface GHG such as CO_2, CH_4 and N_2O as a result of the land use conversion. No study has so far integrated the measurement of changes in C stocks across biomass and soils, and in soil GHG emissions of mangroves side by side with the land uses that replaced them. The findings from such studies are necessary to estimate the total C emissions due to land use/land cover change in mangrove (Murdiyarso et al. 2013).

Carbon dioxide, CH_4 and N_2O are the three main GHGs being monitored in the land use sector by the International Governmental Panel on Climate Change since 1990 (IPCC 2013). Just like other wetlands, mangrove soil can contain high density of C and can act as significant sources of greenhouse gases based on previous studies (Lovelock 2008; Poungparn et al. 2009; Chen et al. 2010; Allen et al. 2011; Chanda et al. 2014; Chen et al. 2014). However, the soil greenhouse gas emissions in intact mangroves (in comparison to deforested mangroves) remain poorly characterised. Quantifying and accurate reporting of GHG emissions from mangrove soil is, therefore, important for regional and national emissions inventories.

Furthermore, the difference in C stocks between intact mangrove forest and land uses that replaced mangroves (i.e. deforested mangroves) can be used to estimate the C emissions owing to mangrove conversion as employed in previous studies (e.g. Kauffman et al. 2013; Bhomia et al. 2016; Kauffman et al. 2016). However, there is a need to supplement the C stock accounting with gas flux measurements, to quantify the emissions of gases that do not accumulate in the biomass and soil such as CH_4 and N_2O. Available estimates of C emissions from mangrove conversion are based on a number of assumptions (e.g. Donato et al. 2011; Pendleton et al. 2012; Siikamäki et al. 2012). These include the following: a) assuming C losses of 50% and 75% in biomass, and 25% and 75% in soil (Donato et al. 2011); b) assuming 25% to 100% C losses in biomass and top 1 m of soil (Pendleton et al. 2012); and c) assuming C losses of 75% in biomass, and 27.25% and 90% in soil C (Siikamäki et al. 2012). Empirical studies, on the other hand, are very few and limited only to two cases: mangrove - abandoned aquaculture pond

(Kauffman et al. 2013; Bhomia et al. 2016; Duncan et al. 2016) and mangrove - pasture (Kauffman et al. 2016). Other land uses that replaced mangroves such as coconut palm plantation, cleared mangrove and abandoned salt pond have not been evaluated regarding their C stocks and soil surface gas fluxes particularly CO_2, CH_4, and N_2O. Also, the implication of the degradation of mangrove forests in terms of the changes in C stock and soil GHG fluxes is poorly understood like in other tropical forests (Lasco 2002). When closed canopy mangrove is degraded into open canopy forest type, the magnitude of change in C density and the soil GHG fluxes are also not well understood.

There could be changes in C stocks and soil surface GHG emissions resulting from mangrove deforestation and forest degradation. While it can be inferred that C stock will decline as mangrove forest is converted to non-forest land use or as intact mangrove is converted to open canopy forest, the magnitude of change has not been fully understood to date. Furthermore, there could be changes in the emissions/fluxes of these GHGs from the soil surface of mangrove once subjected to deforestation, land use conversion and forest degradation. These disturbances could cause a dramatic change in soil chemistry through the increases in the soil temperature and soil microbial activity (Pendleton et al. 2012), resulting to rapid soil surface gas emissions (Alongi 2014). With lack of empirical studies, it is not well understood so far whether or not the land use/land cover change happening in mangrove is a significant source of anthropogenic C emission.

In the Philippines and other developing countries, there are high interests in REDD+ and other similar C payment schemes (Lasco et al. 2013). These programs require robust estimates and sound information on baseline ecosystems C stocks of mangroves, both in the aboveground and belowground C pools. These may also include estimating the soil GHG emissions and the potential C emissions when the current forest disturbance continue (Donato et al. 2011; Kauffman et al. 2011; Adame et al. 2013; Murdiyarso et al. 2013; Hossain 2014). These information are currently not available in mangrove areas in many developing countries including the Philippines (Murdiyarso et al. 2013). The generated findings will be important for potential C credit calculation and projection, and in estimating future C emissions due to mangrove deforestation and biomass degradation (Locatelli et al. 2014).

Using either optical or radar imagery data, previous satellite remote sensing-based biomass retrieval and mapping studies in coastal areas have dealt mostly on mangrove forests alone (e.g. Simard et al. 2006; Proisy et al. 2007; Fatoyinbo et al. 2008; Jachowski et al. 2013; Aslan et al. 2016) but did not cover the land uses that replaced mangroves. The recently launched new-generation Sentinel satellite missions of Copernicus program of the European Space Agency provide both Synthetic Aperture Radar (SAR) and multispectral imagery data. Both could be used for biomass estimation and mapping. However, to my knowledge, the retrieval and mapping of biomass of mangrove forests and their replacement land uses using Sentinel imagery data have not been reported in the scientific literature.

Moreover, the site-scale spatial distribution/variability of soil C stocks and soil GHG emissions in mangroves have not been fully understood and mapped/modelled as available studies are all in plot-scale (e.g. Donato et al. 2011; Kauffman et al. 2013; Chen et al. 2014; Tue et al. 2014). While GIS-based spatial interpolation technique such as Kriging has been used in inland terrestrial soil to generate site-scale soil C stocks distribution, its application in mangrove soil, forested or otherwise, is not well understood. Knowing these sets of information is important to better understand the variations of C stocks and soil GHG fluxes, and help refine the local, regional and global estimates.

Finally, proximal sensor-derived canopy biophysical variables such as Leaf Area Index (LAI) and Canopy Gap Fraction have not been fully described in mangrove forests and land uses that replaced mangroves including their relationships with biomass C stocks. Such information can be useful for large-scale biomass estimation using remote sensing-derived canopy biophysical variables (e.g. Dusseux et al. 2015).

1.3 Significance of the Study

Quantifying the magnitude of changes in the C budget (C stock and soil GHG emission) from mangrove conversion and forest degradation would improve our understanding and knowledge of the consequences of land use/land cover change and forest disturbance in mangrove. This information is necessary to better inform policy

making and resource management to address C emissions and mitigation (Pendleton et al. 2012; Chen et al. 2013). Evaluating the impact of mangrove forest land use/land cover change on C budget could give us the needed but usually absent local "emission factors" necessary for higher tier GHG inventory of C emissions (Murdiyarso et al. 2013).

This thesis provides scientific information on the magnitude of change in C stocks from aboveground and belowground C pools, and soil GHG fluxes of mangrove forests and land uses that replaced them. The generated information can also be used as an empirical basis to estimate emissions from land use change and forest degradation in mangrove. In addition, the results of the study could be used for the following applications:

- Input to updating of the IPCC 2006 emission factors. This could also give us information on whether the land use that replaced mangroves is a net source or sink of GHG.
- Input to periodic reporting of the country's GHG emissions to the UNFCCC (Lasco et al. 2013; Murdiyarso et al. 2013).
- Basis to come up with policies and management strategies to stop the continuing mangrove deforestation
- Up-to-date information for mangrove policy-making, resource management and coastal land use planning in the country.
- Input in revising local, regional and global estimates of C emissions resulting from mangrove deforestation and forest degradation (Donato et al. 2011; Pendleton et al. 2012).

Aside from quantifying the C stocks and soil GHG emissions of mangroves and land uses that replaced them, it is also important to determine and map their distributions and understand spatial variations using available GIS and remote sensing technologies. Generating this information can be important for a number of applications including conservation planning, developing adaptation plans in the coastal area or as baseline for future C studies (Murdiyarso et al. 2012; Alongi 2014). This research is the first to evaluate and map the spatial variation in biomass of mangrove and replacement land uses for the entire study site using both SAR and multispectral imagery from the newly launched new-generation Sentinel satellite system. In addition, the study is the first to investigate the applicability of GIS-based

geostatistical technique (i.e. Ordinary Kriging) in mangrove soil to predict and map the variations of soil C stock and soil GHG fluxes for the entire study site.

Finally, the approach and methodology adopted in this study can be used in the quantification and evaluation of bay-wide total C stocks and soil GHG emissions. On the other hand, the generated maps can be used for developing plans and programs for the coastal zones. This research work is the first comprehensive study in mangrove area by combining a set of methods that employ field-based and laboratory analyses in combination with satellite remote sensing (both radar and multispectral) and GIS-based techniques in the evaluation and mapping of C stocks in four major C pools, and soil fluxes of the three major greenhouse gases (CO_2, CH_4 and N_2O), as well as the investigation of the associated changes in C stocks and soil GHG fluxes owing to conversion of mangrove forests into other land uses.

1.4 Aim and Objectives

This study aims to evaluate and quantify the C stocks and soil GHG fluxes in mangrove forests and the non-forest land uses that replaced mangroves following land use change and forest degradation. Specifically, the study has the following objectives:

1. to quantify and evaluate the biomass and carbon stocks from aboveground biomass (AGB), belowground biomass (BGB), and downed woody debris biomass (DWB) of mangrove forest and the non-forest land uses that replaced mangroves. Associated within this objective was to investigate the relationship of biomass stocks with proximal sensor-derived canopy biophysical variables such as Leaf Area Index and canopy gap fraction;
2. to evaluate the performance of Sentinel satellite imagery-based biomass models and the output predictive biomass maps for site/large-scale biomass retrieval and mapping of mangrove and non-forest replacement land uses.
3. to quantify and evaluate the soil C stocks of mangrove forest and the non-forest replacement land uses, and to examine the relationship with site environmental variables. Associated within this objective was to evaluate the performance of GIS-based Ordinary Kriging in mapping the soil C stocks in the study site

4. to quantify the soil surface gas fluxes of CO_2, CH_4 and N_2O of mangrove forest and the non-forest land uses that replaced mangrove, and to determine the relationship with site environmental variables. Associated within this objective was to evaluate the potential of GIS-based Ordinary Kriging in mapping the soil GHG fluxes in the study site.

1.5 Scope and Limitations of the Study

The scope of the study included the assessment of C stocks in the aboveground and belowground pools of mangrove forests, as well as the non-forest land uses that replaced mangroves. These non-forest land uses include abandoned aquaculture pond, coconut plantation, abandoned salt pond and cleared mangrove site. This study also covered the quantification and assessment of soil GHGs fluxes of not only CO_2 but also CH_4 and N_2O in all of the study land uses. In addition, this research included the use and evaluation of satellite-based remote sensing and GIS-based techniques in the estimation and mapping of biomass and soil C stocks and soil GHG fluxes in mangroves and the land uses that replaced them, respectively.

The C budget assessment of the study was limited to quantifying and evaluating the C stocks and soil surface GHG fluxes. Destructive sampling of mangrove biomass in the country was not allowed so that the estimation of biomass utilised the existing allometric equations developed for Southeast Asian mangroves that have similar agro-ecological characteristics with the study site, while the biomass' C fraction value was taken from the literature. Due to financial limitation, one field campaign was undertaken to measure soil GHG fluxes. With restricted access across other coconut plantations, only one site was sampled for the coconut plantation. Finally, due to unavailability of replicate sites, the abandoned salt pond and cleared mangroves were surveyed with only one site each.

1.6 Conceptual Framework

The conceptual framework of the study is presented in Figure 1.1. Deforestation and forest degradation are activities that decrease the C stocks in both aboveground and belowground pools of forest ecosystems like mangroves. To

determine the impact of the forest disturbance on C budget, the C stocks in biomass and soils of mangroves and land uses that replaced them were determined. Together with the C stocks, the GHG fluxes/emissions in the soil surface were also measured in each of those land uses. These biomass and soil C stocks, and soil GHG fluxes were first estimated using field plots. Then, using field plots as validation points, the aboveground biomass distribution for the whole study site was estimated and mapped using the new-generation SAR and multispectral imagery data from the newly launched Sentinel satellite system. Likewise, the distribution of soil C stocks and soil surface GHG emissions for the whole study site were also mapped but using GIS-based geostatistical interpolation technique. From these results, the C stocks and the C losses in soil and biomass were estimated and evaluated. Likewise, the soil surface GHG emissions in mangrove forest and the changes in soil emissions arising from mangrove conversion to other land uses were also determined.

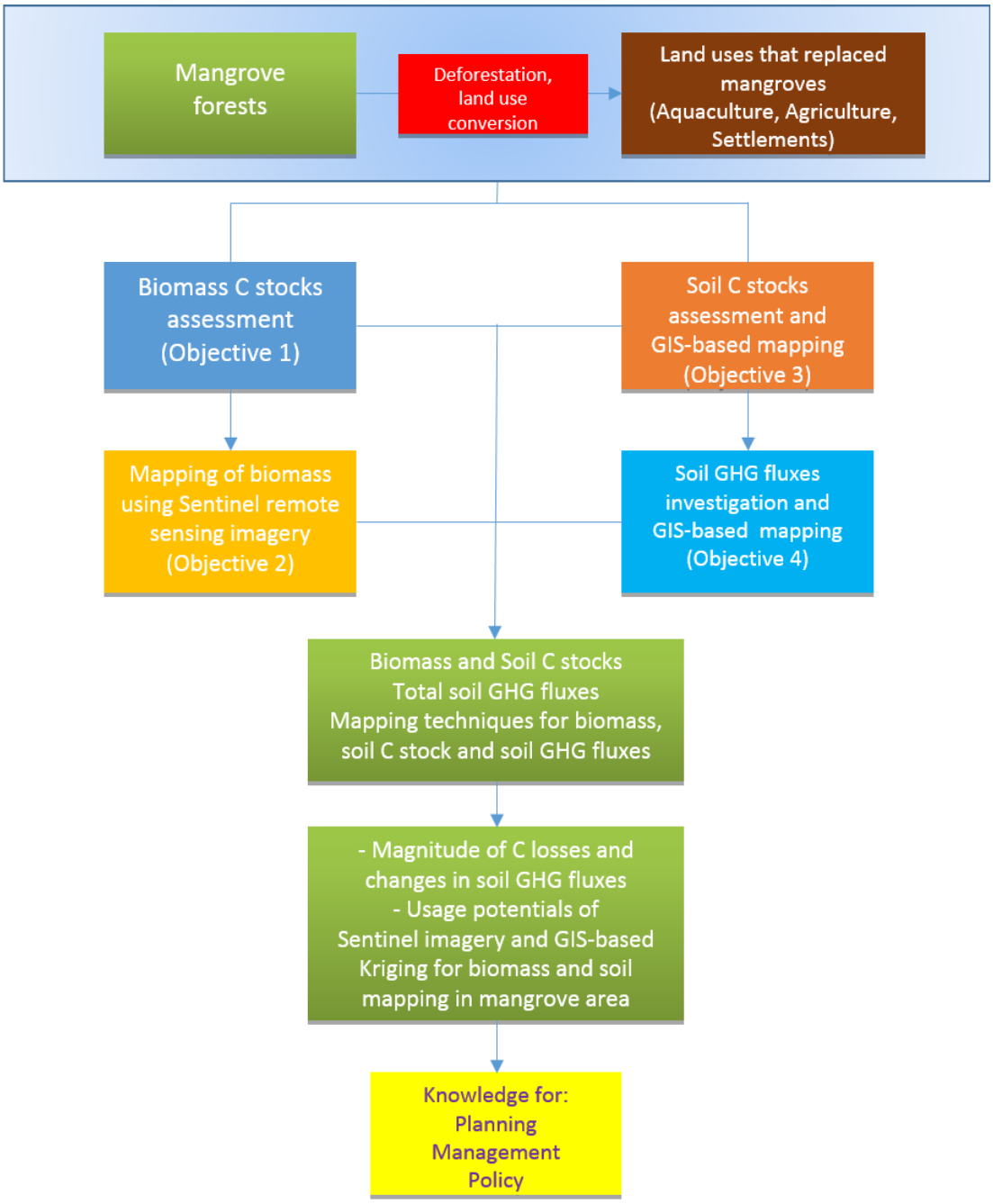

Figure 1.1 Conceptual framework of the study

1.7 Organisation of the Dissertation

This thesis is organised into eight chapters. **Chapter 1**, Introduction, presents the background of the study, identifies the research gaps, enumerates the significance and the broad aim and objectives of the present work, and defines its scope and limitations.

Chapter 2, Review of Literature, reviews the current knowledge sets relevant to the study. These include the following topics: carbon emissions due to global deforestation and degradation, quantification of carbon in biomass and soils in mangrove, quantification of soil-borne fluxes of the three important greenhouse gases, CO_2, CH_4 and N_2O, in mangrove soils, use of remote sensing technology in the biomass retrieval and mapping in mangrove, and use of GIS-based techniques in the prediction and spatial mapping of soil attributes.

Chapter 3 discusses the Research Methods adopted by the study. It describes the study area, the general design of the study, as well as the data capture and acquisition, data pre-processing and analysis.

Chapter 4 and **Chapter 5** discuss the biomass component of the study. **Chapter 4** covers the quantification of biomass and carbon stocks of mangrove forest and the land uses that replaced them using plot-scale estimation. It also evaluates the relationships between biomass carbon stock and canopy biophysical variables (e.g. Leaf Area Index, Canopy Gap Fraction, Mean Leaf Angle) that could be used for site/large-scale biomass retrieval and mapping using remote sensing technologies. **Chapter 5** is about the site-/large-scale biomass retrieval and mapping, and evaluation of the potential of the new Synthetic Aperture Radar and Multispectral imagery from the newly launched new-generation satellite remote sensing system, Sentinel-1 and Sentinel-2, of the European Space Station.

On the other hand, **Chapter 6** and **Chapter 7** deal on soils. **Chapter 6** quantifies the soil C stocks in mangrove and non-forest land uses using field plot-scale estimations and the magnitude of change. This Chapter also evaluates the performance of GIS-based geostatistical technique (Ordinary Kriging) to predict and map the soil C stocks in the entire study site. **Chapter 7** evaluates the soil-borne

fluxes of the three greenhouse gases in mangrove and their non-forest replacement land uses which were estimated from the field plots. The performance of Ordinary Kriging to predict and spatially map the fluxes of each GHG in the entire study site is also presented.

Lastly, the final chapter, **Chapter 8**, presents the overall conclusions, implications, research contributions of the study, and finally enumerates the recommendations for future studies.

Chapter 2

LITERATURE REVIEW

2.1 Introduction

The previous Chapter presented the overall framework of the study, highlighting the need to investigate the carbon (C) stocks in biomass and soil, and the soil greehouse gas (GHG) fluxes of mangrove forest along with their non-forest replacement land uses to determine the impacts of land use change in mangrove's C budget. In this second Chapter, the current literature on C stock assessment in biomass and soil pools, as well as the evaluation of soil GHG fluxes in mangrove and replacement land uses are reviewed. The specific and detailed reviews of literature for each technical chapter are presented in Chapters 4 to 7.

The rest of this chapter is divided into five sections. Section 2.2 is about the anthropogenic emissions of GHG in general and the problem on mangrove conversion. Section 2.3 deals about the major Carbon pools in a mangrove forest ecosystem in both biomass and soil pools. Section 2.4 reviews the studies on soil fluxes of CO_2, CH_4 and N_2O in mangrove forests. Section 2.5 is about the use of satellite remote sensing for mapping the biomass in mangroves. Section 2.6 is about the use of GIS-based Geostatistics in mapping the soil C in mangrove area. Section 2.7 deals on studies on whole-ecosystem C stocks in mangrove. The chapter ends in Section 2.8 where a summary of the Chapter is given.

2.2 Anthropogenic GHG emissions and mangrove conversion

For the last 261 years (1750 to 2011), human activities have emitted a cumulative total of 2,040 $GtCO_2$ to the atmosphere, of which about 50 % have only been emitted in the last 40 years (IPCC 2014b). Deforestation/land use change, mainly from terrestrial sources, is the second highest source of anthropogenic emission next to fossil fuel burning and cement production (Figure 2.1). Since 1970,

cumulative emissions from deforestation/land use change have increased by about 40 %. Deforestation contributed an average annual emission of 3.3 $GtCO_2$ per year during the period 2002-2011 (IPCC 2014). It has been hypothesised that the increased anthropogenic emission to the atmosphere is considered as the "extremely likely" cause of the recent warming of the ocean and the atmosphere, and climate variability (IPCC 2014).

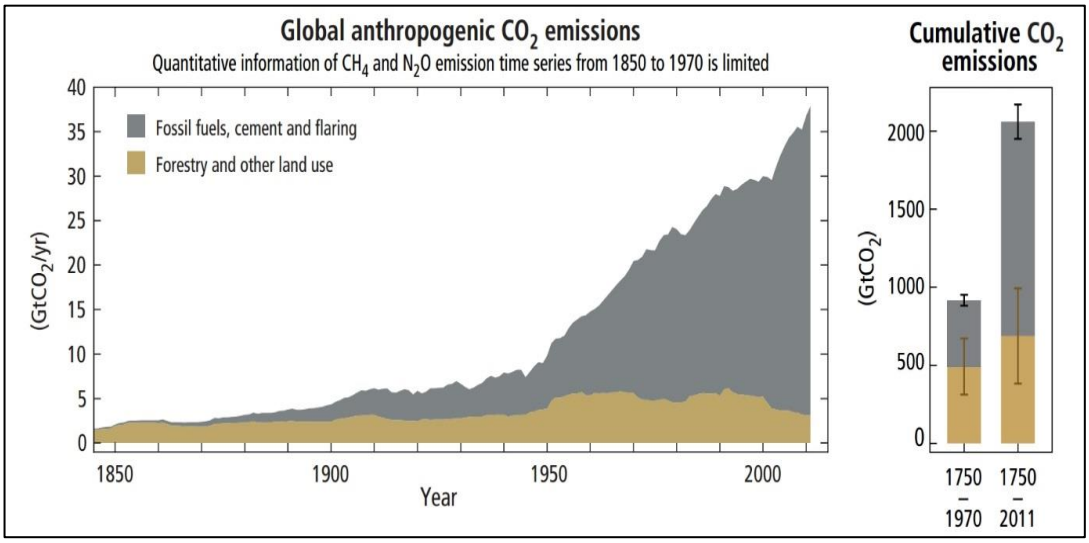

Figure 2.1 Historical yearly global anthropogenic carbon dioxide emissions from fossil fuel and cement production, and deforestation
Source: IPCC (2014a)

As of 2000, the world's mangrove forests were estimated at 137,760 km^2, of which about 75% are located in just 15 countries (Table 3.1, Giri et al. 2011). However, mangroves around the world have been deforested at an unprecedented rate. There has been about 50 % decline in mangrove area over the last 50 years (Alongi 2012). Since 1980, a total of 3.6 M ha of mangroves has been deforested (FAO 2007). The conversion of mangrove forests to other land uses still continue in many parts of the world. In Southeast Asia, more than 100,000 ha of mangrove forests were deforested and converted during 2000–2012 to other non-forest land uses especially aquaculture (Richards & Friess 2016). Among the major causes of area decline include conversion to aquaculture ponds, salt ponds, agricultural plantation, timber extraction, coastal development, settlements, and urban expansion (Primavera 2000; Alongi 2002; Giri et al. 2011; Long et al. 2013; Richards & Friess

2016). Intact mangroves and other coastal wetlands sequester and store a large amount of carbon in their soil and biomass (Howard et al. 2017). The disturbance of mangrove forest through deforestation and drainage (Figure 2.2) will release a significant amount of C back to the atmosphere (Alongi 2012; Pendleton et al. 2012; Siikamäki et al. 2012).

Table 2.1 Top 15 mangrove forest-rich countries in the world

SN	Country	Area (ha)	% of global total	Cumulative %	Region
1	Indonesia	3,112,989	22.6	22.6	Asia
2	Australia	977,975	7.1	29.7	Oceania
3	Brazil	962,683	7.0	36.7	South America
4	Mexico	741,917	5.4	42.1	North and Central America
5	Nigeria	653,669	4.7	46.8	Africa
6	Malaysia	505,386	3.7	50.5	Asia
7	Myanmar (Burma)	494,584	3.6	54.1	Asia
8	Papua New Guinea	480,121	3.5	57.6	Oceania
9	Bangladesh	436,570	3.2	60.8	Asia
10	Cuba	421,538	3.1	63.9	North and Central America
11	India	368,276	2.7	66.6	Asia
12	Guinea Bissau	338,652	2.5	69.1	Africa
13	Mozambique	318,851	2.3	71.4	Africa
14	Madagascar	278,078	2.0	73.4	Africa
15	Philippines	263,137	1.9	75.3	Asia

Source: Giri et al. (2011)

Current global estimates of C emissions from mangrove deforestation/ disturbance vary from 0.07-0.44 Pg CO_2 y^{-1} (Donato *et al.* 2011) to 0.09 – 0.45 Pg CO_2 y^{-1} (Pendleton et al. 2012). Although these estimates are based on assumptions and field plot-scale estimates, and crude (cf. Alongi 2014), these figures nonetheless indicate that greater effort must be exerted to conserve the stored C and prevent their release from disturbance. This also points out the need for empirical studies on C stocks and soil GHG fluxes of mangrove forest side by side with their replacement land uses. This is to better understand the magnitude of C emissions in mangroves as a consequence of land use change, and reduce the uncertainty of emissions estimate.

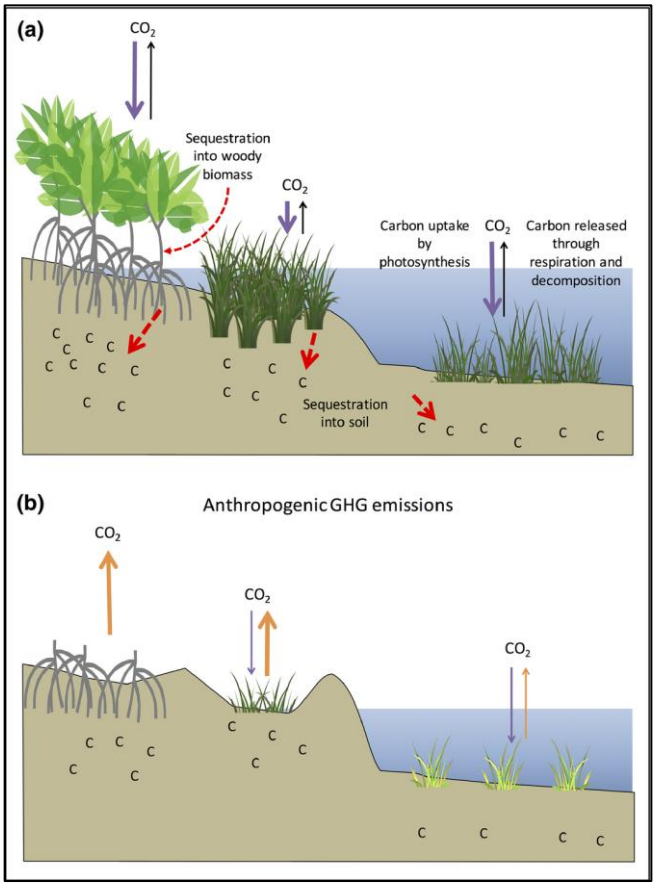

Figure 2.2 Carbon cycle in coastal wetlands, a) Intact mangrove forest and other coastal wetlands and b) Deforested and drained coastal wetlands
Source: Howard et al. (2017)

2.3 Carbon pools and storage in mangrove forest ecosystem

Carbon pools are reservoirs of carbon such as vegetation, soil, atmosphere and water that absorb and emit carbon (Howard et al. 2014). C pools in a mangrove forest ecosystem can be divided into soil and biomass pools, similar to most terrestrial forest ecosystems. However, unlike in upland forests where the greater proportion of total C stocks is in biomass (Brown 1997; Lasco 2002; Maraseni 2007; Ziegler et al. 2012), bulk of C storage in mangrove is in organic C rich soil/sediment, making up 75%, on the average, (Donato et al. 2011; Alongi 2014). High carbon storage in mangrove soil is due to sediment accumulation for over centuries from both autochthonous (C produced and deposited within the mangrove site) and allochthonous (C produced from adjacent ecosystem and deposited in the mangrove)

C sources. The slow decomposition of deposited organic matter in the sediment due to water-logged, anaerobic condition of the soil, also allows the continuous build-up of C over time (Kauffman & Donato 2012; Howard et al. 2014).

The biomass pools can be further subdivided into aboveground biomass (AGB) and belowground biomass (BGB), and the downed woody debris biomass (DWB; Figure 2.3). Leaf litter and understorey vegetation (e.g. seedlings, herbaceous) are negligible components in mangroves and are usually not included in the C stock quantification (Kauffman & Donato 2012; Howard et al. 2014; Phang et al. 2015). All trees in mangrove forest, which dominate the AGB (Kauffman & Donato 2012), are included in the C stock assessment since they are easy to measure, heavily affected by land use change and form a significant proportion of up to 21 % the total C stock (Howard et al. 2014).

The BGB is also an important C pool in mangrove and generally within 33 % to 50 % of aboveground biomass (Komiyama et al. 2008; Jachowski et al. 2013). The DWB is also an important component of biomass in mangroves and performs various ecological functions (e.g. habitat of mangrove invertebrates). It comprised about 2.5 % to 5 % of the total C stock (Howard et al. 2014). Furthermore, the soil in mangroves comprised the largest proportion of the total C stock, comprising 49 % to 98 % (Donato et al. 2011) and about 75 % on the average, of the total stock (Alongi 2014).

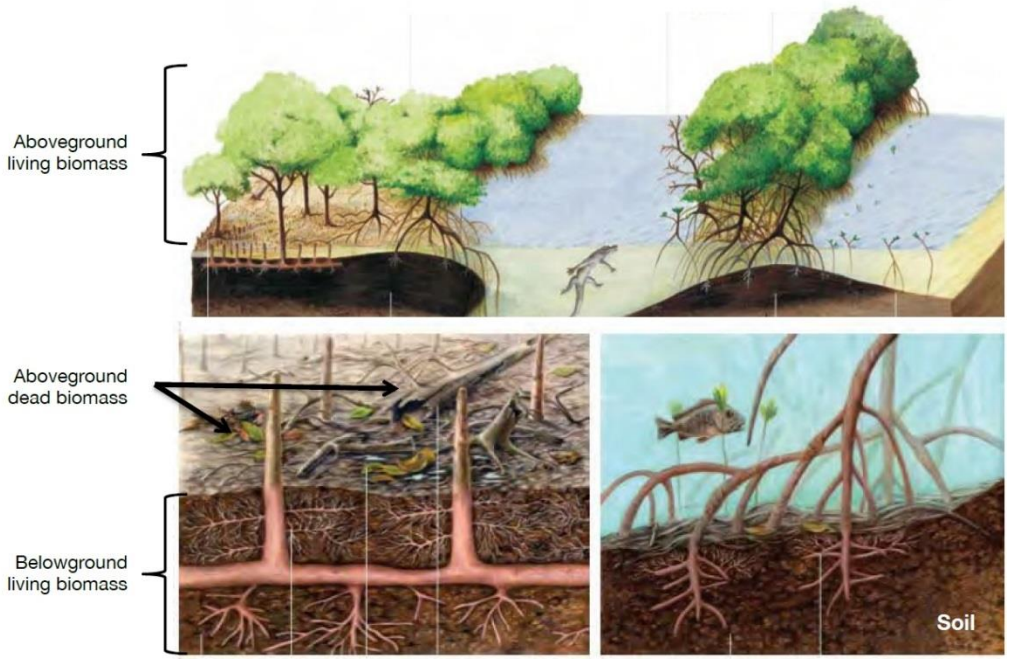

Figure 2.3. Biomass and soil Carbon pools in mangrove ecosystem
Source: Howard et al. (2014)

2.3.1 Biomass Carbon accounting in mangrove forest ecosystem

Carbon stock is the total amount of organic carbon stored in a blue carbon ecosystem of a known size. It is the sum of one or more C pools (Howard et al. 2014). On average, biomass store 25 % of total C stock in mangrove whilst the remaining 75 % is stored in soil (Alongi 2014). Studies that simultaneously measured the AGB, BGB and DWB and their C storage in mangrove forest have been growing since 2011 (e.g.(Donato et al. 2011; Kauffman et al. 2011; Adame et al. 2013; Kauffman et al. 2013; Sitoe et al. 2014; Tue et al. 2014; Murdiyarso et al. 2015; Stringer et al. 2015; Kauffman et al. 2016). Biomass and C stock densities have been quantified in undisturbed (Donato et al. 2011; Kauffman et al. 2011; Murdiyarso et al. 2015), and managed (Adame et al. 2013; Thompson et al. 2014; Tue et al. 2014; Adame et al. 2015; Vien et al. 2016) mangrove forests. Almost all of these studies have utilised published allometric equations (Table 2.2) to determine the biomass of tree individuals based easily measured variables such as diameter and height. The C fraction that is used to convert biomass density to biomass C stock density is usually 48 % for AGB, 39 % for BGB and 50 % for DWB based on Kauffman and Donato (2012).

High total biomass C stock reported in the literature on undisturbed mangrove forest was 453.8 MgC ha^{-1} in Kosrae, Micronesia (Donato et al. 2011), 340.6 MgC ha^{-1} in Mozambique (Stringer et al. 2015), 382 MgC ha^{-1} in West Papua, Indonesia (Murdiyarso et al. 2015), 339.7 MgC ha^{-1} in Sumatra, Indonesia (Murdiyarso et al. 2015) and 334.8 MgC ha^{-1} in Yap, Micronesia (Kauffman et al. 2011) whilst total biomass C stock reported for a disturbed mangrove stand in Java, Indonesia was only 21.2 MgC ha^{-1} (Murdiyarso et al. 2015). Most of the reported total biomass C stocks measurements are below 200 MgC ha^{-1}. The reported proportion of biomass components to the total biomass C stocks ranged from 33 % to 88 % for AGB, 8 % to 46 % for BGB and 0.2 % to 56 % for DWB, with most of the reported proportion below 70 % for AGB, 34 % for BGB and 11 % DWD. Belowground C storage has a positive but weak correlation to aboveground C storage (Donato et al. 2011). In addition, due to difficulty in measuring BGB, most of the estimates are based on allometric equation (Murdiyarso et al. 2013). About 10 % - 15 % of total stored C in mangrove is in belowground roots (Alongi 2014).

Whilst most of biomass and C stocks studies have been conducted in undisturbed and managed mangrove forests, these important parameters have not been fully quantified in the secondary mangrove forests especially in data-poor developing countries in the tropics where this mangrove type is common (Fortes 2004). Also, the measurement and variation of biomass in closed canopy side by side with open canopy mangrove have rarely been reported that could give indications of biomass loss due to forest degradation. This gap is addressed in Chapter 4 (**Objective 1**) of the Thesis.

Table 2.2 Allometric equations for various mangrove species based on diameter at breast height (cm)

Above-ground tree weight (W_{top} in kg)	Below-ground tree weight (W_R in kg)
Avicennia germinans $W_{top} = 0.140DBH^{2.40}$ $r^2 = 0.97$, $n = 45$, $D_{max} = 4$ cm, Fromard et al. (1998)[a] $W_{top} = 0.0942DBH^{2.54}$ $r^2 = 0.99$, $n = 21$, D_{max}: unknown, Imbert and Rollet (1989)[a]	*Avicennia marina* $W_R = 1.28DBH^{1.17}$ $r^2 = 0.80$, $n = 14$, $D_{max} = 35$ cm, Comley and McGuinness (2005)
A. marina $W_{top} = 0.308DBH^{2.11}$ $r^2 = 0.97$, $n = 22$, $D_{max} = 35$ cm, Comley and McGuinness (2005)	*Bruguiera* spp. $W_R = 0.0188(D^2H)^{0.909}$ r^2: unknown, $n = 11$, $D_{max} = 33$ cm, Tamai et al. (1986) c.f., $H = D/(0.025D + 0.583)$
Laguncularia racemosa $W_{top} = 0.102DBH^{2.50}$ $r^2 = 0.97$, $n = 70$, $D_{max} = 10$ cm, Fromard et al. (1998)[a] $W_{top} = 0.209DBH^{2.24}$ $r^2 = 0.99$, $n = 17$, D_{max}: unknown, Imbert and Rollet (1989)[a]	*Bruguiera exaristata* $W_R = 0.302DBH^{2.15}$ $r^2 = 0.88$, $n = 9$, $D_{max} = 10$ cm, Comley and McGuinness (2005)
Rhizophora apiculata $W_{top} = 0.235DBH^{2.42}$ $r^2 = 0.98$, $n = 57$, $D_{max} = 28$ cm, Ong et al. (2004)	*Ceriops australis* $W_R = 0.159DBH^{1.95}$ $r^2 = 0.87$, $n = 9$, $D_{max} = 8$ cm, Comley and McGuinness (2005)
Rhizophora mangle $W_{top} = 0.178DBH^{2.47}$ $r^2 = 0.98$, $n = 17$, D_{max}: unknown, Imbert and Rollet (1989)[a]	*R. apiculata* $W_R = 0.00698DBH^{2.61}$ $r^2 = 0.99$, $n = 11$, $D_{max} = 28$ cm, Ong et al. (2004) c.f., $W_{stilt} = 0.0209DBH^{2.55}$ $r^2 = 0.84$, $n = 41$
Rhizophora spp. $W_{top} = 0.128DBH^{2.60}$ $r^2 = 0.92$, $n = 9$, $D_{max} = 32$ cm, Fromard et al. (1998)[a] $W_{top} = 0.105DBH^{2.68}$ $r^2 = 0.99$, $n = 23$, $D_{max} = 25$ cm, Clough and Scott (1989)[a]	*Rhizophora stylosa* $W_R = 0.261DBH^{1.86}$ $r^2 = 0.92$, $n = 5$, $D_{max} = 15$ cm, Comley and McGuinness (2005)
Bruguiera gymnorrhiza $W_{top} = 0.186DBH^{2.31}$ $r^2 = 0.99$, $n = 17$, $D_{max} = 25$ cm, Clough and Scott (1989)[a]	*Rhizophora* spp. $W_R = 0.00974(D^2H)^{1.05}$ r^2: unknown, $n = 16$, $D_{max} = 40$ cm, Tamai et al. (1986) c.f., $H = D/(0.02D + 0.678)$
Bruguiera parviflora $W_{top} = 0.168DBH^{2.42}$ $r^2 = 0.99$, $D_{max} = 25$ cm, $n = 16$, Clough and Scott (1989)[a]	*Xylocarpus granatum* $W_R = 0.145DBH^{2.55}$ $r^2 = 0.99$, $n = 6$, $D_{max} = 8$ cm, Poungparn et al. (2002)
Ceriops australis $W_{top} = 0.189DBH^{2.34}$ $r^2 = 0.99$, $n = 26$, $D_{max} = 20$ cm, Clough and Scott (1989)[a]	Common equation $W_R = 0.199p^{0.899}D^{2.22}$ $r^2 = 0.95$, $n = 26$, $D_{max} = 45$ cm, Komiyama et al. (2005)
Xylocarpus granatum $W_{top} = 0.0823DBH^{2.59}$ $r^2 = 0.99$, $n = 15$, $D_{max} = 25$ cm, Clough and Scott (1989)[a]	
Common equation $W_{top} = 0.251pD^{2.46}$ $r^2 = 0.98$, $n = 104$, $D_{max} = 49$ cm, Komiyama et al. (2005) $W_{top} = 0.168pDBH^{2.47}$ $r^2 = 0.99$, $n = 84$, $D_{max} = 50$ cm, Chave et al. (2005)	

D_{stilt}: the weight of prop root of *R. apiculata*.
[a] After Saenger (2002), Table 8.3 on p. 260. D_{max}: the upper range of samples.

Source: Komiyama et al. (2008)

Studies that deal on quantifying mangrove C stocks side by side with those of non-forest land uses that replaced mangroves on the same site have been reported in the literature, albeit they are very few and limited only to Mexico, India and central Philippines. Available studies so far are limited to mangrove - abandoned aquaculture pond (Kauffman et al. 2013; Bhomia et al. 2016; Duncan et al. 2016) or mangrove – pasture (Kauffman et al. 2016). Based on these studies, biomass C stock declined by a range of 33 - 86.6 MgC ha^{-1} (68 – 100 %) and by 163 MgC ha^{-1} (92 %) when mangroves are converted to aquaculture pond and cattle pasture, respectively. However, other land uses that replaced mangroves such as coconut palm plantation, cleared mangrove and abandoned salt pond have not been evaluated yet. In terrestrial upland forests, biomass C stocks in terrestrial forests in Asia declined by 22-67 % after logging, whilst the coconut plantation biomass C stock is 43 % less than the natural forest in the same area (Lasco 2002).

AGB in mangrove forest tends to increase with distance from downstream position/seaward edge (Kauffman et al. 2011; Wang et al. 2014) where salinity is low, with lower influence of tidal inundation and wave action, and higher sediment

input from the upland. BGB increase with distance from seaward/downstream position (Wang et al. 2014). Forest structure influenced root biomass, where highest values were observed in forest with high density (Adame et al. 2014). The ratio of BGB to AGB ranges from 0.35 – 0.49 (Jachowski et al. 2013; Wang et al. 2014) and increases from upstream to downstream positions (Wang et al. 2014). Total biomass generally decreases from upstream to downstream as with soil elevation (Wang et al. 2014).

Whilst existing mangrove C stocks studies have examined the relationships between biomass and site factors such as salinity, distance to shore, and elevation, among others (Donato et al. 2011; Adame et al. 2013; Wang et al. 2014), canopy biophysical variables (e.g. leaf area index, canopy gap fraction) of mangroves and their relationship with biomass and C stocks have not been fully studied. This is addressed in Chapter 4 (**Objective 1**) of the Thesis. Salmo et al. (2013) measured the Leaf Area Index (LAI) of a secondary natural mangrove stand as a reference and a set of chrono-ages mangrove *Rhizophora* plantations in the Philippines using proximal instrument sensor (*Plant Canopy Imager)*. They found out that LAI and AGB are both positively correlated with stand age, and those plantations older than 11 years had similar values of LAI as the secondary natural mangrove stand (4.13 to 4.54 m^2 m^{-2}). However, they did not evaluate the relationship between LAI and AGB, and did not mention any measurements of canopy gap fraction. Determining the relationship between biomass and canopy biophysical variables in mangroves could be important to remote sensing-based biomass estimation and mapping since LAI and other canopy physical variables could be generated and mapped using remotely sensed imagery data (e.g. Dusseux et al. 2015).

2.3.2 Soil Carbon accounting in mangrove

Soil contains 75%, on average, of the total C storage in mangrove, as mentioned previously in this Chapter. Past studies on soil C stocks in mangrove are mostly done at the upper 100 cm of the sediment due to difficulty in obtaining samples. However, studies are growing that measured mangrove soils deeper than 100 cm due to availability of soil augers that can collect samples below 1 m soil depth. Whilst the global average of soil C storage is 75 % of the total C storage (Alongi 2014), individual measurements of soil C ranged from 49 % to 98 % of the

total C stock (e.g. Donato et al. 2011; Kauffman et al. 2011; Kauffman et al. 2016; Vien et al. 2016). The global mean soil C stocks is about ~717 MgC ha^{-1} (Alongi 2014) whilst those reported in the literature from individual mangrove studies ranged from a low of 155 MgC ha^{-1} for a depth of 152 cm in India (Bhomia et al. 2016) to a high of 1255 MgC ha^{-1} for a 300 cm depth in Borneo (Donato et al. 2011).

The amount of soil C increases with forest age (Alongi 2012) and with distance from seaward edge/downstream to landward/upstream (Donato et al. 2011; Kauffman et al. 2011; Wang et al. 2014) with decreasing salinity and increasing soil elevation. Soil C stock is negatively correlated with salinity and N:P ratio, but positively correlated with soil surface phosphorus concentration (Adame et al. 2013). Soil C concentration (% C) is positively correlated with tree biomass (Wang et al. 2014) and generally decreases with depth (Kauffman et al. 2011; Adame et al. 2013).

In terrestrial ecosystem, the conversion of forest to agriculture results in the loss of 20-50 % soil C (Lal 2005). In Queensland, Australia, soil C stocks declined by 22 % when terrestrial forest is converted to agricultural land and by 60 % when scrubland is converted to cultivated land (Maraseni 2007). In the coastal mangrove area, whilst some studies have been conducted on mangrove soil C stocks, the knowledge of the soil C stock of closed canopy and open canopy mangrove forests, and of land uses that replaced mangroves such as aquaculture and agriculture are still limited. The few available studies are limited to mangrove and abandoned aquaculture pond as well as mangrove and cattle pasture. For conversion to aquaculture, soil C loss of 60 % (95 MgC ha^{-1}) in India (Bhomia et al. 2016) and 86 % (686 MgC ha^{-1}) in the Dominican Republic (Kauffman et al. 2013) have been reported in the literature. For mangrove to cattle pasture conversion, soil C loss was 23 % for 7-year-old pasture and > 70 % for 30-year-old pasture (~235 MgC ha^{-1}). We have limited knowledge if the same magnitude is true when mangrove forests are converted into non-forest land uses other than abandoned aquaculture pond and cattle pasture. Such knowledge is important for accurately estimating the impact on C stocks owing to land use change. This gap is addressed in Chapter 6 (**Objective 3**) of the Thesis.

2.4 Soil GHG Fluxes in mangrove and competing land uses

In land-based sector, carbon dioxide (CO_2), methane (CH_4) and nitrous oxide (N_2O) are the three greenhouse gases (GHG) being monitored and regularly reported by the Intergovernmental Panel on Climate Change (IPCC). As shown in Figure 2.4, CO_2 accounts for 76 % of the total anthropogenic emissions in 2010, while CH_4 and N_2O comprise 16 % and 6.2 % of the total emissions, respectively (IPCC 2013). CO_2, CH_4 and N_2O contribute approximately 56%, 32% and 6%, respectively of the global warming effect in 2011 relative to year 1750. CH_4 and N_2O have 28 and 265 times global warming potential (GWP), respectively, than CO_2 in a 100-year time horizon (IPCC 2013). Forest clearing, especially in mangrove with high soil C, results in the emission of stored C and other GHG through oxidation of soil C (Lovelock et al. 2011). In addition, aquaculture and agriculture are activities that add nutrients to the system in the form of feeds for shrimps and fish, and fertiliser for crops which can enhance the metabolism of soil microorganisms resulting in emissions of N_2O and CH_4 (Chen et al. 2010).

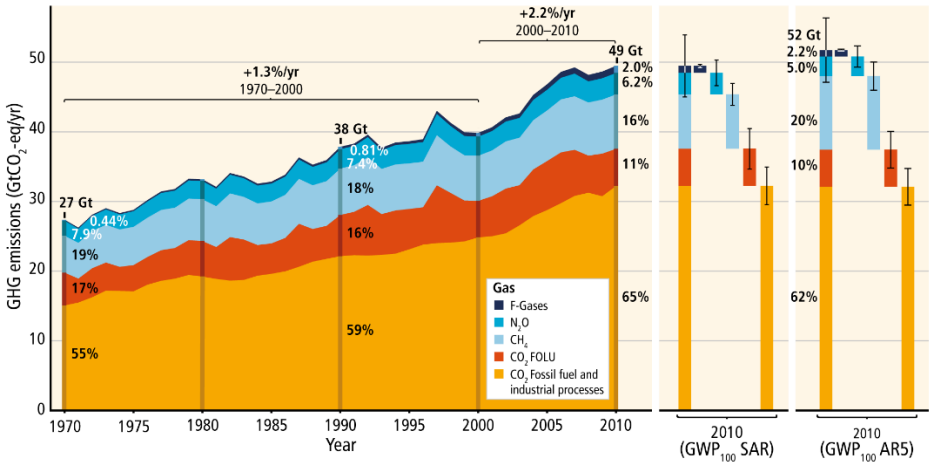

Figure 2.4 Total annual anthropogenic GHG emissions by gases, 1970-2010
Source: IPCC (2013)

Previous studies on mangrove soil GHG emission have mostly dealt on either CO_2 fluxes (Lovelock 2008; Poungparn et al. 2009; Chanda et al. 2014) or CO_2 and N_2O (Chen et al. 2010), or CH_4 and N_2O (Allen et al. 2011) whilst only a few have simultaneously measured the fluxes of the three GHG (Chen et al. 2010; Chen et al.

2014). However, despite its importance, no study has so far simultaneously measured all the GHG fluxes on soil of land uses that replaced mangroves. Fluxes of CH_4 and N_2O have not been assessed for replacement land uses of mangroves. Measuring the three GHG simultaneously would be necessary for determining the relative importance of these gases (Murdiyarso et al. 2012) since they can be brought to a common unit (i.e. CO_2 equivalent). This gap on soil GHG fluxes in mangrove forest and replacement land uses is addressed in Chapter 7 (**Objective 4**) of the Thesis.

For mangrove forests, the reported fluxes of CO_2 ranged from -0.25 to 2.97 μmol m^{-2} s^{-1} in 11 mangrove sites in Caribbean, New Zealand and Australia (Lovelock 2008) to 0.07 to 8.67 μmol m^{-2} s^{-1} in Hong Kong (Chen et al. 2010) while CH_4 fluxes ranged from 0.19 to 1087 μmol m^{-2} h^{-1} in subtropical mangrove in Southeast Queensland, Australia (Allen et al. 2011) to 10 to 5168 μmol m^{-2} h^{-1} in Shenzhen, China (Chen et al. 2010). Reported N_2O fluxes ranged from minus (-) 0.04 μmol m^{-2} h^{-1} in North Sulawesi, Indonesia (Chen et al. 2014) to 0.14 to 23.8 μmol m^{-2} h^{-1} in south China (Chen et al. 2010). Fluxes are reported to be related to soil temperature, nutrient/organic matter content, redox potential, and to some extent salinity (Alongi 2014, Chen *et al*. 2014). In addition, CO_2 fluxes are higher in landward position as compared to N_2O and CH_4 which are the same regardless of tidal positions, and are related to soil organic matter content and soil moisture content (Chen et al. 2014), redox potential, salinity and porosity whilst N_2O flux is related to salinity and porosity and CH_4 to NH_4-N (Chen et al. 2010). Furthermore, it has been reported that the soil CO_2 fluxes of 11 mangrove sites in Caribbean, New Zealand and Australia are positively correlated with their Leaf Area Index (Lovelock 2008).

For the non-forest land uses that replaced mangrove forests, CO_2 flux in soil cleared of mangrove vegetation over 20 years for tourism development levelled to 2 mmol m^{-2} s^{-1}, approximately 2,900 tCO_2 km^{-2} y^{-1}, after four years from disturbance in Belize and found not related to soil temperature (Lovelock et al. 2011). For shrimp aquaculture ponds, the rates of CO_2 flux in Indonesia ranged 4.37 kg CO_2 m^{-2} y^{-1} from the walls of the pond and 1.60 kg CO_2 m^{-2} y^{-1} from its floors (Sidik & Lovelock 2013), and 220 to 5,000 (mean 1,750) tCO_2 km^{-2} y^{-1} in shrimp ponds in Australia (Burford and Longmore 2001 as cited in Lovelock *et al*. 2011).

While the relationship between LAI and CO_2 flux has been reported in forested mangrove soils, the relationship between soil GHG fluxes and soil C stock in mangrove and its replacement land uses is still poorly understood. We also do not know if the same relationship holds true between LAI and the other two GHGs. Knowing the relationship of these GHGs with LAI is important for prediction purposes as LAI map can be generated using satellite remote sensing imagery data. This gap is addressed in Chapter 7 (**Objective 4**) of this Dissertation.

Compared to GHG studies on mangrove soil, research on GHG emissions from peat land (a type of wetland but more terrestrial and inland of the coastal zone), under peat forests and their non-forest replacement land uses, have been reported by several authors (Inubushi et al. 2003; Hadi et al. 2005; Melling et al. 2005; Hergoualc'h & Verchot 2011; Hergoualc'h & Verchot 2012). Several land uses under terrestrial peat soils have been studied and measured for their annual emissions (Table 2.3). Emissions were reported to be strongly influenced by land use type and hydrologic zone, with fluxes exhibiting seasonal changes.

Table 2.3 Annual CO_2, CH_4 and N_2O emissions from peatlands of Kalimantan

Land use	Soil flux		
	CO_2 (g C m^{-2} y^{-1})	CH_4 (g C m^{-2} y^{-1})	N_2O (mg N m^{-2} y^{-1})
Secondary forest	3460	4.4	1338
Paddy field	1389	19.6	24.7
Rice-soybean field	2019	2.6	203.6

Source: Hadi et al. (2005)

2.5 Satellite remote sensing-based biomass estimation and mapping of mangroves

Traditional mangrove biomass studies have utilised field plots to estimate biomass and infer the stock for the whole study site. This approach is sufficient only for a few hectares, but costly and slow if implemented over large areas. This is also difficult to implement in remote and treacherous portions of the land under study, especially for mangrove forests which have extensive root systems that can make it difficult to access to the interior of the forest. Satellite remote sensing technology

offer cost and time advantages in collecting data over larger area and in implementing large-scale biomass assessment due to its synoptic view and routine collection of imagery data (Samalca 2007).

Mapping of biomass through satellite remote sensing technology can make use of radar (active) and multispectral (passive) imagery data (Campbell & Wynne 2011; Aslan et al. 2016; Wicaksono et al. 2016). Multispectral imagery data are composed of many spectral bands including infrared and red edge which are sensitive to the presence of vegetation. Cloud-free multispectral data can be used to characterise canopy cover, species composition and leaf greenness (Aslan et al. 2016). However, a major part of the mangrove growing area are in the tropics where clouds are persistent. On the other hand, radar sensors such as Synthetic Aperture Radar (SAR) have low dependence on atmospheric condition and can operate during cloudy weather and at night (Lam-Dao et al. 2009; Campbell & Wynne 2011).

Studies have been growing on the use of satellite imagery to retrieve and map the aboveground biomass in mangrove ecosystem. Global mangrove biomass map (Hutchison et al. 2014) have been produced and a number of site-specific mangrove biomass maps derived from space-borne optical (Li et al. 2007; Proisy et al. 2007; Jachowski et al. 2013; Wicaksono et al. 2016) and radar (Simard et al. 2006; Li et al. 2007; Fatoyinbo et al. 2008; Thapa et al. 2015; Aslan et al. 2016) imagery data.

However, there is paucity of reports that compare the performance of both satellite radar and optical imagery to predict and map the biomass of mangrove forests. Information is also very limited on the performance of radar and optical satellite imagery to retrieve and map the biomass of non-forest land uses that replaced mangroves. The recent launch of the new-generation Sentinel-1 (SAR) and Sentinel-2 (multispectral) satellite missions of the Copernicus program of the European Space Agency is expected to provide new and enormous radar and optical data for monitoring and mapping of biomass in the coastal zone of the tropics. However, pioneering studies are needed to assess these new-generation satellite imageries especially in the retrieval and mapping of the biomass of mangrove forest. Also needed to analyse are the land uses that replaced mangroves from data acquired by these newly launched multispectral and SAR instruments on-board the Sentinel-1 and Sentinel-2 satellite missions which have not been reported in the scientific literature. These gaps are addressed in Chapter 5 (**Objective 2**) of the dissertation.

For satellite optical imagery data, Proisy et al. (2007) used very high-resolution IKONOS imagery (resolution 1 to 4m) to estimate and map the mangrove aboveground biomass in French Guiana through textural ordination technique. They obtained higher biomass prediction accuracy in using panchromatic band than using NIR band. Jachowski et al. (2013) used very high-resolution GeoEye-1 satellite image and a machine learning biomass algorithm (SMOreg) to build aboveground biomass model for a mangrove forest in Thailand. They found that Band 2 (green), Band 4 (near infrared) and their ratio (Band 2/Band 4) in combination with ASTER GDEM elevation data produced the optimal biomass model, with a correlation of predicted and observed value at 0.81. More recently, Wicaksono et al. (2016) used vegetation indices and PCA bands derived from ALOS-AVNIR-2 imagery for Indonesian mangrove and obtained 77.1 % and 77.8 % predicted map accuracy, respectively.

For radar (SAR) satellite data, Simard et al. (2006) used the traditional linear regression to model the relationship between field-measured plot biomass and mean stem height derived from LIDAR-calibrated SRTM DEM elevation data to compute and map the landscape-scale biomass of mangroves in the Everglade. Fatoyinbo et al. (2008) used the equation developed by Simard et al. (2006) to calibrate SRTM elevation data into canopy height data of mangrove in Mozambique, Africa and used the same in combination with field measured plot biomass and an existing global biomass-height equation to map the landscape-scale standing biomass of mangroves in the country. Thapa et al. (2015) used the L-band ALOS PALSAR imagery and obtained a strong correlation for biomass of mangrove in Sumatra, Indonesia (r^2 = 0.84) from the combination of HH and HV individual polarisations and their ratios. More recently, Aslan et al. (2016) used SRTM DEM-derived mangrove height model, similar to Simard et al. (2006) to estimate and map the mangrove biomass in Papua, Indonesia and found the developed prediction model only explained 47 % of the variation in field biomass.

Moreover, studies that compare satellite radar and optical imagery are almost non-existent in mangrove biomass study. The lone study, Li et al. (2007), used Radarsat imagery backscatter coefficient and compared it with Landsat TM-derived NDVI to predict the mangrove biomass in southern China. They found that polynomial model from Radarsat had higher correlation with biomass and lower

error of biomass prediction than Landsat NDVI model, and model that combined Radarsat backscatter and Landsat NDVI (r = 0.84 vs 0.67 and 0.77).

2.6 GIS-based mapping of mangrove soil C stocks and GHG fluxes

There is a paucity of reports on mapping the site/landscape-scale C stock in mangrove although a global mangrove soil C stock map (Jardine & Siikamäki 2014) has been produced. Most studies on soil C stocks in mangrove forest and other land use in the coastal zone were done using sample plots and have not attempted to map the variation in the entire study site. Scaling up to above plot-level (i.e. study site, bay/landscape and region) will increase our understanding of the spatial distribution and variability of soil C stocks in the coastal zone and can help improve estimates of soil C stocks and emissions.

Whilst GIS-based geostatistical technique such as Kriging has been successfully used in inland terrestrial soils to predict the soil C-related parameters in un-sampled locations and map their site-scale distribution (e.g. Mishra et al. 2009; Umali et al. 2012; Kucuker et al. 2015), its application in mangrove soil is not well understood for lack of any similar studies. Further review of Ordinary Kriging is discussed in the methodology section of Chapter 6.

Results of previous soil C stocks-related predictive mapping in inland soils revealed that it was possible to accurately map the soil organic C for the entire study site by 82-83 % (Umali et al. 2012) and 97 % for soil C stock (Mishra et al. 2009). The prediction accuracy was computed from the given RMSE and dataset range data of the two studies, respectively. Kucuker et al. (2015) were also successful in mapping the soil C stock distribution in their study site in Turkey using Ordinary Kriging, but they did not validate the accuracy of the generated soil C stock map. This gap is addressed in Chapter 6 (**Objective 3**) of this Thesis.

Also, no studies on spatial modelling of the variability/distribution of soil GHG fluxes in mangrove and competing land uses have been done so far. This is despite of the relationship between LAI and CO_2 in mangrove soil (Lovelock 2008). This gap is addressed in Chapter 7 (**Objective 4**) of the Dissertation.

2.7 Whole-ecosystem C stock accounting in mangroves

There have been growing numbers of studies on quantifying the whole-ecosystem carbon stocks of mangroves. Alongi (2014) made a recent review of mangrove's C cycling and storage and showed a consolidated mean global whole-ecosystem C stock of mangrove of 956 MgC ha^{-1}, 2 to 4 times higher than terrestrial forests such as rainforests (241 MgC ha^{-1}) and peat swamps (408 MgC ha^{-1}). About 75 % of total C stock in mangroves is stored in the soil compared to rainforests (44 %) and peat swamp (70 %). Mangrove roots store approximately 13-15 % of the total C, just like rainforests. However, based on individual studies, the values of whole ecosystem C stock ranged from 1023 MgC ha^{-1} for Indo-Pacific sites, 937 MgC ha^{-1} for mainland Southeast Asia, and 381 to 987 MgC ha^{-1} in the Caribbean Mexico with the C stored in soils accounting for 49 – 98 % of the total mangrove C stocks (Donato et al. 2011; Adame et al. 2013; Thompson et al. 2014; Tue et al. 2014; Murdiyarso et al. 2015; Duncan et al. 2016; Vien et al. 2016). Ecosystem C stock in mangroves increase from high salinity/seaward fringe to low saline/interior/landward zone (Kauffman et al. 2011; Mizanur Rahman et al. 2014; Tue et al. 2014) and is strongly related to tree basal area and height but has weak correlation with tree density and crown cover (Mizanur Rahman et al. 2014).

In contrast, the whole-ecosystem C stock of abandoned shrimp pond was only 11 % (Kauffman et al. 2013), 25 % (Bhomia et al. 2016) and 57 % (Duncan et al. 2016) of the C stock of their neighbouring mangroves, with range of C stock decline from 163 to 768 MgC ha^{-1}. Likewise, C stocks of cattle pasture that replaced mangroves in Mexico was only 34 % of the adjacent mangrove forest, with C stock decline of 399 MgC ha^{-1} in the top 1 m of soil or 900 MgC ha^{-1} if the entire soil depth is considered (Kauffman et al. 2016). Despite their importance for establishing baseline C stocks and estimating C emissions from conversion and forest degradation, however, there remains paucity of reports on the whole-ecosystem C stocks secondary mangroves under closed canopy and open canopy stands outside protected areas, and other non-forest land uses that replaced mangroves such as palm plantation, salt pond and cleared mangroves. These information gaps are addressed and summarised in Chapter 8 of the Thesis.

2.8 Summary

From the preceding review of previous studies, the following research gaps related to understanding of the C budget in mangrove forests and the C losses arising from their conversion to non-forest replacement land uses are summarised below:

- C emission estimates from mangrove conversion are based only on assumptions. Available estimates of C losses from mangrove conversion are limited to only a few cases.
- The biomass and C stocks in the secondary mangrove forests are little understood, as well as the C losses from biomass due to conversion to replacement land uses of mangroves. Also, the measurement and variation of biomass in closed canopy, side by side with open canopy mangrove, have rarely been reported that could give indications of biomass C loss due to forest degradation. Canopy biophysical variables (e.g. leaf area index, canopy gap fraction) of mangroves and their relationship with biomass and C stocks have not been fully studied.
- The soil C stocks of closed canopy and open canopy mangrove forests, and the soil C losses from their conversion to non-forest land uses are little understood.
- The whole-ecosystem C stocks of secondary mangroves under closed canopy and open canopy stands outside protected areas, and the C losses from mangrove conversion to other non-forest land uses that replaced mangroves such as palm plantation, salt pond and cleared mangroves, have not been fully evaluated.
- The soil surface fluxes of the three GHGs (CO_2, CH_4 and N_2O) in secondary mangrove forests and the changes due to mangrove conversion are little understood. No study has so far simultaneously measured the soil fluxes of all the three GHGs (CO_2, CH_4 and N_2O) on mangrove forest side by side with their replacement non-forest. The relationship between the mangrove soil GHG fluxes and stand parameters (e.g. C stock, leaf area index) is still poorly understood.
- We have limited knowledge on the performance of satellite radar imagery in comparison with optical imagery to predict and map the biomass of mangrove

forests and non-forest land uses that replaced mangroves. The utility of imagery data from the newly launched multispectral and SAR instruments on-board the Sentinel-1 and Sentinel-2 satellite missions for biomass retrieval and mapping in mangrove forest and replacement land uses in the coastal zone has not been reported in the scientific literature.

- There is a paucity of reports on mapping the site/landscape-scale C stock in mangrove. Most studies on soil C stocks in mangrove forest and other land use in the coastal zone were done using sample plots and have not attempted to map the variation in the entire study site. The utility of geostatistics (e.g. Ordinary Kriging) in the spatial interpolation and mapping of soil carbon in mangrove soil is not well understood for lack of any studies. The same is true for the application of geostatistics to spatial modelling of the variability/distribution of soil GHG fluxes in mangrove and replacement non-forest land uses as no studies have been done so far.

The next Chapter presents the methodology and approaches used in this study to attain the objectives enumerated in Chapter 1.

Chapter 3

RESEARCH METHODS

3.1 Introduction

The previous two chapters discussed the problem of the on-going mangrove deforestation and forest degradation, and the associated C losses arising from conversion to non-forest land uses. Also presented on those chapters are the works that have been done so far to understand the C budget in mangrove forest and the carbon implication of mangrove land use change. Chapter 2 also presents the current research gaps on the topic that need to be filled up, and these gaps served as the basis for developing the aim and objectives of the study. The present chapter discusses the approach, design and methods of the study adopted to achieve the objectives enumerated in Chapter 1. This chapter describes the following subsections: a) Description of the Study Area, b) Research Design, c) Data Capture and Acquisition, and d) Data Processing and Analysis. More specific discussion of methods could be found in Chapters 4 to 7 corresponding to the four specific objectives of this Thesis.

3.2 The Study Area

The study site is located in the central to the southern coast of Honda Bay on the eastern coast of Puerto Princesa City, island-province of Palawan (Figure 3.1). It is geographically located between latitude 9.8028^0 to 9.9612^0N and longitude 118.725^0 to 118.805^0E. The city is approximately 567 km southwest of Manila, the Philippines' capital. Puerto Princesa City is Palawan province's capital and is located in the central part of the province in the westernmost part of central Philippines. Palawan province including Puerto Princesa City and neighbouring towns are famous for its white sand beaches, and favourite vacation destinations among local and international tourists.

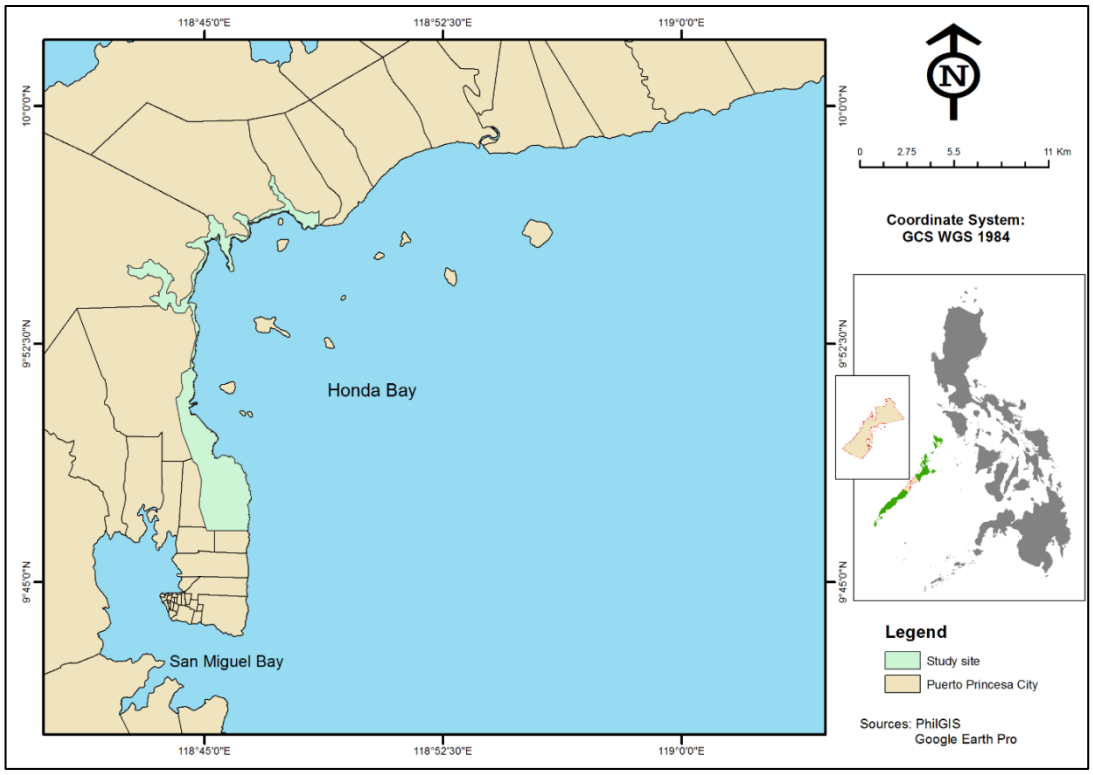

Figure 3.1. The location map of the study site. Inset: Philippine map showing Palawan province (green) and Puerto Princesa City (beige) at province's midsection

The climate in the study site is tropical, monsoon-type climate with two seasons (dry and wet) and under Type 3 (i.e. no very pronounced maximum rain period, with one to three months only of dry season) based on Modified Corona's Climate Classification. The city receives an annual rainfall of 1,527.3 mm. Rainfall is highest during months of October (216.1 mm) to November (211 mm) and lowest from January to April (less than 55 mm), with February (23.7 mm) as the driest month (Figure 3.2). Rainfall from May to September and December is at least 150 mm (PAGASA 2016). The city's annual mean temperature is 27.4 ^{0}C. The lowest temperature (26.8 - 26.9 ^{0}C) is during the months of January and February while the highest (28.5 - 28.6 ^{0}C) is during April and May (PAGASA 2016).

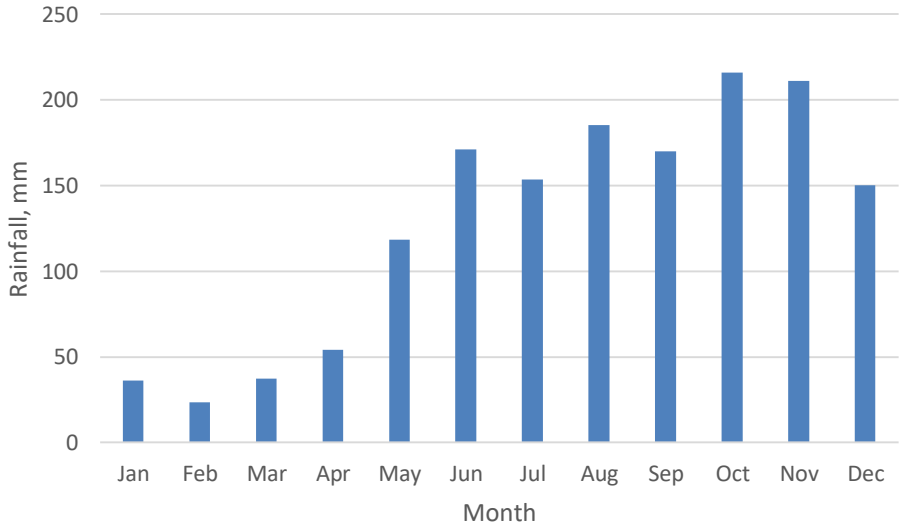

Figure 3.2 Mean monthly rainfall in Puerto Princesa City, Palawan, Philippines
Source: PAGASA (2016)

The population of the city is 255,166 as of 2015 (PSA 2016), from only 92,147 in 1990 (NSO 2011). The city's yearly population growth rate was 3.24 % during the period 2000-2010 and 5.79 % during 1990-2000. The last 20-years (1990-2010) annual population growth rate was 4.51 % which was higher compared to the national rate of only 2.12 % during the 1990-2010 period (NSO 2011). Nineteen (19) of the city's total 66 barangays (villages), the smallest political unit in the Philippines, are located along the coast of Honda Bay and has a total population of 118,969 as of 2015 (PSA 2016). The six villages that cover the study area (i.e. Salvacion, Santa Cruz, Bacungan, Santa Lourdes, Tagburos, and San Jose) have a total population of 36,329 (14.2 % of the city's population). About 15 of the 19 villages that lie along Honda Bay's coast, including the six villages that cover the study site, are directly dependent on Honda Bay, with fishing either as a primary or alternative source of livelihood (Ibrahim, pers. com).

The city has a total land area of 253, 982 ha (PPC 2017). The eastern coast of the city faces the Sulu Sea where two bays can be found: San Miguel Bay near the Central Business District (city proper) and further north, Honda Bay. The coastline of Honda Bay stretches some 82 km from the Langogan village in the north to down south in San Miguel village near the Puerto Princesa Airport. Honda Bay's central and southern coast is lined with a long band of mangrove forests, some 40 km in

length, running north to south of the study site, along the coast (fringing mangrove), and along the mouths and upstream (estuarine mangrove) of the three rivers in the northern part of the study site. The fringing mangroves are interrupted by non-forest land uses such as agriculture, aquaculture, and built-up areas/settlements especially in the central and southern portion of the study site (Figure 3.3).

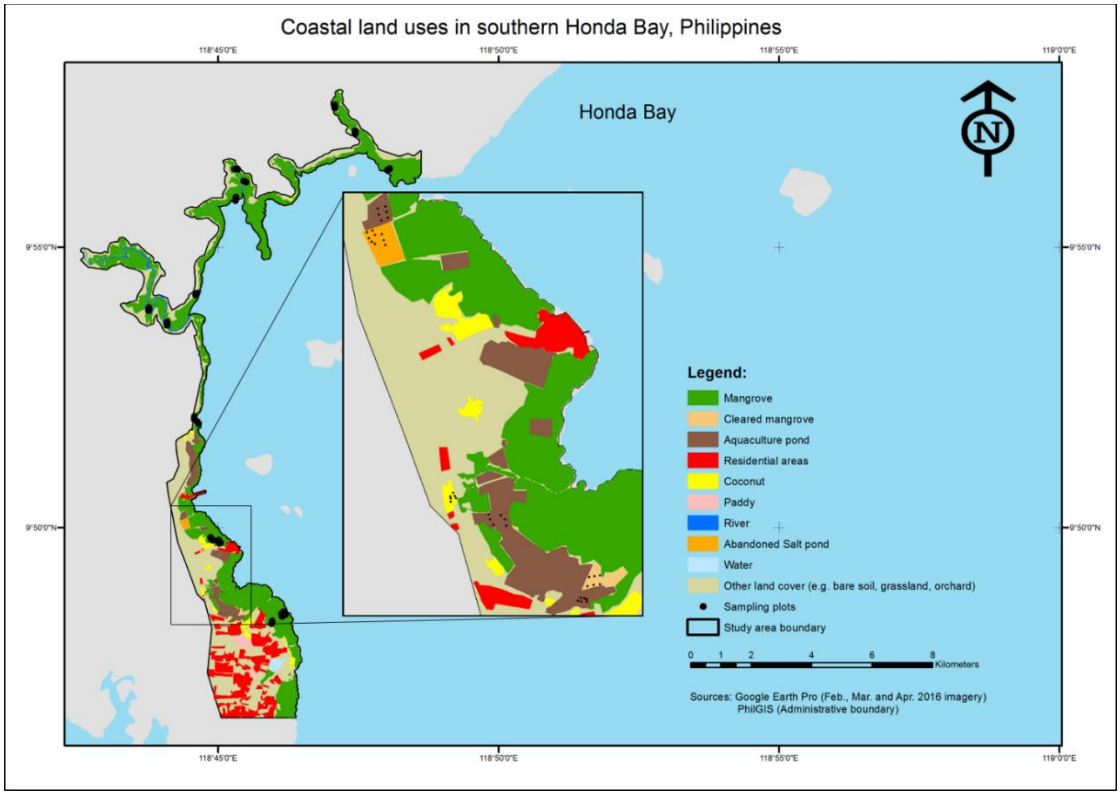

Figure 3.3 Land use map of the study site showing the location of mangrove forest relative to the land uses that replaced mangroves and the location of the sampling plots (black dots)

The non-forest land uses mostly encroached the landward and middle portions of the fringing mangrove in the case of aquaculture, agriculture and built-up areas. However, the encroachment was sometimes within the whole band (landward to seaward) of the mangrove, disrupting the north-south continuity of the forest lining the shore. Encroachment is also apparent with local boat stations where clearings for access and some human settlements are prominent. The width of the remaining fringing mangrove forest varies from 10 m to about 500 m while the width of the estuarine mangroves varies from 250 m to 560 m at the river mouth to some 90

m to 200 m upstream. The estuarine mangroves extend some 1 km to about 6 km upstream from the river mouth. The mangroves in the northern portion of the study site have high tree density (>1,100 trees ha^{-1}) and closed canopies (herein termed 'closed canopy forest') while the mangroves in the central and southern portions of the study site, where the non-forest replacement land uses of mangroves are all located, mostly have lower tree density (<1,00 trees ha^{-1}) and open canopies (herein called 'open canopy forest').

Sites under mangrove forests were selected as well as non-forest land uses that replaced mangroves on deforested mangrove lands (i.e. competing land uses of mangroves) such as aquaculture ponds, coconut plantation, abandoned salt pond and cleared mangrove area. The study site has an area of 2,750 ha, of which some 1,216.4ha is covered by mangrove forests, both under closed and open canopies. The mangroves in the site are dominated mostly by *Rhizophora* species. They can be classified into two canopy types: closed canopy mangrove forest and open canopy mangrove forest. Closed canopy mangroves are dense, intact mangrove vegetation, with no significant open spaces or gaps. These forests are located mostly in areas far from built-up areas. They have a mean Leaf Area Index (LAI) of 2.25 and canopy gap fraction of 14 % or about ~86 % canopy foliage cover. On the other hand, open canopy mangroves have open spaces with fewer trees, and mostly near built-up areas, with mean LAI of 0.62 and canopy gap fraction of 64 % (~36 % canopy foliage cover).

In contrast, the non-forest land uses were historically occupied by mangroves prior to their conversion. The aquaculture ponds and abandoned salt ponds were former mangrove forests until they were cleared in the early 1990s and were both in operation until early 2000s. The coconut plantation is a 20-year-old stand planted at the back of an open canopy mangrove forest and seemed not actively managed. This plantation has thick growth of the mangrove fern *Acrostichum* sp. on the base of the individual coconut (see Fig. 3.4d). The cleared mangrove is a deforested mangrove area that was gradually cleared from 2005 to 2008 as a site earmarked for resettlement but remained unutilized at the time of survey. Table 3.1 shows the area of mangrove forest and the non-forest land uses that replaced mangroves.

Table 3.1 Area of mangrove forest and the non-forest land uses that replaced mangroves

Land use	Area (ha.)	% share
Mangrove	1,216.4	44.2
Abandoned aquaculture pond	237.8	8.6
Coconut plantation	69.5	2.5
Abandoned salt pond	14.4	0.5
Cleared mangrove	9.6	0.3
Other non-forest land uses	1,202.3	43.7
Total	2,750	100

3.2.1 Basis in Selecting the Study Site

The criteria used in site selection include the following:

1. Presence of mangrove forest in closed and open canopy conditions, and non-forest land uses that replaced mangroves, such as aquaculture pond and non-aquaculture alike in the same coast.
2. Palawan has been identified as one with the highest mangrove deforestation rate from 1990 to 2010 (Long et al. 2013).
3. Accessibility, peacefulness, and orderly situation of the study area.

3.3 Field Sampling Design

Stratified random sampling was adopted in this study where land use (e.g. mangrove forest) was used as strata. In each strata, sites were selected through simple random sampling. The mangroves had three sites for closed canopy forest and three sites for open canopy forest. The non-forest replacement land uses had three sites for abandoned aquaculture ponds. Due to access restriction to other coconut plantations in the site and absence of other abandoned salt ponds and cleared mangrove in the area, only one site for each of these non-aquaculture land uses was measured.

In each site of mangrove forest, three transects were established, except for one thin (width: 20-25 m) open canopy mangrove forest where only two transects were established (Figure 3.5). Each transect was established near the sea margin

(seaward), middle/midstream and near the land/upstream (landward) to cover the natural tidal gradient in mangrove (cf. Kauffman & Donato 2012). In each mangrove transect, three circular plots, 7 m in radius, were established 50 m apart along a line parallel to the coast. For non-forest replacement land uses, only two transects were established at each site, but each transect also had the same three 7m-radius circular plots, spaced about 25 m apart. At each plot, all the measurements (e.g. tree diameter, soil depth) necessary to determine biomass C stock, soil C stock and soil GHG fluxes were undertaken. In each plot, geographic coordinates were recorded using a *Garmin* hand-held GPS receiver. In total, 90 plots were established, of which 51 plots were in mangrove forests, and 39 from non-forest land uses that replaced mangroves (i.e. 18 plots in abandoned aquaculture ponds, nine plots in abandoned salt pond, six plots in a coconut plantation and six plots in cleared mangrove area). The plot layout for biomass and soil C sampling was adopted from Kauffman and Donato (2012). The number of plots per transect was reduced to only three instead of six to sample more transects.

(a)

(b)

(c)

(d)

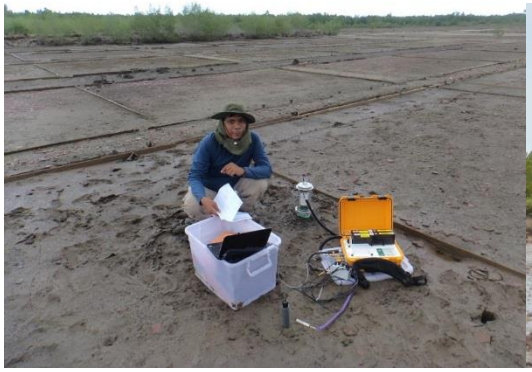

(e)

(f)

Figure 3.4 The mangrove forests and the non-forest land uses that replaced mangroves in the coast of southern Honda bay - a) closed canopy mangrove forest, b) fresh mangrove stump in open canopy mangrove forest, c) abandoned aquaculture pond, d) coconut plantation, (e) abandoned salt pond, and (f) cleared mangrove

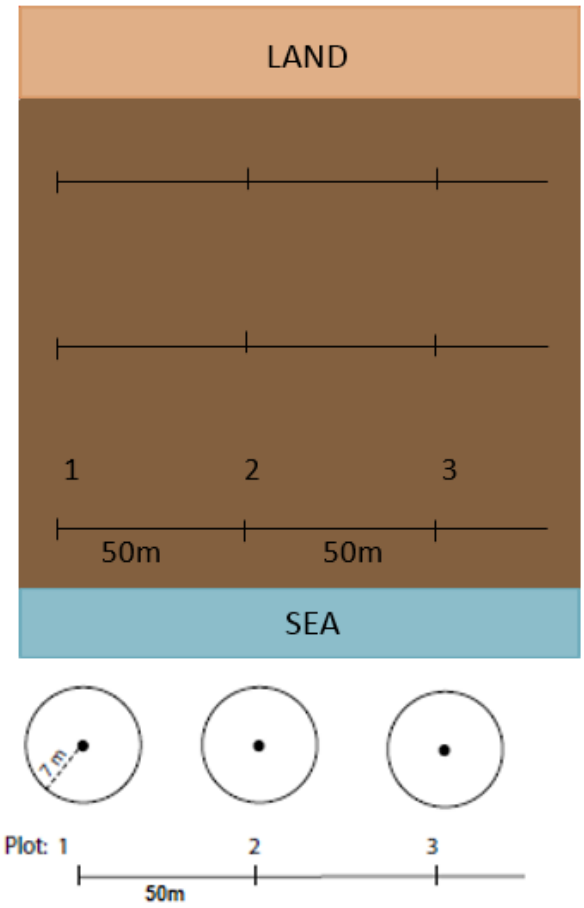

Figure 3.5 General field layout of sampling plots
Source: Kauffman and Donato (2012), modified

3.4 Data Capture and Acquisition

Figure 3.6 gives an overview of the study showing the data inputs, data analyses, and the outputs to achieve its four objectives. The details and methods of data capture and acquisition for each technical chapter are discussed in the succeeding sections of this Thesis. As data capture and acquisition are different for each technical chapter, only a general overview is provided in this section as summarised below in Figure 3.6 and Table 3.1. Briefly, GIS layers (e.g. land use, administrative boundary) were secured and used as the basis for field plot data collection for vegetation biomass, and soil C stock and soil GHG fluxes. The geographic coordinates of the plots were collected. The field data were supplemented by remotely sensed data such as those from the 30m- DEM from Shuttle Radar Topography Mission (SRTM) downloaded from EarthExplorer (USGS 2016), and

the new 10m- satellite Synthetic Aperture Radar (SAR) and multispectral data from the newly launched Sentinel satellite system downloaded from Sentinel Data Hub (ESA 2016). Ancillary measurements in each plot were also done to supplement the biomass, soil C and soil GHG flux data collected. These measurements include canopy variables (i.e. Leaf Area Index (LAI), Transmission Coefficient, Mean Leaf Angle); soil pore water pH, pore water salinity, soil redox potential, soil porewater temperature, and soil temperature.

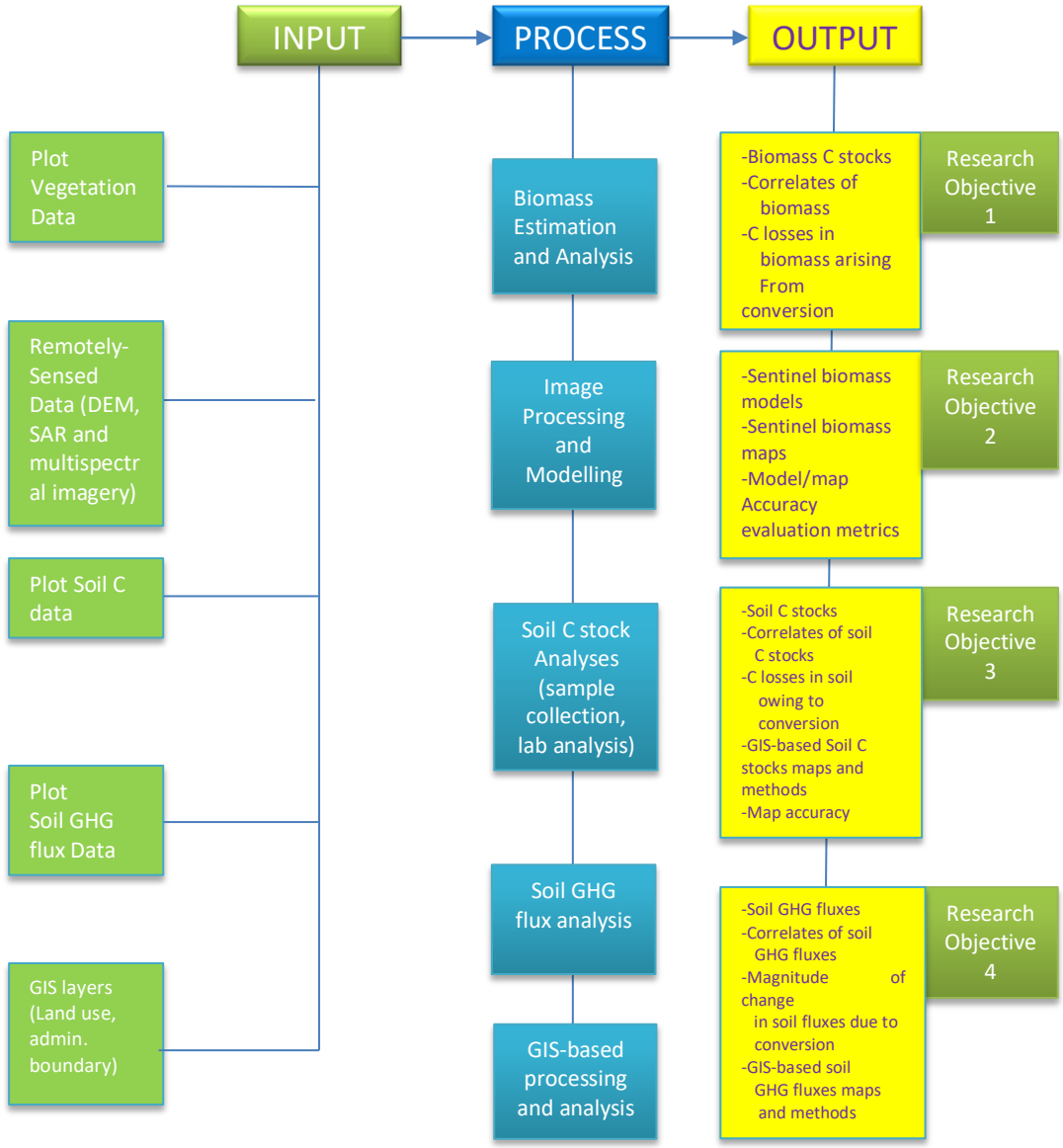

Figure 3.6 Input-Process-Output Model of the study

Table 3.2 Types of data collected for the study

Data type	Acquisition year/period
I. Field plot data	
A. Biomass stock	June - July 2015
Species of plant	
DBH, basal area, height	
Count of individuals, tree density	
Downed woody debris (DWD) diameter	
DWD wood density, count of DWD pieces	
B. Soil C stock	June - July 2015
Soil depth interval, total depth	
Bulk density, %C	
C. Soil GHG fluxes	July 2015
CO_2 flux	
CH_4 flux, N_2O flux	
D. Ancillary data	June - July 2015
Leaf Area Index, Transmission Coefficient	
Mean Leaf Angle, GPS coordinates	
Soil porewater pH, porewater salinity	
Soil temperature, porewater temperature	
II. Remotely sensed data	
A. Synthetic Aperture Radar (Sentinel-1)	
Image 1 (with VV, VH channels in 10 m resolution)	October 2015
Image 2 (with VV, VH channels in 10 m resolution)	December 2015
Image 3 (with VV, VH channels in 10 m resolution)	January 2016
B. Multispectral data (Sentinel-2)	
Bands 1 to 12 (VNIR (10m), Red Edge and SWIR (20 m)	April 2016
C. Digital Elevation Model (SRTM, ~30 m*)*	February 2000
III. GIS layers	
A. Digitised by author from Google Earth Pro	
Selected land cover of the study site	Feb., Mar., Apr. 2016
B. Acquired from other sources	
Administrative boundary, villages (PhilGIS)	No information
2010 Land cover map of Philippines (NAMRIA)	2010
IV. Other Data	
A. Population count; growth rate (PSO 2017)	2015; 2010
B. Climatic data (PAGASA 2016)	Last 30-year period
C. Length of coastline, width and length of mangrove forests (measured from Google Earth Pro image)	2015
D. History of the site, livelihood of people (pers. com)	June – July 2015
E. Biomass allometric models; wood density values	

3.5 Data Processing and Analysis

Figure 3.6 also presents the processing and analyses done to achieve the objectives of the study. The details of each data processing and analysis are discussed in detail in the method of the following technical chapters. As the technical chapters have different data processing and analysis, only an overview is presented in this section. Briefly, for Research Objective 1 (biomass C stock of mangrove and replacement land uses), published allometric equations were used to convert the individual tree diameter-at-breast-height and wood density into biomass per tree, which was then summed for all trees in the plot to come up with biomass per plot. The relationship of plot biomass with selected field measured canopy and site variables (termed here as *ancillary data*) were determined through correlation analysis. Potential C losses from biomass were determined using Stock Change Method. Statistical tests (e.g. correlation analysis, regression, analysis of variance) were done using the IBM SPSS Statistics software version 22.

For Research Objective 2 (Satellite remote sensing-based biomass mapping), new-generation satellite SAR and multispectral imagery data from Sentinel Satellite system were evaluated for their potential for predictive biomass retrieval and mapping in the mangrove area. Pre-processing of radar imagery (calibration, speckle reduction, terrain correction) and multispectral imagery (atmospheric correction, conversion from top-of-atmosphere reflectance to bottom-of-atmosphere reflectance) were done first. Vegetation indices (NDVI, IRECI, TNDVI, and NDI45)[1] and canopy biophysical variables (LAI, fCover, Leaf Chlorophyll, and fPAR)[1] were derived. These Sentinel image-derived vegetation variables plus the raw bands of SAR and multispectral imagery were used as biomass predictors and were regressed with the plot biomass data from Objective 1 to predict and map the biomass in the study area. The regression analysis was accomplished using the traditional linear regression and new machine learning algorithms. The accuracy of prediction was analysed using root mean square error (RMSE), and agreement (r) of predicted and observed values from leave-one-out cross-validation method. The pre-processing of SAR and multispectral imagery, and derivation of vegetation indices and biophysical variables were implemented in SNAP software version 4.0 (ESA 2016) while the

[1] These acronyms are defined in Acronyms and Chapter 5.

biomass modelling/regression analysis and model accuracy assessment were done in WEKA Machine Learning software version 3.8.0 (Hall et al. 2009). The predictive mapping and map accuracy assessment were done using the Spatial Analyst extension of ArcMap version 10.3.1.

For Research Objective 3 (Soil C stock and GIS-based mapping), the same plot for biomass was evaluated for its soil C stock. The collected soil samples were processed in the laboratory for bulk density and % C determination. Soil C stock per plot was determined as the product of soil bulk density (BD), %C and soil depth interval. The relationship of soil C stock with ancillary data was also determined using correlation analysis. C losses from soil were computed using the Stock Change Method of IPCC. A GIS-based geostatistical spatial interpolation technique was used to predict the soil C stock at non-sampled locations and map the soil C stock distribution at the study site. The accuracy of prediction was also analysed using root mean square error (RMSE), and agreement (*r*) of predicted and observed values from leave-one-out cross-validation method. Statistical tests (correlation, analysis of variance) were done using IBM SPSS Statistics version 22. The geostatistical spatial interpolation and accuracy assessment were done using Geostatistical Analyst extension of ArcMap version 10.3.1.

For Research Objective 4 (soil fluxes of the 3 GHGs and GIS-based mapping), soil fluxes of CO_2 were determined *in situ* while fluxes of CH_4 and N_2O were quantified in the Gas Chromatography laboratory. The fluxes of each GHG were brought to a common unit (CO_2 equivalent) using their Global Warming Potential and added to determine total emission. The relationship of each soil GHG flux with selected ancillary data was also determined using correlation analysis. Changes in soil GHG fluxes owing to conversion were determined from the difference of fluxes in mangrove and the replacement land uses. A GIS-based geostatistical spatial interpolation technique was used to predict the soil fluxes of the three GHGs at non-sampled locations and map the distribution of soil fluxes of the three GHGs in the study site. The accuracy of prediction was also analysed using the methods in Research Objectives 2 and 3. The Geostatistical Analyst extension of ArcMap version 10.3.1 was used for geostatistical spatial interpolation and accuracy assessment while IBM SPSS Statistics version 22 was used for statistical tests such as correlation analysis and analysis of variance.

3.6 Summary

This Chapter presents the overall approach and general methods used to achieve the four objectives of the study. As the detailed methods are discussed in the ensuing technical chapters, the methods used were given here briefly. In summary, the biomass C stock was determined by field plot sampling and using published allometric models, while C loss from biomass owing to land use conversion was determined using Stock Change Approach. The potential of new-generation SAR and multispectral imagery data from the newly launched Sentinel Satellite System for predictive biomass retrieval and mapping were determined by modelling using linear regression and machine learning algorithms, and GIS-based implementation. The soil C stock was determined by field plot sampling while C loss from soil from mangrove land use conversion was determined using Stock Change Approach. Predictive mapping of soil C stocks was done using GIS-based geostatistical modelling. Soil fluxes of CO_2, CH_4 and N_2O were determined by field plot sampling and laboratory analysis while changes in soil fluxes of these GHGs as a result of mangrove land use conversion were determined by bringing the three GHGs into a common unit using their Global Warming Potential. Predictive mapping of soil GHG fluxes was done by modelling using the GIS-based geostatistical technique.

The next chapter, Chapter 4, presents the first technical chapter of the thesis and discusses the field investigation on biomass C stock estimation in mangrove forest and non-forest land uses that replaced mangroves. It also includes the reports on the potential C losses from biomass owing to land use conversion in mangrove.

Chapter 4

BIOMASS AND CARBON STOCKS IN MANGROVE FORESTS AND LAND USES THAT REPLACED MANGROVES

4.1 Introduction

Chapter 2 highlighted the knowledge gap in our understanding of the biomass and carbon (C) storage in mangrove, in both closed canopy and open canopy forests, and in the non-forest land uses that replaced mangroves. The gap in the relationship of biomass with the canopy biophysical variables such as Leaf Area Index was also emphasised. These information offer critical bases for various applications such as biomass mapping, estimation of productivity, and estimation of C losses in biomass owing to mangrove conversion and forest degradation, among many others. In this Chapter, the aboveground biomass (AGB), belowground biomass (BGB), downed woody debris biomass (DWB) of secondary mangroves and the land uses that replaced them (aquaculture pond, coconut plantation, salt pond and cleared mangrove) were investigated. This Chapter has the following objectives: 1) to quantify the biomass and carbon stocks from AGB, BGB, DWB of mangrove forests and the non-forest land uses that replaced mangroves, and 2) to determine the relationship of biomass stock with canopy biophysical variables.

This Chapter is organised into five sections. The Background section presents and discusses the information on previous works undertaken about the topic and the knowledge gaps on biomass C accounting. These knowledge gaps were used as basis to form the objectives of the Chapter. Then the Chapter proceeds with the Methods section wherein the approaches and methodologies are discussed to achieve the objectives. The Results as well as the Discussion sections follow. The Chapter ends with the Conclusion highlighting the new knowledge and insights generated from this biomass study.

The novel outputs of the study presented in this Chapter include the following: a) all the biomass components (aboveground, belowground and downed woody debris) of mangroves and non-forest mangrove replacement land uses (aquaculture and non-aquaculture alike) were analysed which have been partially considered in the past studies; b) canopy variables in mangroves and their relationship with biomass were characterised; and c) potential C losses from biomass owing to mangrove conversion and mangrove forest degradation were estimated. This Chapter also reports the downed woody debris biomass of mangrove forests in the Philippines for the first time.

4.2 The need for biomass study in mangrove and replacement land uses

Mangrove forest is a valuable coastal resource in the tropics. It provides various products which include timber and other construction materials, fuelwood, fishery products and ecosystem services such as storm protection, sediment regulation, and habitat for coastal and marine biodiversity (Alongi 2014). It is increasingly recognised as among the most C dense tropical forests, storing three to five times higher than terrestrial forests (Donato et al. 2011). However, despite its importance, there has been a massive reduction in the global mangrove area in the past owing to conversion to other land uses (FAO 2007; Spalding et al. 2010; Giri et al. 2011). Overexploitation and conversion of mangroves to aquaculture, agriculture, urban, tourism and industrial uses are considered to be among the drivers of mangrove loss especially in Southeast Asia (Richards & Friess 2016). In the Philippines, for instance, mangrove vegetation have been cleared and reduced by half (51.8 %) in just over 92 years, from around 450,000 hectares in 1918 (Brown & Fischer 1920) to only 240,824 ha in 2010 (Long et al. 2013). It is essential, therefore, to monitor the mangroves and quantify its attributes such as its role in the global C cycling, biodiversity conservation, and as a potential source of renewable biomass energy.

Biomass in the form of AGB, BGB and DWB are significant carbon pools in an ecosystem (Kauffman & Donato 2012; Howard et al. 2014). It has been recently

reported in the global 2015 Forest Resource Assessment that forest biomass and C stock densities were highest in tropical sub-regions of South America (122.4 Mg C ha^{-1}) as well as in Western and Central Africa (120.6 Mg C ha^{-1}) while the dead wood C density was highest (12.1 Mg C ha^{-1}) in North America (Köhl et al. 2015). In mangrove forest, previous studies had quantified the biomass and C stock densities in undisturbed (Donato et al. 2011; Kauffman et al. 2011; Murdiyarso et al. 2015), and managed (Adame et al. 2013; Thompson et al. 2014; Tue et al. 2014; Adame et al. 2015; Vien et al. 2016) mangrove forest stands.

However, the values of biomass and C stock densities have not been fully quantified in the secondary mangrove forests especially in data-poor developing countries in the tropics where this mangrove type is common due to various disturbances (Fortes 2004). Also, very few have dealt on quantifying mangrove C stocks side by side with those of non-forest land uses that replaced mangroves on the same site. Available studies so far are limited to mangrove and abandoned aquaculture pond (Kauffman et al. 2013; Bhomia et al. 2016; Duncan et al. 2016) or mangrove and pasture (Kauffman et al. 2016), and did not include other land uses that replaced mangroves such as coconut palm plantation, cleared mangrove and abandoned salt pond.

Furthermore, existing mangrove biomass C stocks studies mostly deal with biomass and C stock quantification and their relationships with site factors such as salinity, distance to shore, elevation and porewater pH, among others (Donato et al. 2011; Adame et al. 2013; Wang et al. 2014). However, the relationship of mangrove biomass C stock with canopy variables (e.g. leaf area index, canopy gap fraction) has not been fully studied. Knowing the relationship between biomass and canopy variables such as LAI might assist in biomass mapping in mangrove areas since LAI, for instance, can be generated from satellite imagery.

Quantification of biomass from these land uses in the plot-scale is an important input for the evaluation of productivity, C sequestration and storage, estimation of associated C losses from conversion, and coastal biodiversity (Alongi 2014). It is also necessary for the estimation of available fuelwood from downed woody debris, as support to planning for renewable energy generation (Kumar et al.

2012) and to support large-scale biomass monitoring assessment using remote sensing techniques (Aslan et al. 2016).

4.3 Methods

4.3.1 Study Site

The study site is a coastal area located in the southern coast of Honda Bay on the eastern coast of Puerto Princesa City in the island-province of Palawan (between latitude 9.8028^0 to 9.9612^0N and longitude 118.725^0 to 118.805^0E). The city is located in the central part of Palawan province, approximately 567 km south-west of Manila, the Philippines' capital and located in the central part of Palawan province. The climate is tropical, with two seasons (dry and wet) and under Type 3 based on Modified Corona's Climate Classification (i.e. no very pronounced maximum rain period, with one to three months only of the dry season). Palawan has minimal rain (24-54 mm per month) from January to April and relatively wet (>115 mm per month) during the rest of the year (PAGASA 2016). The mean annual rainfall is 1,527.3 mm which is highest during October (216.1 mm) and lowest in February (23.7 mm) (PAGASA 2016).

The coast of southern Honda Bay is a mosaic of a long band of mangrove forests interrupted by non-forest land uses such as agriculture, aquaculture, and built-up areas/settlements. The Bay is drained by several rivers and creeks where mangroves thrive. Rivers in varying length dissect the mangrove forests, both estuarine and fringing types. Mangroves, especially in the northern part of the study site, are extensive. A detailed description including maps of study site is given in Chapter 3.

4.3.2 Field sampling design and biomass C accounting process

Mangrove forests (represented by closed canopy mangroves and open canopy mangroves) along with non-forest land uses that replaced mangroves in Honda Bay such as abandoned aquaculture pond, coconut plantation, abandoned salt pond and cleared mangrove were assessed for their AGB, BGB, DWB and total biomass, and

C stocks. The non-forest land uses were previously occupied by mangroves. The study site was stratified based on land use. In each land use, sites were selected through simple random sampling. The mangrove forests had three sites for closed canopy stand and another three sites for open canopy mangroves. The land uses that replaced mangroves also had three sites for abandoned aquaculture ponds. However, the non-aquaculture land uses had only one site each due to access restriction to other coconut plantations and absence of other sites for abandoned salt pond and cleared mangrove. For mangrove forest, three transects were established at each site (except for one open canopy mangrove which had only two transects due to thin cover): near the sea (seaward), middle/midstream and near the land/upstream (landward) to cover the natural tidal gradient in a mangrove ecosystem (*cf.* Kauffman and Donato 2012). The seaward transects were about 15m-20 m from the mangrove-sea interface. Each transect has three circular plots, 7 m in radius, spaced 50 m apart (Figure 4.1). For non-forest land uses, two transects were established at each site except for salt pond which had three. Each transect also had three circular plots, 7 m in radius, established about 25m apart.

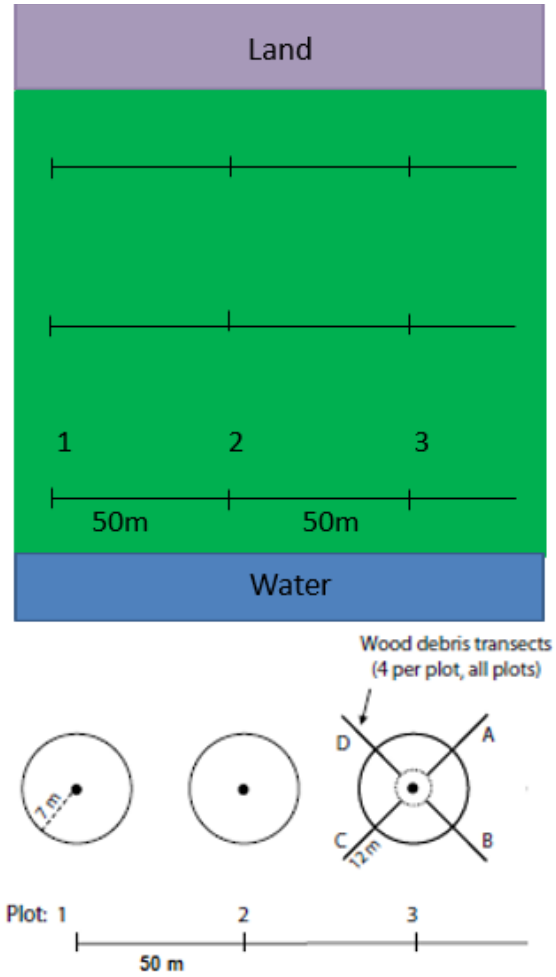

Figure 4.1 Plot layout for biomass sampling
Source: Kauffman and Donato (2012), modified

Following the method of Kauffman & Donato (2012) for biomass C accounting, all the measurements (e.g. tree diameter) necessary to determine the biomass were undertaken for each plot. In total, 90 plots were established, of which 51 plots were located in mangrove forests. The whole process of biomass C accounting implemented in this study is summarised in Figure 4.2.

With geographic coordinates recorded in each plot using a *Garmin* hand-held GPS receiver, canopy variables such as Leaf Area Index (LAI), and gap fraction/Transmission Coefficient were measured using the *CI-110 Plant Canopy Imager (CID Bio-Science, Washington, USA*) (see Figure 4.3). LAI is the one-sided leaf area per unit ground area and is a measure of photosynthetic area (Salmo et al. 2013). Canopy gap fraction is the amount of the sky visible from beneath the canopy

and indicates fraction of canopy foliage cover (CID Bioscience 2016). As well as LAI, a proxy for Canopy gap fraction called fraction of vegetation cover (fCover), could also be generated and mapped using satellite imagery.

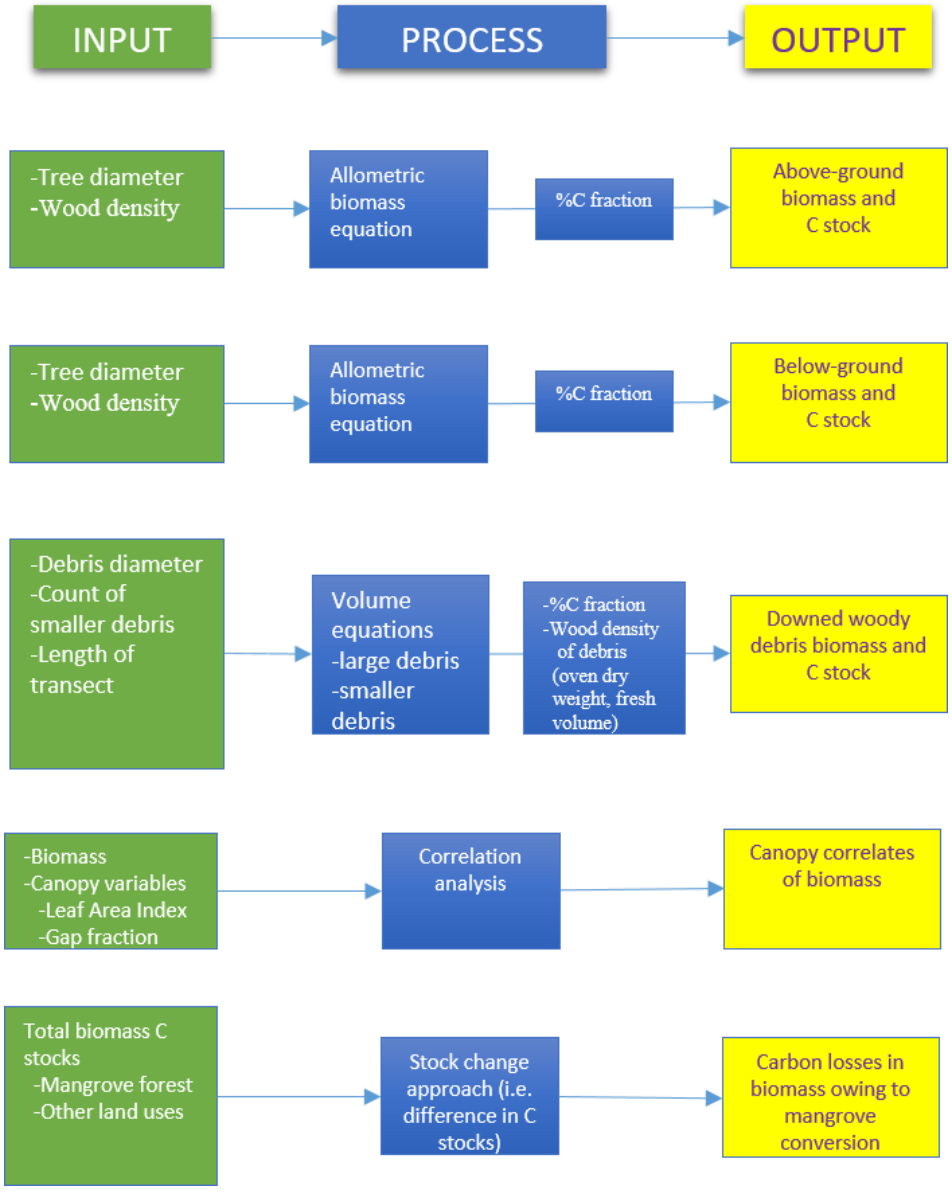

Figure 4.2 Input-Process-Output model for biomass C accounting component (Chapter 4) of the Thesis

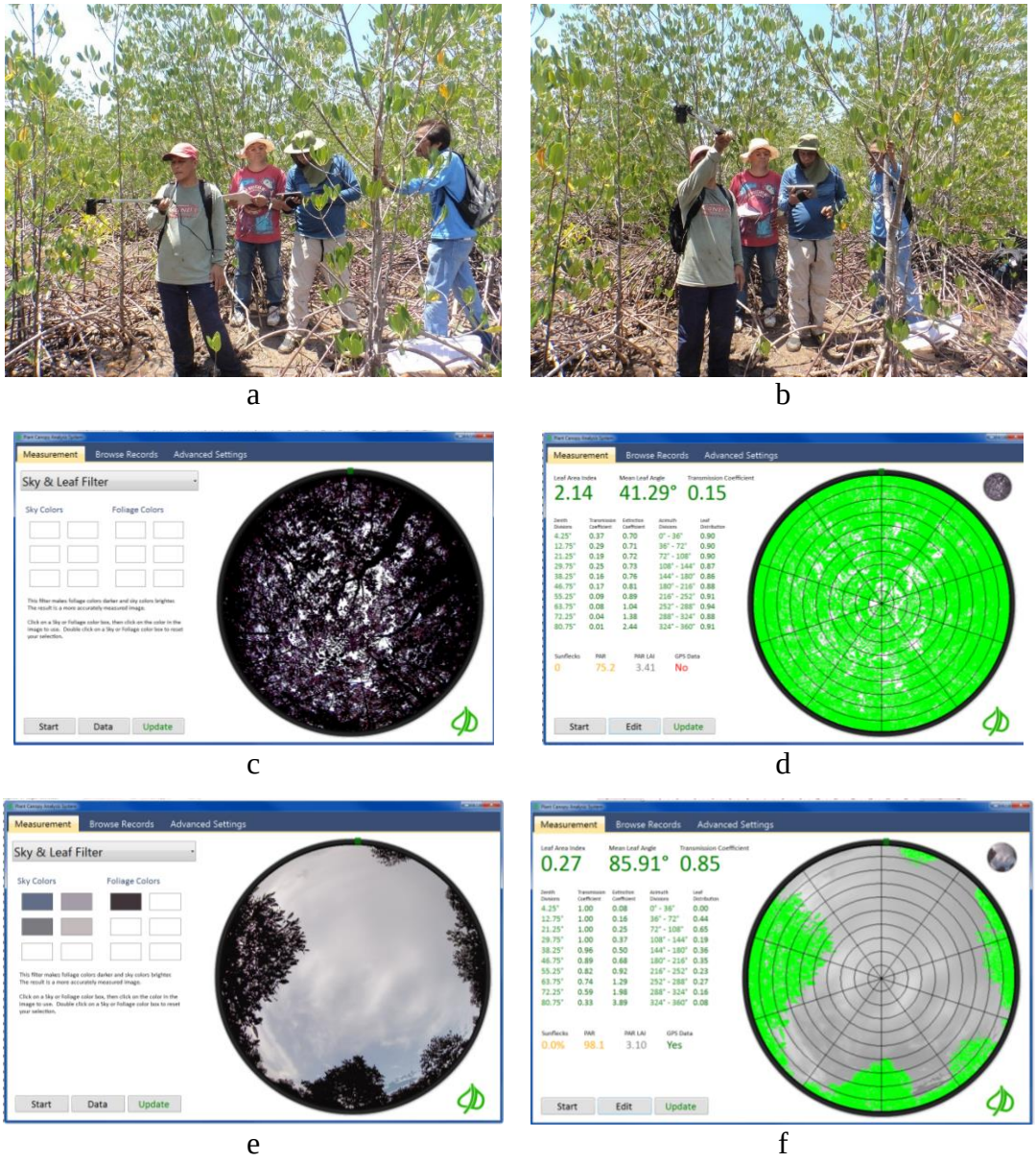

Figure 4.3 Canopy image and calculated canopy metrics, respectively, of closed canopy mangrove (c, d), and open canopy mangrove (e, f) taken from Plant Canopy Imager CI-110 instrument (CID Bioscience, USA)

4.3.3 Estimation of biomass

In each plot, the species of each tree was recorded and measured of its diameter at breast height (1.3 m from the ground) or 30 cm above the highest prop root for stilt-rooted species like *Rhizophora* spp (Figure 4.4). As there were no specific allometric equations published for the study site and for the Philippine mangroves, published allometric equations were used to compute for the aboveground and belowground biomasses of each tree (Komiyama et al. 2005; Kauffman & Donato 2012; Adame et al. 2013; Tue et al. 2014). For AGB of mangroves, equations specific for the species/genus were used; otherwise, the common allometric equation of Komiyama et al. (2005) for other species was utilised (Table 4.1). Mangrove BGB was estimated using the common allometric equation of Komiyama et al. (2005). Species-specific wood density values in the Philippines for some mangrove species and genus as reported in Brown and Fischer (1920) were used. For others with no available data on wood density, data from published literature were used such as those compiled by Howard et al. (2014). For coconut biomass, the allometric model given in Brown (1997) as used by Zamora (1999) for coconut plantation in Mt Makiling, Philippines was adopted. The result of Zamora (1999) of ~4% belowground - aboveground biomass ratio to compute for the belowground biomass of each coconut individual was also used.

Also, the mass of DWB at all sites in each land use was measured in each of the biomass plot using planar intercept technique as described in Kauffman and Donato (2012) and in Howard et al. (2014), and as used by Kauffman et al. (2013) and Kauffman et al. (2016). The DWB material consisting of fallen twigs, branches, and stems were classified by diameter as fine (<0.6 cm), small (0.6-2.5 cm), medium (2.6-7.6 cm) and large (>7.6 cm). In the centre of each 7m-radius plot, four 12-m sub-transect lines were laid down, the first being 45^0 off the direction of the main transect line and the remaining three established clockwise, 90^0 off from the previous sub-transects. In each sub-transect, the large woody debris was recorded at the entire length of the sub-transect (i.e. 0-12 m) while fine, small and medium debris were sampled at 10 m-12 m, 7 m-10 m, 2 m-7 m marks of the sub-transect line, respectively (Figure 4.5). For each large debris, the diameter was measured while for

the rest of the debris classes, the number of pieces was classified by diameter class using a metal fuel gauge and was tallied.

a

b

c

d

Figure 4.4 Data collection for biomass estimation. a) measuring the tree diameter, b) classifying the diameter of downed woody debris (DWD) using a fuel gauge, c) laboratory works for DWD samples to estimate the volume using water displacement method, and d) ovendrying the DWD samples

Table 4.1. Biomass allometric equations and wood density values used in the study

Species	Aboveground	Belowground[+]	References for aboveground biomass equations	Wood Density (g cm^{-3})
Aegiceras floridum	Biomass (kg) = $0.251*\rho*D^{2.46}$	Biomass (kg) = $0.199*\rho^{0.899}D^{2.22}$	Komiyama *et al.* (2005)	0.71[a]
Bruguiera gymnorrhiza	Biomass (kg) = $0.186 D^{2.31}$	Biomass (kg) = $0.199*\rho^{0.899}D^{2.22}$	Clough and Scott (1989)	0.85[b]
B. parviflora	Biomass (kg) = $0.168D^{2.42}$	Biomass (kg) = $0.199*\rho^{0.899}D^{2.22}$	Clough and Scott (1989)	0.89[b]
B. sexangula	Biomass (kg) = $0.168D^{2.42}$	Biomass (kg) = $0.199*\rho^{0.899}D^{2.22}$	Clough and Scott (1989)	0.87[b]
Camptostemon philippinense	Biomass (kg) = $0.251*\rho*D^{2.46}$	Biomass (kg) = $0.199*\rho^{0.899}D^{2.22}$	Komiyama *et al.* (2005)	0.71[a]
Ceriops tagal	Biomass (kg) = $0.251*\rho*D^{2.46}$	Biomass (kg) = $0.199*\rho^{0.899}D^{2.22}$	Komiyama *et al.* (2005)	0.89[b]
Cocos nucifera	Biomass (kg) = $0.7854*D^2*H*\rho*1.6$	Biomass (kg) $=0.7845*D^2*H*\rho*1.6$ *0.04 (Zamora 1999)	Brown (1997); Zamora (1999)	0.25[c]
Heritiera littoralis	Biomass (kg) = $0.251*\rho*D^{2.46}$	Biomass (kg) = $0.199*\rho^{0.899}D^{2.22}$	Komiyama *et al.* (2005)	0..84[a]
Lumnitzera racemosa	Biomass (kg) = $0.251*\rho*D^{2.46}$	Biomass (kg) = $0.199*\rho^{0.899}D^{2.22}$	Komiyama *et al.* (2005)	0.71[a]
Rhizophora apiculata	Biomass (kg) = $0.235D^{2.42}$ + $Biomass_{stilt}$ (kg) = $0.0209D^{2.55}$	Biomass (kg) = $0.199*\rho^{0.899}D^{2.22}$	Ong et al. (2004)	1.04[b]
R. mucronata	Biomass (kg) = $0.235D^{2.42}$ + $Biomass_{stilt}$ (kg) = $0.0209D^{2.55}$	Biomass (kg) = $0.199*\rho^{0.899}D^{2.22}$	Ong et al. (2004)	0.98[b]
R. stylosa	Biomass (kg) = $0.235D^{2.42}$ + $Biomass_{stilt}$ (kg) = $0.0209D^{2.55}$	Biomass (kg) = $0.199*\rho^{0.899}D^{2.22}$	Ong et al. (2004)	0.98[b]
Sonneratia alba	Biomass (kg) = $0.251*\rho*D^{2.46}$	Biomass (kg) = $0.199*\rho^{0.899}D^{2.22}$	Komiyama *et al.* (2005)	0.83[b]
Xylocarpus moluccensis	Biomass (kg) = $0.251*\rho*D^{2.46}$	Biomass (kg) = $0.199*\rho^{0.899}D^{2.22}$	Komiyama *et al.* (2005)	0.66[b]
X. granatum	Biomass (kg) = $0.251*\rho*D^{2.46}$	Biomass (kg) = $0.199*\rho^{0.899}D^{2.22}$	Komiyama *et al.* (2005)	0.66[b]

[a]Howard *et al.*, 2014 [b]Brown and Fisher, 1920 [c]Brown 1997; Zamora, 1999 [+]Equations from Komiyama et al. (2005) unless stated otherwise

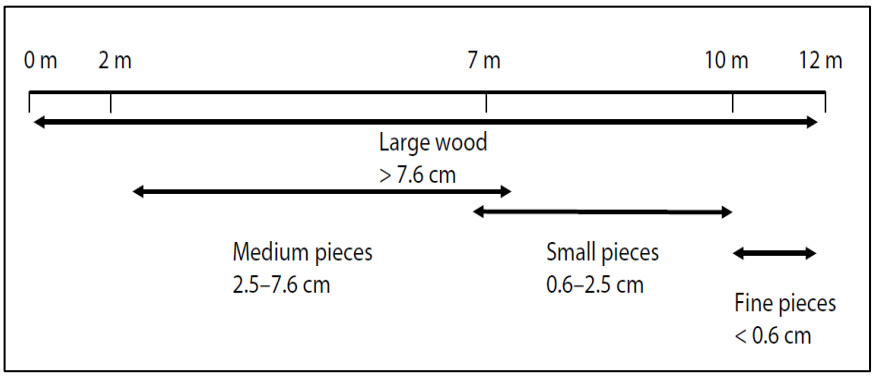

Figure 4.5 Guide to sampling the downed woody debris biomass
Source: Kauffman and Donato (2012)

Samples of debris in each class were collected for calculations of site-specific mean diameter, quadratic mean diameter and wood specific density of each debris class. Prior to oven-drying, the volume of each wood debris sample was determined using the water displacement method as suggested by Kauffman and Donato (2012) and Howard et al. (2014). The same samples were then oven-dried until constant weight at 100 ^{0}C. The specific gravity of each woody debris sampled in each class was then determined by dividing the oven-dry weight of each sample with its fresh volume.

The volume per hectare for each debris class was computed using scaling equations discussed in Kauffman and Donato (2012) and Howard et al. (2014), and given as:

a. large DWD class: $v = \pi^2 (\Sigma d^2/8L)$ (Equation 1)

b. other DWD classes: $v = \pi^2 (N_i\ QMD_i^2/8L)$ (Equation 2)

where: v = volume ($m^3\ ha^{-1}$)

d = diameter of piece (cm)

L = length of sampling line (m)

N_i = count of intersecting woody debris in debris size class i

QMD = quadratic mean diameter of debris size class i (cm)

The volume of each woody debris class was multiplied by its wood density value to obtain DWB.

4.3.4 Biomass C stock calculation

The AGB and BGB data were converted to their C stock equivalent using C fraction of 48 % and 39 %, respectively as suggested by Kauffman and Donato (2012) and adapted by Adame et al. (2013), Kauffman et al. (2013) and Kauffman et al. (2016) for mangroves. Also, the DWB was multiplied by C fraction of 50 % to determine DWB C stock as suggested by Kauffman and Donato (2012) and applied

in a number of published mangrove biomass studies (e.g. Adame et al. 2013; Kauffman et al. 2013; Kauffman et al. 2016). In addition, for coconuts, the 48 % C fraction to convert the ABG to its carbon stock equivalent was also used while for its BGB, the 39 % C fraction based on the result of Zamora (1999) for coconut plantation biomass study in Philippines was adopted. Jaramillo et al. (2003) also found that the C content of roots in tropical forests and pastures of Mexico to be between 35.9% - 41.6%, which give a median of about 39%.

The sum of C stocks of AGB, BGB and DWB was calculated to determine the biomass C stock per plot and averaged per site and per land use to get the mean biomass C stock per land use. The value was converted to its CO_2-equivalent (CO_2e) based on the protocol of IPCC to monitor the changes in C stocks (Pendleton et al. 2012).

4.3.5 Statistical analysis

Non-parametric Kruskal-Wallis H Test was used to compare the biomass carbon stocks among land uses. If the differences are significant, a pairwise comparison was employed using Mann-Whitney U Test. These tests are used in place of the parametric one-way Analysis of Variance and its post-hoc tests when the number of observations in the groups are unequal, and the assumptions of data normality and homoscedasticity are sufficiently violated (Zaiontz 2015; McDonald 2016). These non-parametric tests have also been used by Murdiyarso et al. (2015) and Phang et al. (2015) for their mangrove carbon stock studies. Correlation analysis was used to determine the relationships between AGB and DWB and as well as the relationships between biomass C stock and canopy biophysical variables. All tests were conducted at 5 % significance level.

4.4 Results

The mangrove forests were dominated by *Rhizophora apiculata* and *R. mucronata*. A total of 14 mangrove species were recorded, eight species in closed mangrove forests and 13 in open canopy mangroves (Table 4.1). In abandoned aquaculture ponds, individuals of *R. apiculata* and *Ceriops tagal* were also

encountered, but only one site (site 3) had vegetation albeit very few. The tree density in mangrove forests was between 865 ± 55 trees ha^{-1} (open canopy forest) and 1,621 ± 139 trees ha^{-1} (closed canopy forest). In the coconut plantation, the tree density was 195 ± 24 trees ha^{-1} while it was only 40 ± 28 trees ha^{-1} in aquaculture ponds. Trees were absent in both the abandoned salt pond and the cleared mangrove. The basal area in closed mangrove forests was 11.4 ± 1.1 m^2 ha^{-1} and ranged from 9.9 to 13 m^2 ha^{-1} across sites while the open canopy mangroves had 5.25 ± 2.2 m^2 ha^{-1} and ranged from 1.6 to 11.9 m^2 ha^{-1} from one site to another. The coconut plantation's basal area was 3.23 ± 0.8 m^2 ha^{-1} while it was only 0.01 ± 0.01 m^2 ha^{-1} in the abandoned aquaculture site (Table 4.2). Furthermore, the wood density values of DWD were almost similar in fine, small and medium size classes and was highest in large woody debris class (0.63 ± 0.03 g cm^{-3}; Table 4.3). The quadratic mean diameter values for fine, small and medium woody debris were computed as 0.45 cm, 1.37 cm and 4.61 cm, respectively.

Table 4.2. Dominant species and structural diversity in mangrove forest and replacement land uses of mangroves in Honda Bay, Palawan, Philippines

Land use/site	Tree density (Individuals $ha^{-1*)}$	Basal Area* (m^2 ha^{-1})	Dominant Species
Closed canopy mangrove			
Bacungan	1,890 ±312	9.9 ±1.1	*Rhizophora apiculata*
Santa Cruz	1,429 ±104	11.5 ±0.7	*R. mucronata*
Salvacion	1,544 ±200	13 ± 3	*R. apiculata*
Open canopy mangrove			
Tagburos 1	772 ±136	1.6 ±0.7	*R. apiculata*
Santa Lourdes	963 ±171	11.9 ±8.5	*R. apiculata*
San Jose 1	859 ±210	4.4 ±1.1	*Ceriops tagal*
Abandoned aquaculture pond			
San Jose 2	0 ±0.0	0.0 ±0.0	None
Tagburos 2	0 ±0.0	0.0 ±0.0	None
Tagburos 3	119 ±76	0.03 ±0.02	*R. apiculata*
Coconut plantation			
Tagburos 4	346 ±32	3.2 ±0.8	*Cocos nucifera*
Abandoned Salt pond			
Tagburos 5	0 ± 0.0	0.0 ±0.0	none
Cleared mangrove			
San Jose 3	0 ±0.0	0.0 ±0.0	none

*data are mean ± standard error

Table 4.3. Mean diameter and wood density of DWD of mangroves in Honda Bay, Palawan, Philippines

Size class diameter (cm)	Mean diameter (cm)*	Quadratic mean diameter (cm)	No. of pieces measured	Wood density (g/cc)*	No. of pieces measured
Fine (≤0.6)	0.44 ±0.02	0.45	62	0.46 ±0.01	93
Small (0.6-2.5)	1.29 ±0.06	1.37	64	0.47 ±0.01	81
Medium (2.5-7.6)	4.33 ± 0.45	4.61	13	0.46 ±0.05	17
Large (≥7.6)				0.63 ±0.03	38

*data are mean ±standard error

4.4.1 Biomass

Among mangrove sites, AGB and BGB of closed canopy mangroves were 99.7 ± 5.1 Mg ha-^{1} and 50.1 ± 4.5 Mg ha^{-1}, respectively and were significantly higher than open canopy mangroves that had only 27.4 ± 7.3 Mg ha^{-1} and 15.1±4.5 Mg ha^{-1}, in that order ($p < 0.001$). However, their downed woody debris biomass (DWB) were not significantly different ($p > 0.05$), with 8.5 ± 2.3 Mg ha^{-1} in closed mangrove forests and 6.9 ± 3.2 Mg ha^{-1} in open canopy mangroves (Table 4.4). In sum, the total biomass (AGB + BGB + DWB) stock of closed canopy mangrove was 158.4 ± 13.3 Mg ha^{-1} and was significantly higher than open canopy mangrove (68.8 Mg ha^{-1} ± 8.9; $p < 0.05$). Among the three closed canopy mangroves, there were no significant differences in the biomass stocks, be it within the AGB ($p > 0.7$), BGB ($p > 0.4$), DWB ($p > 0.07$) and total biomass ($p > 0.5$). Similarly, there were no significant differences among open canopy sites, except for the DWB where site 2 was significantly higher than the site 1 and site 3 ($p < 0.05$).

Table 4.4. Biomass stock density (Mg ha^{-1} ± standard error) of mangroves and their non-forest competing land uses in Honda Bay, Palawan, Philippines

Land use/site	AGB	BGB	DWB
Closed canopy mangrove			
Bacungan	89.66±15	43.25±6	6.44 ± 1
Santa Cruz	103.29±8	48.42±3	6.03 ±1
` Salvacion	106.20± 20	58.67±14	13.26 ±3
mean	**99.72±5**	**50.11±4**	**8.58 ±2**
Open canopy mangrove			
Tagburos 1	13.20±6	6.72±3	2.45 ±1
Santa Lourdes	37.49±14	22.01±10	13.13 ±2
San Jose 1	31.65±8	16.68±5	5.22 ±2
mean	**27.44±7**	**15.13±5**	**6.93 ±3**
Abandoned aquaculture pond			
San Jose 2	0	0	0
Tagburos 2	0	0	0
Tagburos 3	0.11±0	0.08 ±0	0.07 ±0
mean	**0.04 ±0**	**0.03 ±0**	**0.02 ±0**
Coconut plantation			
Tagburos 4/**mean**	**11.36±3**	**0.60±0**	**0**

AGB = aboveground biomass BGB = belowground biomass DWB = downed woody debris biomass
biomass of Abandoned salt pond and Cleared mangrove are zero and not included in the table.

In closed canopy mangroves, the biomass generally increases from seaward to landward where fringe/seaward transects were lower than the interior ones in all of AGB, BGB, DWB and total biomass (Figure 4.6). For example, the AGB in seaward transect was lower (79.6 Mg ha^{-1}) as compared to 102.2 Mg ha^{-1} and 117.3 Mg ha^{-1} in the interior and landward transects. However, the difference was not significant for all the biomass components ($p > 0.2$). This trend was less clear in open canopy mangrove where the seaward transects were generally higher than the landward transect. However, the difference between the biomass in seaward transects and the interior ones were also not significant ($p > 0.08$). Also, about 78 % of DWB in closed canopy mangroves were from large and medium size classes. The same was true for open canopy mangrove where the mass of fine class debris was only 2 % of the total while the large and medium debris contributed 80 % to the biomass (Table 4.3). Non-significant relationships were also found between DWB and AGB in both closed canopy mangrove forest ($r = -0.21$, $p = 0.30$) and open canopy forest ($r = 0.32$, $p = 0.13$), and even from the pooled data ($r = 0.23$, $p = 0.10$).

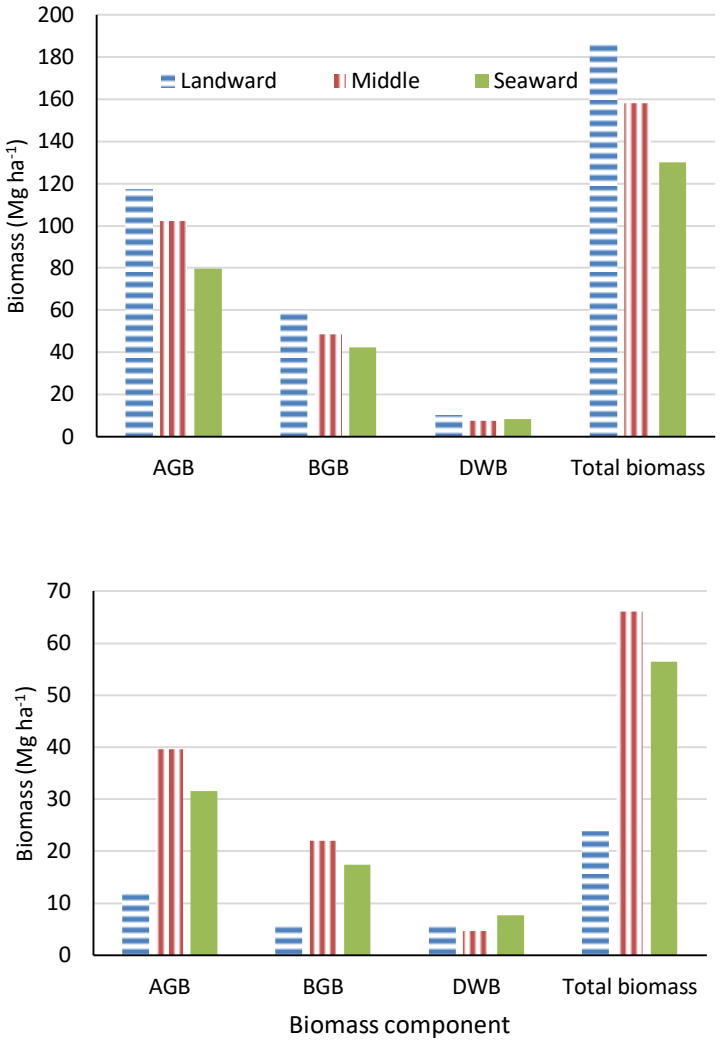

Figure 4.6 Variation in biomass stock along geomorphic/tidal position: Closed canopy mangrove (above) and Open canopy mangrove (below)

In contrast, the total biomass of non-forest competing land uses of mangroves was negligible to low and ranged from zero to 0.26 Mg ha^{-1} in abandoned aquaculture pond and 11.9 to 12 Mg ha^{-1} in coconut plantation (Table 4.4). There were no DWB sampled in the coconut plantation, the abandoned salt pond and the cleared mangrove site while the abandoned aquaculture ponds had only 0.02 Mg ha^{-1}.

4.4.2 Biomass carbon stock

The total biomass C stock of closed mangrove forest was 71.7 ± 5.9 MgC ha^{-1} (range: 63.12 to 80.48 MgC ha^{-1}) and was higher than the open canopy mangrove forest (mean: 21.2±3.9 MgC ha^{-1}; range: 10.18 to 33.14 MgC ha^{-1}; $p < 0.05$; Figure 4.7). In mangrove forests, the contribution of AGB, BGB and DWB to the total biomass C stock (47.94±5.1 MgC ha^{-1}) was 63%, 27% and 10%, respectively. Also, biomass C stock in mangrove forests generally increased from seaward to landward. In contrast, the total biomass C stock in the coconut plantation was only 5.7±1.5 MgC ha^{-1} while the abandoned aquaculture pond had only 0.12±0.1 MgC ha^{-1}. C losses in biomass (difference in biomass C stocks of mangrove forests and replacement land uses) were 46.5 Mg C ha^{-1}, on average or about 97% decline in biomass C stock arising from mangrove conversion.

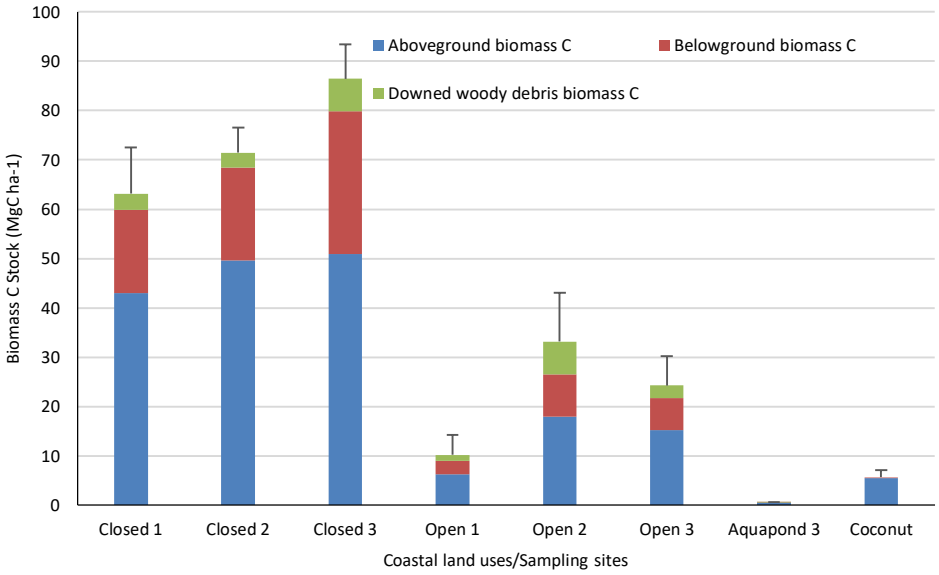

Figure 4.7 Total biomass C stock of mangroves (± standard error) and their competing land uses in Honda Bay, Palawan, Philippines. Biomass in Abandoned aquaculture pond sites 1 and 2, Abandoned salt pond and cleared mangroves are zero and not included in the graph.

4.4.3 Canopy biophysical variables

The Leaf Area Index (LAI) across all mangrove sites was 1.48±0.13. The LAI of closed canopy mangroves (mean: 2.24 ± 0.1; range: 1.53 to 2.71) was higher than the open canopy mangroves (mean: 0.62 ± 0.1; range: 0.05 to 1.79). The

coconut plantation's LAI was only 0.26 ±0.1. Furthermore, the canopy gap fraction of closed mangrove forests was only 0.14 ± 0.01 (range: 0.09 to 0.26) while the open canopy mangroves had 0.64 ± 0.1 or 0.38 ± 0.04 for the whole mangroves. The coconut plantation's canopy gap fraction was 0.79 ± 0.0.04 (range: 0.09 to 0.97).

4.4.4 Relationship of total biomass carbon stock with canopy variables

Leaf Area Index was significantly correlated with biomass C stock (r = 0.67). The correlation of canopy gap fraction with mangrove biomass C stock was also significant (r = -0.65, Figure 4.8).

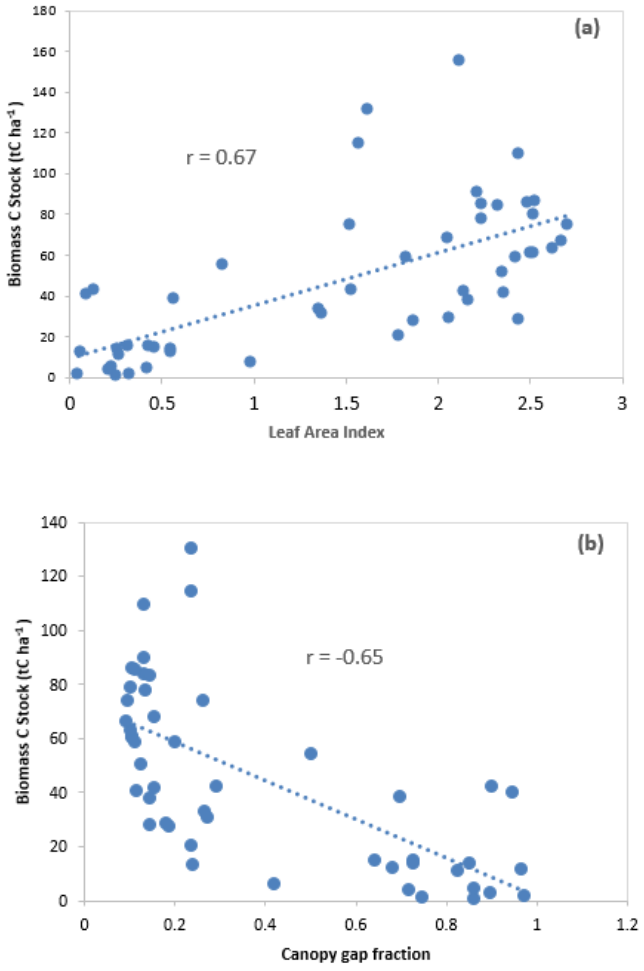

Figure 4.8 Scatter plot of canopy biophysical variables in relation to mangrove (pooled) biomass C stocks

4.5 Discussion

The study demonstrated the available biomass and C stocks in mangroves as compared to the land uses that replaced them in the coast of Honda Bay. The results also indicate the significant difference of these attributes between mangroves and the land uses that replaced them.

4.5.1 Biomass and C stocks of mangroves and land uses that replaced them

The biomass C stocks of land uses that replaced mangroves were 97%, on average, less than that of mangrove forests. The mean C stock of mangroves in this study was 71.7 Mg C ha^{-1} for closed canopy mangroves and 22.5 Mg C ha^{-1} for open canopy mangroves as compared to only 5.7 Mg C ha^{-1} for coconut plantation and zero to 0.04 Mg C ha^{-1} for abandoned aquaculture ponds, salt ponds and cleared mangrove site. The loss in mangrove biomass (along with the stored C) due to conversion is a significant amount considering the role of mangroves in global C cycling, maintaining C balance, nutrient cycling, aesthetic and recreation, as habitat for plants and animals, maintenance of biodiversity, storm and flood protection and regulation of water quality. These benefits are in addition to the provision of products (fuel wood, construction material, food, etc.) in the coastal zone.

The closed canopy mangroves in this study were not old-growth, but the mean C stocks from biomass of non-forest land uses studied were at most 8 % only of C stocks of closed canopy mangroves. In Mexico, the C stock from biomass of pasture was only 9 % of C stocks of mangroves that they replaced (138 versus 12 Mg C ha^{-1}; Kauffman *et al*. 2016). A similar trend was reported in the Dominican Republic (Kauffman et al. 2013) and India (Bhomia et al. 2016) from an abandoned aquaculture pond which had negligible biomass C stock as compared to the mangrove in their vicinity (10 to 161 Mg C ha^{-1} and 65-100 Mg C ha^{-1}, respectively).

Also, this study had also shown that the C stock of open canopy mangrove forest was 69 % lower than closed canopy mangrove forest (71.7 versus 22.5 Mg C ha^{-1}), which could indicate a form of forest C degradation by 49.2 Mg C ha^{-1}.

Biomass C stock data from Kauffman et al. (2016) showed that potential emissions due to biomass loss from converting mangroves to pasture could be 462 Mg CO_2e ha^{-1} as well as 37 to 591 Mg CO_2e ha^{-1} for converting mangroves to shrimp ponds (Kauffman et al. 2013) using stock change approach (or difference in C stocks between intact mangrove forest and deforested mangrove). The results from this study suggest that deforesting mangrove forest and converting them to non-forest land uses such as aquaculture, coconut plantation or cleared mangrove could result in the emission of 82 to 263 Mg CO_2e ha^{-1} from biomass C losses alone using the same approach, consistent with the reports of Kauffman et al. (2013) and Kauffman et al. (2016).

The closed canopy mangroves in this study generally had low stem diameters ($\leq$10 cm) indicative of being second-growth forests. Indeed, one of the closed canopy stands that were measured (i.e. Bacungan mangrove) was once commercially logged during the 1980s (Ismael Ibañez, *pers. com.*) and since then were allowed to regrow while being protected by the community. This stand is probably one of the common types of closed canopy mangroves that are now being degraded into open canopy forests due to biomass harvesting or being deforested for non-forest uses in some cases. Old-growth mangrove stands are now very rare in the Philippines due to rampant harvesting and massive conversion in the past.

The aboveground and belowground biomass carbon of the closed mangrove forests and open canopy mangrove forests reported here (59.9 to 73.9 Mg C ha^{-1} and 8.9 to 26.6 Mg C ha^{-1}, respectively) are within the range of values reported for Philippine mangroves (Abino et al. 2013; Salmo et al. 2013) and in IPCC (2014c). However, the biomass C stock of closed canopy mangrove reported here is 3 to 6 times lower than the biomass C stock value reported by Murdiyarso et al. (2015) for mangroves in Indonesia and those reported by Donato et al. (2011) in Kosrae and Kauffman et al. (2011) in Yap, Micronesia and Stringer et al. (2015) in Zambezi River delta, Mozambique in Africa (Table 4.5). Those workers had measured primary forests, thus the difference. The lowest tree biomass carbon value in open canopy mangrove forest reported here is similar to Cilacap mangrove in Java, also the lowest among the mangrove stands reported by Murdiyarso et al. (2015) in Indonesia. Variation in biomass was said to be due to the differences in

anthropogenic influence, stand age, composition, climate and geomorphology, among many other factors (Bouillon et al. 2008; Alongi 2012, 2014). In addition, the result of this study shows a general increase in biomass from sea edge to landward. This is consistent with the known inverse relationship of biomass and salinity as documented in a number of mangrove studies (e.g. Kauffman et al. 2011; Wang et al. 2014).

The DWB C stock of mangroves in this study (1.23 Mg C ha^{-1} to 6.63 Mg C ha^{-1}) is within the range of values reported from previous studies in mangroves (e.g. Allen et al. 2000; Adame et al. 2013; Stringer et al. 2015; Kauffman et al. 2016). In terms of biomass, this is on the range of 6.9 to 8.5 tonnes per hectare of mangrove forest (Table 4.4). The result indicates another importance of retaining a mangrove forest. This is in terms of providing that much amount of downed woody debris biomass per hectare of mangrove forest that can serve as habitat for mangrove invertebrates aside from being a significant storage of sequestered atmospheric C. The mean diameter, quadratic mean diameter and wood density values in each DWB size class generated from this study can serve as reference in estimating the downed woody debris mass of other mangrove stands in the country with similar conditions.

The lack of significant relationships between DWBs and AGB in both types of mangrove forests studied (r = -0.21, $p = 0.30$ for closed mangrove forest; r = 0.32, $p = 0.13$ for open mangrove forest) is similar to the findings of Allen et al. (2000) who also found no relationship between standing wood and downed wood volume in Micronesian mangrove stands. This suggests that DWD cannot be accurately estimated on the basis of aboveground biomass alone. Furthermore, the C stocks from total biomass of competing land uses of mangroves in this study are very low as compared to the C stocks of mangroves that they replaced, similar to the results obtained by Kauffman et al. (2013) and Kauffman et al. (2016) in Latin America.

Table 4.5. Biomass carbon (C) stocks of natural mangrove stands from recent studies that simultaneously reported AGB, BGB and DWB C stocks

Location		Dominant Species	AGB C stock (Mg C ha^{-1})	BGB C stock (Mg C ha^{-1})	DWB C stock (Mg C ha^{-1})	Reference
Asia-Pacific	Honda Bay, Palawan, Philippines (Bacungan, mangrove)	*Rhizophora apiculata*	43.04	16.87	3.22	This study
	Honda Bay, Palawan, Philippines (Santa Cruz closed canopy mangrove)	*Rhizophora mucronata*	49.58	18.88	3.01	This study
	Honda Bay, Palawan, Philippines (Salvacion closed canopy mangrove)	*Rhizophora apiculata*	50.97	22.88	6.63	This study
	Honda Bay, Palawan, Philippines (Tagburos open canopy mangrove)	*Rhizophora apiculata*	6.3	2.6	1.2	This study
	Honda Bay, Palawan, Philippines (Santa Loudes open canopy mangrove)	*Rhizophora apiculata*	18.0	8.6	6.6	This study
	Honda Bay, Palawan, Philippines (San Jose open canopy mangrove)	*Ceriops tagal*	15.9	6.5	2.6	This study
	Cilacap, Java, Indonesia (disturbed stand)	*Sonneratia alba*	6.9	2.5	11.8	Murdiyarso et al. (2015)
	Sembilang, Sumatra, Indonesia	*Rhizophora apiculata; Bruguiera gymnorrhiza*	300.5	27.9	11.3	Murdiyarso et al. (2015)
	Kubu Raya, Kalimantan, Indonesia	*R. apiculata*	134.8	14.3	24.2	Murdiyarso et al. (2015)
	Tanjung Putting, Kalimantan, Indonesia	*R. apiculata*	140.9	21.3	18.6	Murdiyarso et al. (2015)
	Bunaken, Sulawesi, Indonesia	*R. mucronata*	69.2	14.9	42.7	Murdiyarso et al. (2015)
	Bintuni, West Papua, Indonesia	*B. gymnorrhiza*	323.6	43.6	14.8	Murdiyarso et al. (2015)
	Mekong Delta, Vietnam	*Avicennia* sp.	102.7	34.7	~1.7	Tue et al. (2014)
	Borneo	*Rhizophora-Bruguiera*	67.1	22.4	11.2	Donato et al. (2014)
	Borneo	*Rhizophora* sp.	178.7	61.9	17.9	Donato et al. (2011)
	Sundarbans, Bangladesh	*Heritiera-Excoecaria*	79.7	42.9	4.1	Donato et al. (2011)
	Kosrae	*Sonneratia-Bruguiera*	242.5	203.7	7.6	Donato et al. (2011)
	Airai, Palau	*Rhizophora* sp.	104.4	80	14.8	Kauffman et al. (2011)
	Yap, Micronesia	*Sonneratia alba*	169.2	144	21.6	Kauffman et al. (2011)
America	Pantanos de Centla. Mexico	*R. mangle*	125.3	42.7	12	Kauffman et al. (2016)
	Pantanos de Centla. Mexico	*R. mangle-Lumnitzera racemosa*	118	57	21	Kauffman et al. (2016)
	Montecristi, Dominican Republic	*Rhizophora mangle* Tall mangrove	125	46	12	Kauffman et al. (2013)
	Montecristi, Dominican Republic	*Rhizophora mangle* Medium mangrove	27.6	18.2	1.5	Kauffman et al. (2013)
	Quitana Roo, Mexico	*Rhizophora mangle* Tall mangrove	77.1	59.2	11.8	Adame et al. (2013)
	Quitana Roo, Mexico	*Rhizophora mangle* Medium mangrove	52.6	29.2	4.9	Adame et al. (2013)
	Zambezi River delta, Mozambique	*Xylocarpus granatum-Avicennia marina*	68.5	23.8	6.7	(Stringer et al. 2015)
Africa	Zambezi River delta, Mozambique	*Xylocarpus granatum-Avicennia marina*	255.3	72.8	12.5	Stringer et al. (2015)
	Beira City, Mozambique	*Avicennia marina*	29.7	25.2	0.13	(Sitoe et al. 2014)

AGB = Aboveground biomass Belowground biomass DWB = Downed woody debris biomass

This study has demonstrated that biomass C stocks vary substantially between mangrove forests and land uses that competed and replaced them. Despite its importance, few studies have looked into the factors that correlate with the variability of biomass C stocks in mangrove and their competing land uses. Canopy variable especially LAI also correlate strongly with the biomass C stocks of mangrove. This is an important information since LAI can be derived from satellite imagery using the biophysical variable processor based on PROSAIL algorithm (Jacquemoud et al. 2009) which is available in SNAP (Sentinels Application Platform) software (SNAP 2016). This means that the LAI map derived from satellite imagery could be calibrated from the LAI measurements in the field and related/regressed to plot biomass to generate a biomass map. Dusseux et al. (2015) used the relationship of field biomass and LAI derived from satellite imagery to map the grassland biomass in France. The same LAI-based biomass map could be done for mangrove forest and the replacement land uses in this study.

4.5.2 Implications for management and conservation

The results suggest that if proper protection is afforded to existing stands of mangroves, the open as well as the young closed canopy stands that were studied can be managed to potentially store an additional carbon of up to at least 284 Mg C ha^{-1} (~1,042 Mg CO_2e ha^{-1}), assuming they can attain the biomass C stock of the old-growth mangrove measured by Abino et al. (2014) in nearby Ulugan Bay (~356 Mg C ha^{-1}). Reforesting abandoned aquaculture pond, abandoned salt pond, cleared mangroves and coconut plantation could each sequester and store 264 to 1,307 Mg CO_2e ha^{-1} by early stage (~25 years) to late mature stage stands (>30 years), respectively. This suggests that proper financial incentives should be made to encourage land owners to protect their mangroves and revert the land use back to the mangrove forest.

Reducing emissions from deforestation, forest degradation, and other activities that enhance C stocks (REDD+), as well as other result-based schemes, are strategies that give monetary incentives for reducing deforestation and biomass removal, for not converting forests to agriculture, and conservation of carbon to mitigate climate change, among others. REDD+ could increase C stocks (Pandey et

al. 2014), deliver livelihood benefits (Pandey et al. 2016) and be a significant source of C financing for forestry projects in developing countries (Lasco et al. 2013). In the case of REDD+, the rate of mangrove deforestation in the Philippines, as in other countries, has been slowing down (FAO 2010) and so the country stand to gain carbon credits much from reducing forest degradation and enhancement of C stocks, similar to terrestrial forests in the country (Lasco et al. 2013). Unfortunately, there is much less information on the extent of forest degradation in many countries, especially for mangroves. This suggests that more studies should be done on the topic to generate more data and information for policy and decision-making.

The study results suggest that the potential C emission from degrading an intact, closed-canopy mangrove forest into open canopy forest could be at least 182 Mg CO_2e ha^{-1}. The reduction in biomass C stocks is about 68%, which is consistent albeit higher than the findings of Lasco et al. (2013) on logging operations in the southern Philippines. In that site, logging removed up to 50% of total biomass and yet the site logged is still classified as forest based on definition which is a land with an area of more than 0.5 ha and more than 10% tree crown cover (FMB 2014).

In 2010, the mangrove forest cover in the Philippines was 240,824 ha (Long et al. 2013). Data of the annual rate of forest degradation in mangrove areas of the country is not available. However, the data shows that the difference in biomass C stocks of secondary closed canopy mangrove forest and open canopy mangrove forest is 49 Mg C ha^{-1} or 179.8 CO_2e Mg ha^{-1} (i.e. 68% loss in biomass C stock, 71.7 vs 22.5 Mg C ha^{-1}). If we assume that the open canopy forests in this study were still closed canopy 20 years ago, then we can estimate that C emission from degrading secondary closed canopy mangrove forest to open canopy forest could be 8.9 Mg CO_2e ha^{-1} $year^{-1}$ or about 3.4% reduction every year. The next question to ask is how many hectares of closed canopy mangroves are degraded to open canopy every year? While the practice is being done for terrestrial forests, this is an important research gap at the moment highlighting the need for mapping closed canopy and open canopy mangrove forests in the country. Closed canopy terrestrial forests in the Philippines shrunk from 2,560,872 ha in 2003 (FMB 2005) to 1,934,032 ha in 2010 (FMB 2014). This is 24.5% reduction in the span of seven years which is about 3.5% annually, similar to the assumption for mangroves of 3.4% annually. However, C

emissions from forest degradation are not included in GHG inventories for use in national communications such as in the Philippines, which can grossly underestimate forest C emissions (Lasco et al. 2013).

This study contributes to better understanding of biomass and C stocks of mangrove and the non-forest land uses that replaced them. The results could also serve as input for use in higher tiers (Tier 2 and Tier 3) GHG inventory reporting in wetlands as well as in refining regional and global mangrove biomass estimates.

4.6 Conclusion

Aboveground biomass, BGB and DWB and their C stocks are significantly high relative to non-forest land uses that replaced mangroves that were studied. This underscores the need for more active forest protection in the management of the country's mangrove forest and the need for financial incentives to landowners and managers to not convert the mangrove forests to agriculture/aquaculture. There is also a need for distinguishing and mapping closed and open canopy mangrove stands, similar to what is being done to their terrestrial forest counterparts, to facilitate monitoring and a better understanding of forest degradation in mangrove forests. The relationship that exists between biomass and LAI could be used to pursue and evaluate biomass mapping in mangroves as LAI could be generated using satellite optical imagery. It is argued that mangroves are good in biomass production, and C sequestration and storage only when they are not converted into some other land uses. Mangroves should, therefore, be managed and protected to maximise its role in global C cycling, in the maintenance of coastal biodiversity and in providing wood products to the local community.

In the next Chapter, Chapter 5, the retrieval and mapping of aboveground biomass in mangrove area using the new Sentinel-1 Synthetic Aperture Radar and Sentinel-2 multispectral imagery are presented.

Chapter 5

ESTIMATION AND MAPPING OF ABOVEGROUND BIOMASS OF MANGROVE FORESTS AND THEIR REPLACEMENT LAND USES USING SENTINEL IMAGERY

5.1 Introduction

The previous Chapter, Chapter 4, quantified the biomass in mangrove and replacement land uses using geographically referenced plots. Correlation analysis in Chapter 4 also revealed that field biomass is related to Leaf Area Index. As mentioned in Chapter 2, relating field plots biomass data with satellite imagery data would allow the possible retrieval and predictive mapping of biomass in larger geographic scales. The recent launches of Sentinel-1 and Sentinel-2 satellite missions of the European Space Agency (ESA) offer enormous new-generation imagery data in the present and coming years. While literature are growing on the use of Sentinel-1 and Sentinel-2 imagery data, their applications for biomass estimation and mapping of mangrove forests and other land uses in the tropical coasts are still not reported in the literature.

In this study, the potential of Sentinel-1 and Sentinel-2 imagery data for the retrieval and predictive mapping of aboveground biomass of mangroves and the associated replacement land uses in a coastal area in the tropics were evaluated. The specific objectives of the study were the following: 1) to determine and model the relationship between field-measured aboveground biomass and Sentinel-1 SAR backscatter coefficients and Sentinel-2 multispectral reflectance from mangrove forest and replacement non-forest land uses, 2) to evaluate the accuracy of the biomass prediction models, and 3) to evaluate the accuracy of the output predictive biomass maps. The aboveground biomass models and predictive maps derived from Sentinel-1 SAR imagery, Sentinel-2 multispectral bands, Sentinel-2-derived vegetation indices (e.g. NDVI) and Sentinel-2-derived vegetation biophysical

variables (e.g. LAI) were developed and evaluated. This study attempted to contribute in developing remote sensing-based biomass predictive mapping techniques for mangrove area. It is a pioneering study that utilised Sentinel imagery for biomass modelling and mapping of mangrove forests and non-forest land uses that replaced mangroves in tropical areas.

This Chapter is organised in six sections. Section 1 enumerates the objectives of the Chapter, while Section 2 discusses the background literature and previous works and research gaps on using satellite data for mapping biomass in mangrove area. Section 3 describes the Methods that were used to achieve the objectives of the Chapter. Section 4 presents the results of the correlation and regression analyses between field biomass and Sentinel-1 and Sentinel-2 imagery data, as well as the evaluation and validation of the biomass models and the predictive biomass maps generated by the study. Section 5 discusses and interprets the results in lieu of the objectives and research gaps identified in Section 2. The Chapter concludes in Section 6 with implications of the results and recommendations for future studies.

This study is the first to report the application of Sentinel-1 and Sentinel-2 imagery data in the retrieval and predictive mapping of aboveground biomass of mangroves and their replacement land uses in the tropics.

5.2 Satellite remote sensing-based mapping of mangrove biomass

Mangroves are an important coastal resource in the tropics. They provide many ecosystem goods and services including the provision of wood for construction and fuel, habitat of coastal fauna and nursery of juvenile marine organisms, carbon (C) storage in biomass and soil, protection from strong winds during typhoons and coastal erosion mitigation (Alongi 2009; Donato et al. 2011). However, there have been large reduction in the global mangrove forest cover due to conversion to non-forest land uses such as aquaculture, perennial agriculture and clearing for human settlement (FAO 2007). This is especially true in tropical Southeast Asia where more than 100,000 ha of mangroves were deforested and converted to other land uses during the last 15 years, notably for aquaculture and agriculture (Richards & Friess

2016). It is crucial, therefore, to monitor the mangroves against land use change and forest degradation.

Empirical studies that quantify the carbon stocks of mangroves and the land uses that replaced them are needed in order to provide emission estimates based on actual measures of carbon stocks and reduce uncertainty of estimates. In addition, climate mitigation programs such as Reducing Emissions from Deforestation and Forest Degradation and other activities that increase C stocks (REDD+) are being proposed to prevent large emissions from deforestation and forest degradation in the tropics. These programs will require accurate assessment and mapping to establish the baseline biomass and C stocks against which to monitor future changes (Maraseni et al. 2005). Integrated coastal management would also require relevant maps such as biomass maps for better planning and decision-making.

Aboveground biomass is one of the important carbon pools in mangrove ecosystem (Kauffman & Donato 2012; Howard et al. 2014). There has been a growing body of literature on mangrove biomass and their carbon stocks (e.g.(Ong et al. 2004; Komiyama et al. 2005; Kauffman & Cole 2010; Murdiyarso et al. 2010; Donato et al. 2011; Abino et al. 2013; Abino et al. 2014; Hossain 2014; Sitoe et al. 2014; Tue et al. 2014; Phang et al. 2015; Stringer et al. 2015; Vien et al. 2016). However, only a few studies have quantified biomass and carbon stock of mangrove forest side by side their replacement land uses such as aquaculture pond (Kauffman et al. 2013; Bhomia et al. 2016; Duncan et al. 2016) and cattle pastures (Kauffman et al. 2016). Such studies could help in quantifying the differences in carbon stock and hence the emission from conversion (Maraseni et al. 2008). These studies, however, have utilised field plots to estimate biomass and infer the stock for the whole study site. This approach is sufficient only for a few hectares, but costly and slow if implemented over large areas. It is difficult to implement in remote and treacherous portions in a larger landscape. The use of satellite remote sensing techniques offers cost and time advantages in implementing large-scale biomass assessment. For this approach, remote sensing-based biomass assessment utilises the relationships between field-measured biomass data, imagery and other thematic maps to develop models that predict biomass in different locations of the study site. The outcome of

remote sensing-based biomass estimation is a spatially-explicit pattern of the total aboveground biomass and its variations for the entire area (Samalca 2007).

Satellite image-based biomass prediction models can be derived from radar backscatter polarisations, multispectral bands, vegetation index [e.g. Normalised Difference Vegetation Index (NDVI)], and vegetation cover biophysical variables [e.g. Leaf Area Index (LAI)]. These models can be developed with or without ancillary thematic map data such as elevation (Lu et al. 2004; Simard et al. 2006; Fatoyinbo et al. 2008; Kumar et al. 2012; Jachowski et al. 2013; Dusseux et al. 2015). In the tropics, however, during the rainy season where clouds are persistent, the use of multispectral image is challenging. In contrast, data from space-borne synthetic aperture radar (SAR) sensors are independent of daytime and weather conditions and can provide valuable data for the monitoring of land cover.

Previous satellite remote sensing-based biomass retrieval and mapping studies in coastal areas have dealt mostly on mangrove forest alone (e.g. Simard et al. 2006; Proisy et al. 2007; Fatoyinbo et al. 2008; Jachowski et al. 2013; Aslan et al. 2016), and did not cover the land uses that replaced mangroves. This gap could be an important basis for productivity quantification and comparison with original land use. Simard et al. (2006) utilised the Shuttle Radar Topography Mission (SRTM) elevation data to map the height of mangroves in the Everglades using linear regression with field data, and used that mangrove height map and a local mangrove tree height-biomass equation to eventually map the biomass of mangroves therein. Proisy et al. (2007) used high-resolution IKONOS imagery and field data, and employed Fourier-based textural ordination from canopy grain analysis to model and map the mangrove biomass in French Guiana. Fatoyinbo et al. (2008) also used STRM elevation data and field data to map the mangrove height in Mozambique using linear regression and applied a general mangrove height-biomass equation to map the mangrove biomass in the area. In contrast, Jachowski et al. (2013) made use of high-resolution GeoEye-1 imagery and field data to estimate and map the biomass mangroves in Thailand using a suite of machine learning algorithm. Aslan et al. (2016) also used SRTM elevation and field data to map the mangrove height in Indonesia using linear regression, but utilised non-linear quartile regression to

generate map of mangrove biomass in the area using the mangrove height map and field biomass.

The recent launch of the new-generation Sentinel-1 (SAR) and Sentinel-2 (multispectral) satellite missions of the Copernicus program of the European Space Station is expected to provide new capabilities for monitoring and mapping of biomass in the coastal zone of the tropics. In contrast to other space-borne SAR sensors, Sentinel-1 provides radar imagery with HH+HV or VV+VH polarisations (C-band) in 250 km swath width and 10 m pixel size for interferometric wide swath acquisition mode (Sentinel-1 Team 2013). Likewise, compared to other optical sensors, the Sentinel-2 offers 13 multispectral bands including four vegetation red edge bands and two infrared bands at 20 m resolution, in addition to visible and near infrared bands in 10 m resolution and 100 km swath width (Sentinel-2 Team 2015). These imagery have high temporal resolution (every 6 and 5 days for twin satellites, respectively) and are freely accessible which could benefit developing countries in the tropics. However, the retrieval and mapping of biomass of mangrove forest and land uses that replaced them from data acquired by these newly launched multispectral and SAR instruments onboard the Sentinel-1 and Sentinel-2 satellite missions have not been reported in the scientific literature. Therefore, pioneering studies are needed to assess these new-generation satellite imagery.

5.3 Methods

5.3.1 Study site

The study site is situated on the southern coast of Honda Bay within the administrative jurisdiction of Puerto Princesa City in the island province of Palawan, Philippines. The southern coast of Honda Bay is presently a mosaic of a long band of mangrove forests interrupted by non-forest land uses such as agriculture, aquaculture, and built-up areas/settlements. The study site has an area of 2,749 ha, of which ca. 1,216 ha is covered by mangrove forests. The mangrove forests in the area are dominated mostly by the genus *Rhizophora* and are extensive in the northern part of the study site. They can generally be classified as either closed canopy and open canopy stands. The former are dense, intact mangrove vegetation, with no significant

open spaces or gaps inside, and are located mostly in areas far from roads and built-up areas. The open canopy mangroves, on the other hand, have open spaces, with lower tree density, with fresh stumps and cut branches. In contrast, the non-forest land uses were historically occupied by mangroves prior to their conversion. The aquaculture ponds and salt ponds were mangrove forests until they were cleared in the early 1990s and were in operation until their abandonments in the early 2000s. The coconut plantation is a 20-year-old stand planted at the back of an open canopy mangrove forest and not actively managed as evidenced by the proliferation of dried leaves and fruits. The cleared mangrove is a deforested mangrove area that was gradually cleared from 2005 to 2008 but remained unutilised. The full details of the study site are described in Chapter 3.

5.3.2 Field data

The results of biomass estimation in Chapter 4 were used in this study. The data was gathered from five coastal land uses, i.e. mangrove forest (closed canopy and open canopy), abandoned aquaculture pond, coconut plantation, abandoned salt pond, and cleared mangrove. The non-forest land uses were previously occupied by mangroves. The whole study site was stratified based on land use. In each land use, sites were taken using simple random sampling. The mangrove forests had three sites for closed canopy mangroves and three sites for open canopy mangroves. The land uses that replaced mangroves had three sites for abandoned aquaculture ponds. However, due to access restriction and availability of sites for replication, the coconut plantation, salt pond and cleared mangroves have only one site each. Circular plots with 7 m in radii, established along line transects, were used in each land use to collect plot data necessary to estimate the biomass of each tree in a plot.

For mangrove forests, three transects were established at each site (except for one open canopy mangrove which had only two transects due to thin cover). Each transect has three circular plots spaced 50 m apart. For non-forest land uses, two transects were established at each site except for salt pond which had three. Each transect also had three circular plots established about 25 m apart. At each plot, all the measurements (e.g. tree diameter) necessary to do biomass stock accounting were undertaken, following the method of Kauffman and Donato (2012). In each plot, geographic coordinates were recorded using a *Garmin* hand-held GPS receiver. In

total, 90 plots were established, of which 51 plots were in mangrove forests, 18 plots in abandoned aquaculture ponds, nine plots in abandoned salt pond and six plots each for coconut and cleared mangrove areas. In each plot, stem diameters of all individuals were measured at breast height (1.3 m from the ground) or 30 cm above the highest prop root for stilt-rooted species like *Rhizophora* spp. Allometric equations were used to compute for the aboveground biomass of each individual.

$$\text{Biomass (kg)} = 0.251*\rho*D^{2.46} \quad \text{(Equation 5.1)}$$

$$\text{Biomass (kg)} = 0.186\ D^{2.31} \quad \text{(Equation 5.2)}$$

$$\text{Biomass (kg)} = 0.168D^{2.42} \quad \text{(Equation 5.3)}$$

$$\text{Biomass (kg)} = 0.235D^{2.42} + \text{Biomass}_{\text{stilt}}\,(\text{kg}) = 0.0209D^{2.55} \quad \text{(Equation 5.4)}$$

$$\text{Biomass (kg)} = 0.7854*D^{2}*H*\rho*1.6 \quad \text{(Equation 5.5)}$$

Equation 5.1, from Komiyama et al. (2005), was used for eight species (*Aegiceras floridum, Sonneratia alba, Xylocarpus moluccensis, X. granatum, Camptostemon philippinense, Ceriops tagal, Heritiera littoralis* and *Lumnitzera racemosa*). Equations 5.2 and 5.3 were from Clough and Scott (1989) and were used for *Bruguiera gymnorrhiza,* and *B. parviflora* and *B. sexangula,* respectively. Equation 5.4 was from Ong et al. (2004) and used for *Rhizophora apiculata, R. mucronata,* and *R. stylosa,* while Equation 5.5 was from Brown (1997) and used for coconut.

In summary, the mangrove forests were dominated by *Rhizophora apiculata* and *R. mucronata*. In the abandoned aquaculture pond, individuals of *R. apiculata* and *Ceriops tagal* were also encountered. The tree density in the mangroves averaged 1,260 trees per hectare. In the land uses that replaced mangroves such as coconut, the tree density was only 195 per hectare while it was only 40 trees per hectare in aquaculture pond. Trees were absent in both abandoned salt pond and cleared mangrove. Furthermore, the aboveground biomass of mangrove was 65.1 Mg ha^{-1} (range: 1.1 to 210 Mg ha^{-1}). In contrast, the aboveground biomass in the coconut plantation was only 11.4 Mg ha^{-1} (range: 0.2 to 19.7 Mg ha^{-1}) and 0.07 Mg ha^{-1} (range: 0.2 to 19.7 Mg ha^{-1}) in the abandoned aquaculture pond. Figure 5.1 shows the profile of the aboveground biomass in the 90 study plots. Mangroves were in plots 1 to 51, aquaculture ponds were in plots 52 to 69, coconut plantations were in plots 70

to75, salt ponds in plots 76 to 84, and cleared mangroves in plots 85 to 90. Biomass in abandoned aquaculture pond ranged from negligible to zero, while there was no biomass present in abandoned salt pond and cleared mangrove.

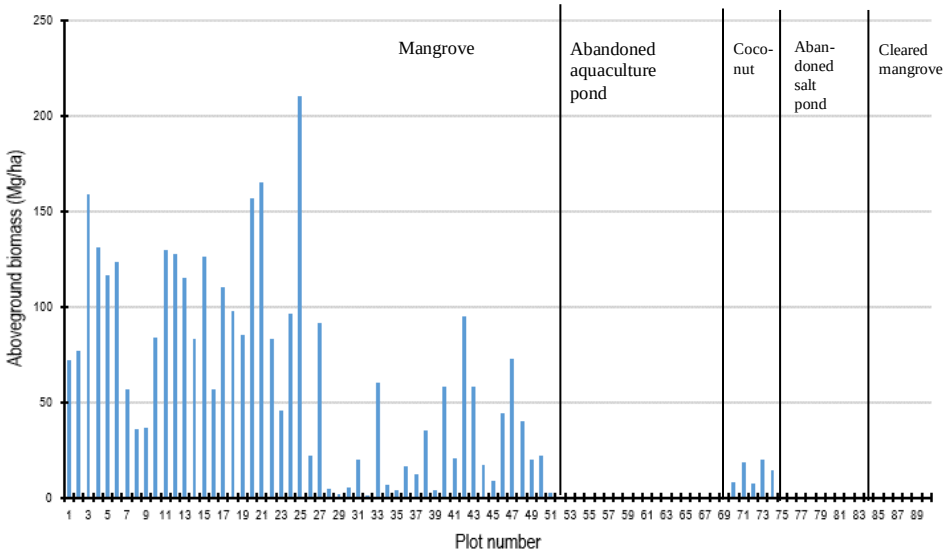

Figure 5.1. Field plots profile of aboveground biomass in the study site. Plots 1 to 51 are areas covered for mangrove plots, 52 to 69 for abandoned aquaculture pond plots, 70 to 75 for coconut plantation plots, 76 to 84 for abandoned salt pond plots, and 85 to 90 for cleared mangrove plots

5.3.3 Satellite data collection and pre-processing

This study used data from Sentinel-1 (Synthetic Aperture Radar) and Sentinel-2 (Multispectral) imagery (Figures 5.2 and 5.3) of the European Space Station downloaded from the station's Copernicus Sentinels Scientific Data Hub (ESA 2016). The list of Sentinel images used for the study is presented in Table 5.1. The acquired Sentinel-1 C-band (5.405 GHz) images were collected in Interferometric Wide Swath mode with a swath width of 250 km, of VH (Vertical transmit – Horizontal receive) and VV (Vertical transmit – Vertical receive) polarisations, and in high-resolution (HR) Level-1 Ground Range Detected (GRD) processing level. The images are already multi-looked (5 x 1) and with a pixel size of 10 m (Sentinel-1 Team 2013). The collected Sentinel-2 imagery, on the other hand, is an orthorectified, top-of-atmosphere reflectance (Level 1C), 100 km x 100 km image in UTM/WGS84 projection, with 13 spectral bands in the visible, near

infrared and short-wave infrared regions. The imagery is in 10 m (4 bands), 20 m (6 bands) and 60 m (3 bands) spatial resolutions. Accordingly, Level-1C product has been processed for radiometric and geometric corrections including orthorectification and spatial registration on a global reference system (Sentinel-2 Team 2015). In addition, elevation data (1-arc second, ~30m) from SRTM product was acquired from the United States Geological Service's Earth Explorer (USGS 2016) for inclusion in the analysis of the Sentinel data.

Table 5.1 List of Sentinel imagery acquired for the study

Mission	Product	Observation date	Cell size (m)	Swath width (km)
Sentinel-1A	Level-1GRD-HR	October 31, 2015	10	250
Sentinel-1A	Level-1 GRD-HR	December 30, 2015	10	250
Sentinel-1A	Level-1 GRD-HR	January 11, 2016	10	250
Sentinel-2A	Multispectral image Level-1C	April 11, 2016	10	100

A flowchart of data processing steps used in the study is summarised in Fig. 2. The software SNAP (Sentinel's Application Platform) version 4.0 of the European Space Agency was used to pre-process the Sentinel-1, Sentinel-2 and elevation data. The pre-processing steps for the acquired Sentinel-1 SAR data adopted the Sentinel-1 Toolbox pre-processing steps described by Veci (2015) for multi-look SAR image. It consisted of 1) image calibration; 2) speckle reduction, and 3) terrain correction. Image calibration radiometrically corrects the SAR image pixel value into one that represents the radar backscatter of the reflecting surface, as well as correction for incidence angle effect and replica pulse power variation. This process converts the pixel values of the SAR image into radar intensity backscatter coefficient (Sigma naught, σ^0). Furthermore, speckle reduction using Refined Lee Filter was done to reduce the speckle effect in the image to allow better backscatter analysis and interpretation. Finally, terrain correction was performed using the Range-Doppler Terrain Correction to reproject the SAR image into a map projection (Veci 2015; Liu 2016).

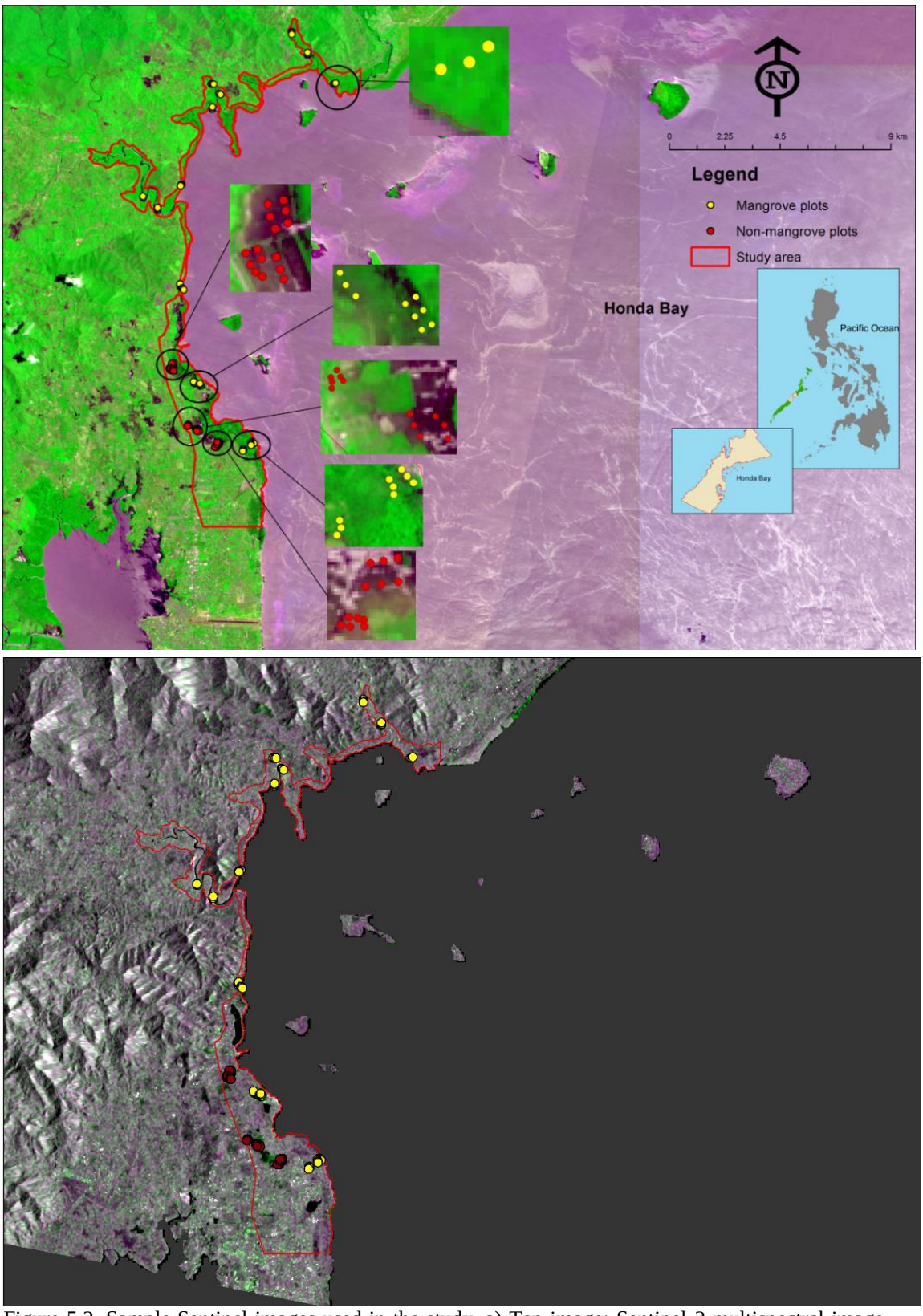

Figure 5.2. Sample Sentinel images used in the study. a) Top image: Sentinel-2 multispectral image acquired on April 2016 in false colour composite (RGB = R, NIR, B). Sampling locations were zoomed-in to show the number of plots. b) Bottom image: Sentinel-1 SAR image acquired on October 2015 (RGB = VV, VH, VV in dB). Yellow and red dots are sampling plots. Inset maps: 1. Philippine map showing the relative location of Palawan province (green) with Puerto Princesa City at its midsection (beige); 2. Puerto Princesa map showing the Honda Bay area.

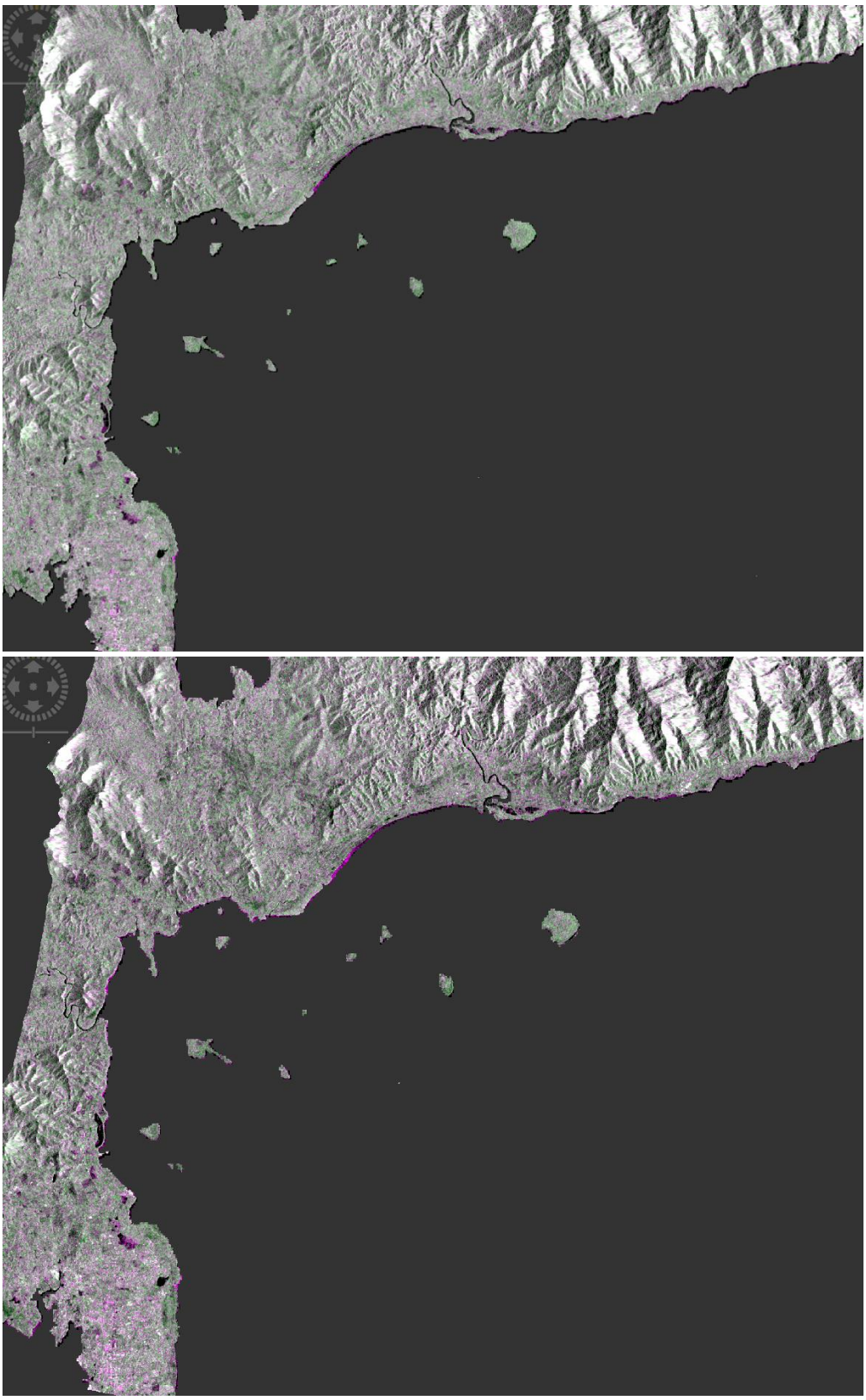

Figure 5.3 Other Sentinel-1 images used in the study, a) Top image: Sentinel-1 SAR image acquired on December 2015. b) Bottom image: Sentinel-1 SAR image acquired on January 2016. In RGB = VV, VH, VV in dB.

For the optical Sentinel-2 image, the acquired Level-1C orthorectified, top-of-atmosphere image was atmospherically corrected and processed to Level-2A product to obtain bottom-of-atmosphere corrected reflectance image. This was also done in SNAP software using the recent radiative transfer model-based SEN2COR atmospheric correction processor (version 2.2.1). The pre-processed Sentinel images, as well as the elevation data, were brought into a common map projection (i.e. UTM Zone 50 WGS84) and resampled to 10 m pixel size. Subsetting was done each for the Sentinel SAR and multispectral images and the SRTM DEM to reduce the image size and the processing time, and to cover only the general area along the coast of Honda Bay.

5.3.4 Modelling the relationship between field biomass and satellite data

The Sentinel imagery data were divided into four predictor groups of biomass: 1) multi-date SAR raw channels (Figure 5.4), 2) multispectral bands, 3) derived Vegetation Indices, and 4) derived biophysical variables. The predictors of biomass and their combination used in each group and their brief description are given in Table 5.2. Thus, modelling the relationship of Sentinel image data and field measured biomass was done in four parts and consisted of four groups (Table 5.2). The first part, Group 1 (SAR biomass models), consisted of relating the field data with Sentinel SAR polarisation channels (i.e. VH and VV). The SAR biomass models included the VH and VV channels for October 2015, December 2015 and January 2016 scenes, used singly or in combination with each other and elevation data.

Furthermore, the second part, Group 2 (multispectral band biomass models), proceeded with relating the field biomass with Sentinel 2 multispectral bands and their combination. The Multispectral band biomass models were composed of the 10 bands in the visible, near infrared and short wave infrared regions of the electromagnetic spectrum, used singly or in combination with other bands, and elevation data. The third part, Group 3 (Vegetation index biomass models), involved relating the field biomass with Sentinel-2-derived vegetation indices such as Normalised Difference Vegetation Index (NDVI), Normalised Difference Index

(NDI45), Inverted Red-Edge Chlorophyll Index (IRECI) and Transformed Normalised Difference vegetation Index (TNDVI), used singly and in combination with elevation. The last part, Group 4 (Biophysical biomasss models) , used Sentinel-2-derived vegetation cover biophysical variables such as Leaf Area Index (LAI), Fraction of Absorbed Photosynthetically Active Radiation (fPAR), Fraction of Vegetation Cover (fCover) and Chlorophyll (Chlorophyll content in the leaf) to predict the biomass, either singly or in combination with elevation data.

The Sentinel backscatter and reflectance data were supplemented with elevation data from SRTM DEM to assess whether the inclusion of elevation can improve the biomass prediction. LAI and other biophysical cover variables (see Table 5.2) were also derived in SNAP from its biophysical processor that uses neural network algorithm (SNAP 2016) based on PROSAIL radiative transfer model (Jacquemoud et al. 2009). The retrieval of these biophysical variables was also done for the SPOT image by Dusseux et al. (2015).

All modelling tasks were implemented using IBM SPSS Statistics version 23 (IBM, USA) and the Waikato Environment for Knowledge Analysis (WEKA, version 3.8.0, The University of Waikato, NZ). The WEKA software is a collection of machine learning algorithms (Hall et al. 2009). The models were prepared using the entire dataset. The models were first subjected to linear regression, producing models with minimum number of predictor variables by eliminating insignificant and collinear variables. This process steps through the variables, removing the one with the smallest standardised coefficient until no improvement was observed in the estimate of the error (as given by the Akaike Information Criterion (AIC)), eliminating collinear variable/s. To assess the model performance, a leave-one-out approach with 90-fold cross-validation was performed to compute the prediction error (Root Mean Square Error; RMSE) and correlation coefficient/agreement (*r)* between the observed and predicted data. In the leave-one-out approach, each sample was excluded one by one while the model is trained with the remaining samples to predict the excluded sample.

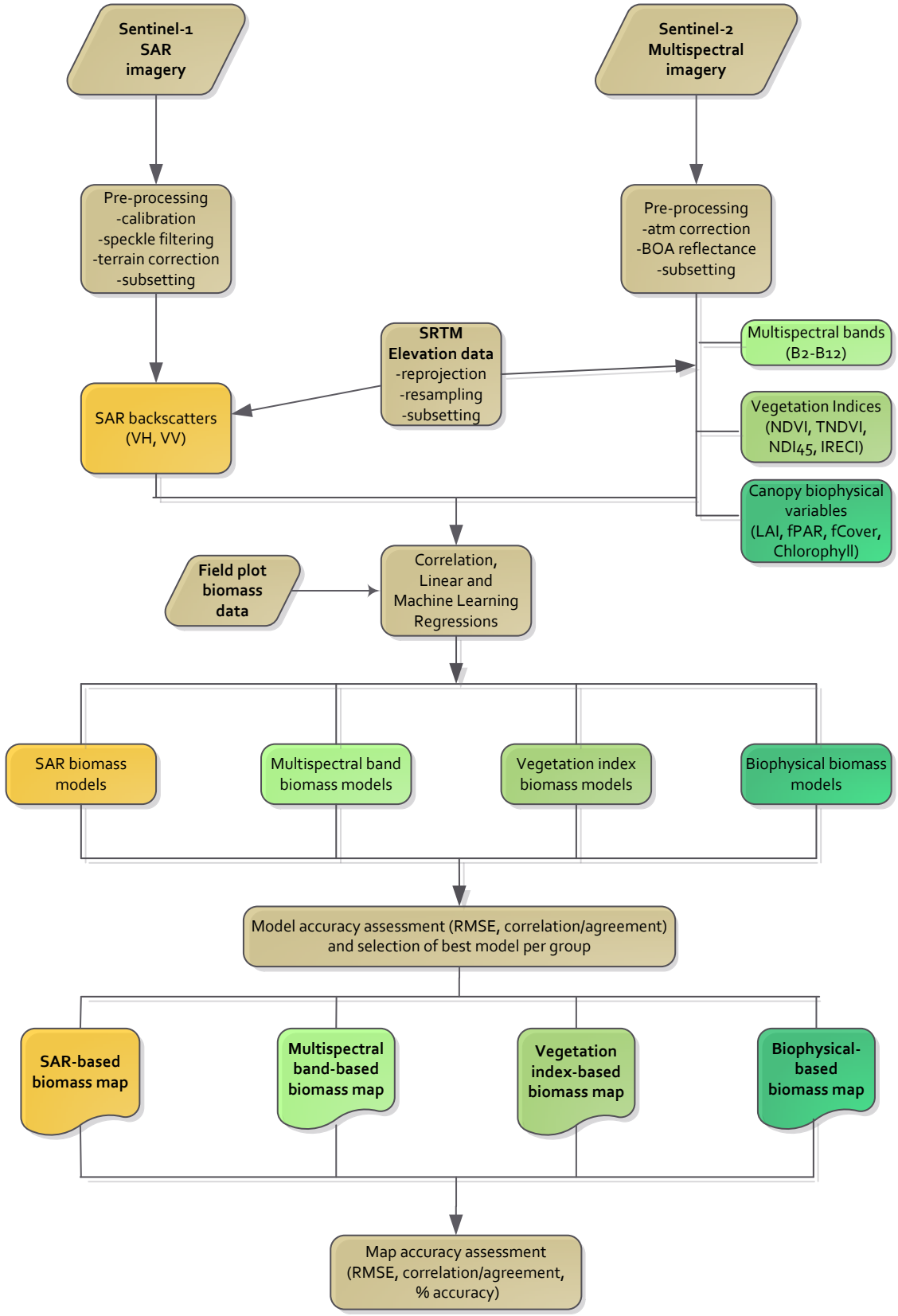

Figure 5.4. Flowchart of the study showing the steps used for the aboveground biomass retrieval and mapping of mangrove forests and their non-forest replacement land uses using the Sentinel SAR and multispectral imagery. There were four Sentinel groups considered in the study: 1. SAR-based group, 2. Multispectral band-based group, 3. Vegetation indices-based group, and 4. Vegetation biophysical variables-based group.

Table 5.2 Sentinel-based imagery data predictors of aboveground biomass including space-borne elevation data

Group	Source Image	Predictor Variable Group	Predictor/s set	Description
1	Sentinel-1	Polarisation/ channel	VH-Oct VV-Oct VH-Dec VV-Dec VH-Jan VV-Jan VV-Oct, VH-Dec, VV Jan VV Oct, VH Jan, Elevation	VH channel (dB) for October 2015 VV channel (dB) for October 2015 VH channel (dB) for December 2015 VV channel (dB) for December 2015 VH channel (dB) for January 2016 VV channel (dB) for January 2016 Multi-date VH, VV combination Multi-date VH, VV, elevation combination
2	Sentinel-2	Multispectral bands	Band 2 Band 3 Band 4 Band 5 Band 6 Band 7 Band 8 Band 8a Band 11 Band 12 NIR, SWIR 2 Red, Red Edge 1 Red, Red Edge 2 Red, Red Edge 1, NIR, Elevation Red, Red Edge 1, Red Edge 3, Elev.	Blue, 490nm Green, 560 nm Red, 665nm Red edge 1, 705 nm Red edge 2, 749 nm Red edge 3, 783 nm Near Infrared, 842 nm Near Infrared a, 865 nm Short Wave IR 1, 1610 nm Short Wave IR 2, 2190 nm NIR, SWIR 2 combination Red, Red Edge 1 combination Red, Red Edge 2 combination Red, Red Edge 1, NIR, Elevation combination Red, Red Edge 1, Red Edge 3, Elev. combination
3	Sentinel-2	Vegetation Indices	NDVI NDI45 IRECI TNDVI NDI45, Elevation IRECI, Elevation	(Band 8 – Band 4) / (Band 8 + Band 4)* (Band 5 – Band 4) / (Band 5 + Band 4)** (Band 7 – Band 4) / (Band 5/Band 6)*** $[(\text{Band 8} - \text{Band 4}) / (\text{Band 8} + \text{Band 4}) + 0.5]^{1/2}$**** NDI45, Elevation combination IRECI, Elevation combination
4	Sentinel-2	Vegetation biophysical variables	LAI fCover fPAR Chlorophyll (Cab) LAI, Elevation Chlorophyll, Elevation	Leaf Area Index Fraction of Vegetation Cover Fraction of Absorbed Photosynthetically Active Radiation Chlorophyll content in the leaf LAI, Elevation combination Chlorophyll, Elevation combination
	SRTM DEM	Elevation		Elevation, 30 m resolution

IRECI = Inverted Red-Edge Chlorophyll Index; TNDVI = Transformed Normalised Difference Vegetation Index
*Rouse et al. 1973 as cited in SNAP (2016) **Delegido et al. 2011 as cited in SNAP 2016)
***Clevers et al. 2000 as cited in SNAP (2016) ****Senseman et al. 1996 as cited in SNAP (2016)

To assess if the correlation with biomass and prediction error from the linear models can still be improved, the set of predictors from the linear models with the highest *r* and lowest RMSE for each part was further subjected to 17 machine learning algorithms (available in the WEKA machine learning software; Table 5.3). The model/algorithm with highest *r* and lowest RMSE was selected for use in predictive mapping of biomass which was implemented in ArcGIS (version 10.3.1,

ESRI, USA). Four biomass predictive maps were produced which were derived from Sentinel-1 SAR channels, Sentinel-2 multispectral bands, Sentinel-2 vegetation index, and Sentinel-2 vegetation biophysical variable.

Table 5.3 Machine learning algorithms used in the study. These algorithms are available from WEKA machine learning software (Hall et al. 2009)

Algorithm	Classifier type	Key description
ElasticNet	Functions	Coordinate descent-based regression for 'elastic net'-related problem
GaussianProcesses	functions	Gaussian processes for regression
IsotonicRegression	Functions	Learns an isotonic regression model
LeastMedSq	Functions	Least median squared linear regression
MultilayerPerceptron	Functions	Backpropagation to classify instances
PaceRegression	Functions	Pace regression linear models
RBFNetwork	Functions	Normalized Gaussian radial basis function network.
RBFRegressor	Functions	Supervised Radial basis function networks
SMOreg	Functions	Support vector machine for regression
AlternatingModelTree	Trees	An alternating model tree by minimising squared error
DecisionStump	Trees	Building and using a decision stump
RandomForest	Trees	Construction a forest of random trees
RandomTree	Trees	Tree construction based on K-randomly chosen attributes
REPTree	Trees	Fast decision tree learner
IBk	Lazy	K-nearest neighbour classifier
KStar	Lazy	Instance-based classifier
LWL	Lazy	Locally weighted learning

The accuracy of the predicted maps was assessed for their overall RMSE, agreement/correlation coefficient (*r)* between predicted and observed values, and map accuracy (%) based on the range value (i.e. maximum – minimum) of the dataset (Christensen et al. 2004). Extraction of the pixel value of the 90 plots for each of the four predictive maps was done using ArcGIS. The prediction errors (RMSE) were also computed for each land use in each Sentinel image-derived map. An elevation range of zero to 15 m was used as a mask to remove, in the predicted maps, areas that are far from the study site. All the land uses were all covered within this elevation range.

5.4 Results

5.4.1 Relationship of field biomass and Sentinel Image data, and model assessment

5.4.1.1 Sentinel-1 (SAR) polarisations

There was an increase in the backscatter values as the aboveground biomass increases, i.e. from nil in aquaculture ponds, the salt pond and the cleared mangrove to low biomass in the coconut plantation, and low to high biomass in mangroves (Figure 5.5). The backscatter (dB) values of vegetated mangrove and coconuts were comparable, -13.41 and -13.19 in VH polarisation, and -7.51 and -7.86 in VV polarisation, respectively. Non-vegetated areas under aquaculture ponds, the salt pond and the cleared mangrove had lower dB in VH polarisation (i.e. -18.098 for aquaculture ponds, -19.80 for the salt pond, and -16.16 for the cleared mangrove). For VV polarisation, the trend was less clear for non-vegetated areas, with lower backscatter value of -9.22 and -10.77 for aquaculture ponds and the salt pond, but higher backscatter for the cleared mangrove of -6.83.

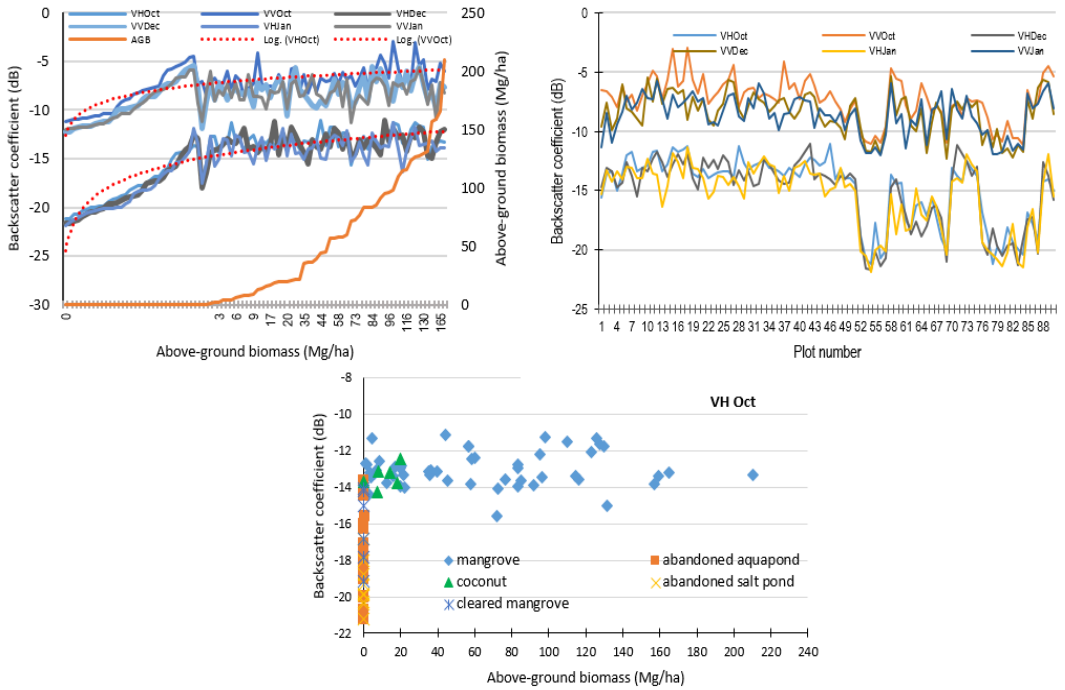

Figure 5.5 Relationships of observed aboveground biomass and Sentinel-1 SAR backscatter coefficient (σ^o, dB) in the different coastal land uses. Plots were arranged from nil to high biomass (top left), according to land use/plot number (top right) and in October 2015 for VH polarisation (bottom). Plots are arranged per land use, as: 1 to 51 (mangrove), 52 to 69 (abandoned aquaculture), 70 to 75 (coconut plantation), 76 to 84 (abandoned salt pond) and 85 to 90 (cleared mangrove).

Single-date VH channel had higher correlations with biomass (r = 0.48 – 0.51 vs. r = 0.28 – 0.45) than VV polarisation. The multi-date combination of VH and VV polarisations had a higher correlation with biomass than single date imagery, albeit the relationship is only moderate (r = 0.55). However, when elevation was added to multi-date VH-VV channels, the relationship with biomass was greatly improved (*r* = 0.84). This model was able to explain 69 % of the biomass variability and had the lowest prediction error of 28.36 Mg ha^{-1}, among the SAR models evaluated (Table 5.4).

Table 5.4 Correlations of observed aboveground biomass and Sentinel-based predictors

Modelling Group	Predictor/s	*Correlation with biomass, r*	*p* value	*Agreement/ Correlation of observed and predicted value, r*	Model prediction error, RMSE (Mg ha^{-1})
1. Sentinel-1 (SAR) polarisation	VH Oct	0.50	<0.001	0.47	44.16
	VV Oct	0.45	<.001	0.42	45.50
	VH Dec	0.51	<.001	0.49	43.67
	VV Dec	0.33	0.001	0.28	48.03
	VH Jan	0.48	<.001	0.45	44.72
	VV Jan	0.28	0.007	0.21	48.99
	VV Oct, VH Dec, VV Jan	0.55	<.001	0.47	44.33
	VV Oct, VH Jan, Elevation	0.84	<.001	0.82	28.36
2. Sentinel-2 (multispectral) raw bands	Blue	0.57	<0.001	0.53	42.40
	Green	0.54	<0.001	0.51	43.03
	Red	0.65	<0.001	0.63	38.74
	Red Edge 1	0.50	<0.001	0.47	44.16
	Red Edge 2	0.69	<0.001	0.67	37.09
	Red Edge 3	0.72	<0.001	0.71	35.34
	NIR	0.72	<0.001	0.71	35.45
	NIRa	0.72	<0.001	0.70	35.60
	SWIR 1	0.42	<0.001	0.38	46.23
	SWIR 2	0.59	<0.001	0.56	41.37
	NIR, SWIR 2	0.80	<0.001	0.79	30.90
	Red, Red Edge 1	0.71	<0.001	0.68	36.59
	Red, Red Edge 2	0.77	<0.001	0.76	32.68
	Red Edge 1, Red Edge 2	0.79	<0.001	0.77	31.83
	Red, red edge 1, NIR, Elevation	0.84	<0.001	0.82	28.92
	Red, Red edge1, Red edge3, Elev.	0.84	<0.001	0.82	28.47
3. Sentinel-2 derived vegetation indices	NDI45	0.80	<0.001	0.79	30.74
	IRECI	0.80	<0.001	0.79	30.73
	TNDVI	0.72	<0.001	0.70	35.54
	NDVI	0.74	<0.001	0.73	34.44
	NDI45, Elevation	0.84	<0.001	0.82	28.83
	IRECI, Elevation	0.84	<0.001	0.83	28.02
4. Sentinel-2 derived biophysical variables	LAI	0.80	<0.001	0.79	30.91
	fPAR	0.77	<0.001	0.75	32.89
	fCover	0.78	<0.001	0.77	32.11
	Chlorophyll content	0.77	<0.001	0.76	32.32
	LAI, Elevation	0.84	<0.001	0.82	28.33
	Chlorophyll, Elevation	0.84	<0.001	0.82	28.38

5.4.1.2 Sentinel-2 Multispectral bands and combination

Figure 5.6 presents the reflectance in the visible, red edge and infrared bands of mangroves and the non-forest land uses that replaced them. Bands in the Red edge 2, Red edge 3, and Near-infrared have better correlations (r = 0.69 to 0.72) with aboveground biomass than bands in the visible and short-wave infrared regions. Raw band combination of Red edge 1 and Red edge 2, as well as NIR and SWIR2 bands, had stronger and higher correlations with aboveground biomass than individual raw bands and other raw band combinations. However, the inclusion of elevation with band combination of Red, Red edge 1, and Red edge3 greatly improved the correlation (r = 0.89). This raw band-elevation combination had the least prediction error (28 Mg ha^{-1}; Table 4).

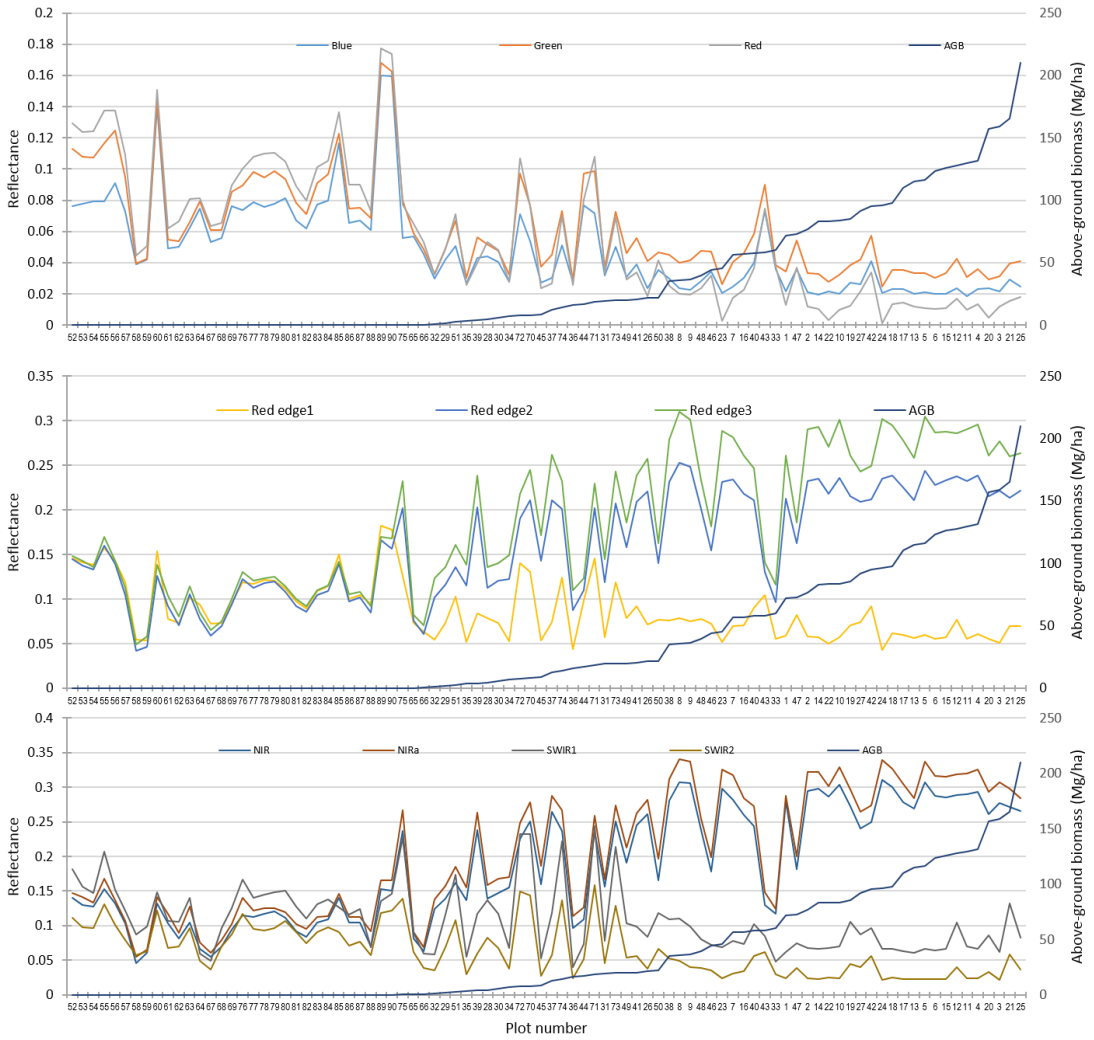

Figure 5.6 Relationships of observed aboveground biomass with Sentinel-2 multispectral bands in the visible, red edge and infrared regions. Plots were arranged from nil to high biomass, regardless of land use. Plots 1 to 51 are in mangroves, 52 to 69 are in abandoned aquaculture ponds, 70 to 75 are in the coconut plantation, 76 to 84 are in the abandoned salt pond and 85 to 90 are in the cleared mangrove.

5.4.1.3 Sentinel-2-derived Vegetation Indices

Figure 5.7 shows the plot profile of vegetation indices in the study site. Indices close to zero for NDVI, IRECI and NDI45 were plots under aquaculture ponds, the salt pond and the cleared mangrove, respectively. Among the Sentinel-derived vegetation indices, NDI45 and IRECI had the highest correlation (r = 0.80) to biomass. Adding elevation to the indices slightly improved the correlation, of which the highest was in IRECI and elevation combination (r = 0.84; Table 5.4). This combination also had the lowest prediction error of 28 Mg ha^{-1}.

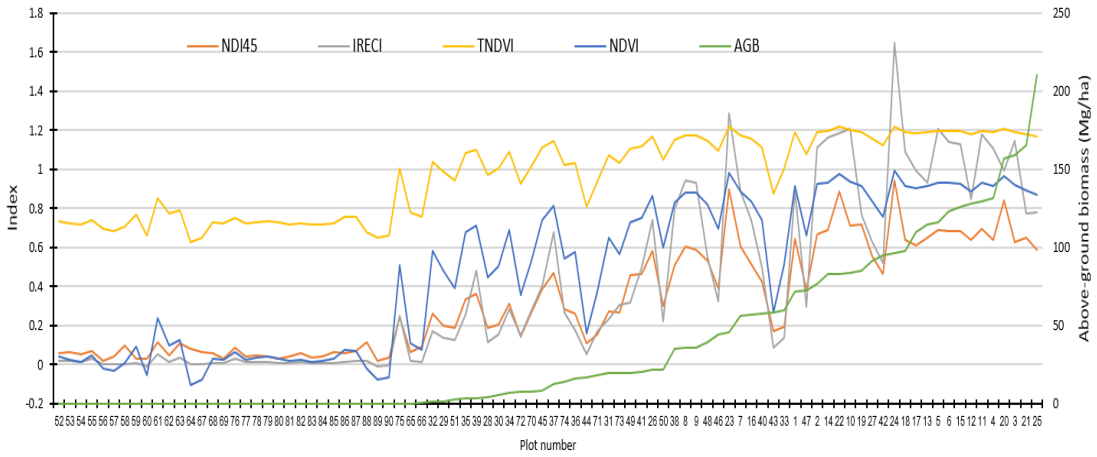

Figure 5.7 Relationship of observed aboveground biomass with Sentinel-2-derived vegetation indices. Plots were arranged from nil to high biomass. Plots 1 to 51 are in mangroves, 52 to 69 are in abandoned aquaculture ponds, 70 to75 are in the coconut plantation, 76 to 84 are in the abandoned salt pond and 85 to 90 are in the cleared mangrove.

5.4.1.4 Sentinel-2-derived Vegetation biophysical variables

Figure 5.8 presents the plot profile of the Sentinel-2-derived vegetation biophysical variables included in the study. Areas under aquaculture ponds, saltpond and cleared mangrove had values close to zero whereas vegetated areas under coconut had lower value of vegetation cover (less than 0.5 on average) compared to mangroves. Leaf Area Index (LAI) had better correlation with biomass (r = 0.80) than the other vegetation cover variables evaluated (Table 5.4). Adding elevation data improved the correlation and reduced the error of prediction. The highest correlation with biomass and lowest prediction error was for the combination of LAI and elevation (r = 0.84; RMSE = 28.38 Mg ha^{-1}).

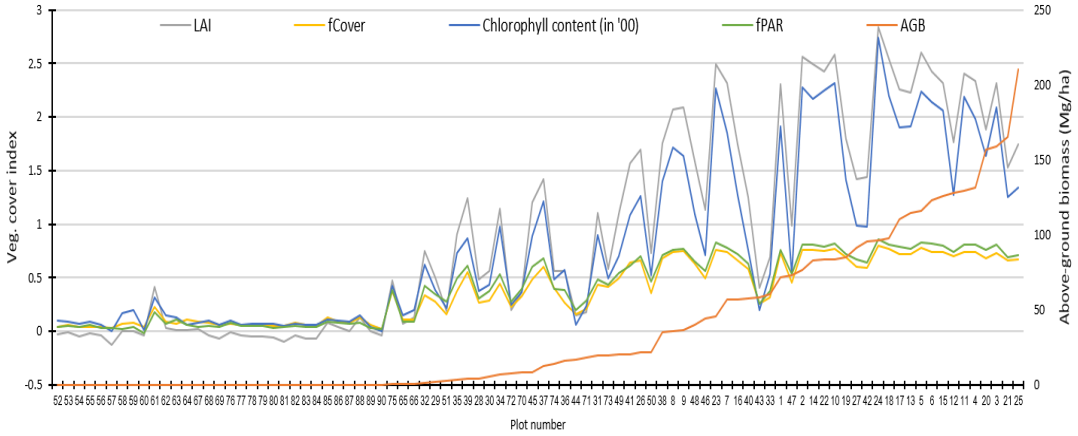

Figure 5.8 Relationship of observed aboveground biomass with Sentinel-2-derived biophysical variables. Plots were arranged from nil to high biomass. Plots 1 to 51 are in mangroves, 52 to 69 are in abandoned aquaculture ponds, 70 to75 are in the coconut plantation, 76 to 84 are in the abandoned salt pond and 85 to 90 are in the cleared mangrove.

5.4.2 Linear regression versus machine learning algorithms

Compared to linear regression, the use of machine learning algorithms SMOreg and ElasticNet gave better biomass prediction from Sentinel-1 SAR and Sentinel-2-derived vegetation cover data, respectively. However, for Sentinel-2 multispectral band combination and Sentinel-2 derived vegetation index, linear regression gave better biomass prediction than the machine learning algorithms. Table 5.5 shows the evaluation of biomass prediction from machine learning algorithms and traditional linear regression in terms of the agreement of observed and predicted values as well as the prediction error.

Table 5.5 Algorithms used in the study and their accuracy evaluation for biomass prediction

Algorithm	**S-1 SAR**		**S-2 raw bands**		**S-2 veg. index**		**S-2 LAI**	
	r	RMSE	r	RMSE	r	RMSE	r	RMSE
Linear Regression	0.82	28.36	**0.82**	**28.47**	**0.83**	**28.02**	0.82	28.33
ElasticNet	0.82	28.34	0.82	28.61	0.82	28.35	**0.83**	**28.25**
GaussianProcesses	0.78	33.23	0.78	31.35	0.82	41.14	0.81	41.64
IsotonicRegression	0.80	30.48	0.80	29.99	0.79	31.26	0.80	30.48
LeastMedSq	0.82	43.98	0.65	48.69	0.74	44.61	0.82	43.28
MultilayerPerceptron	0.77	32.98	0.76	33.33	0.78	31.86	0.78	31.90
PaceRegression	0.82	28.38	0.81	29.04	**0.83**	**28.03**	0.82	28.33
RBFNetwork	0.46	44.32	0.76	32.34	0.76	32.53	0.76	32.32
RBFRegressor	0.78	31.40	0.80	29.94	0.80	42.06	0.78	31.92
SMOreg	**0.83**	**27.75**	0.80	29.81	0.82	29.18	0.80	30.58
AlternatingModelTree	0.58	55.81	0.71	35.92	0.44	59.12	0.38	62.48
DecisionStump	0.71	35.58	0.73	34.40	0.67	37.64	0.70	36.05
RandomForest	0.76	32.95	0.75	33.81	0.75	33.71	0.72	35.13
RandomTree	0.54	48.75	0.65	42.42	0.67	41.17	0.61	43.15
REPTree	0.79	31.26	0.76	32.96	0.77	31.89	0.77	32.04
IBk	0.69	38.80	0.61	43.20	0.59	44.67	0.59	43.35
KStar	0.74	33.93	0.71	36.75	0.78	31.15	0.77	31.74
LWL	0.75	33.07	0.86	27.54	0.77	33.82	0.69	36.68

5.4.3 Biomass predictive mapping

The model from the best algorithm (lowest RMSE and highest *r)* from each of the four biomass prediction groups was then used to estimate and map the aboveground biomass (AGB) values throughout the study area, as shown in the equations below:

Sentinel 1-derived AGB = -32.0684 + 1.7712 * VVOct - 1.8129 * VHJan + 12.6514 * elevation (Equation 5.6)

Sentinel-2 multispectral bands-derived AGB = -9.3577 + 792.5243 * Band 4 - 987.7312 * Band 5 + 234.2441 *Band 7 + 10.082 * elevation (Equation 5.7)

Sentinel-2 vegetation index-derived AGB = -12.7514 + 36.0378 * IRECI + 8.0015 * elevation (Equation 5.8)

Sentinel-2 vegetation cover-derived AGB = -16.067 + 7.474 *LAI + 9.296 *elevation (Equation 5.9)

Figure 5.9 and Figure 5.10 present the biomass maps derived from Sentinel-1 SAR and Sentinel-2 multispectral images, in conjunction with SRTM elevation data. The spatial variation of predicted AGB conforms to those observed in the field. The predicted high biomass areas were in the northern part of the study site which is in agreement with the field observation where closed canopy mangrove forest can be found. Likewise, the lowest AGB estimates were found in the middle to southern part of the study site and consistent with field condition where non-forest land uses that replaced mangroves are usually found.

The accuracy assessment of the Sentinel-based predicted biomass maps revealed that their RMSE values were almost similar (range: 28.05 to 30.92 Mg ha^{-1}), but lowest in Sentinel-2-LAI-derived biomass map and highest in Sentinel-2 optical raw bands-derived map (Figure 5.11). The overall map accuracy ranged from 85.3 % (Sentinel-2 optical raw bands-based map) to 86.6 % (Sentinel-2-derived LAI-based map). Correlation coefficients/agreements (r) between measured and predicted biomass were all significant at 0.01 level and computed at 0.838, 0.821, 0.831 and 0.835 for models derived from Sentinel SAR-, Sentinel-2 multispectral bands, Sentinel-2 IRECI vegetation index and Sentinel-2 LAI datasets, respectively. There was no significant difference between the observed and predicted biomass values for each of the biomass map based on paired t-tests ($p > 0.05$).

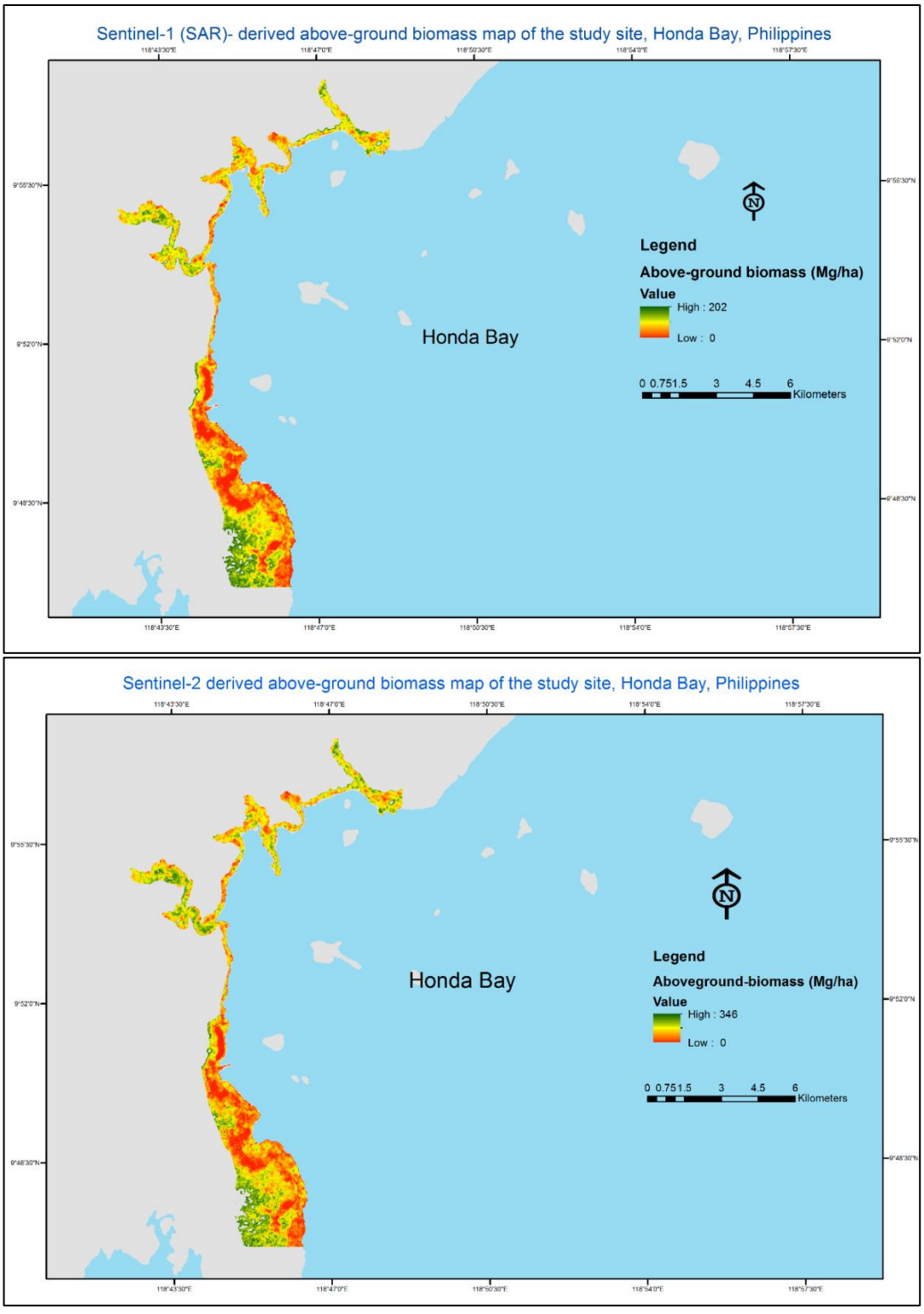

Figure 5.9 Predicted maps of aboveground biomass in the study site derived from biomass models from Sentinel-1 SAR raw channels (top, equation 5.6) and Sentinel-2 multispectral bands (bottom, equation 5.7)

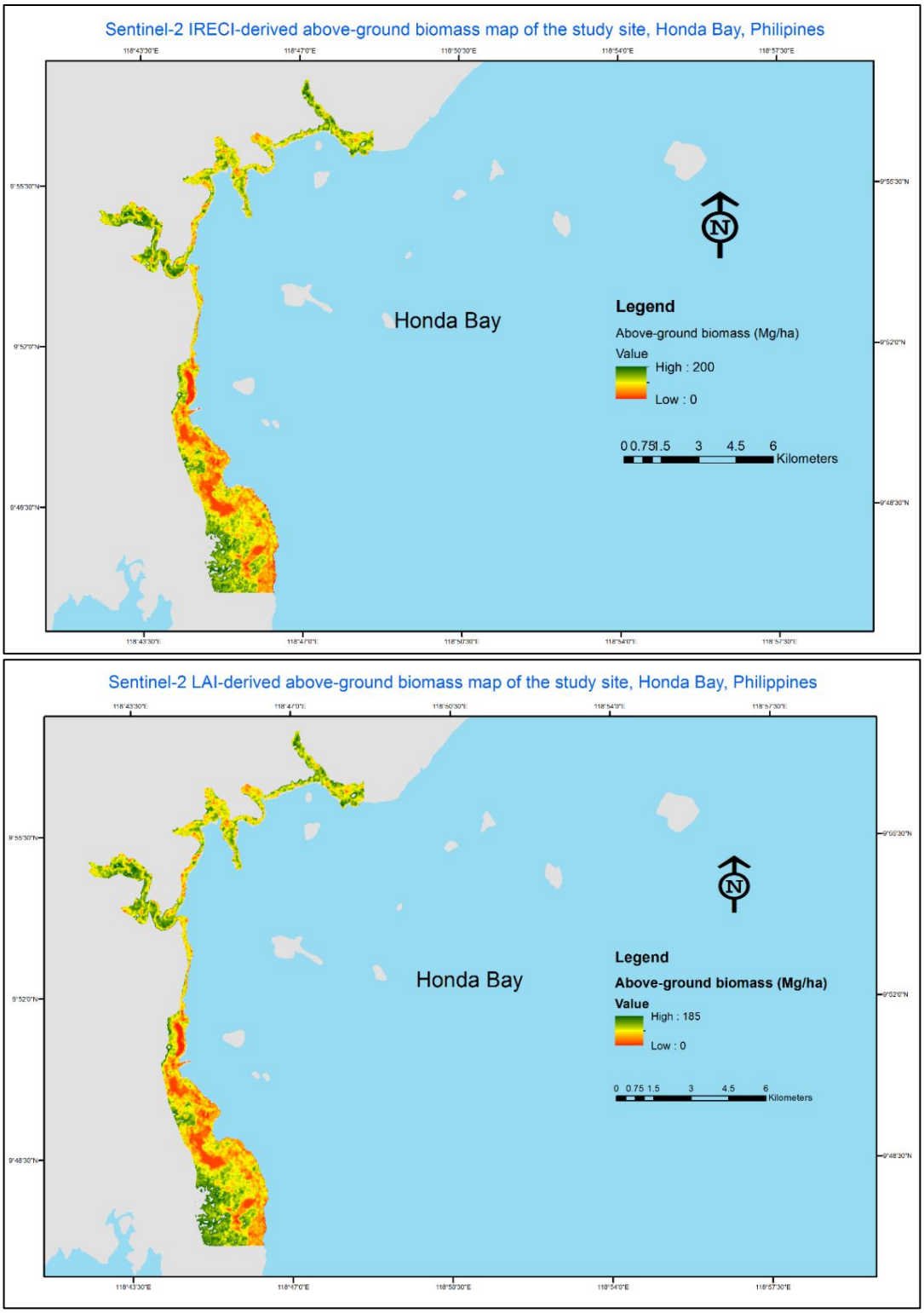

Figure 5.10 Predicted maps of aboveground biomass in the study site derived from biomass models from Sentinel-2 IRECI vegetation index (top, equation 5.8) and Sentinel-2 based Leaf Area Index (bottom, equation 5.9)

Also, among the land uses, the prediction errors for mangrove forest were similar for the four Sentinel-derived biomass maps (36.13 to 38.96 Mg ha^{-1}) but lowest in Sentinel LAI-derived biomass map (Figure 5.12). For coconut plantation biomass, Sentinel-2 optical raw bands-derived biomass map had the lowest prediction error (21.42 Mg ha^{-1}) while the vegetation index (IRECI)-derived biomass map had the highest error (26.7 Mg ha^{-1}). The SAR-derived biomass map had the lowest biomass prediction error for aquaculture ponds, salt pond and cleared mangrove, which are all low biomass area, if not devoid of vegetation. Sentinel-2 multispectral band-derived biomass map had the highest prediction error for the retrieval of biomass from cleared mangrove (25.7 Mg ha^{-1}) compared to the three other biomass maps which had almost similar prediction error (3.5 to 4.5 Mg ha^{-1}).

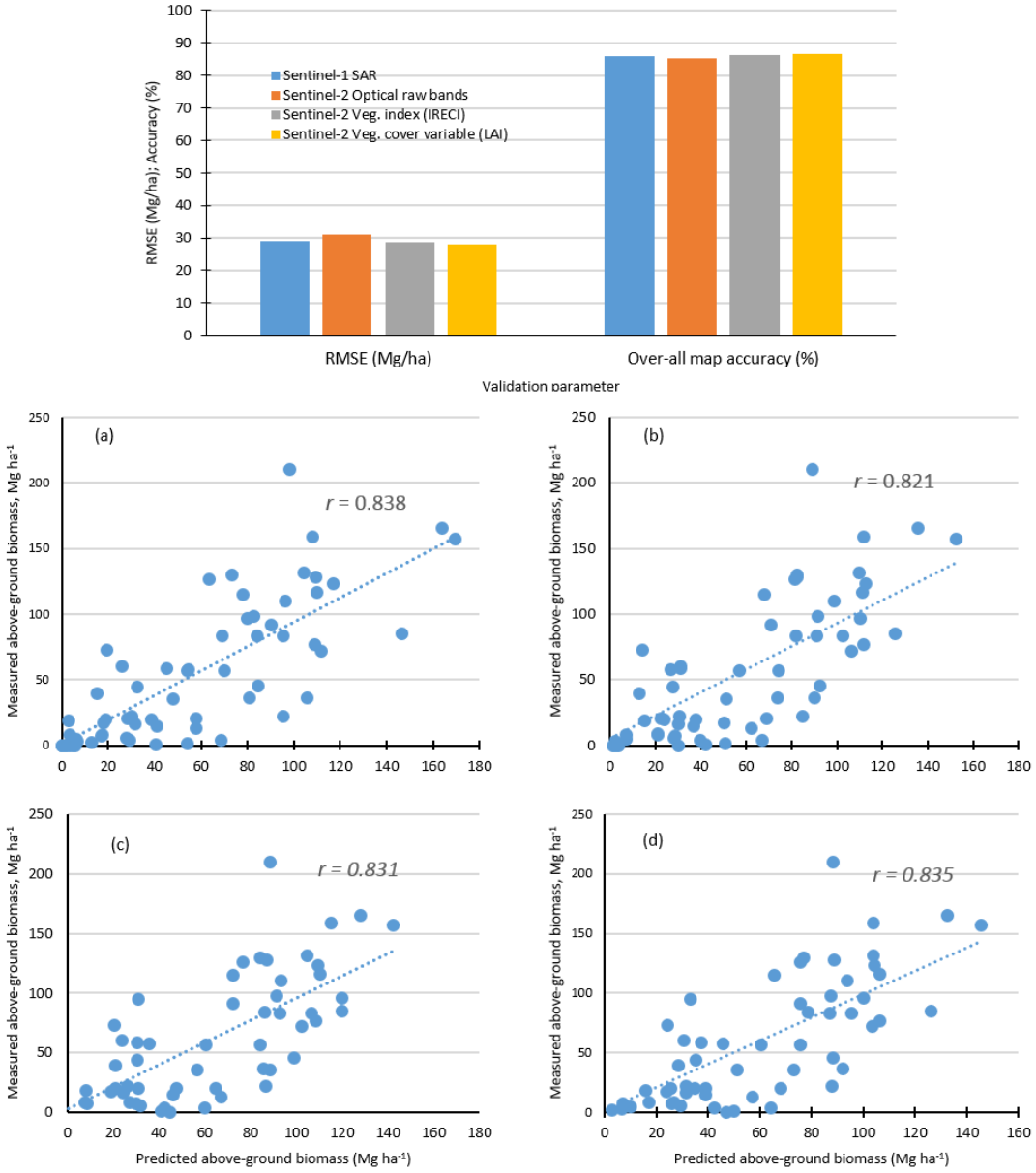

Figure 5.11. Accuracy assessment of predicted biomass maps produced from the four Sentinel-based models (top panel). Scatter plots of observed and predicted biomass values correspond to (a) Sentinel-1-based model, (b) Sentinel-2 multispectral band-based model, (c) Sentinel-2 vegetation index-based model and (d) Sentinel-2 biophysical variable-based model, respectively

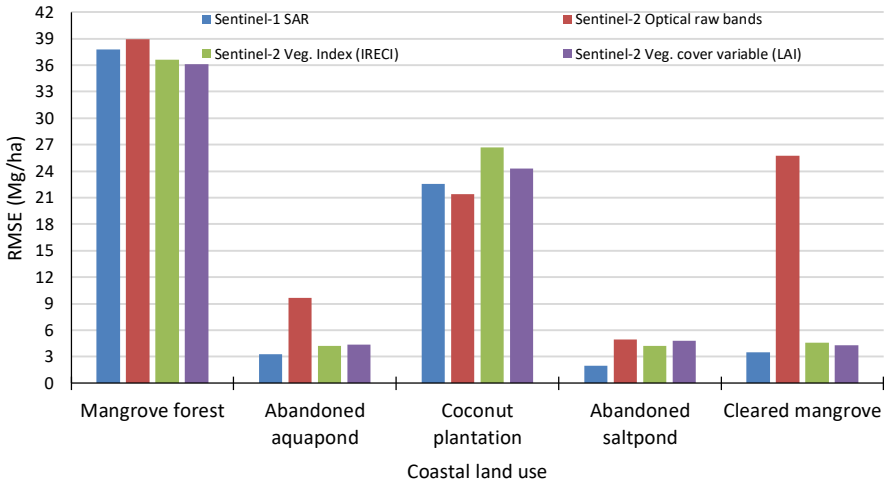

Figure 5.12 Comparative prediction errors of the four Sentinel-based aboveground biomass models for predicting biomass of mangrove forest and the four land uses that replaced mangroves in Honda Bay coast

5.5 Discussion

5.5.1 Relationship of field biomass with Sentinel SAR polarisations and multispectral bands

Single-date SAR VH channel had a higher correlation with biomass than VV polarisation. However, the combination of multi-temporal VH and VV polarisations correlated better with biomass than single-date SAR imagery. Proisy et al. (2003) also reported similar observation for the C-band of the airborne-AIRSAR where cross-polarised HV channel had better correlation with biomass than co-polarised VV channel for both mangrove forests in Northern Australia and French Guiana. Also, Kumar et al. (2012) found that multi-date Envisat ASAR images had a better correlation than single-date ASAR image in retrieving tropical forest biomass in India.

Bands in the Red edge (B6 and B7) and NIR (B8) had a higher correlation with aboveground biomass than bands in the visible (B2, B3, B4) and short wave infrared (B11, B12) regions. Raw band combination in the Red edge (B5 and B6), as well as NIR (B8) and SWIR (B12) bands combination, had strong and better correlation with aboveground biomass than individual raw bands and other raw band combinations. The red edge and NIR regions are bands known to correlate well with

biomass (Sibanda et al. 2015; Dube et al. 2016). In addition, among the Sentinel-derived vegetation indices, NDI45 and IRECI gave the highest correlation with biomass compared to NDVI and other vegetation index evaluated. NDI45 and IRECI are vegetation indices that use red edge bands which are known to relate well with biomass as mentioned above. Also, LAI had better correlation with biomass (r = 0.80) than the other vegetation cover biophysical variables evaluated. This is consistent with the findings of Dusseux et al. (2015) where correlation with biomass was highest with LAI than the other biophysical variable tested (i.e. fPAR). The LAI gives information on the density of vegetation and describes more accurately the status of vegetation compared to other canopy variables (Dusseux et al. 2015).

Among the Sentinel predictor groups, the highest correlation with biomass was obtained when elevation was included as covariate. This is consistent with the results of Jachowski et al. (2013) for their mangrove biomass estimation in Thailand where the best biomass model was from the combination of multispectral bands and elevation. Elevation and tree height in mangrove area are related (Simard et al. 2006; Fatoyinbo et al. 2008; Aslan et al. 2016) probably due to the close proximity of mangrove to the sea where elevation is usually set as zero. Tree height and biomass are allometrically related (Cintron & Novelli 1984; Chave et al. 2005; Komiyama et al. 2005).

5.5.2 Accuracy assessment of biomass prediction

The LAI-based model derived from the Sentinel-2 image was more accurate in predicting the overall aboveground biomass of the different coastal land uses studied, out-performing the models based on SAR raw polarisation backscatter, raw multispectral bands and multispectral-based vegetation index. The lowest accuracy was observed for optical raw band-based model. Comparing the prediction per land use, the LAI-based model was also the best model for predicting mangrove biomass. The result is consistent with the study of Dusseux et al. (2015) and Saatchi et al. (2007) where LAI-based biomass model also gave the highest prediction for biomass compared to models based on vegetation index and other vegetation cover variables. However, the Sentinel SAR-based model was more accurate in predicting the biomass in the usually deficient to low vegetation cover non-forest replacement land uses such as abandoned aquaculture pond, cleared mangrove and abandoned salt

pond. This is probably due to its ability to accurately detect non-vegetated areas such as water and open area whose surface are smooth to radar wave and with low backscatter coefficient compared to vegetation (Kumar et al. 2012; Kumar et al. 2015; Sinha et al. 2015). C-band SAR, as in the case of Sentinel-1, is favoured for biomass study of low biomass sites such as forest clearings, grassland and forest regeneration sites because of its stronger backscattering in these areas as compared to L and P bands (Sinha et al. 2015).

Using Sentinel-1 SAR and Sentinel-2 multispectral imagery data can give good results in the retrieval and predictive mapping of the aboveground biomass of mangroves and the replacement non-forest land uses, especially with the inclusion of elevation data. Agreement/correlation of predicted and observed biomass values from the Sentinel-1 SAR biomass model was 0.83. This value is almost similar to the value reported for Radarsat SAR (0.84) reported by Li et al. (2007) but lower than the value reported for PALSAR (0.91; Thapa et al. (2015) as shown in Table 5.6. Sentinel-1 and Radarsat are both in C-band, which has a shorter wavelength than the L-band in PALSAR that has higher canopy penetration capability (Sinha et al. 2015). For Sentinel-2 biomass models, the agreement between the predicted and observed values was 0.83. This value is the same for biomass prediction using ALOS VNIR-2 reported by Wicaksono et al. (2016), slightly higher than the biomass model derived from GeoEye-1 (0.81; Jachowski et al. (2013), higher than Landsat-based model (0.67; Li et al. (2007), but lower than the IKONOS-based model (0.93; Proisy et al. (2007). In addition, for Sentinel-1 model, the prediction error (RMSE) is comparable with the error reported by Thapa et al. (2015) on PALSAR, within the range computed by Simard et al. (2006) but higher than the error reported by Li et al. (2007). For Sentinel-2 model, the prediction error obtained in this study is much lower than the error reported by Jachowski et al. (2013) from using GeoEye image and Proisy et al. (2007) for IKONOS (Table 5.6).

Overall, the results obtained in this study are comparable to the previous studies above. However, one of the key benefits in using Sentinel imagery is that both the SAR and multispectral images are available, is free of charge, comes with open-source processing software (SNAP) and has a discussion forum for queries. This availability is important especially in developing countries in the tropics where

funds for the imagery and software procurement are limited and where there is persistent cloud cover, especially during rainy season.

Also, compared to other free imagery, Sentinel-1 and Sentinel-2 have higher spatial and temporal resolutions. Sentinel imagery have larger swath width compared to commercial imagery, which can be advantageous in mapping for biomass in regional and national coverage. Potential issues with the use of Sentinel imagery may include difficulty in downloading and pre-processing of the imagery due to large imagery files (from the many bands and larger swath width), especially with the increased demand for the imagery in the future. These can be an issue for developing countries with slow internet connection and limited funding for the procurement of high-speed computer processor and larger memory.

It is acknowledged, however, that the biomass estimations here are not from destructive sampling but by using allometric biomass equations. The true accuracy of models depends on how accurate are the field-based measurements. The agreement/correlation between the predicted and observed biomass values (i.e. 0.82 to 0.83) suggest that there is a good potential for the retrieval and mapping of biomass in mangrove area in using the Sentinel imagery. The method used in the study allowed to generate cross-validated coastal biomass maps predicted from this free, open-source imagery. The predictive biomass maps produced could be used as a baseline for which to compare results from future intervention such as reforestation.

Table 5.6 Satellite-based biomass retrieval and mapping studies in mangrove area

Sensor	Correlation/agreement of predicted and observed values	RMSE (Mg/ha)	Source
Radar			
Sentinel-1 SAR	*0.83*	*27.75*	*This study*
SRTM SAR	0.50	146.88	Aslan et al. (2016)
PALSAR	0.91	28.39	Thapa et al. (2015)
Radarsat SAR	0.84	9.46	Li et al. (2007)
SRTM SAR	0.82	20-40	Simard et al. (2006)
Multispectral			
Sentinel-2	*0.83*	*28.02*	*This study*
ALOS VNIR-2	0.83	Not reported	Wicaksono et al. (2016)
GeoEye	0.81	53.4	Jachowski et al. (2013)
IKONOS	0.93	42	Proisy et al. (2007)
Landsat	0.67	7.38	Li et al. (2007)

Furthermore, Sentinel-1A was launched on April 3, 2014. The earliest available image that covered the study site was only on October 31, 2015. The three Sentinel-1A images used in the study were, in fact, the earliest first three images in GRD mode available for the study site. On the other hand, Sentinel-2A was launched on June 23, 2015. The earliest available Sentinel-2A image that covered the study site was only on January 12, 2016. The next earliest dates were February 11, 2016 and April 11, 2016. However, the images for January and February 2016 were both cloudy, thus the April 11, 2016 image was the one used. Therefore, the imagery data used in the study were the closest to the field data acquisition time. The time elapsed between the field data collection and image acquisition (i.e. three to five months for Sentinel-1, and eight months for Sentinel-2) is acknowledged.

However, considering the available Sentinel images for the study site, it was assumed that the difference in field biomass is still negligible after three to eight months have passed (i.e. field data collection was conducted from June 2015 to July 2015). The mangrove forests and coconut plantation that were studied are all mature stands and presumed in a steady state. Also, five (i.e. December, January, February, March and April) of the eight months elapsed time were dry season months where growth is minimum. Indeed, Proisy et al. (2007) in mapping the mangrove biomass

in French Guiana also considered the time difference of 1 year between field data acquisition and imagery date as "not required" for biomass value adjustment. Future studies should consider using Sentinel images as close as possible to the field data collection to avoid the assumption that was made, considering that the Sentinel-1 and Sentinel-2 are now on their routine data collection.

5.6 Conclusion

Sentinel-1 (SAR) and Sentinel-2 (multispectral) image data can be used for biomass retrieval and mapping in the coastal land uses, mangrove and non-mangrove alike, of Honda Bay and adjacent coastal areas in Puerto Princesa City, Philippines. The prediction accuracy is comparable to imagery from current commercial sensors. High correlation values (r = 0.84) between biomass and Sentinel imagery data were obtained from the combination of dual-date SAR VH and VV channels, red and red edge bands, red edge-based vegetation indices and leaf area index, respectively. The developed Sentinel-based models can explain 67 % to 69 % of the biomass variance, with prediction error of < 29 Mg ha^{-1} while the output predictive biomass maps had prediction accuracy of 85.3 % to 86.6 % and agreement/correlation (r) of observed and predicted biomass value of 0.82 to 0.84. The Sentinel SAR-based model was more accurate in predicting the biomass in the usually deficient to low vegetation cover non-forest replacement land uses such as abandoned aquaculture pond, cleared mangrove and abandoned salt pond. The study indicates satisfactory results to map the coastal land uses in the study area.

The free and open-source Sentinel imagery in both SAR and multispectral data and the associated open-source SNAP software should encourage the conduct of biomass mapping and monitoring in the coastal zone of resource-poor countries especially in the tropics. In addition, the methods developed might be used to map and estimate the aboveground biomass of mangrove and non-forest land uses in the coastal zone similar to the study site. Follow-up studies should aim for the generation of DEM from Sentinel-1 InSAR in order to test its capability for biomass retrieval and mapping in combination with Sentinel backscatter and multispectral data.

In addition, the accuracy of the map might be improved with additional plots distributed strategically in areas far from the current plots, and additional sites for each land use especially for coconut plantation, abandoned saltpond and cleared mangrove. Lastly, the use of various data transformation techniques, as well as non-linear multiple regression forms, should be also pursued with the aim of finding the highest correlation for predicted and observed value, and lower prediction error compared to the current values. The results of the study could be useful for monitoring the status of mangrove plantings in the region.

The next Chapter, Chapter 6, will present and discuss the soil C stock quantification and predictive mapping in mangroves and replacement land uses.

Chapter 6

SOIL C QUANTITIES OF MANGROVE FORESTS, THEIR COMPETING LAND USES, AND THEIR SPATIAL DISTRIBUTION

6.1 Introduction

The Literature Review mentioned the knowledge gap on carbon (C) loss in soil and biomass of the on-going mangrove conversion. Studies are growing on quantifying the C stocks of mangrove forests while very few has been reported on land uses that replaced mangroves. It is not surprising, therefore, that most estimates of C losses from soil owing to mangrove conversion are based only on assumptions. Also, the application of geostatistical technique such as Kriging in soil C stock mapping in mangrove has not been reported in the literature as compared with inland terrestrial soils.

While Chapters 4 and 5 discussed about the biomass, the present Chapter and Chapter 7 dealt on soils in intact and deforested mangrove area. In this Chapter, the soil C stocks of mangrove forests with the non-forest land uses that competed and replaced mangroves (i.e. aquaculture pond, salt pond, coconut plantation and cleared mangrove) were evaluated and compared. Specifically, this Chapter aimed 1) to quantify the soil C stocks of mangrove forest under closed and open canopies and their competing land uses; 2) examine the relationship between soil C stock and site variables; and 3) to model the spatial distribution of soil C stock in the study site. Results from this study could help inform current discussions on Blue Carbon (Howard et al. 2014) and in including mangroves under REDD+, and for policy and program development that advance soil C conservation in forested coastal wetlands.

This Chapter is arranged into six sections as follows: 1) Introduction, 2) Background literature on soil C stock accounting in mangrove soil, 3) Methods, 4)

Results, 5) Discussion, and 6) Conclusion. This Chapter has been published in the journal *Geoderma* (Castillo et al. 2017) with some reformatting done to suit the format of the Thesis.

The new and significant contributions of this Chapter include: 1) the evaluation of the soil C stocks of not only mangrove forests and aquaculture ponds but also other land uses that replaced mangroves such as coconut plantation, cleared mangroves and abandoned salt pond; and 2) the application of GIS-based Kriging for predicting and mapping the soil C stocks in mangrove area.

6.2 Soil Carbon stock accounting and mapping in mangrove area

Mangrove forests in the tropical and subtropical coastal regions are important ecosystems that provide goods and services, including C sequestration and storage functions. Mangroves are increasingly recognised as a huge storage of C, storing at least two to three times higher than terrestrial forests (Donato et al. 2011; Pendleton et al. 2012; Kauffman et al. 2016). They are the most productive ecosystem in the coastal zone sequestering a net of 11.1 Mg C ha^{-1} $year^{-1}$ in aboveground biomass (Alongi 2014). At least half of total C stock in mangroves is stored in the soil (Donato et al. 2011; Murdiyarso et al. 2015; Kauffman et al. 2016).

However, there has been massive global mangrove deforestation in the past, i.e. 0.75 % to 2.1 % are lost annually, converting mangrove forests to other land uses such as agriculture and aquaculture (FAO 2007; Giri et al. 2011; Thompson et al. 2014). The conversion of mangrove forests to other land uses still continue in many parts of the globe. In Southeast Asia, more than 100,000 ha of mangrove forests were deforested and converted during 2000–2012 to other non-forest land uses especially aquaculture (Richards & Friess 2016). The disturbance of mangrove forest, especially in its soil, will release a significant amount of C back to the atmosphere in the form of CO_2 (Alongi 2012).

Soil is considered as one of the largest global C pool, next to oceanic and geologic pools. The soil organic C exceeds the amount of C in the atmospheric and

biotic global pools (Lal 2008; Maraseni & Pandey 2014). Wetland soil covers an area of 5,961 x 10^3 km^2 and contains 513 Pg of organic C globally (Bridgham et al. 2006). It, therefore, has a high C stock per unit area that is susceptible to mineralisation when disturbed. When mangrove forests are converted to other land uses, trees and other vegetation are removed which in effect stops the sequestration of atmospheric C (Chmura et al. 2003; Navarrete & Tsutsuki 2008). When mangroves are converted into aquaculture ponds, the soil top layer (1.5m - 2m) is excavated exposing and oxidising C-rich soils (Eong 1993; Thompson et al. 2014).

While some studies have been conducted on mangrove soil C stocks (see for example Donato et al. 2011; Kauffman et al. 2011; Tue et al. 2014; Murdiyarso et al. 2015), our knowledge on how C stocks of mangrove forests compare with those of non-forest land uses that replaced them is still limited. Such knowledge is important for accurately estimating the impact on C stocks of and emissions due to land use change. In terrestrial ecosystem, the conversion of forest to agriculture results in the loss of 20-50 % soil C (Lal 2005), while the conversion of native scrubland to cultivation lost about 60 % of soil C (Maraseni 2007; Maraseni et al. 2008). There is limited knowledge if the same magnitude is true when mangrove forests are converted into other non-forest land uses. The assessment of soil C stocks in soils of mangrove and their comparison with non-forest land uses is important in determining emission baselines (Adame *et al*. 2013), in estimating soil C for trading (Maraseni & Pandey 2014), and for land use decision-making in the coastal zone.

Previous studies on soil C stocks in mangrove forest and other land use in the coastal zone were done using sample plots (e.g. Donato et al. 2011; Kauffman et al. 2011; Murdiyarso et al. 2015; Kauffman et al. 2016). Scaling up to above plot-level (i.e. study site, bay/landscape and region) will increase our understanding of the spatial distribution and variability of soil C stocks in the coastal zone and will help improve estimates of soil C stocks and emissions. While spatial interpolation technique such as Kriging has been used in inland terrestrial soils to generate site-scale soil C stocks, its application in mangrove soil is not yet well understood.

6.3 Methods

6.3.1 Study Site

Mangrove forests and the non-forest land uses that replaced mangroves were investigated for their soil C stocks (Table 6.1). These coastal land uses were studied in the coast of Honda Bay. The non-forest coastal land uses were historically occupied by mangroves prior to their conversion. Detailed description of the study site is provided in Chapter 3.

Table 6.1 Characteristics of sampling sites in Honda Bay, Palawan, Philippines

Land use	Dominant Species	Location	Soil Depth (cm)	Pore water Salinity (ppt)	Elevation (masl)
A. Mangrove forest					
Closed canopy mangrove					
Closed 1	*Rhizophora apiculata*	N9.903^0, E118.74376 to N9.89866^0, E118.72935^0	236	16.8	8.3
Closed 2	*R. mucronata*	N9.93048^0, E118.75513^0 to N9.93988^0, E118.75481^0	300[1]	21	7.8
Closed 3	*R. apiculata*	N9.93953^0, E118.8002^0 to N9.95895^0 to E118.78475^0	231	22.6	9.4
Open canopy mangrove					
Open 1	*R. apiculata*	N9.83041^0, E118.7477^0 to N9.82923^0, E118.75033^0	195.9	32	3.6
Open 2	*R. apiculata*	N9.86631^0, E118.74291^0 to N9.8642^0, E118.74421^0	79.3	21.9	4.5
Open 3	*Ceriops tagal*	N9.80515^0, E118.76605^0 to N9.80828^0, E118.76936^0	33.9	79.3	3.6
B. Non-forest land uses that replaced mangroves					
Abandoned aquaculture pond					
Aquapond 1	None	N9.80615^0, E118.75575^0	63.3	26.7	1
Aquapond 2	None	N9.81263^0, E118.74971^0	90	34.9	1.2

Table 6.1 continued

Aquapond 3	*R. apiculata*	N9.83698^0, E118.74035^0	99.2	39.2	1.2
Coconut plantation					
Coconut	*Cocos nucifera*	N9.814483^0, E118.74575^0	51.2	16.1	3.5
Abandoned Salt pond					
Saltpond	none	N9.83433^0, E118.74026^0	79.2	53.8	1.4
Cleared mangrove					
Cleared	none	N9.80813^0, E118.75678^0	69.7	68.2	1

data are mean; ppt – parts per thousand; masl – meters above sea level

[1]the depth is at least 300 cm since the soil is deeper than the 300-cm soil auger and depth rod.

6.3.2 Field sampling design and soil C stock accounting

Mangrove forests (represented by closed canopy mangrove and open canopy mangroves) and competing land uses of mangroves represented by abandoned aquaculture pond, coconut plantation, abandoned salt pond and cleared mangrove were investigated for their soil C stocks and other soil properties. The study site was stratified based on land use. In each land use, sites were selected through simple random sampling. The mangrove forests had three sites for closed canopy stand and another three sites for open canopy mangroves. The land uses that replaced mangroves also had three sites for abandoned aquaculture ponds. However, the non-aquaculture land uses had only one site each due to access restriction to other coconut plantations and absence of other sites for abandoned salt pond and cleared mangrove. For mangrove forests, three transects were established in each site except in one thin open canopy mangrove where only two transects were made. In each transect, three circular plots with 7m radius were established 50 m apart along a line established parallel to the coast (Figure 6.1). Each transect was located near the sea (seaward), middle/midstream and near the land/upstream (landward) to cover the natural tidal gradient in a mangrove ecosystem (cf. Kauffman & Donato 2012). For non-forest land uses, only two transects were established at each site, but each transect also has three 7 m circular plots spaced about 25 m apart, except for the salt pond where an additional transect was formed. In total, 90 plots were sampled, of which 51 plots were in mangrove forests. The whole process of soil C accounting adopted in this study is summarised in Figure 6.2

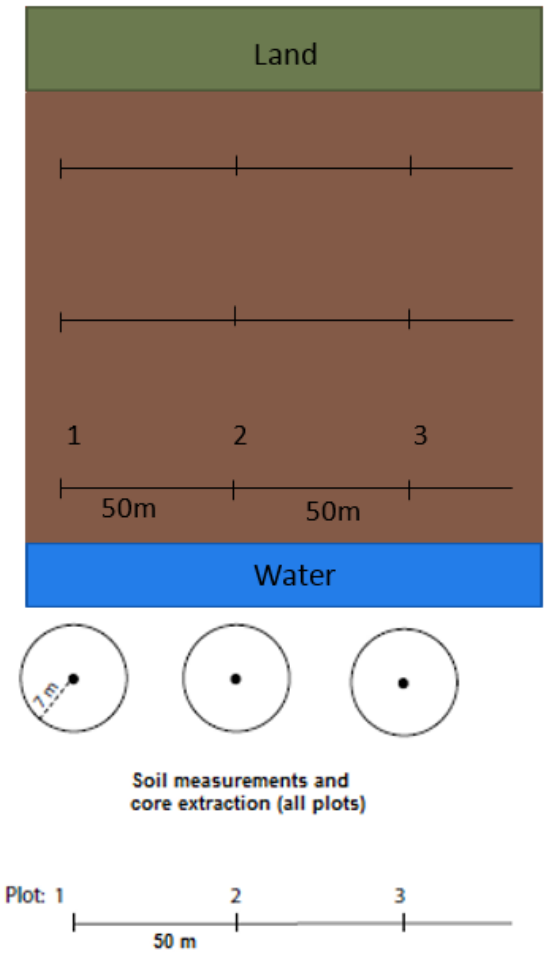

Figure 6.1. Plot layout for soil C sampling
Source: Kauffman and Donato (2012), modified

6.3.3 Soil sampling and laboratory analysis

Soil measurements, collection and analyses were done in each of the plots, following the method of Kauffman and Donato (2012). In each plot, soil core was taken from an undisturbed spot nearest the centre by driving an open-face stainless steel tube peat auger capable of obtaining sample to a depth of 300 cm (Figure 6.3). Each core was divided into depth intervals of 0-15 cm, 15-30 cm, 30-50 cm, 50-100 cm, and >100 cm if parent materials (marine sand/sediment or rock) were not encountered before the depth of 100 cm. A 5-cm sample was taken in the middle of each layer, stored in a labelled container and brought to the laboratory for oven drying and analysis. In each plot, soil depth to parent material was measured three times near the centre by driving a graduated aluminium rod until refusal. The rod is

300 cm in length, the inference limit of the study. In addition, *in situ* pore water salinity was measured using refractometer and pore water pH, redox potential and temperature using hand-held pH-mV-temperature meter (*Aqua pH 2.2, TPS, Australia)*. The geographic coordinates of each plot were determined using a handheld *Garmin* GPS receiver.

Samples were oven-dried to constant weight at 60 ^{0}C and were weighed individually for bulk density (BD) determination. Dry samples were grounded, homogenised and brought to Analytical Services Laboratory of the International Rice Research Institute in Los Baños, Laguna, Philippines for C and N concentrations (% mass) by dry combustion method using *Thermo Finnigan Flash Elemental Analyzer 1112*. The inorganic C was not measured as it was assumed to be be negligible/minimal (see Donato et al. 2011) since the study site has no nearby karst formation, coral reefs and seagrass beds, and is associated with rivers.

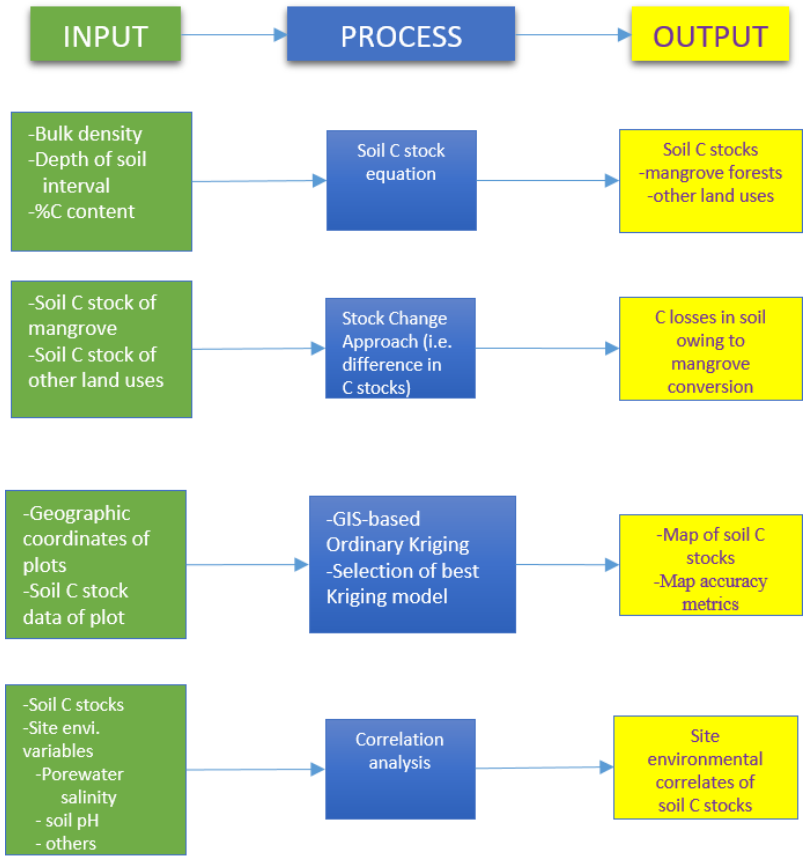

Figure 6.2 Input-Process-Output model for soil C accounting component of the Thesis

6.3.4 Soil C Stock Estimation

Soil C stock (Mg C ha^{-1}) per depth interval was computed as the product of BD (g cm^3), depth interval (cm) and % C content, and were added together to get the total soil C stock per site, following Kauffman and Donato (2012). BD (g cm^{-3}) was computed as the ratio of the dry weight (g) of soil sample over its fresh volume (cm^{-3}).

6.3.5 Statistical Analysis

The soil C stocks of mangrove forests and their competing land uses were compared using Analysis of Variance (ANOVA). If the difference is significant, Tukey's posthoc test (or Games-Howell if the variance is not homogenous from Levene's test) was employed to determine which of the land uses are different. The normality of the data was assessed using Shapiro-Wilk Test and visually inspected using the histogram and Quantile-Quantile (QQ) plot. Correlation analysis was performed using Pearson's correlation to determine if the relationship between soil C stock and soil parameters exist. ANOVA and Tukey's posthoc test are used for comparing means of measurements for three or more categories (Zaiontz 2015; McDonald 2016). Kauffman et al. (2011), Kauffman et al. (2013), Adame et al. (2015) and Tue et al. (2014) also used the tests for their wetland C stocks studies. Statistical analysis was performed using IBM SPSS Statistics version 22.


a


b


c


d


e


f


g


h


i


j

Figure 6.3 Soil site data and core samples collections

a) measuring the soil depth, b) measuring porewater pH, temperature, c) driving the soil auger into the mangrove soil, d) soil auger with the 2-m extension arm, e) soil sampling in mangrove forest, f) soil sampling in abandoned aquaculture pond, g) collected soil core, h) soil core being prepared for partitioning, i) partitioning the soil core by soil layer j) collection of the 5 cm soil sample for laboratory analysis.

6.3.6 Spatial Modelling of Soil C Stock

To generate a map of soil C stock spatial distribution and variability for the entire study site, spatial interpolation of soil C stocks was done using Ordinary Kriging method. The Kriging interpolation was done independently each for mangrove forests and their competing non-forest land uses. Non-forest land uses that were not under study such as built-up areas, paddy and others were excluded in the interpolation and was given a "No Data" pixel value. The generated maps were then mosaicked together to form a seamless spatial distribution map of soil C stock. The spatial modelling and analysis were implemented in *Geostatistical Analyst* and *Spatial Analyst* extensions of *ArcMap* 10.3 (ESRI, CA, USA) using 10 m x 10 m pixel size. Ordinary Kriging, as successfully used in a number of soil studies (Mishra et al. 2009; Umali et al. 2012; Kucuker et al. 2015), was applied in this study to estimate the value of soil C stock at unsampled locations as expressed in the following equation:

$$\hat{Z}(x_o) = \sum_{i=1}^{n} \lambda_i Z(x_i)$$

where:

$\hat{Z}(x_o)$ is the estimate of soil C stock (MgC ha^{-1}) at location x_o;

$Z(x_i)$ is the measured value of soil C stock at x_i locations; and

λ_i are weights of measured x_i locations surrounding location x_o.

The Kriging estimate at unsampled location is the linear weighted sum of adjacent measured data points (Mishra et al. 2009). The weights are not only based on distance but also on the overall spatial relationships among measured data points around the location being predicted (Johnston et al. 2001). A detailed theoretical description of Ordinary Kriging is discussed in Johnston et al. (2001). In this study, several model types were tested (Table 6.2) and were ranked according to their Pearson correlation coefficient (*r*) and Root Mean Square Error (RMSE):

$$\text{RMSE} = \sqrt{\frac{1}{n}\sum_{i=1}^{n}(x_i - y_i)^2}$$

where:

x_i = measured soil C stock value of ith *sample*;

y_i = predicted soil C stock value.

A set of 51 data points for mangroves and 39 for non-mangroves were used in each spatial interpolation. To evaluate the performance of several models, the observed and predicted soil C stock values were plotted and regressed, and their *r* values were computed. Cross-validation was done using the Leave-One-Out (LOO) approach to give an idea of how well the model predicted the unknown values as indicated in their RMSE. Using this approach, each sample was excluded sequentially, with a model built using the remaining samples to predict the value of the excluded sample, and compared it to the measured value (Johnston et al. 2001; He & Guo 2006; Jachowski et al. 2013). The extent of current mangrove cover in the study area, as well as the four non-forest land use areas, were digitised from a high-resolution image of the study site as viewed from Google Earth (Google Inc., USA).

6.4 Results

6.4.1 Soil depth, BD and C content

Soil depth was considerable in mangrove forests (i.e. 255.6 cm for closed canopy mangrove and 106 cm for open canopy mangrove; Table 6.1). In contrast, the soil depth of aquaculture ponds and the rest of non-forest land uses that replaced mangroves were significantly lower ($p < 0.05$) and did not exceed 100 cm, i.e. 84 cm for abandoned aquaculture ponds, 51.7 cm for the coconut plantation, 79.2 cm for the abandoned salt pond and 69.7 cm for the cleared mangrove.

In addition, the mean BD of mangrove forests (0.56 g cm^{-3}) was lower than their competing land uses (0.77 g cm^{-3} for abandoned aquaculture ponds to 1.35 g cm^{-3} for the coconut plantation) except for the cleared mangrove (0.62 g cm^{-3}; $p < 0.05$; Table 6.2). The effect of mangrove conversion to other land use was prominent

in the topmost soil layer (0-15 cm) of the competing non-forest land uses (mean: 1.15 g c m^{-3}, range: 0.95- 1.36 g cm^{-3}), compared to mangrove forests' much lower BD in the same soil layer (0.53 g cm^{-3}; $p < 0.05$). Some 54% of non-forest plots had BD of $\geq$ 0.89 g cm^{-3} while 50% of the mangrove forest plots had BD of < 0.55 g cm^{-3}. Mean BD of closed canopy mangroves (0.53 g cm^{-3}) and open canopy mangroves were not significantly different ($p = 0.68$) and the former represented only 39 % of the coconut plantation (1.35 g cm^{-3}), 51 % of the abandoned salt pond (1.03 g cm^{-3}) and 68 % of abandoned aquaculture ponds (0.77 g cm^{-3}).

Furthermore, the mean soil C content (%) in mangrove forests (8.64 %) was significantly higher as compared to their competing land uses especially the coconut plantation (0.54 %) and the abandoned salt pond (5.2%; $p < 0.05$). The mean soil C content of the four competing non-forest land uses was only 5.55 % which was significantly lower than that in mangroves ($p < 0.05$). The effect on soil C content of mangrove conversion to other land uses was also noteworthy in the topsoil (0-15 cm) layer (mangroves: 9.4 % vs. competing land uses: 4.3 %; $p<0.05$). Soil C content of topsoil (0-15 cm) in closed canopy mangroves (8.47 %) and open canopy mangrove forests (10.28 %) were significantly higher than aquaculture ponds (2.9 %), the salt pond (4.1 %) and the coconut plantation (0.8 %; $p <0.05$). In general, the % C decreased with depth across land use types.

Table 6.2 Bulk density and % C of soil under mangrove forests and their competing land uses in Honda Bay, Philippines

Land Use	Soil core depth interval (cm)				
	0-15	15-30	30-50	50-100	>100
A. Mangrove Forest					
1. Closed canopy mangrove					
Bulk density	0.48	0.49	0.52	0.50	0.62
%C	8.47	6.64	7.54	8.73	6.43
2. Open canopy mangrove					
Bulk density	0.59	0.57	0.52	0.63	0.65
%C	10.28	9.56	10.50	9.48	8.74
Mean					
Bulk density	0.54	0.53	0.52	0.57	0.65
%C	9.4	8.1	9.02	9.11	7.59
B. Competing land uses					
1. Aquaculture pond					
Bulk density	0.95	0.72	0.68	0.75	
%C	2.91	7.64	10.25	8.08	
2. Coconut plantation					
Bulk density	1.36	1.36	1.30	1.47	
%C	0.77	0.54	0.34	0.46	
3. Salt pond					
Bulk density	1.15	1.06	0.80	1.09	
%C	4.11	4.65	8.23	4.01	
4. Cleared mangrove					
Bulk density	0.43	0.55	0.71	0.66	
%C	9.31	13.3	7.57	6.7	
Mean					
Bulk density	0.97	0.92	0.87	0.99	
%C	4.3	6.5	6.6	4.8	

6.4.2 Soil C Stock

The mean C stock was higher in mangrove forests (851.93 Mg C ha^{-1}) compared to the non-forest land uses that replaced mangroves ($p < 0.05$, Figure 6.4). C stocks in the aquaculture ponds, salt pond, cleared mangrove and coconut plantation were only 53 %, 47 %, 48 % and 5 %, in that order, of mangrove forests. Among mangroves, closed mangrove forests had higher C stock (1,040 Mg C ha^{-1}) than open canopy forests (640 Mg C ha^{-1}; $p < 0.05$). Mean C stock of non-forest land uses was 365.15 Mg C ha^{-1}. Overall, the reduction in soil C stock due to land use conversion in mangroves ranged from 398 to 809 Mg C ha^{-1} (mean: 486.8 Mg C ha^{-1}) or a decline of 57 % in soil C stock, on the average. The decrease in soil C stock in mangrove soil could indicate soil C losses and emissions due to the conversion of mangrove forests to other land uses.

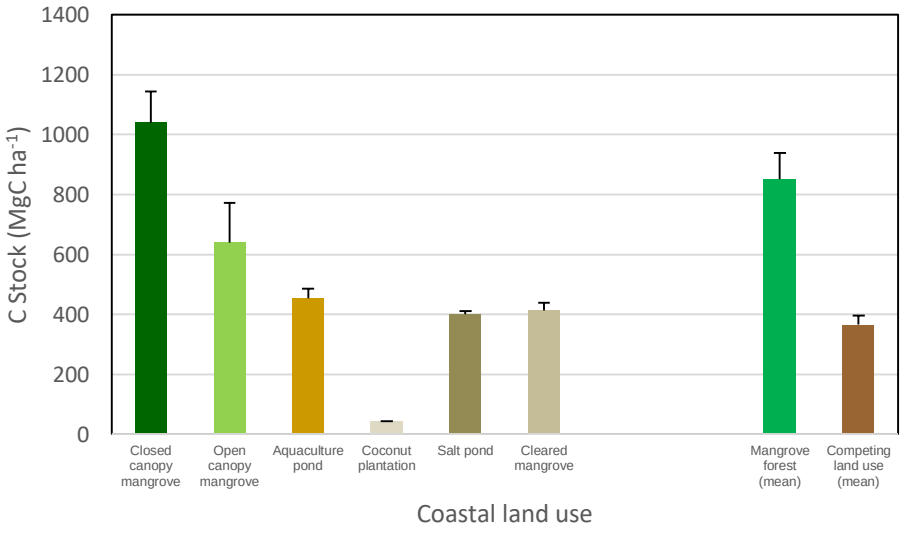

Figure 6.4 Soil C stocks of mangrove forests and their competing land uses in Honda Bay, Philippines

Significant positive relationship existed between soil C stock and total soil depth in mangrove forests ($r = 0.51$, $p<0.01$) and their competing land uses ($r = 0.71$, $p <0.01$), as well as with soil salinity (mangrove: $r = 0.32$, $p<0.05$; non-mangrove: *$r = 0.45$, $p<0.01$)*. There were no significant relationships between soil C stock and porewater pH, temperature or redox potential (Table 6.3).

Table 6.3 Relationship (r) between soil C stock and site variables in mangrove forests and competing land uses

Variable	Mangrove forest	Land uses that replaced mangroves
Soil depth (cm)	0.51**	0.71**
Salinity (ppt)	0.32*	0.45**
pH	-0.05	-0.19
Redox Potential (mV)	0.02	0.19
Soil temperature	0.17	-0.20

* Correlation is significant at the 0.05 level (2-tailed).
**Correlation is significant at the 0.01 level (2-tailed)

6.4.3 Mapping the Soil C Stock

For mangrove forest, the Stable model type gave the lowest RMSE and highest correlation coefficient, while it was the Exponential model type for non-forest land uses (Table 6.4). These models were then used to predict and map the spatial distribution of soil C stocks in the study site for the mangrove forest and non-forest land uses, respectively. The slope of the best-fit line of the Ordinary Kriging model was 0.69 for mangrove and 0.73 for non-forest land uses, short of 0.31 and 0.27, respectively, for a 1:1 ratio of predicted vs. measured values. This means that the model overestimates the prediction at low values and underestimate the high values, which is typical of Kriging model (Johnston et al. 2001). Nevertheless, the overall prediction certainty is about 83.7% (RMSE = 16.3%) for mangrove and 85.7% (RMSE = 14.3%) for competing non-forest land uses based on the normalised RMSE, which may be sufficient for general site-scale estimation purposes.

Table 6.4 Comparison of Ordinary Kriging model types applied to the dataset

Model type	RMSE	ME	*r*
A. Mangrove forest			
1. Stable	346.97	13.06	0.83
2. Exponential	353.09	10.61	0.82
3. Spherical	355.04	16.71	0.82
4. Gaussian	354.25	14.18	0.82
5. Circular	356.59	14.35	0.82
B. Non-forest land uses			
1. Exponential	123.82	-0.13	0.76
2. Spherical	125.25	0.30	0.75
3. Stable	126.67	-0.23	0.75
4. Circular	126.11	0.43	0.75
5. Gaussian	132.45	0.41	0.72

RMSE = Root Mean Square Error ME = Mean Error
r = correlation/agreement of observed and predicted values

Figure 6.5 shows the graphs and the parameters of the semivariogram models for mangrove forest and non-forest land uses. The spatial distribution map of the soil C stock in the study area is given in Figure 6.6. In general, the predicted map showed higher soil C stocks in the central and northern part than the southern part of the study site. The lower soil C stock areas (<300 Mg C ha^{-1}) were concentrated along the southern part, which was heavily altered and where built-up areas were mostly concentrated. In contrast, the high soil C stock areas (>1,000 Mg C ha^{-1}) were in the northern part, where closed canopy mangroves can be found. The predicted map had an overall prediction accuracy of 83.7 % (RMSEP = 16.3 %) for mangrove forest and 85.7 % (RMSEP = 14.3 %) for non-forest land uses based from the normalised RMSE using the range of the measured data (*sensu* Christensen *et al*. 2004). Using the zonal statistics tool of *ArcMap 10*, the spatial mean soil C stock of mangrove forest was computed at 807.98 ± 194.1 (range: 46.77 – 2014.56) Mg C ha^{-1}, while it was 394.53 ± 66.2 (range: 42.80 – 583.72) Mg C ha^{-1} for the non-forest land uses.

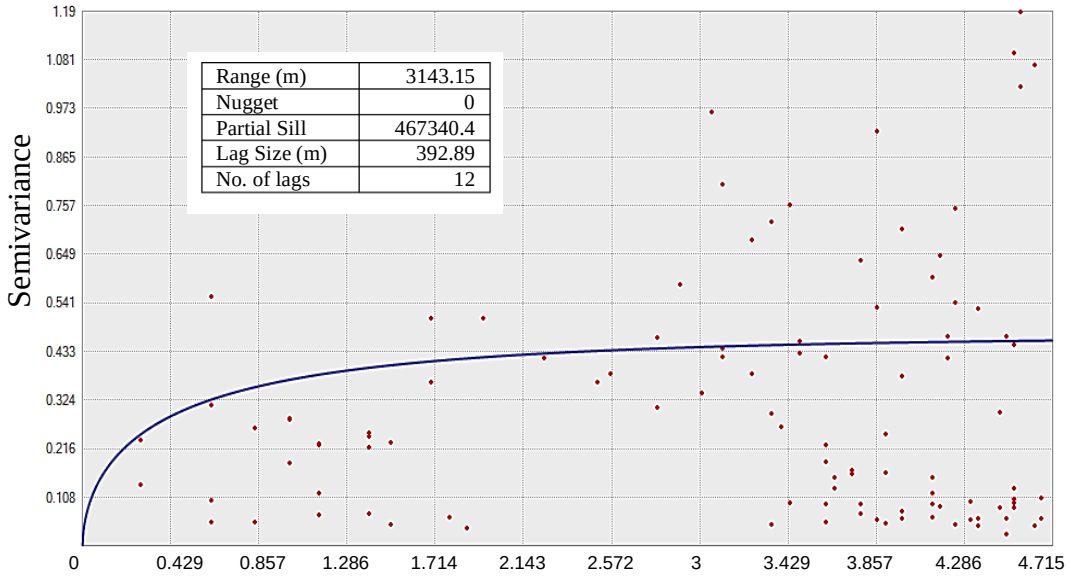

(a) Lag distance (m, 10^3)

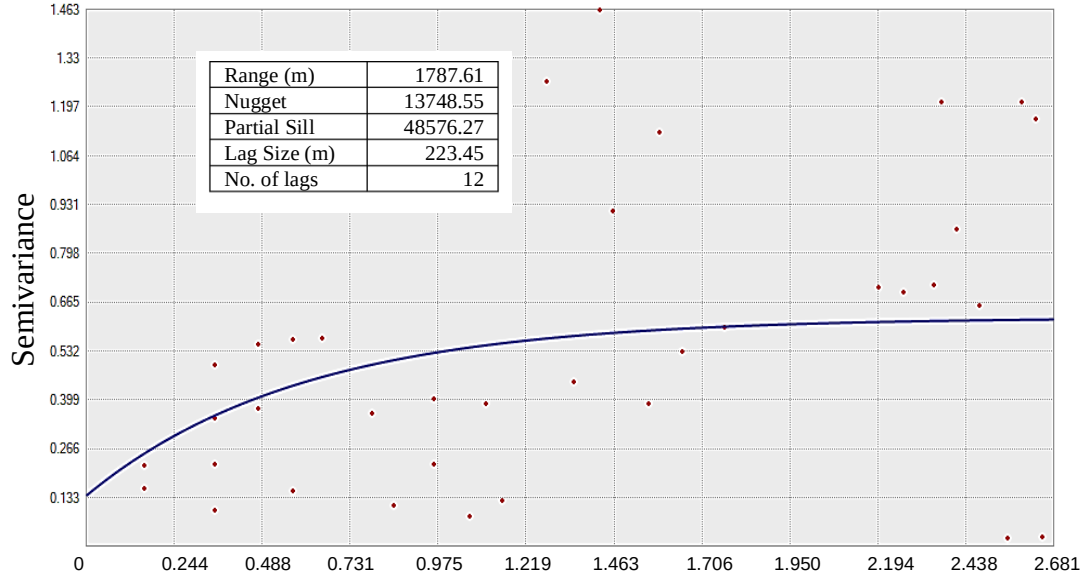

(b) Lag distance (m, 10^3)

Fig. 6.5 Empirical semivariogram cloud (red dots) and fitted model (blue line) for (a) mangrove forest and (b) non-forest land uses. The model parameters (range et al.) are inset in each graph.

The soil C stock in the mangrove forest (area: 1,216 ha) of the study site was estimated to be about 982,503 Mg C. On the other hand, the soil C stock in the four non-forest land uses (area: 178 ha) was estimated at 70,226 Mg C.

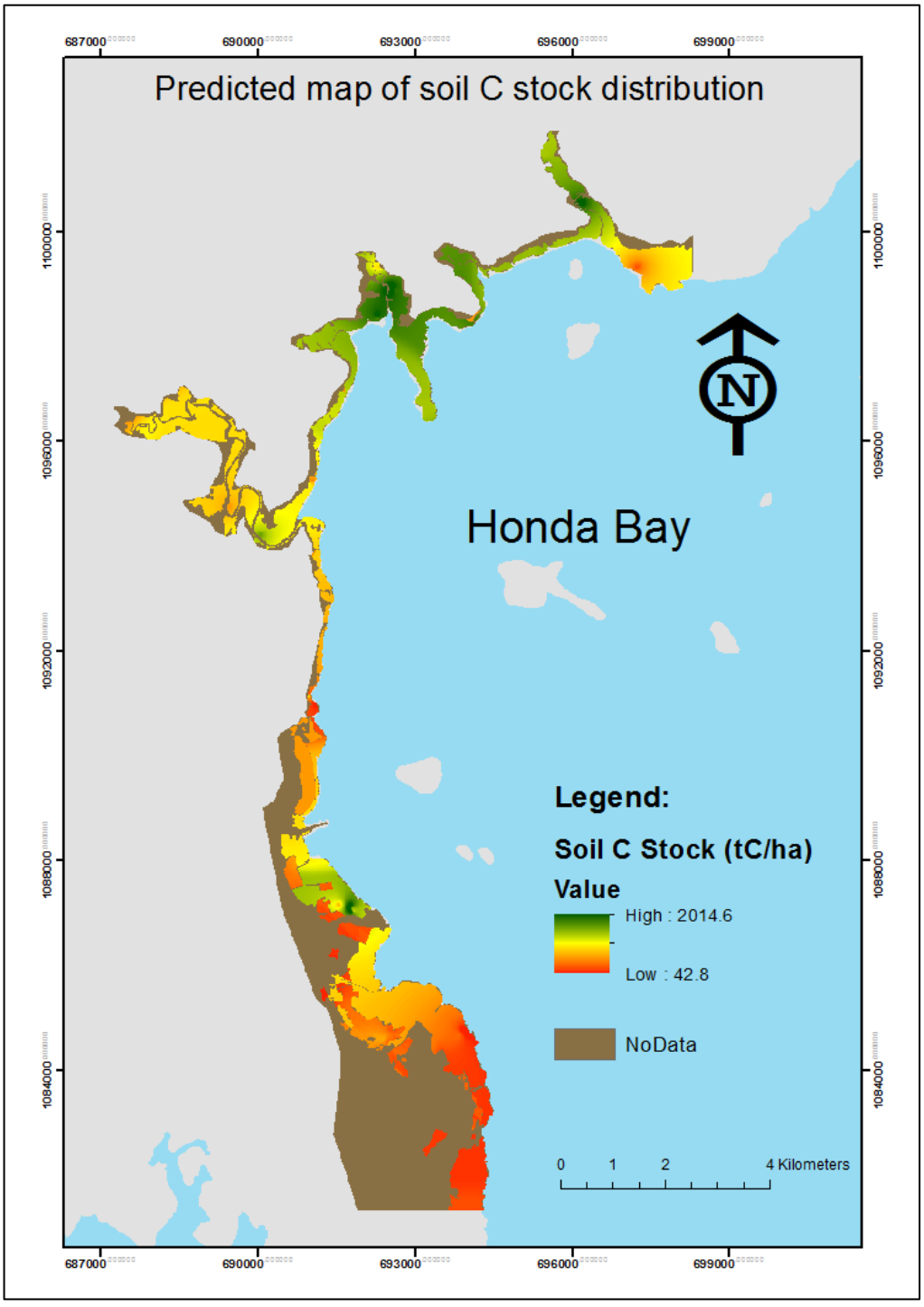

Figure 6.6 Predicted map of soil C stock spatial distribution in the coast of southern Honda Bay, Philippines

6.5 Discussion

6.5.1 Soil C stocks of mangrove forests and land uses that replaced mangroves

The mean C stock in mangrove forests (851.93 Mg C ha^{-1}) in this study was significantly higher than that of the land uses that replaced mangroves (365.15 Mg C ha^{-1}, on average). The difference in soil C stock could indicate soil C loss and C emission. Using a stock change approach, the estimated soil C loss from converting mangrove forests to non-forest land uses was 486.78 Mg C ha^{-1} (range: 398 – 809), on the average. This is equivalent to an emission of 1,786.5 t CO_2e ha^{-1} (range: 1461.6 to 2971.7 t CO_2e ha^{-1}). The estimate of C stock in this study might be liberal since inorganic C was not excluded in the estimate. The high amount of soil C in mangrove forests could be due to the contribution of local organic matter sources in the site as well as from the C captured by the living organisms from external sources (i.e. land and adjacent coastal ecosystems) which are transported to the mangroves via tidal actions.

The decline in soil %C content by 36 % when mangroves were converted to their competing non-forest land uses is about 1.65-fold higher compared to when terrestrial forests were converted to agriculture (22 %; Maraseni and Pandey (2014). This is probably due to the C-rich and deep soft soil of mangroves that were excavated and exposed when converted to other land uses. The shallow soil depths in the land uses that replaced mangroves are probably due to the effect of excavating the soft top layer of the soil during the pond preparation. Pond preparation in the Philippines involves the excavation of around 1.5 m mangrove soil (Thompson et al. 2014).

One of the obvious impacts of converting mangrove forests to non-forest land uses is in soil bulk density and % C content. The BD of the top 30cm soil layer in mangrove forest is only 0.54 g cm^{-3} as compared to 0.95 g cm^{-3} in non-forest competing land uses. Similarly, the top 30 cm of mangrove forest soil contains 8.8% mean C content compared to only 5.4% in the non-forest land uses. This is probably due to the land preparation involved during conversion which entails excavation of

the C-rich top layer of soil, about 1.5 m to 2 m in the case of aquaculture ponds (Ong 2002; Thompson et al. 2014), usually using machine which makes the soil more compact. This is consistent with the observations of Kauffman et al. (2013) and Kauffman et al. (2016) that the soil of aquaculture pond and pasture are more compact and contain less % C content as compared to their adjacent mangroves.

The relationship of total soil depth with soil C stock was evaluated using the Pearson's correlation test. Their relationship is positive. This may suggest that mangrove soil with deeper/higher depth (e.g. 200 cm) has higher soil C stock than those with shallower/lower depth (e.g. 80 cm). This is expected since soil C stock is first computed from the product of %C, Bulk density and soil depth interval and then added together to get the total soil C stock.

The soil C stocks of mangrove forests reported here (i.e. 640.1 Mg C ha^{-1} for open canopy mangrove forest and 1,040.2 Mg C ha^{-1} for closed canopy mangrove) are within the range reported in mangrove literature (Donato et al. 2011; Kauffman et al. 2011; Adame et al. 2013; DelVecchia et al. 2014; Hossain 2014; Jones et al. 2014; Thompson et al. 2014; Wang et al. 2014; Adame et al. 2015; Murdiyarso et al. 2015; Phang et al. 2015; Vien et al. 2016); Table 6.5). In addition, the mean mangrove forest C stock (851.93 Mg C ha^{-1}) in this study is higher by 135 Mg C ha^{-1} when compared to the global mean soil C stock (~717 Mg C ha^{-1} out of the 956 Mg C ha^{-1}) which also considered the total depth of mangrove soil (Alongi 2014). Furthermore, the study's mean C stock is also higher by 68.43 MgC ha^{-1} when compared to the mangrove mean soil C stock in the Indo-Pacific region (783.5 MgC ha^{-1}; Donato *et al*. 2011); higher by 229 Mg C ha^{-1} to mangroves in Vietnam (Tue *et al*. (2014) but very similar to the mean soil C stock of Indonesian mangroves (848.9 Mg C ha^{-1}; Murdiyarso *et al*. 2015). However, when only the top 1 m of the soil was considered, mean mangrove soil C stock in this study (347.6 Mg C ha^{-1}) is lower as compared to the global average of 471 Mg C ha^{-1} as reported by IPCC (Hiraishi *et al*. 2014).

For non-forest land uses, the soil C stocks of abandoned aquaculture pond in the present study (454 Mg C ha^{-1}) is higher than the abandoned aquaculture pond in India (Bhomia et al. 2016) which had only 61 Mg C ha^{-1} and 95.5 Mg C ha^{-1} in

Dominican Republic (Kauffman et al. 2013), but comparable to the C stock of cattle pastures on former mangrove (437 MgC ha^{-1}) in Mexico (Kauffman et al. 2016 ; Table 5).

Table 6.5 Some of the reported soil carbon (C) stock and depth of mangrove and non-forest land uses

Location	Land use	Soil C Stock (Mg C ha^{-1})	Soil depth (cm)	Reference
Borneo	Mangrove	813.9 – 1,255	300	Donato et al. (2011)
Bangladesh (Sundarbans)	Mangrove	386 - 491.8	300	Donato et al. (2011)
Palau	Mangrove	520.6	117	Donato et al. (2011)
Micronesia (Kosrae)	Mangrove	427.5-1222.3	74 -299	Donato et al. (2011)
Mexico (Quitana Roo)	Mangrove	286 – 1,166	$\leq$200	Adame et al (2013)
Mexico (Chiapas)	Mangrove	505.9	$\leq$200	Adame et al. (2015)
Dominican Republic (Montecristi)	Mangrove	753	174.3	Kauffman et al. (2013)
Malaysia (Selangor)	Mangrove	488.04	100	Hossain (2014)
Madagascar (Mahajamba)	Mangrove	429.2	150	Jones et al. (2014)
Ecuador (Esmeraldas)	Mangrove	365	100	DelVecchia et al. (2014)
China (Guandong)	Mangrove	197.28-270.27	100	Wang et al. (2014)
Mozambique (Sofala Bay)	Mangrove	160	100	Sitoe et al. (2014)
Vietnam (Mui Ca Mau)	Mangrove	622.7	250	Tue et al. (2014)
Philippines (Aklan/Iloilo)	Mangrove	206.5	150	Thompson et al. (2014)
Mexico (Tabasco/Campeche)	Mangrove	1107.43	300	Kauffman et al. (2016)
Indonesia (Cilacap and Tanjung Puting)	Mangrove	571.6 -1059.2	211-300	Murdiyarso et al. (2015)
Singapore (Chek Jawa)	Mangrove	307	100	Phang et al. (2015)
Vietnam (Cau Mau)	Mangrove	759.9	300	Vien et al. (2016)
India (Odisha)	Mangrove	155.5	152	Bhomia et al. (2016)
Philippines (Puerto Princesa)	Mangrove	640 - 1040.21	103 - 255.6	This study
Dominican Republic (Montecristi)	Abandoned shrimp pond	95.5	71.3	Kauffman et al. (2013)
Mexico (Tabasco/Campeche)	Cattle Pasture	437	300	Kauffman et al. (2016)
India (Odisha)	Abandoned aquaculture pond	61	70	Bhomia et al. (2016)

The results of the study have also shown the good potential of the GIS-based Ordinary Kriging approach for mapping the soil C stocks in mangrove areas (accuracy of 85%). The result is within the range reported in the literature (Mishra et al. 2009; Umali et al. 2012). However, some portions of the study area were far from the locations which were sampled due to resources constraint and therefore the estimate in that portion may be associated with higher prediction errors compared to those portions near the sampled locations. Future studies should consider to evenly distribute the plots to reduce the prediction errors. The use of this GIS-based Kriging method for mangrove soil C stock mapping complements the biomass C mapping using remote sensing techniques. Together, the two methods play an important role for mapping the ecosystem (biomass plus soil) C stocks in mangrove areas for the first time. The soil C stock distribution map produced in the present study could guide coastal managers to pinpoint high soil C stock areas in prioritising conservation and protection efforts. This is relevant to current schemes to combat emissions from land use change such as REDD+.

6.5.2 Implications for management and conservation

Primavera and Esteban (2008) reported that around 50 % of the 279,000 ha mangrove lost in the Philippines during the period 1951-1988 was due to conversion to aquaculture. Using the emission factor derived from this study (1,786.5 t CO_2e ha^{-1}), it is estimated that the emission due to soil C loss from mangrove conversion to aquaculture during 1951-1988 was about 249.21 Mt CO_2e. This is assuming that the soil C stocks of mangroves and the competing land uses studied here are representative of the whole country. On the same vein, during 2001-2012, Philippines lost some 1,157 ha of mangrove forest to aquaculture (522.8 ha), deforestation (464.8 ha), palm plantation (157.5 ha) and rice cultivation (12.4 ha) (Richards & Friess 2016). Again, using the study's emission factor from soil C loss, the potential emission estimate from these mangrove conversions during the period was 2.07 Mt CO_2e. Together, these emissions from mangrove conversion to non-forest land uses, estimated at 251.3 Mt CO_2e, add considerably to the alarming increased CO_2 concentration in the atmosphere.

Furthermore, it is of paramount importance to protect and manage the mangrove forests and the blue carbon they store from conversion to other land uses due to the numerous coastal protections they offer to the coastal communities especially during strong typhoon and tsunami events. These benefits are in addition to opportunities for additional funds being developed in the global scene as part of climate change mitigation (Howard et al. 2014).

6.6 Conclusion

While the importance of mangrove forest as a huge storage of C is increasingly being recognised, the deforestation of mangrove forests and their conversion to other land uses still continue. In this study, the mean soil C stock of mangrove forest was estimated to be 851.93 Mg C ha^{-1} while their competing non-forest land uses contain only 365.15 Mg C ha^{-1}. The decrease/loss in soil C of 57 % indicates C emission. When mangrove forests are lost and converted to other land uses, not only the stored C is lost and released to the atmosphere. The conversion also significantly reduced the ecosystem goods and services provided by mangroves such as biodiversity, habitat for marine organisms and coastal protection. This makes mangrove forests fit into Payment for Ecosystem Services schemes such as REDD+ that provide monetary incentives for the lost income made from the competing land uses of mangroves. Communities and landowners could tap into those schemes to protect their existing mangrove forests from conversion to other land uses, reduce the C emissions and benefit from the myriad of goods and services that mangrove forests provide.

The next Chapter presents a comparison of the soil-atmosphere fluxes of greenhouse gases CO_2, CH_4 and N_2O in mangrove forests and land uses that replaced mangroves as well as the magnitude of changes in soil GHG fluxes owing to mangrove conversion.

Chapter 7

SOIL GREENHOUSE GAS FLUXES IN TROPICAL MANGROVE FORESTS AND IN LAND USES ON DEFORESTED MANGROVE LANDS

7.1 Introduction

The limited knowledge about the impact of mangrove conversion on soil C stock and GHG fluxes in mangroves is highlighted in the Review of Literature. Such information is important for estimating C losses and emissions owing to mangrove conversion. The previous Chapter examined the soil C stocks of mangroves and the land uses that replaced them, the C losses arising from mangrove conversion, and the potential of geostatistical technique, Ordinary Kriging, to map the soil C stocks in mangrove area.

In this Chapter, the soil fluxes of CO_2, CH_4 and N_2O were examined under mangrove forests and compared with four non-forest land uses that replaced mangroves (i.e. abandoned aquaculture ponds, coconut plantations, abandoned salt ponds and cleared mangroves). Specifically, the objectives were to: 1) quantify the fluxes of CO_2, N_2O and CH_4 in mangrove forests and non-forest land uses that replaced mangroves; 2) determine the relationship of these GHGs with selected environmental site variables; and 3) evaluate the accuracy of the output from GIS-based spatial modelling/interpolation and mapping of GHG fluxes.

This Chapter is organised into six sections. Section 7.2 gives the background literature on mangrove conversion and soil-atmosphere fluxes of greenhouse gases in mangrove area. Section 7.3 provides the Methods of the study, while Section 7.4 presents the Results. Section 7.5 discusses and interprets the results of the study. Finally, the Chapter ends with Section 7.6 that provides the conclusion.

The novelty and significant contributions of this Chapter include: 1) the evaluation of all the three major GHGs (CO_2, CH_4 and N_2O) of not only from mangrove forests but also in replacement land uses; and 2) the application of GIS-based geostatistical technique for mapping the soil fluxes of each of the three GHGs and their combined fluxes.

7.2 Land use conversion and soil-atmosphere fluxes of greenhouse gases in mangrove areas

Mangrove forests are important ecosystems inhabiting the coastal wetland of tropical and subtropical countries. They provide timber and other construction materials, fuelwood, fishery products and performs critical ecological functions such as biodiversity conservation, storm protection, sediment regulation, and coastal stabilisation, among others (Koch et al. 2009; Barbier et al. 2011; Salmo et al. 2013). Recently, mangroves have been increasingly recognised as among the most carbon dense tropical forests (Murdiyarso et al. 2010; Kauffman et al. 2011; Adame et al. 2013; Murdiyarso et al. 2015; Bhomia et al. 2016). Southeast Asian countries hold >30% of the remaining mangroves in the world, estimated to be between 13,776,000 and 15,236,000 ha (Spalding et al. 2010; Giri et al. 2011).

On a global scale, approximately 3.6 million ha of mangroves had been deforested and converted to other land uses since 1980. However, deforestation rate has declined to 102,000 ha yr^{-1} during the period 2000-2005 from 185,000 ha yr^{-1} in the 1980s (FAO 2007). In Southeast Asia, recent estimates of mangrove deforestation and land use conversion were about 9,535 ha per year during the period 2000-2012, mostly to make way mostly for aquaculture, rice farms and oil palm plantations (Richards & Friess 2016).

Among the drivers of global mangrove loss are overexploitation, conversion of mangroves to aquaculture, agriculture, urban, tourism and industrial developments in the coastal area (Alongi 2002; Giri et al. 2011; Murdiyarso et al. 2013; Richards & Friess 2016). In the Philippines, for example, conversion of mangroves to aquaculture ponds is considered the main reason for mangrove loss. Other causes are

overexploitation and conversion to other non-forest land uses such as agriculture, salt ponds and settlements (Primavera & Esteban 2008). Mangrove clearing and land reclamation results in the emission of stored carbon (C) in the form of CO_2 and other GHG through oxidation (Lovelock et al. 2011). Also, aquaculture and agriculture add nutrients to the system in the form of feeds and fertilisers, respectively, which can enhance the metabolism of soil microorganisms resulting in the emissions of N_2O and CH_4 (Chen et al. 2010).

Carbon dioxide, CH_4 and N_2O are the three main GHGs being monitored in the land use sector by the International Governmental Panel on Climate Change since 1990 (IPCC 2013). Accurate reporting of GHG emissions from wetlands is, therefore, essential for regional and national emissions inventories. Compared to tropical peatlands (Hadi et al. 2005; Hergoualc'h & Verchot 2011; Hergoualc'h & Verchot 2012), the effects of mangrove land use conversion on soil fluxes of the three GHGs are not yet fully understood. For mangroves, the soil GHG fluxes could be minimal to substantial depending on anthropogenic influences (Chen et al. 2010; Chen et al. 2014).

Several soil and vegetation characteristics (referred to in this Chapter as environmental site variables) are reported to influence the GHG fluxes in mangrove soil. For instance, CO_2 fluxes are related to soil organic matter content, soil moisture content, redox potential, salinity and porosity (Chen et al. 2010; Chen et al. 2014), and Leaf Area Index (Lovelock 2008). CH_4 fluxes in wetlands are related to salinity (Purvaja & Ramesh 2001; Allen et al. 2011; Poffenbarger et al. 2011). Furthermore, N_2O flux is influenced by nitrate loading, salinity and porosity (Allen et al. 2007; Chen et al. 2010; Howard et al. 2014).

The soil fluxes of the three GHGs, however, have not been measured simultaneously in non-forest land uses in deforested mangroves along with the mangrove forest that they replaced. Fluxes of CH_4 and N_2O have not been assessed for aquaculture ponds, salt ponds and coconut plantations that are formerly occupied by mangroves as well as in mangrove areas that were cleared of vegetation. Simultaneous measurements of the three GHG fluxes is necessary to evaluate their relative importance (Cobb et al. 2012).

Furthermore, site-scale information on the spatial variation of soil GHG fluxes is needed in order to identify priority areas for management intervention. Available studies on GHG fluxes in coastal wetlands are based on few plots from which the spatial variation in the entire study site is inferred. Maps of soil GHG fluxes produced from modelling the spatial variation of the soil GHG fluxes is, therefore, essential for designing effective programs aimed at reducing GHG emissions from soil.

7.3 Methods

7.3.1 Site description

The soil GHG emissions of mangrove forests and the non-forest land uses that replaced mangroves were investigated in Honda Bay. A summary of the characteristics of the land uses of the study site is shown in Table 7.1. Honda Bay's southern coast is lined with a contiguous mangrove forests, running north to south of the study site. The mangroves are interspersed with non-forest land uses such as agriculture, aquaculture, and built-up areas/settlements especially in the central and southern portion of the study site. More details of the study site are presented in Chapter 3.

More details of the study site are presented in Chapter 3 while a summary of the characteristics of the land uses of the study sites is shown in Table 7.1.

Table 7.1 Characteristics of sampling sites in Honda Bay, Palawan, Philippines; data are mean values

Land use/site	Dominant Species	Tree density (Individuals $ha^{-1)}$	Basal Area (m^2 ha^{-1})	Salinity (ppt)	Location
Closed canopy mangrove					
Bacungan	*Rhizophora apiculata*	1,890	9.9	16.8	N9.903^0 , E118.74376
Santa Cruz	*R. mucronata*	1,429	11.5	21	N9.93048^0, E118.75513^0
Salvacion	*R. apiculata*	1,544	13	22.6	N9.93953^0, E118.8002^0
Open canopy mangrove					
Tagburos	*R. apiculata*	772	1.6	32	N9.86631^0, E118.74291^0
Santa Lourdes	*R. apiculata*	963	11.9	21.9	N9.86631^0, E118.74291^0
San Jose	*Ceriops tagal*	859	4.4	79.3	N9.80515^0, E118.76605^0
Abandoned aquaculture pond					
San Jose	None	0	0.0	26.7	N9.80615^0, E118.75575^0
Tagburos a	None	0	0.0	34.9	N9.81263^0, E118.74971^0
Tagburos b	*R. apiculata*	119	0.03	39.2	N9.83698^0, E118.74035^0
Coconut plantation					
Tagburos	*Cocos nucifera*	346	3.2	16.1	N9.814483^0, E118.74575^0
Abandoned Salt pond					
Tagburos	None	0	0	53.8	N9.83433^0, E118.74026^0
Cleared mangrove					
San Jose	None	0	0	68.2	N9.80813^0, E118.75678^0

7.3.2 Field sampling design and soil GHG fluxes study process

Mangrove forests (represented by closed canopy mangrove and open canopy mangrove forests), along with non-forest land uses in deforested mangrove lands (represented by abandoned aquaculture ponds, coconut plantations, abandoned salt ponds and cleared mangroves), were used in this study. The study site was stratified based on land use. In each land use, sites were selected through simple random sampling. The mangrove forest had three sites for closed canopy forests and another three sites for open canopy mangroves. The land uses that replaced mangroves also had three sites for abandoned aquaculture ponds. However, the non-aquaculture land uses (i.e. coconut plantation, abandoned salt pond and cleared mangrove) had only one site each due to access restriction to other coconut plantations and absence of other sites for abandoned salt pond and cleared mangrove.

Within the mangrove forest, three transects were established, except for one thin open canopy mangrove forest (width: 20-25 m) where only two transects were established. Each transect was established near the sea margin (seaward), middle/midstream and near the land (landward) to cover the natural tidal gradient in mangrove forests (cf. Kauffman & Donato 2012). In each mangrove transect, three circular plots with 7-m radii were established and positioned 50 m apart along a line parallel to the coast. For non-forest replacement land uses, however, only two transects were established for each site, but each transect had the same three 7m-radii circular plots, spaced about 25 m apart. In each of the mangrove and non-mangrove plots, two random points at least 1 m apart were selected for soil GHG flux measurement. The whole process of soil GHG fluxes study is summarised in Figure 7.1.

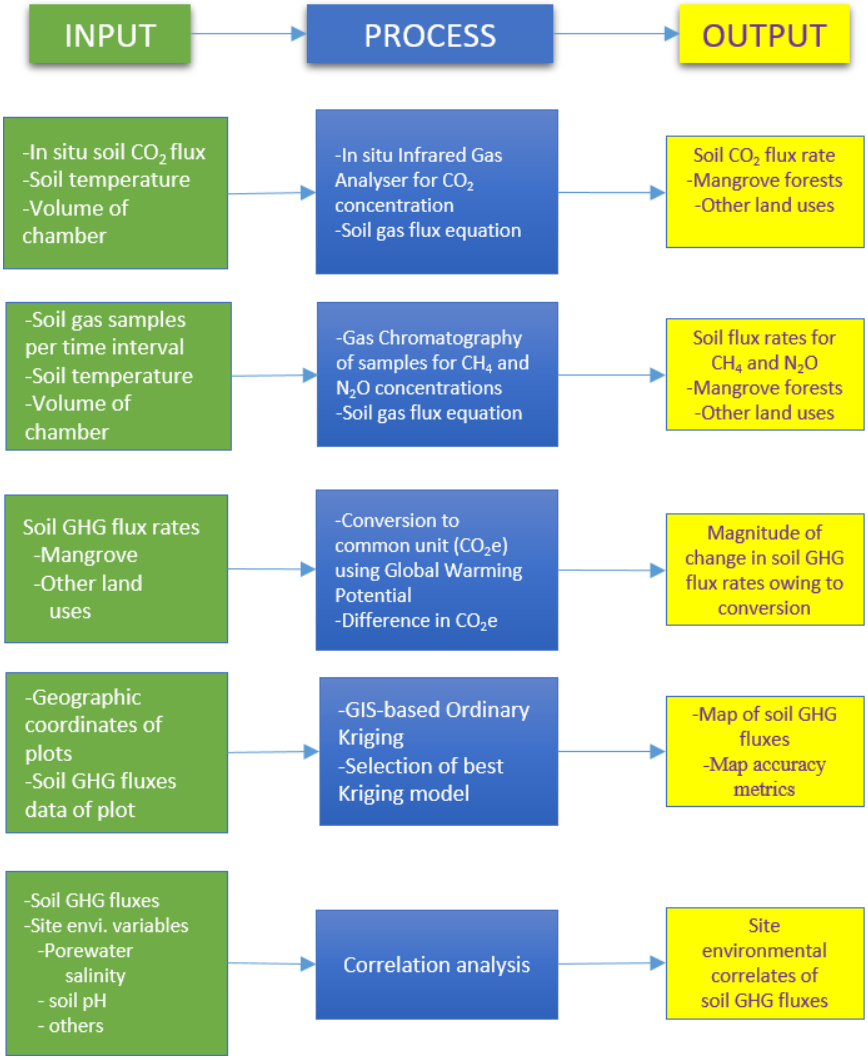

Figure 7.1 Input-Process-Output model for soil GHG fluxes study

7.3.3 Gas sampling and flux determination

As the land uses are subjected to regular tidal inundation, the soil gas measurements and sampling were done during daytime low tide period. A survey-type *LiCor 8100A Automated Soil CO_2 Flux System* (LiCor Corp, USA) was used to measure the soil CO_2 fluxes, *in situ* (Figure 7.2). The system is composed of an analyser control unit containing the infrared gas analyser, 10 cm chamber, a computer and soil collar. The soil collars, made up of 10 cm diameter and 9 cm height PVC pipes, were driven 3 cm deep into the soil. The soil gas flux chamber was placed on top of the collar to start the measurement. CO_2 fluxes were measured *in situ*, following manufacturer's manual.

Gas samples for CH_4 and N_2O analyses were also collected through the gas sampling kit which was appended to the LICOR instrument. Samples were drawn from the kit using a 60-ml syringe at 0-, 1-, 2- and 3- minute intervals after the system has started recording the *in situ* CO_2 concentration. The collected samples were then injected to labelled pre-evacuated glass vials with 35 ml volume capacity. Samples were sent to the Gas Chromatography Laboratory of the International Rice Research Institute (IRRI) in Los Baños, Philippines for the analyses of GHG concentrations. The CH_4 and N_2O concentrations were analysed and quantified using a gas chromatograph (SRI Greenhouse GC System, Germany) equipped with electron capture detector, flame ionisation, and methanizer. Flux rates were calculated based on the rate of change in gas concentrations per unit time and the total volume of the chamber per unit soil area. using the following equation (Pumpanen et al. 2004; Howard et al. 2014; Warner et al. 2017):

$$F = \left(\frac{dC}{dt}\right)\left(\frac{Vc}{Ac}\right)\frac{P}{\left(R * (T + 273.15)\right)}$$

where F is the flux of a gas, dC/dt is the change in concentration over time (ppm s^{-1}), Vc is the volume of the system in liters, Ac is the chamber area in m^{-2}, P is the atmospheric pressure (assumed to be 1 atm), R is the Universal gas constant (0.0820 L*atm/mol*K), T is the measured soil temperature (^{o}C), and 273.15 is the conversion factor from Celsius to Kelvin.

GHG fluxes were converted to a common unit (i.e. CO_2-equivalent, CO2e) to compare and add them together using the Global Warming Potential of 28 for CH_4 and 265 for N_2O set by the Intergovernmental Panel on Climate Change (IPCC 2013).

a

b

c

d

e

f

Figure 7.2 LICOR soil flux system consisting of a) analyser control unit, b) flux chamber, c) soil collar, d) laptop computer, e) soil temperature probe set, and f) soil GHG flux measurements in abandoned salt pond.

7.3.4 Ancillary measurements

Soil temperature, redox potential and pH were also simultaneously measured in each plot using a hand-held *Aqua pH-mV-temperature meter* (Aqua pH 2.2, TPS, Australia). The salinity of porewater was measured using a refractometer (Vee Gee STX-3, USA) after suctioning the same with a syringe. These variables were measured at a depth of 30 cm. The geographic coordinates of each plot were determined using a hand-held *Garmin GPS* receiver.

Vegetation canopy variables such as Leaf Area Index (LAI) and canopy gap fraction were measured using *CI-110 Plant Canopy Imager (CID Bio-Science, USA).* Tree density and basal area were determined in each plot. Biomass data was taken from Chapter 4 of this thesis. Tree density is the number of tree individuals in a plot while basal area per plot is the sum of all tree basal area [= 0.7854 x (tree diameter)^2] in a plot. Biomass was computed using allometric equations for each species (Brown 1997; Komiyama et al. 2008).

Soil C stock data was collected from the same study site and taken from Chapter 6 of this thesis. Soil C stock was computed as the product of bulk density, % C and soil depth interval. Soil samples were sectioned at 0-15 cm, 15-30 cm, 30-50 cm, 50-100 cm, and >100 cm if marine sediments/sands or impenetrable rocks were not encountered before the 100-cm depth (Kauffman et al. 2013; Bhomia et al. 2016; Kauffman et al. 2016). The soil cores were taken in an undisturbed location near the plot centre using an open-face auger capable of obtaining a sample up to a depth of 300 cm. Only one soil core per plot was obtained. Soil depth to parent material was measured three times near the plot centre by driving a 3-m graduated aluminium rod. The sampling procedure for soil C stock assessment was discussed thoroughly in Chapter 6, Castillo et al. (2017), Kauffman and Donato (2012), Howard et al. (2014) and Maraseni et al. (2008).

7.3.5 Statistical Analysis

Differences in fluxes of CO_2, CH_4 and N_2O between mangrove and the non-forest land uses that replaced mangroves were tested using Welch's Test Analysis of Variance (ANOVA). If the main effect (land use) was significant, Games-Howell

posthoc test was applied to determine differences among means. Normality and symmetry were assessed by visual inspection of histogram and box plot. Plot was the unit of replication used. Pearson's correlation coefficient was determined to assess the relationship between GHG fluxes and environmental parameters. Statistical analyses were run using IBM SPSS Statistics for Windows, version 22 (IBM Corp., USA).

7.3.6 Mapping/Spatial modelling of soil GHG fluxes

Geostatistical technique, particularly Ordinary Kriging (Mishra et al. 2009; Umali et al. 2012; Kucuker et al. 2015), was used to model the site-scale spatial variation of soil GHG fluxes in the study site. This technique was also used to predict the soil GHG fluxes at un-sampled locations. The extent of current mangrove cover in the study area, which was used for the spatial interpolation, was digitised from a high-resolution image of the study site as viewed in Google Earth (Google Inc., USA). Ordinary Kriging was implemented using the following equation. A detailed theoretical description of Ordinary Kriging has been discussed in Johnston et al. (2001).

$$\hat{Z}(x_o) = \sum_{i=1}^{n} \lambda_i Z(x_i)$$

where:

$\hat{Z}(x_o)$ is the estimate of soil GHG fluxes ($\mu mol\ m^{-2}\ s^{-1}$) at location x_o

$Z(x_i)$ is the measured value of soil GHG fluxes at x_i locations

λ_i are weights of measured samples at x_i locations surrounding location x_o

The spatial modelling and analysis of the GHG fluxes were implemented using Geostatistical Analyst and Spatial Analyst extensions of ArcGIS 10.3 (ESRI, USA) using 10 m x 10 m pixel size. At least five runs were made to model the site-scale spatial variation of fluxes of each GHG. Cross-validation was done in each run using the Leave-One-Out (LOO) approach to determine how well the model predicted the unknown values based on Root Mean Square Error (RMSE), among

other measures of prediction accuracy. In this approach, each measured data/sample was excluded sequentially while a model was built using the remaining data/samples in order to predict the value of the excluded sample. To estimate the errors, the predicted value was then compared to the measured value (Johnston et al. 2001; He & Guo 2006; Jachowski et al. 2013). In this study, the model with the lowest RMSE was selected and used for further GIS processing required for the spatial interpolation task. RMSE is defined by the equation:

$$\mathrm{RMSE} = \sqrt{\frac{1}{n}\sum_{i=1}^{n}(x_i - y_i)^2}$$

where:

x_i = measured soil GHG flux value of the i^{th} sample

y_i = predicted soil GHG flux value.

7.4 Results

7.4.1 GHG fluxes

The mean CO_2 emission varied significantly between mangrove forests (0.24 to 9.25 μmol m^{-2} s^{-1}) and non-forest land uses that replaced mangroves (0.07 to 4.32 μmol m^{-2} s^{-1}; $P < 0.001$; Figure 7.3). The mean CO_2 emission rate in mangrove forests (2.90 μmol m^{-2} s^{-1}) was 61.2 % higher than the non-forest land uses (1.12 μmol m^{-2} s^{-1}, $P < 0.001$). The mean emission rate in non-forest land uses was highest in the abandoned salt pond (2.25 μmol m^{-2} s^{-1}) and lowest under the cleared mangroves and the coconut plantation which are both below 0.50 μmol m^{-2} s^{-1}. Soil under mangrove forests was a net source of CO_2. The non-forest land uses were also a net source of CO_2 although in lower emission rates.

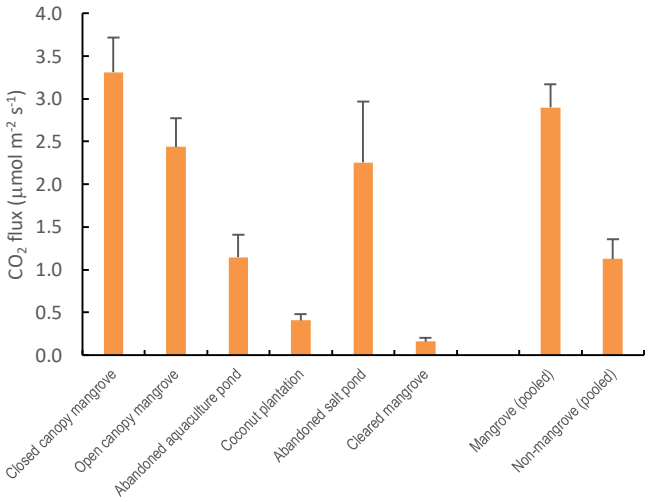

Figure 7.3 CO_2 fluxes in soils under mangrove forest and non-forest land uses that replaced mangroves.

For CH_4, the mean fluxes ranged from 4.55 to 7.64 µmol m^{-2} h^{-1} under mangrove forests, and from -5.95 to 17.53 µmol m^{-2} h^{-1} under non-forest land uses. The mean CH_4 emission in mangrove forests (6.15 µmol m^{-2} h^{-1}) was higher by 84.8 %, on the average, as compared to non-forest land use types (0.93 µmol m^{-2} h^{-1}), but not statistically significantly different ($P > 0.05$; Figure 7.4). The soil of mangrove forests was a net source of CH_4. The response of mangrove soil CH_4 flux to land use conversion was variable: a) net sink/consumer in the case of abandoned aquaculture ponds, and b) net source/producer in the case of the cleared mangrove, the coconut plantation and the abandoned salt pond.

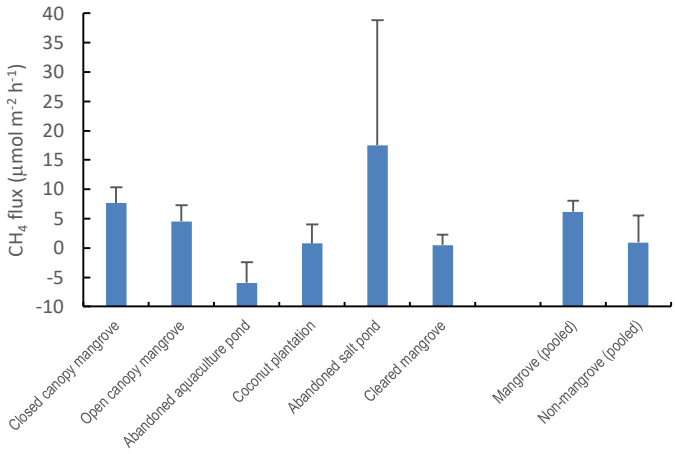

Figure 7.4 CH_4 fluxes in soils under mangrove forest and non-forest land uses that replaced mangroves

The mean fluxes of N_2O across all land uses ranged from -0.67 to 5.54 µmol m^{-2} h^{-1}. The mean emission in mangrove forests was only 0.01 µmol m^{-2} h^{-1} and was 38 times lower than non-forest land uses (0.49 µmol m^{-2} h^{-1}), albeit the difference was also not significantly different ($P > 0.05$; Figure 7.5). Among non-forest land uses that replaced mangroves, the abandoned salt pond had the highest mean emission rate (5.54 µmol m^{-2} h^{-1}) followed by abandoned aquaculture ponds (0.33 µmol m^{-2} h^{-1}). On average, all sites were net sources of N_2O, although N_2O emissions tended to be higher in magnitude for non-forest land uses.

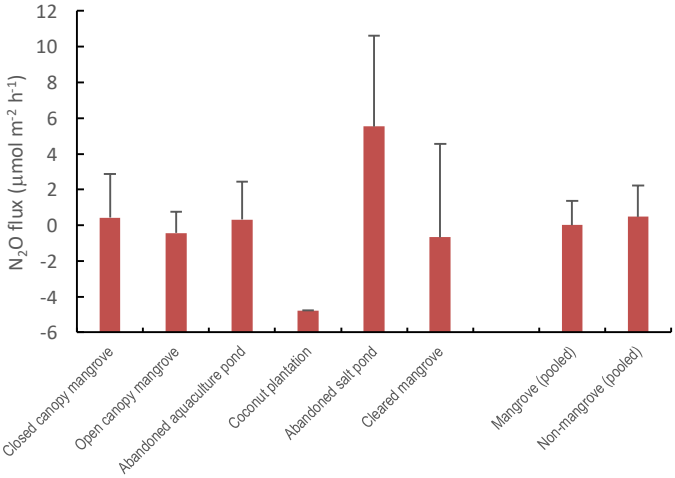

Figure 7.5 N_2O fluxes in soils under mangrove forest and non-forest land uses that replaced mangroves

All converted land uses were net sources of GHGs, although in varying magnitude; highest from the abandoned salt pond, followed by abandoned aquaculture ponds. The abandoned salt pond was found to have higher emission as compared to open canopy mangrove forests (Table 7.2). The coconut plantation had the least soil GHG emission among the non-forest land uses. CO_2 was still the dominant gas before and after conversion, accounting for 99% in mangrove forests and 97% in land uses that replaced mangroves. The CH_4 and N_2O fluxes accounted for 0.59 % and 0.04 % of the total emissions in mangrove forests as compared to 0.23 % and 3.07 %, respectively, for non-forest land uses. In general, the total emission in mangrove forests was 2.5 times higher than non-forest land uses. Soil fluxes of CO_2 and CH_4 decreased by 2.6 and 6.6 times, respectively, while that of N_2O increased by 34 times in non-forest land uses as compared to mangrove forests.

Table 7.2 Mean soil GHG fluxes (± *SE)* and their total in mangrove forest and non-forest replacement land uses in deforested mangrove lands

Land use	Flux (kg CO_2e ha^{-1} day^{-1})			
	CO_2	CH_4	N_2O	Total
Mangrove forest	*110.25±10.42* *n = 49*	*0.66±0.21* *n = 29*	*0.04±3.81* *n = 29*	*110.94*
Replacement land uses	*42.77±8.73* *n = 32*	*0.10±0.50* *n = 16*	*1.36±5.00* *n = 16*	*44.23*
Abandoned aquaculture pond	43.45±10.19 n = 15	-0.64±0.37 n = 7	0.91±5.89 n = 7	43.72
Coconut plantation	15.47±2.74 n = 6	0.08±0.28 n = 3	-13.40±0.06 n = 3	2.16
Abandoned salt pond	85.65±27.08 n = 7	1.88±2.29 n = 3	15.50±14.17 n = 3	103.03
Cleared mangrove	6.08±1.68 n = 4	0.05±0.18 n = 3	-1.88±14.65 n = 3	4.26

7.4.2 Relationship between GHG fluxes and environmental variables

In mangrove forests, the CO_2 fluxes were significantly correlated to tree density ($P < 0.05$), leaf area index ($P < 0.01$) and canopy gap fraction ($P < 0.01$). LAI, canopy gap fraction and tree density all had moderate relationships with CO_2. LAI could only explain 15% of the variability of CO_2 fluxes among plots of mangroves forests. For non-forest land uses, no site variables were correlated with CO_2 fluxes. CO_2 fluxes from both mangrove forests and non-forest land uses were not related to carbon content (%C) of the surface soil (0-15cm), pore water salinity or soil depth (Table 7.3).

Table 7.3 Pearson's correlation coefficient (*r*) between site variables and GHG fluxes in soils under mangrove forests and non-forest land uses that replaced mangroves

Site variables	CO_2		CH_4		N_2O	
	Mangrove forests	Non-forest land uses	Mangrove forests	Non-forest land uses	Mangrove forests	Non-forest land uses
Tree density	0.333*	n.a	0.112	n.a	0.384*	n.a
Basal area	0.112	n.a	-0.04	n.a	-0.049	n.a
Biomass C stock	0.147	n.a	-0.026	n.a	-0.073	n.a
Soil C stock	0.202	.121	.485**	-0.086	-0.03	-0.073
Soil Depth	0.234	.236	.379*	-0.273	-0.019	0.052
Bulk Density	-0.072	.051	0.147	0.292	-0.116	-0.39
Mean %C / Mean %N[1]	0.003	.068	-0.179	-0.181	0.103	0.538*
%C 0-15 / %N 0-15[1]	-0.358	-.332	-0.301	0.227	0.406*	0.70*
Porewater Salinity	-0.278	-.068	-.496**	0.15	0.042	0.178
Porewater pH	-0.120	-.026	-0.062	0.036	-0.278	-0.458
Porewater redox potential	0.293	.021	0.064	-0.037	0.257	0.46
Leaf Area Index	0.392**	n.a	0.196	n.a	0.048	n.a
Photosynthetically Active Radiation	-0.256	n.a	-.404*	n.a	-0.071	n.a
Canopy gap fraction	-0.367**	n.a	-0.203	n.a	-0.054	n.a

*significant at 0.05 alpha level **significant at 0.01 alpha level

[1]Mean %N and %N 0-15 applied only to N_2O, n.a. = not applicable

The mean fluxes of CH_4 in mangrove soil were positively correlated to soil C stock and soil depth, and negatively correlated to porewater salinity and photosynthetically active radiation ($P<0.05$). Porewater salinity and soil C stock accounted for 25 % and 24 % of the variation of CH_4 fluxes. Such relationships were not observed in the non-forest land uses (Table 7.3).

Fluxes of N_2O in soil under mangrove forests were correlated with tree density and %N (0-15 cm), but not with the other variables ($P < 0.05$). In non-forest land uses, there was a significant positive correlation between N_2O fluxes and % N (0-15 cm), as well as with mean % N ($P < 0.05$).

7.4.3 Modelling the spatial variation of GHG fluxes

The semi-variograms of fluxes for CO_2, CH_4, N_2O and CO_2e are given in Table 7.4. The overall prediction accuracies obtained were 82.4 % for CO_2, 79.8 % for CH_4, 75.3 % for N_2O and 83 % for combined fluxes in CO_2e, based on the normalised root mean square error (RMSE). The RMSE for CO_2, CH_4, N_2O and CO_2e fluxes were 1.62 μmol m^{-2} s^{-1}, 15.163 μmol m^{-2} h^{-1}, 7.44 μmol m^{-2} h^{-1} and 65.04 kgCO_2e ha^{-1} day^{-1}, respectively.

Table 7.4 Best fit model semi-variograms for Kriging analysis

Variable	Model	Nugget	Range (m)	Partial Sill	No. of lags	Lag size (m)
CO_2	Exponential	0	69.28	1.83	8	8.66
CH_4	Exponential	0	296.49	333.72	10	29.64
N_2O	Stable	36.33	10,813.72	35.82	12	980
CO_2e	Exponential	0	64	3,204.35	8	8

The southern portion of the study site was found to have lower CO_2 emission as compared to the middle and northern parts (Figure 7.6). On the other hand, the northernmost section of the study site was observed to have higher CH_4 emission rates as compared to its middle and southern portions. Meanwhile, the middle segment of the study site was found to have higher N_2O emission rates as compared to its northern and southern parts. Overall, when the three GHGs were brought to a common unit and combined, it was clear that the middle and northern areas had higher flux rates as compared to the southern part (Figure 7.6).

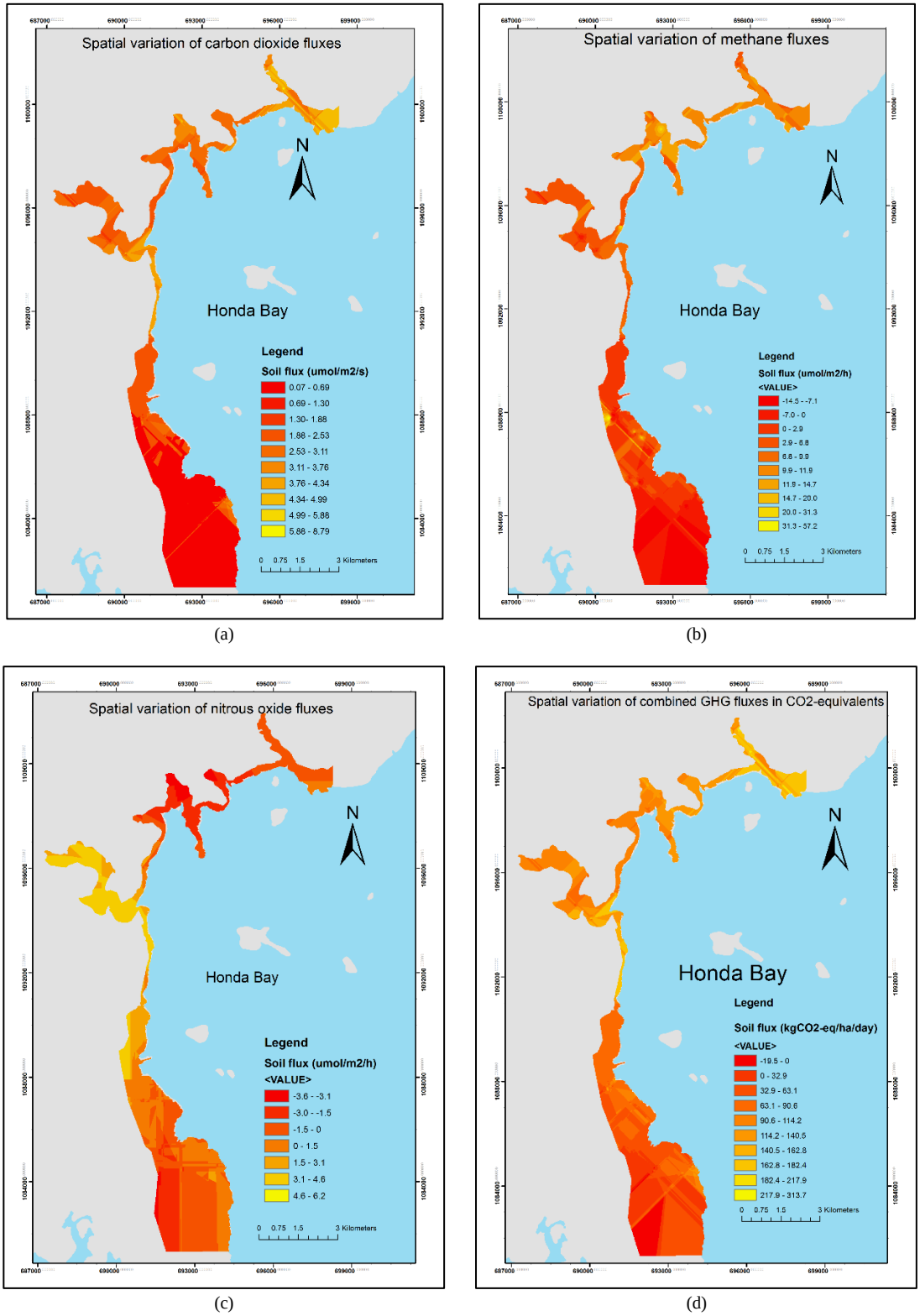

Figure 7.6 Modelled spatial variation of GHG fluxes in the study site using GIS-based Ordinary Kriging. Fluxes of (a) CO_2 is in µmol m^{-2} s^{-1}; (b) CH_4 and (c) N_2O are in µmol m^{-2} h^{-1}; and (d) combined flux is in kg CO_2e ha^{-1} day^{-1}

7.5 Discussion

7.5.1 Soil GHG emissions in mangrove forests and land uses that replaced mangroves

The mean CO_2 flux in mangrove forests is higher than non-forest land uses. The combined autotrophic and heterotrophic respirations in mangrove forest could probably explain the higher CO_2 fluxes in mangrove forests. In contrast, only heterotrophic respiration occurs in land uses that replaced mangroves which are devoid of vegetation. Coincidentally, mangroves' soil C stock is also higher as compared to non-forest land uses. Moreover, the higher flux in N_2O in the non-forest land uses especially in abandoned salt ponds could probably be due to the presence of decomposed feeds in the pond floor and the ponds' proximity to human settlements, the discharges of which are sources of nitrogen (IPCC 2014c). Furthermore, the observed decrease of CH_4 fluxes in non-forest land uses as compared to mangrove forests could be probably due to increased soil drainage. The modification of soil surface elevation in the non-forest land uses including the embankment/levee and canals could have reduced the entry of tidal waters and the inundation period in these systems, and increased the soil drainage. In terrestrial peatland, the methane fluxes were observed to exhibit exponential response to changes in water table depth, before and after the peatland conversion, suggesting higher CH_4 emission with reduced drainage (Hergoualc'h & Verchot 2012).

Total emission per hectare in mangrove forest is greater by 2.5 times (66 %) than non-forest land uses. This is probably due to higher CO_2 emissions in mangroves as well as the large proportion (>95%) of CO_2 in the total GHG flux. In addition, the non-forest land uses are now abandoned and unmanaged, but they could have even higher N_2O fluxes where they are still are actively managed. For example, adding nutrients to the soil, in the form of feeds to nurture shrimps/fish and fertilisers to enhance coconut growth, could increase soil N_2O fluxes.

Very few studies have simultaneously measured the fluxes of three GHG gases in the mangrove soil and in land-uses that are formerly occupied by mangroves. In this study, the mean estimates for the fluxes of the three GHGs under mangrove forests fell within the range reported in the literature (Table 7.5). The GHG flux estimates in this study are five times higher as compared to the fluxes of pristine mangrove forest in Indonesia (Chen et al. 2014) but in the lower limit of the summer GHG fluxes of mangroves in Shenzhen and Hong Kong in southern China (Chen et al. 2010).

The mean CO_2 flux in this study is comparable to the average flux of undisturbed mangroves in Queensland and Western Australia (Lovelock 2008) but higher than the mean values (68.96 mmol m^{-2} day^{-1}; n = 75) from mangrove forests worldwide (Alongi 2009). The measured CO_2 fluxes in this study are probably conservative since the measurement was done in the rainy season (July). In India, fluxes of CO_2 were lower during rainy season as compared to dry/summer season (Chanda et al. 2014). However, such observation was not the same case in Thailand where the dry and wet season fluxes were comparable (Poungparn et al. 2009). Further studies are, therefore, needed to evaluate if there is seasonal variation in CO_2 flux. On the other hand, the calculated mean CH_4 and N_2O flux estimates are in the lower limit of the ranges for the mangrove sediments in Moreton Bay and Brisbane River in Australia (Allen et al. 2011).

As for the GHG fluxes in the soil that are formerly occupied by mangroves, only fluxes of CO_2 are available so far for comparison, and only for aquaculture ponds and cleared mangroves. The mean flux estimate for abandoned aquaculture ponds is similar to mean floor emission of active aquaculture ponds that were drained in Indonesia (Sidik & Lovelock 2013). Furthermore, the measured soil CO_2 flux from the cleared mangrove in the present study is lower as compared to that in Belize (Lovelock et al. 2011). The cleared mangroves in Belize are on peat soil (300 mgC g^{-1}) that has higher soil C content as compared to the cleared mangrove in this study (~92 mgC g^{-1}).

Table 7.5 Reported soil greenhouse gas fluxes in different mangrove forests and other land uses under former mangrove area and in peatland

Location	Land Use	CO_2 flux ($\mu mol\ m^{-2}\ s^{-1}$)	CH_4 flux ($\mu mol\ m^{-2}\ h^{-1}$)	N_2O flux ($\mu mol\ m^{-2}\ h^{-1}$)	Reference
A. Mangrove forests					
Honda Bay, Puerto Princesa, Philippines	Mangrove forest (*Rhizophora*)	2.90	6.15	0.01	This study
North Sulawesi, Indonesia	*Rhizophora-Bruguiera* Mangrove forest	0.55	0.71	-0.04	Chen et al. (2014)
Shenzhen and Hong Kong, China	*Kandelia* mangrove forest	0.15 – 5.71	10.10 – 5,168.62	0.14 – 23.83	Chen et al. (2010)
Mai Po, Hong Kong	*Kandelia* mangrove forest	0.07 – 8.67	Not determined	0.73-1.21	Chen et al. (2012)
Sundarbans, India	*Avicennia* mangrove forests	0.15 - 2.34	Not determined	Not determined	Chanda et al. (2014)
Australia, New Zealand and the Caribbean	Mangrove forest	-0.25 – 2.97	Not determined	Not determined	Lovelock (2008)
Southeast Queensland, Australia	Subtropical mangrove	Not determined	0.19 to 1,087.50	0.09 – 1.48	Allen et al. (2011)
B. Non-forest land uses that replaced mangroves					
Honda Bay, Puerto Princesa, Philippines	Abandoned aquaculture pond	1.14	-5.95	0.33	This study
Honda Bay, Puerto Princesa, Philippines	Abandoned salt pond	2.25	17.53	5.54	This study
Honda Bay, Puerto Princesa, Philippines	Coconut plantation (under mangrove soil)	0.41	0.78	-4.79	This study
Honda Bay, Puerto Princesa, Philippines	Cleared mangrove	0.16	0.49	-0.67	This study
Twin Bays, Central Belize	Cleared mangrove	2.1 – 7.6	Not determined	Not determined	Lovelock et al. (2011)
Bali, Indonesia	Shrimp pond	1.15 - 3.15	Not determined	Not determined	Sidik and Lovelock (2013)
C. Land uses in peatland					
Kalimantan, Indonesia	Peat forest (secondary)	2.49	31.39	3.47	Hadi et al. (2005)
Kalimantan, Indonesia	Paddy field	1.00	139.84	0.06	Hadi et al. (2005)
Kalimantan, Indonesia	Rice-soybean	1.46	18.55	0.53	Hadi et al. (2005)

Several site variables significantly correlate with the three GHGs in mangrove forest and non-mangrove sites. However, the relationships were moderate at the most. This may indicate that the GHG fluxes may be predicted by those site variables but with higher errors. Nonetheless, this could be useful information in attempting to estimate fluxes for larger areas as variable like LAI could be mapped using remote sensing techniques (Lovelock et al. 2011; Dusseux et al. 2015).

The effect on GHG fluxes of the differences in tidal positions between mangrove forests and non-forest land uses was not analysed in this study. This gap should be considered in future studies. In this study, mangrove forests were found to occur in the seaward, middle and landward part of the intertidal zone while non-forest land uses that replaced mangroves were in the middle and landward sections. However, a soil GHG fluxes study of mangroves in Indonesia (Chen et al. 2014) showed that the fluxes of the three GHGs were statistically similar in the landward, middle zone and seaward tidal positions. In subtropical mangroves in Hong Kong-Shenzhen area in southern China, Chen et al. (2010) reported that the summer fluxes of the three GHGs were also statistically similar in the landward and seaward tidal positions, except for CO_2 which had higher fluxes landward. These results may indicate that tidal positions have small effect on GHG fluxes in mangrove soil.

Furthermore, the inundation period at each transect of the land uses under study was not measured. This information is probably important in evaluating if the period of submergence by tidal water has influence on the rate of fluxes of the three GHGs. Are soils with longer inundation period emit more CO_2, CH_4 and N_2O than those with shorter inundation time? Incidentally, previous studies had mixed results. For instance, Poungparn et al. (2009) showed that in a riverine mangrove in Thailand, plots in the river edge/fringe were observed to exhibit higher CO_2 fluxes as compared to plots established away from the river. Plots in the river edge/fringe had longer inundation period than those plots away from the river. However, Chen et al. (2014) and Chen et al. (2010) found that the GHG fluxes are statistically similar along intertidal positions which could have different inundation periods. These results suggest that future studies are needed to investigate the effect of inundation period on GHG fluxes in mangrove soil.

The study demonstrated the good potential of GIS-based Kriging for mapping the GHG fluxes in mangrove soil. The generated maps of soil GHG fluxes in this study have overall prediction errors of 17 % to 24.7 %. These are probably sufficient for general land use planning purposes in the coastal zone and as a baseline for which to compare future management intervention such as reforestation. The accuracy of the map might be improved by adding more plots distributed strategically in areas far from the current plots. This study reported for the first time the mapping of the soil GHG emissions in mangrove area. The soil GHG emissions maps generated by the study could complement the Net Primary Production (NPP) maps in order to generate maps of Net Ecosystem Production (NEP). NEP is obtained by subtracting soil respiration (sum of annualised soil CO_2 and CH_4 fluxes) from NPP as used by Chen et al. (2016).

7.5.2 Implications for management and conservation

The total area covered by mangrove forests in the study site is 1,216.4 ha while for the non-forest land uses, it is 1,533.3 ha. Roughly, the non-forest land uses emit and contribute ca. 24,753 tonnes of CO_2e to the atmosphere annually. Since these land uses are generally devoid of vegetation, they cannot offset this amount of emission on-site through photosynthesis. For mangrove forests, their total annual emission is 49,256 tonnes of CO_2e to the atmosphere. However, mangrove forests can offset this emission through vegetation C uptake which is at a net rate of 40 - 50 tonnes CO_2 ha^{-1} y^{-1} (Lovelock et al. 2011; Alongi 2014). This means that the 1,216.4-ha mangrove forests in the study site can practically offset all of their soil C emissions through photosynthesis at a net rate of 48,656 – 60,820 tonne CO_2 y^{-1}. This highlights the importance of mangrove forests in the study site, acting as a huge absorber of atmospheric CO_2, aside from other ecological goods and services they provide. During the period 2000 – 2012, approximately 1,423 ha of mangrove forests were removed in the Philippines, and 36.7 % of this area were converted to aquaculture (Richards & Friess 2016). Using the results from this study, and assuming all the mangrove soil (forested or otherwise) in the country were similar to the mangrove soil in this study, it is estimated that this 522-ha new aquaculture ponds emit about 8,333 tCO_2e yearly to the atmosphere that is not offset *in situ* by

this land use. This is in addition to the lost atmospheric C sequestration function of approximately 20,880 – 26,100 tonne CO_2 y^{-1} due to the deforestation of 522 ha of mangrove forests. This result could serve as basis to estimate the GHG emissions due to land use change in mangrove in the country.

7.6 Conclusion

The soil CO_2 and CH_4 fluxes in land uses that replaced mangroves were lower than that of mangrove forests, except for N_2O fluxes which are lower in mangroves. The soils of mangrove forests and the non-forest land uses are net sources of the three GHGs. The study also found significant site correlates of the three GHGs. Mapping the spatial variation of the fluxes of the three GHGs is possible using the GIS-based Ordinary Kriging technique, as shown by the good agreement between modelled and measured values. The fluxes emitted by mangrove forest could be offset by its net vegetation uptake through photosynthesis at an almost similar rate (soil emission: 40 vs. uptake: 40.7 to 50 $MgCO_2$ ha^{-1} y^{-1}). However, those emissions from non-forest land uses such as aquaculture pond (~15.8 $MgCO_2e$ ha^{-1} y^{-1}) cannot be offset *in situ* by these land uses as they are generally devoid of vegetation.

The results obtained in the study could be used as emission factors in the conduct of higher tier national GHG inventories, and to refine regional and global emission values from land use change in mangroves. Moreover, the result could provide the scientific basis to estimate the GHG impacts of the estimated 232,000-ha brackish water aquaculture ponds, active and abandoned alike, in the Philippines, majority of which were previously occupied by mangrove forests. Future works should include other land uses such as rice agriculture and oil palm plantations, and consider increasing the sampling campaigns to include dry season and monthly measurements which could improve flux estimates and clarify possible seasonal flux differences. Results of the study could also inform the current discussions on inclusion of mangrove forests under REDD+ and other global change mechanisms.

The next Chapter provides the overall summary and conclusion of this Dissertation.

Chapter 8

CONCLUSION

8.1 Introduction

This study aimed to evaluate the carbon (C) budget of mangrove forests and their competing replacement non-forest land uses, in biomass, soil and soil greenhouse gas (GHG) fluxes. To achieve this aim, the study was divided into four objectives as enumerated in Chapter 1 wherein each was addressed in Chapters 4 to 7.

This Thesis provides a comprehensive study of C budget of mangroves and non-forest land uses that replaced them (aquaculture pond, salt pond, cleared mangrove and coconut plantation), including the four major carbon pools in coastal wetland ecosystem (soils, aboveground biomass, belowground biomass and downed woody debris biomass). It also includes the study of the three major GHGs (CO_2, CH_4 and N_2O) associated with land use change. The study was based on field assessments and laboratory analyses, combined with the use of the new Sentinel satellite remote sensing imagery and Geographic Information System (GIS) techniques.

This study was the first to evaluate the whole-ecosystem (soil and biomass) carbon stocks of mangroves and four land uses that replaced them, and the potential C losses owing to mangrove conversion using empirical measurements. It also covered for the first time the investigation of the CH_4 and N_2O fluxes in the soil of land uses that replaced mangroves. The study was also the first one to investigate the use of new-generation SAR (Sentinel-1) and multispectral (Sentinel-2) imagery data for biomass mapping in mangrove area, and also the first to test and report the application of GIS-based geostatistical Kriging technique to mangrove area for soil C stock mapping and mapping of soil GHG fluxes.

This Chapter presents the summary of findings and overall conclusion of the whole Dissertation and provides a number of recommendations for future research. This Chapter is organised into four sections. Section 8.2 presents the summary of findings, while Section 8.3 provides the overall conclusion and major contributions of the study. The Chapter ends in Section 8.5 with recommendations for future studies.

8.2 Summary of Findings

This study provided new knowledge and fresh insights on C budget assessment of mangrove and the C losses owing to mangrove conversion to competing non-forest land uses through empirical study. This was accomplished using the triad approach of mangrove field measurement techniques in conjunction with novel application of new-generation satellite remote sensing imagery and GIS-based technique, both of which have never been applied in previous studies in mangroves.

8.2.1 Evaluation of biomass, C losses from biomass and canopy predictors

Chapter 4 revealed that the total biomass C stock in mangroves ranged from 21.2 to 71.7 MgC ha^{-1}. In contrast, biomass C stock ranged from zero to 0.12 MgC ha^{-1} in abandoned aquaculture pond, abandoned salt ponds and cleared mangrove site, to 5.7 MgC ha^{-1} in coconut plantation. Carbon losses from biomass owing to mangrove conversion to other land uses ranged from 82 to 263 Mg CO_2e ha^{-1}. The difference in the biomass C stocks of closed and open canopy mangroves of 69% could indicate a form of mangrove forest C degradation by 49.2 Mg C ha^{-1}. The Leaf Area Index (LAI) correlated strongly with mangrove biomass, an important information for biomass mapping in mangrove, as LAI map can generated using satellite imagery.

8.2.2 Biomass mapping using Sentinel satellite imagery

Chapter 5 demonstrated that the model based on biophysical variable Leaf Area Index (LAI) derived from Sentinel-2 was more accurate in predicting the over-

all aboveground biomass. In contrast, the model which utilised optical bands had the lowest accuracy. However, the Synthetic Aperture Radar (SAR)-based model was more accurate in predicting the biomass in the usually deficient to low vegetation cover non-forest replacement land uses such as abandoned aquaculture pond, cleared mangrove and abandoned salt pond. These models had 0.82 to 0.83 correlation/agreement of observed and predicted value, and root mean square error of 27.8 to 28.5 Mg ha^{-1}. Among the Sentinel-2 multispectral bands, the red and red edge bands (bands 4, 5 and 7), in combination with elevation data, were the best variable set combination for biomass prediction. The red edge-based Inverted Red-Edge Chlorophyll Index had the highest prediction accuracy among the vegetation indices. Overall, Sentinel-1 SAR and Sentinel-2 multispectral imagery can provide good results in the retrieval and predictive mapping of the aboveground biomass of mangroves and the replacement non-forest land uses, especially with the inclusion of elevation data. The study demonstrates encouraging results for biomass mapping of mangroves and other coastal land uses in the tropics using the freely accessible and relatively high-resolution Sentinel imagery.

8.2.3 Evaluation of soil C stocks and GIS-based soil C stock mapping

Chapter 6 presented that the soil C stock of mangrove forests was 2.3 times greater than the competing land uses that replaced mangroves. The C losses in soil (i.e. C stock difference between mangrove forests and replacement land uses) owing to mangrove land use conversion was 57%, on average, and ranged from 1,461 to 2,969 Mg CO_2e ha^{-1}. It was possible to model the site-scale spatial distribution of soil C stock and predict their values with 85% overall certainty using Ordinary Kriging approach.

8.2.4 Evaluation of soil fluxes of greenhouse gases and GIS-based soil GHG mapping

Chapter 7 showed that the emissions of CO_2 and CH_4 are higher by 2.6 and 6.6 times in mangrove forests while their N_2O emission is lower by 34 times compared to the average of non-forest land uses. CH_4 and N_2O emissions accounted for 0.59% and 0.04% of the total emissions in mangrove forest compared to 0.23% and 3.07%, respectively, for non-forest land uses. Site-scale soil GHG flux

distribution could be mapped with 75% to 83% accuracy using Ordinary Kriging. In general, total emission (CO_2 + CH_4 + N_2O) in mangrove forest is 2.5 times (66%) higher than non-forest land uses. However, unlike mangroves that can offset all its emissions through CO_2 uptake from photosynthesis, the non-forest land uses cannot offset their emissions on-site as they are usually devoid of vegetation.

8.2.5 Overall summary

In summary, this thesis has shown the following:

a. The whole-ecosystem (total biomass + soil) C stock of mangrove forests was 900 (range: 661.2 to 1,111.7) MgC ha^{-1}, while the competing non-forest replacement land uses of mangroves was only 329 (range: 47.9 in the coconut plantation to 454 in abandoned aquaculture ponds) MgC ha^{-1}.

b. The proportion of soil pool to the total C stock (biomass + soil) increases after conversion, from 95% in mangrove forests to almost 100% in replacement land uses.

c. Carbon losses in biomass and soil owing to conversion were 63% (571 MgC ha^{-1}) or 2,096 tCO_2e ha^{-1} of mangrove forest converted.

d. The total soil flux (CO_2 + CH_4 + N_2O) in mangrove forest is 2.5 times (66%) higher than replacement land uses. Surface fluxes of CO_2 and CH_4 decreased by 2.6 and 6.6 times while N_2O flux increased by 34 times after mangrove conversion.

e. The new Sentinel satellite imagery could be used in mangrove areas to predict and map the biomass in the whole study site with satisfactory results. Furthermore, the GIS-based geostatistical Kriging could be used to predict and map the soil C stocks and soil GHG fluxes in the whole study site with good accuracy.

The above findings may suggest the following:

a. Mangrove conversion to other land uses heavily reduces the C stock in the coastal ecosystem. More than half (~63%) of C stock is lost after conversion. Soil becomes the sole C pool after conversion, in most cases.

b. Mangrove conversion heavily alters the soil-atmosphere fluxes of the three major GHGs, especially the non-CO_2 gases. Conversion of mangroves to other land uses reduces the fluxes of CH_4 by six times but increases the N_2O fluxes by 33 times.

c. The non-forest land uses that replaced mangroves are net sources of carbon.

d. The use of the new-generation Sentinel SAR and Sentinel multispectral imagery data has a good potential for biomass retrieval and mapping of coastal areas similar to the study site.

e. The use of GIS-based geostatistical Ordinary Kriging technique has a good potential for estimating soil C stock and soil GHG fluxes in un-sampled locations and mapping their distribution in coastal areas similar to the study site.

f. Estimating the whole-ecosystem C stocks at un-sampled locations and mapping their site-scale distribution in mangrove area could be possible to accomplish with the methods used in this study utilising the Sentinel imagery for biomass mapping and GIS-based geostatistical Kriging for soil C stock mapping.

g. The global coverage of the Sentinel imagery, in both radar and multispectral, suggests that it would be possible to map the mangrove biomass in higher resolution (10 m) than the currently available in the country, regional and global scales using the Sentinel imagery.

8.3 Conclusion

This study provided improved knowledge and new insights of mangrove forests' biomass C stocks, soil C stocks, soil fluxes of CO_2, CH_4 and N_2O, and their site environmental correlates vis-a-vis land uses that replaced them. The study also clarified, through empirical measurements, the magnitude of changes in soil and biomass C stocks, and soil GHG fluxes owing to mangrove conversion. Such information might be important for refinements of emission factors for mangrove deforestation and conversion to other land uses.

Moreover, this study generated new knowledge into how to map biomass, soil C and the soil fluxes of GHG using the new-generation Sentinel satellite radar and optical imagery and GIS-based geostatistical Kriging technique, both of which have never been applied and evaluated for mangrove area. The study's contributions to the current knowledge of quantifying and mapping the C stocks and soil GHG fluxes of mangrove forests and land uses that replaced mangroves will hopefully help in the better monitoring and management of mangroves' C stocks and soil GHG emissions in the tropics, as well as improve our understanding of the climate impact of mangrove conversion. The approaches used in this study to map the aboveground biomass, soil C stocks and soil fluxes of CO_2, CH_4 and N_2O will also hopefully contribute to the improvements of methods for mapping the ecosystem services of mangrove forests particularly the C storage and emissions.

The major contributions to science of the present work include the following:

- Improved understanding of C stocks in soil and biomass of mangrove forests and the non-forest land uses that replaced them, and the C losses associated with mangrove conversion based on empirical measurements;
- Improved understanding of the soil fluxes/emissions of the three major greenhouse gases (CO_2, CH_4 and N_2O) in mangrove forests in relation to the non-forest land uses that replaced them;
- New knowledge on the potential application of Sentinel radar and optical imagery in mapping the biomass of coastal mangrove area;
- New knowledge on the potential application of GIS-based geostatistical Kriging spatial interpolation in mapping the soil C stock in mangrove area;
- New knowledge on the potential application of GIS-based geostatistical Kriging spatial interpolation in mapping the soil fluxes of CO_2, CH_4 and N_2O in mangrove area; and
- The approaches used in the study could be adopted to possibly map for the first time the whole-ecosystem C stocks, C emissions and Net Ecosystem Production in mangrove area.

8.4 Recommendation

Based on the foregoing discussions, the results of the study could be used for the following practical applications:

- Inform the current discussions on Blue Carbon and REDD+ as well as policy and program development that advance research on soil C conservation and ecosystem services exists in coastal forested wetlands;
- Higher tier national GHG inventory, refine regional and global estimates of GHG emissions in mangrove wetlands, and inform policy-making in coastal wetlands conservation;
- The methods adopted in the study to estimate and map the biomass, soil C stocks and soil GHG fluxes of mangroves and the non-forest land uses that replaced them could be used to other coastal areas similar to the site;
- The equations generated by the study can used for C accounting and mapping tasks in the coastal mangrove area but should be used with caution especially in sites with different environmental and climatic conditions.

Also, the following are recommended for future research:

- There is a need for distinguishing and mapping closed and open canopy mangrove stands, similar to what is being done to their terrestrial forest counterparts, to facilitate monitoring and a better understanding of forest degradation in mangrove forests.
- Follow-up studies should aim for the generation of DEM from Sentinel-1 InSAR in order to test its capability for biomass retrieval and mapping in combination with Sentinel backscatter and multispectral data. In addition, the accuracy of the biomass map might be improved with additional plots distributed strategically in areas far from the current plots, and additional sites for each land use especially for coconut plantation, abandoned saltpond and cleared mangrove. Lastly, the use of various data

transformation techniques, as well as non-linear multiple regression forms, should be also pursued with the aim of finding the highest correlation for predicted and observed value, and lower prediction error compared to the current values.

- Likewise, for soil C stock mapping in mangrove, some portions of the study area were far from sites which were sampled due to resources constraint and therefore the estimate in that portion may be associated with higher prediction errors compared to those portions near the sampled locations. Thus, increasing the number of samples and distribute them evenly in the study site would make the spatial interpolation more robust.

- Include other land uses such as rice agriculture and oil palm plantations, and consider increasing the sampling campaigns to include dry season and monthly measurements which could improve flux estimates and to clarify possible seasonal flux differences. Also, include the measurement of the inundation period in each of the land uses.

REFERENCES

Abino, AC, Castillo, JAA & Lee, YJ 2013, 'Assessment of species diversity, biomass and carbon sequestration potential of a natural mangrove stand in Samar, the Philippines', *Forest Science and Technology*, vol. 10, no. 1, pp. 2-8.

Abino, AC, Castillo, JAA & Lee, YJ 2014, 'Species diversity, biomass, and carbon stock assessments of a natural mangrove forest in palawan, philippines', *PAKISTAN JOURNAL OF BOTANY*, vol. 46, no. 6, pp. 1955-62.

Adame, MF, Santini, NS, Tovilla, C, Vázquez-Lule, A, Castro, L & Guevara, M 2015, 'Carbon stocks and soil sequestration rates of tropical riverine wetlands', *Biogeosciences*, vol. 12, no. 12, pp. 3805-18.

Adame, MF, Kauffman, JB, Medina, I, Gamboa, JN, Torres, O, Caamal, JP, Reza, M & Herrera-Silveira, JA 2013, 'Carbon Stocks of Tropical Coastal Wetlands within the Karstic Landscape of the Mexican Caribbean', *PLoS ONE*, vol. 8, no. 2, p. e56569.

Allen, D, Dalal, RC, Rennenberg, H & Schmidt, S 2011, 'Seasonal variation in nitrous oxide and methane emissions from subtropical estuary and coastal mangrove sediments, Australia', *Plant Biology*, vol. 13, no. 1, pp. 126-33.

Allen, DE, Dalal, RC, Rennenberg, H, Meyer, RL, Reeves, S & Schmidt, S 2007, 'Spatial and temporal variation of nitrous oxide and methane flux between subtropical mangrove sediments and the atmosphere', *Soil Biology and Biochemistry*, vol. 39, no. 2, pp. 622-31.

Allen, J, Ewel, K, Keeland, B, Tara, T & Smith, T 2000, 'Downed wood in Micronesian mangrove forests', *Wetlands*, vol. 20, no. 1, pp. 169-76.

Alongi, DM 2002, 'Present state and future of the world's mangrove forests', *Environmental Conservation*, vol. 29, no. 03, pp. 331-49.

Alongi, DM 2009, *The energetics of mangrove forests*, Springer Science & Business Media.

Alongi, DM 2012, 'Carbon sequestration in mangrove forests', *Carbon Management*, vol. 3, no. 3, pp. 313-22.

Alongi, DM 2014, 'Carbon Cycling and Storage in Mangrove Forests', *Annual Review of Marine Science*, vol. 6, no. 1, pp. 195-219.

Aslan, A, Rahman, AF, Warren, MW & Robeson, SM 2016, 'Mapping spatial distribution and biomass of coastal wetland vegetation in Indonesian Papua by combining active and passive remotely sensed data', *Remote Sensing of Environment*, vol. 183, pp. 65-81.

Barbier, EB, Hacker, SD, Kennedy, C, Koch, EW, Stier, AC & Silliman, BR 2011, 'The value of estuarine and coastal ecosystem services', *Ecological Monographs*, vol. 81, no. 2, pp. 169-93.

Bhomia, RK, MacKenzie, RA, Murdiyarso, D, Sasmito, SD & Purbopuspito, J 2016, 'Impacts of land use on Indian mangrove forest carbon stocks: Implications for conservation and management', *Ecological Applications*, vol. 26, no. 5, pp. 1396-408.

Bouillon, S, Borges, AV, Castañeda-Moya, E, Diele, K, Dittmar, T, Duke, NC, Kristensen, E, Lee, SY, Marchand, C, Middelburg, JJ, Rivera-Monroy, VH, Smith, TJ & Twilley, RR 2008, 'Mangrove production and carbon sinks: A revision of global budget estimates', *Global Biogeochemical Cycles*, vol. 22, no. 2, p. GB2013.

Bridgham, SD, Megonigal, JP, Keller, JK, Bliss, NB & Trettin, C 2006, 'The carbon balance of North American wetlands', *Wetlands*, vol. 26, no. 4, pp. 889-916.

Brown, S 1997, *Estimating biomass and biomass change of tropical forests: a primer*, vol. 134, Food & Agriculture Org.

Brown, WH & Fischer, AF 1920, 'Philippine Mangrove Swamps', in W Brown (ed.), *Minor Products of Philippine Forests* Bureau of Printing, Manila, vol. 1.

Campbell, JB & Wynne, RH 2011, *Introduction to Remote Sensing*, Fifth edn, Guilford Press, New York.

Castillo, JAA, Apan, AA, Maraseni, TN & Salmo Iii, SG 2017, 'Soil C quantities of mangrove forests, their competing land uses, and their spatial distribution in the coast of Honda Bay, Philippines', *Geoderma*, vol. 293, pp. 82-90.

Chanda, A, Akhand, A, Manna, S, Dutta, S, Das, I, Hazra, S, Rao, KH & Dadhwal, VK 2014, 'Measuring daytime CO2 fluxes from the inter-tidal mangrove soils of Indian Sundarbans', *Environmental Earth Sciences*, vol. 72, no. 2, pp. 417-27.

Chave, J, Andalo, C, Brown, S, Cairns, MA, Chambers, JQ, Eamus, D, Fölster, H, Fromard, F, Higuchi, N, Kira, T, Lescure, J-P, Nelson, BW, Ogawa, H, Puig, H, Riéra, B & Yamakura, T 2005, 'Tree allometry and improved estimation of carbon stocks and balance in tropical forests', *Oecologia*, vol. 145, no. 1, pp. 87-99.

Chen, G, Chen, B, Yu, D, Tam, NFY, Ye, Y & Chen, S 2016, 'Soil greenhouse gas emissions reduce the contribution of mangrove plants to the atmospheric cooling effect', *Environmental Research Letters*, vol. 11, no. 12, p. 124019.

Chen, GC, Tam, NFY & Ye, Y 2010, 'Summer fluxes of atmospheric greenhouse gases N2O, CH4 and CO2 from mangrove soil in South China', *Science of The Total Environment*, vol. 408, no. 13, pp. 2761-7.

Chen, GC, Tam, NFY & Ye, Y 2012, 'Spatial and seasonal variations of atmospheric N2O and CO2 fluxes from a subtropical mangrove swamp and their relationships with soil characteristics', *Soil Biology and Biochemistry*, vol. 48, no. 0, pp. 175-81.

Chen, GC, Ulumuddin, YI, Pramudji, S, Chen, SY, Chen, B, Ye, Y, Ou, DY, Ma, ZY, Huang, H & Wang, JK 2014, 'Rich soil carbon and nitrogen but low atmospheric greenhouse gas fluxes from North Sulawesi mangrove swamps in Indonesia', *Science of The Total Environment*, vol. 487, no. 0, pp. 91-6.

Chen, Y, Li, X, Liu, X & Ai, B 2013, 'Analyzing land-cover change and corresponding impacts on carbon budget in a fast developing sub-tropical region by integrating MODIS and Landsat TM/ETM+ images', *Applied Geography*, vol. 45, no. 0, pp. 10-21.

Chmura, GL, Anisfeld, SC, Cahoon, DR & Lynch, JC 2003, 'Global carbon sequestration in tidal, saline wetland soils', *Global Biogeochemical Cycles*, vol. 17, no. 4, pp. n/a-n/a.

Christensen, LK, Bennedsen, BS, Jørgensen, RN & Nielsen, H 2004, 'Modelling Nitrogen and Phosphorus Content at Early Growth Stages in Spring Barley using Hyperspectral Line Scanning', *Biosystems Engineering*, vol. 88, no. 1, pp. 19-24.

CID_Bioscience 2016, *CI-100 Plant Canopy Imager*, CID Bioscience, USA, viewed May 1, 2017, <https://cid-inc.com/plant-science-tools/leaf-area-measurement/ci-110-plant-canopy-imager/>.

Cintron, G & Novelli, YS 1984, 'Methods for studying mangrove structure', in *Mangrove ecosystem: research methods*, Unesco, pp. 91-113.

Clough, BF 2013, *Continuing the journey amongst mangroves*, International Society for Mangrove Ecosystems, Okinawa, Japan.

Clough, BF & Scott, K 1989, 'Allometric relationships for estimating above-ground biomass in six mangrove species', *Forest Ecology and Management*, vol. 27, no. 2, pp. 117-27.

Cobb, A, Agus, F, Warren, M, Applegate, G, Ryan, Z, Engel, V, Handayani, E, Hooijer, A, Husen, E & Jauhiainen, J 2012, 'Greenhouse gas fluxes and flux changes from land-use dynamics in tropical wetlands', in *Tropical wetlands for climate change adaptation and mitigation: Science and policy imperatives with special reference to Indonesia*, Center for International Forestry Research (CIFOR), Bogor, Indonesia.

DelVecchia, AG, Bruno, JF, Benninger, L, Alperin, M, Banerjee, O & de Dios Morales, J 2014, 'Organic carbon inventories in natural and restored Ecuadorian mangrove forests', *PeerJ*, vol. 2, p. e388.

Donato, DC, Kauffman, JB, Murdiyarso, D, Kurnianto, S, Stidham, M & Kanninen, M 2011, 'Mangroves among the most carbon-rich forests in the tropics', *Nature Geosci*, vol. 4, no. 5, pp. 293-7.

Dube, T, Gara, TW, Mutanga, O, Sibanda, M, Shoko, C, Murwira, A, Masocha, M, Ndaimani, H & Hatendi, CM 2016, 'Estimating forest standing biomass in savanna

woodlands as an indicator of forest productivity using the new generation WorldView-2 sensor', *Geocarto International*, pp. 1-11.

Duncan, C, Primavera, JH, Pettorelli, N, Thompson, JR, Loma, RJA & Koldewey, HJ 2016, 'Rehabilitating mangrove ecosystem services: A case study on the relative benefits of abandoned pond reversion from Panay Island, Philippines', *Marine Pollution Bulletin*, vol. 109, no. 2, pp. 772-82.

Dusseux, P, Hubert-Moy, L, Corpetti, T & Vertès, F 2015, 'Evaluation of SPOT imagery for the estimation of grassland biomass', *International Journal of Applied Earth Observation and Geoinformation*, vol. 38, pp. 72-7.

Eong, OJ 1993, 'Mangroves - a carbon source and sink', *Chemosphere*, vol. 27, no. 6, pp. 1097-107.

ESA 2016, *Sentinels Scientific Data Hub*, European Space Agency, viewed August 1, 2016, <https://scihub.copernicus.eu/>.

FAO 2007, *The World's Mangroves 1980–2005*, Food and Agriculture Organisation, Rome, Italy.

FAO 2010, 'Global Forest Resources Assessment 2010: Main report', *Food and Agriculture Organization of the UN: Rome, Italy*, p. 378.

Fatoyinbo, TE, Simard, M, Washington-Allen, RA & Shugart, HH 2008, 'Landscape-scale extent, height, biomass, and carbon estimation of Mozambique's mangrove forests with Landsat ETM+ and Shuttle Radar Topography Mission elevation data', *Journal of Geophysical Research: Biogeosciences*, vol. 113, no. G2, p. G02S6.

FMB 2005, '2003 Philippine Forestry Statistics', *Forest Management Bureau, Department of Environment and Natural Resources: Quezon City, Philippines*, p. 333.

FMB 2014, '2012 Philippine Forestry Statistics', *Forest Management Bureau, Department of Environment and Natural Resources: Quezon City, Philippines*, p. 335.

Fortes, MD 2004, 'Chapter 14 - Wetland Conservation and Management in the Philippines: Where are We Now? The Case of Seagrass and Mangrove', in MH Wong (ed.), *Wetlands Ecosystems in Asia*, Elsevier, Amsterdam, vol. 1, pp. 233-62.

Giri, C, Ochieng, E, Tieszen, LL, Zhu, Z, Singh, A, Loveland, T, Masek, J & Duke, N 2011, 'Status and distribution of mangrove forests of the world using earth observation satellite data', *Global Ecology and Biogeography*, vol. 20, no. 1, pp. 154-9.

Hadi, A, Inubushi, K, Furukawa, Y, Purnomo, E, Rasmadi, M & Tsuruta, H 2005, 'Greenhouse gas emissions from tropical peatlands of Kalimantan,Indonesia', *Nutrient Cycling in Agroecosystems*, vol. 71, no. 1, pp. 73-80.

Hall, M, Frank, E, Holmes, G, Pfahringer, B, Reutemann, P & Witten, IH 2009, 'The WEKA data mining software: an update', *ACM SIGKDD explorations newsletter*, vol. 11, no. 1, pp. 10-8.

Hamilton, SE & Casey, D 2016, 'Creation of a high spatio-temporal resolution global database of continuous mangrove forest cover for the 21st century (CGMFC-21)', *Global Ecology and Biogeography*, vol. 25, no. 6, pp. 729-38.

He, Y & Guo, X 2006, 'Leaf Area Index estimation using remotely sensed data for Grassland National Park', *Prairie Perspectives*, vol. 9, pp. 105-17.

Hergoualc'h, K & Verchot, LV 2011, 'Stocks and fluxes of carbon associated with land use change in Southeast Asian tropical peatlands: A review', *Global Biogeochemical Cycles*, vol. 25, no. 2, p. GB2001.

Hergoualc'h, K & Verchot, LV 2012, *Changes in soil CH4 fluxes from the conversion of tropical peat swamp forests: a meta-analysis*, vol. 9.

Hiraishi, T, Krug, T, Tanabe, K, Srivastava, N, Baasansuren, J, Fukuda, M & Troxler, T 2014, '2013 Supplement to the 2006 IPCC Guidelines for National Greenhouse Gas Inventories: Wetlands', *IPCC, Switzerland*.

Hossain, M 2014, 'Carbon pools and fluxes in Bruguiera parviflora dominated naturally growing mangrove forest of Peninsular Malaysia', *Wetlands Ecology and Management*, vol. 22, no. 1, pp. 15-23.

Howard, J, Hoyt, S, Isensee, K, Telszewski, M, Pidgeon, E & eds 2014, *Coastal blue carbon: methods for assessing carbon stocks and emissions factors in mangroves, tidal salt marshes, and seagrasses*, Conservation International, Intergovernmental Oceanographic Commission of UNESCO, International Union for Conservation of Nature, Arlington, VA, USA.

Howard, J, Sutton-Grier, A, Herr, D, Kleypas, J, Landis, E, McLeod, E, Pidgeon, E & Simpson, S 2017, 'Clarifying the role of coastal and marine systems in climate mitigation', *Frontiers in Ecology and the Environment*, vol. 15, no. 1, pp. 42-50.

Hutchison, J, Manica, A, Swetnam, R, Balmford, A & Spalding, M 2014, 'Predicting Global Patterns in Mangrove Forest Biomass', *Conservation Letters*, vol. 7, no. 3, pp. 233-40.

Inubushi, K, Furukawa, Y, Hadi, A, Purnomo, E & Tsuruta, H 2003, 'Seasonal changes of CO2, CH4 and N2O fluxes in relation to land-use change in tropical peatlands located in coastal area of South Kalimantan', *Chemosphere*, vol. 52, no. 3, pp. 603-8.

IPCC 2013, 'Climate Change 2013: The Physical Science Basis. Contribution of Working Group I to the Fifth Assessment Report of the Intergovernmental Panel on Climate Change', in T Stocker, et al. (eds), Cambridge University Press, Cambridge and New York, p. 1535.

IPCC 2014a, '*Climate Change 2014: Synthesis Report. Contribution of Working Group I, II and III to the Fifth Assessment Report of the Intergovernmental Panel on Climate Change*', in RK Pachauri & LA Meyer (eds), Cambridge University Press, Cambridge, United Kingdom and New York, NY, USA, p. 151.

IPCC 2014b, 'Climate change 2014: Impacts, adaptation, and vulnerability. Part B: Regional aspects. Contribution of working group II to the fifth assessment report of the Intergovernmental Panel on Climate Change', in V Barros, et al. (eds), Cambridge University Press, Cambridge, United Kingdom and New York, NY, USA.

IPCC 2014c, '2013 Supplement to the 2006 IPCC Guidelines for National Greenhouse Gas Inventories: Wetlands', in T Hiraishi, et al. (eds), Intergovernmental Panel on Climate Change, Switzerland.

Jachowski, NRA, Quak, MSY, Friess, DA, Duangnamon, D, Webb, EL & Ziegler, AD 2013, 'Mangrove biomass estimation in Southwest Thailand using machine learning', *Applied Geography*, vol. 45, no. 0, pp. 311-21.

Jacquemoud, S, Verhoef, W, Baret, F, Bacour, C, Zarco-Tejada, PJ, Asner, GP, François, C & Ustin, SL 2009, 'PROSPECT + SAIL models: A review of use for vegetation characterization', *Remote Sensing of Environment*, vol. 113, Supplement 1, pp. S56-S66.

Jaramillo, VJ, Ahedo-Hernández, R & Kauffman, JB 2003, 'Root biomass and carbon in a tropical evergreen forest of Mexico: changes with secondary succession and forest conversion to pasture', *Journal of Tropical Ecology*, vol. 19, no. 4, pp. 457-64, Cambridge University Press, Cambridge Core.

Jardine, SL & Siikamäki, J 2014, 'A global predictive model of carbon in mangrove soils', *Environmental Research Letters*, vol. 9, no. 10, p. 104013.

Johnston, K, Ver Hoef, JM, Krivoruchko, K & Lucas, N 2001, *Using ArcGIS geostatistical analyst*, vol. 380, Esri Redlands.

Jones, T, Ratsimba, H, Ravaoarinorotsihoarana, L, Cripps, G & Bey, A 2014, 'Ecological Variability and Carbon Stock Estimates of Mangrove Ecosystems in Northwestern Madagascar', *Forests*, vol. 5, no. 1, pp. 177-205, item: doi:10.3390/f5010177.

Kanninen, M, Murdiyarso, D, Seymour, F, Angelsen, A, Wunder, S & German, L 2007, *Do trees grow on money?: the implications of deforestation research for policies to promote REDD*, Center for International Forestry Research (CIFOR), Bogor, Indonesia.

Kauffman, JB & Cole, T 2010, 'Micronesian Mangrove Forest Structure and Tree Responses to a Severe Typhoon', *Wetlands*, vol. 30, no. 6, pp. 1077-84.

Kauffman, JB & Donato, D 2012, *Protocols for the measurement, monitoring and reporting of structure, biomass and carbon stocks in mangrove forests*, Center for International Forestry Research (CIFOR), Bogor, Indonesia.

Kauffman, JB, Heider, C, Norfolk, J & Payton, F 2013, 'Carbon stocks of intact mangroves and carbon emissions arising from their conversion in the Dominican Republic', *Ecological Applications*, vol. 24, no. 3, pp. 518-27.

Kauffman, JB, Heider, C, Cole, T, Dwire, K & Donato, D 2011, 'Ecosystem Carbon Stocks of Micronesian Mangrove Forests', *Wetlands*, vol. 31, no. 2, pp. 343-52.

Kauffman, JB, Hernandez Trejo, H, del Carmen Jesus Garcia, M, Heider, C & Contreras, WM 2016, 'Carbon stocks of mangroves and losses arising from their conversion to cattle pastures in the Pantanos de Centla, Mexico', *Wetlands Ecology and Management*, vol. 24, no. 2, pp. 203-16.

Koch, EW, Barbier, EB, Silliman, BR, Reed, DJ, Perillo, GME, Hacker, SD, Granek, EF, Primavera, JH, Muthiga, N, Polasky, S, Halpern, BS, Kennedy, CJ, Kappel, CV & Wolanski, E 2009, 'Non-linearity in ecosystem services: temporal and spatial variability in coastal protection', *Frontiers in Ecology and the Environment*, vol. 7, no. 1, pp. 29-37.

Köhl, M, Lasco, R, Cifuentes, M, Jonsson, Ö, Korhonen, KT, Mundhenk, P, de Jesus Navar, J & Stinson, G 2015, 'Changes in forest production, biomass and carbon: Results from the 2015 UN FAO Global Forest Resource Assessment', *Forest Ecology and Management*, vol. 352, pp. 21-34.

Komiyama, A, Poungparn, S & Kato, S 2005, 'Common allometric equations for estimating the tree weight of mangroves', *Journal of Tropical Ecology*, vol. 21, no. 04, pp. 471-7.

Komiyama, A, Ong, JE & Poungparn, S 2008, 'Allometry, biomass, and productivity of mangrove forests: A review', *Aquatic Botany*, vol. 89, no. 2, pp. 128-37.

Kucuker, MA, Guney, M, Oral, HV, Copty, NK & Onay, TT 2015, 'Impact of deforestation on soil carbon stock and its spatial distribution in the Western Black Sea Region of Turkey', *Journal of Environmental Management*, vol. 147, pp. 227-35.

Kumar, L, Sinha, P, Taylor, S & Alqurashi, AF 2015, 'Review of the use of remote sensing for biomass estimation to support renewable energy generation', *Journal of Applied Remote Sensing*, vol. 9, no. 1, pp. 097696-.

Kumar, S, Pandey, U, Kushwaha, SP, Chatterjee, RS & Bijker, W 2012, 'Aboveground biomass estimation of tropical forest from Envisat advanced synthetic aperture radar data using modeling approach', *Journal of Applied Remote Sensing*, vol. 6, no. 1, pp. 063588-.

Lal, R 2005, 'Forest soils and carbon sequestration', *Forest Ecology and Management*, vol. 220, no. 1–3, pp. 242-58.

Lal, R 2008, 'Carbon sequestration', *Philosophical Transactions of the Royal Society of London B: Biological Sciences*, vol. 363, no. 1492, pp. 815-30.

Lam-Dao, N, Le Toan, T, Apan, A, Bouvet, A, Young, F & Le-Van, T 2009, 'Effects of changing rice cultural practices on C-band synthetic aperture radar backscatter using Envisat advanced synthetic aperture radar data in the Mekong River Delta', *Journal of Applied Remote Sensing*, vol. 3, no. 1, pp. 033563--17.

Lasco, R, Veridiano, R, Habito, M & Pulhin, F 2013, 'Reducing emissions from deforestation and forest degradation plus (REDD+) in the Philippines: will it make a difference in financing forest development?', *Mitigation and Adaptation Strategies for Global Change*, vol. 18, no. 8, pp. 1109-24.

Lasco, RD 2002, 'Forest carbon budgets in Southeast Asia following harvesting and land cover change', *SCIENCE IN CHINA SERIES C LIFE SCIENCES-ENGLISH EDITION-*, vol. 45, no. SUPP, pp. 55-64.

Li, X, Gar-On Yeh, A, Wang, S, Liu, K, Liu, X, Qian, J & Chen, X 2007, 'Regression and analytical models for estimating mangrove wetland biomass in South China using Radarsat images', *International Journal of Remote Sensing*, vol. 28, no. 24, pp. 5567-82.

Liu, C 2016, 'Analysis of Sentinel-1 SAR data for mapping standing water in the Twente region', Masters thesis, University of Twente, Enschede, The Netherlands.

Locatelli, T, Binet, T, Kairo, J, King, L, Madden, S, Patenaude, G, Upton, C & Huxham, M 2014, 'Turning the Tide: How Blue Carbon and Payments for Ecosystem Services (PES) Might Help Save Mangrove Forests', *AMBIO*, vol. 43, no. 8, pp. 981-95.

Long, J, Napton, D, Giri, C & Graesser, J 2013, 'A Mapping and Monitoring Assessment of the Philippines' Mangrove Forests from 1990 to 2010', *Journal of Coastal Research*, pp. 260-71.

Lovelock, C 2008, 'Soil Respiration and Belowground Carbon Allocation in Mangrove Forests', *Ecosystems*, vol. 11, no. 2, pp. 342-54.

Lovelock, CE & McAllister, RRJ 2013, ''Blue carbon' projects for the collective good', *Carbon Management*, vol. 4, no. 5, pp. 477-9, viewed 2015/01/27.

Lovelock, CE, Ruess, RW & Feller, IC 2011, 'CO₂ Efflux from Cleared Mangrove Peat', *PLoS ONE*, vol. 6, no. 6, p. e21279.

Lu, D, Mausel, P, Brondízio, E & Moran, E 2004, 'Relationships between forest stand parameters and Landsat TM spectral responses in the Brazilian Amazon Basin', *Forest Ecology and Management*, vol. 198, no. 1–3, pp. 149-67.

Maraseni, TN 2007, 'Re-evaluating land use choices to incorporate carbon values: a case study in the South Burnett region of Queensland, Australia', PhD thesis, University of Southern Queensland.

Maraseni, TN & Pandey, SS 2014, 'Can vegetation types work as an indicator of soil organic carbon? An insight from native vegetations in Nepal', *Ecological Indicators*, vol. 46, pp. 315-22.

Maraseni, TN, Cockfield, G & Apan, A 2005, 'Community based forest management systems in developing countries and eligibility for clean development mechanism', *Journal of forest and Livelihood*, vol. 4, no. 2, pp. 31-42.

Maraseni, TN, Mathers, NJ, Harms, B, Cockfield, G, Apan, A & Maroulis, J 2008, 'Comparing and predicting soil carbon quantities under different land-use systems on the Red Ferrosol soils of southeast Queensland', *Journal of Soil and Water Conservation*, vol. 63, no. 4, pp. 250-6.

McDonald, J 2016, *Handbook of Biological Statistics*, viewed May 2016, <http://www.biostathandbook.com/onewayanova.html#welch>.

Melling, L, Hatano, R & Goh, KJ 2005, 'Methane fluxes from three ecosystems in tropical peatland of Sarawak, Malaysia', *Soil Biology and Biochemistry*, vol. 37, no. 8, pp. 1445-53.

Mishra, U, Lal, R, Slater, B, Calhoun, F, Liu, D & Van Meirvenne, M 2009, 'Predicting soil organic carbon stock using profile depth distribution functions and ordinary kriging', *Soil Science Society of America Journal*, vol. 73, no. 2, pp. 614-21.

Mizanur Rahman, M, Nabiul Islam Khan, M, Fazlul Hoque, AK & Ahmed, I 2014, 'Carbon stock in the Sundarbans mangrove forest: spatial variations in vegetation types and salinity zones', *Wetlands Ecology and Management*, pp. 1-15.

Murdiyarso, D, Kauffman, JB & Verchot, LV 2013, 'Climate change mitigation strategies should include tropical wetlands', *Carbon Management*, vol. 4, no. 5, pp. 491-9.

Murdiyarso, D, Kauffman, JB, Warren, M, Pramova, E & Hergoualc'h, K 2012, *Tropical wetlands for climate change adaptation and mitigation: science and policy imperatives with special reference to Indonesia*, Center for International Forestry Research (CIFOR), Bogor, Indonesia.

Murdiyarso, D, Donato, D, Kauffman, JB, Kurnianto, S, Stidham, M & Kanninen, M 2010, *Carbon storage in mangrove and peatland ecosystems: a preliminary account from plots in Indonesia*, Center for International Forestry Research (CIFOR), Bogor, Indonesia.

Murdiyarso, D, Purbopuspito, J, Kauffman, JB, Warren, MW, Sasmito, SD, Donato, DC, Manuri, S, Krisnawati, H, Taberima, S & Kurnianto, S 2015, 'The potential of Indonesian mangrove forests for global climate change mitigation', *Nature Clim. Change*, vol. advance online publication.

Navarrete, IA & Tsutsuki, K 2008, 'Land-use impact on soil carbon, nitrogen, neutral sugar composition and related chemical properties in a degraded Ultisol in Leyte, Philippines', *Soil Science & Plant Nutrition*, vol. 54, no. 3, pp. 321-31.

NSO 2011, *2010 Census of Population and Housing*, National Statistics Authority, viewed February 25, 2017, <http://psa.gov.ph/statistics/census/population-and-housing>.

Ong, JE 2002, 'The hidden costs of mangrove services: Use of mangroves for shrimp aquaculture', *International Science Roundtable for the Media*, vol. 4.

Ong, JE, Gong, WK & Wong, CH 2004, 'Allometry and partitioning of the mangrove, Rhizophora apiculata', *Forest Ecology and Management*, vol. 188, no. 1–3, pp. 395-408.

PAGASA 2016, *Climatological Normals*, Philippine Atmospheric, geophysical and Astronomical Services Administration, viewed March 31, 2016, <http://web.pagasa.dost.gov.ph/index.php/climate/climatological-normals>.

Pandey, SS, Maraseni, TN & Cockfield, G 2014, 'Carbon stock dynamics in different vegetation dominated community forests under REDD+: A case from Nepal', *Forest Ecology and Management*, vol. 327, pp. 40-7.

Pandey, SS, Cockfield, G & Maraseni, TN 2016, 'Assessing the roles of community forestry in climate change mitigation and adaptation: A case study from Nepal', *Forest Ecology and Management*, vol. 360, pp. 400-7.

Pendleton, L, Donato, DC, Murray, BC, Crooks, S, Jenkins, WA, Sifleet, S, Craft, C, Fourqurean, JW, Kauffman, JB, Marbà, N, Megonigal, P, Pidgeon, E, Herr, D, Gordon, D & Baldera, A 2012, 'Estimating Global "Blue Carbon" Emissions from Conversion and Degradation of Vegetated Coastal Ecosystems', *PLoS ONE*, vol. 7, no. 9, p. e43542.

Phang, VXH, Chou, LM & Friess, DA 2015, 'Ecosystem carbon stocks across a tropical intertidal habitat mosaic of mangrove forest, seagrass meadow, mudflat and sandbar', *Earth Surface Processes and Landforms*, vol. 40, no. 10, pp. 1387-400.

Poffenbarger, HJ, Needelman, BA & Megonigal, JP 2011, 'Salinity Influence on Methane Emissions from Tidal Marshes', *Wetlands*, vol. 31, no. 5, pp. 831-42.

Poungparn, S, Komiyama, A, Tanaka, A, Sangtiean, T, Maknual, C, Kato, S, Tanapermpool, P & Patanaponpaiboon, P 2009, 'Carbon dioxide emission through soil respiration in a secondary mangrove forest of eastern Thailand', *Journal of Tropical Ecology*, vol. 25, no. 04, pp. 393-400, viewed 2009.

PPC 2017, *Puerto Princesa: The Official Website of the City Government*, Puerto Princesa City Government, viewed February 27, 2017, <http://puertoprincesa.ph/?q=about-our-city/key-facts>.

Primavera, JH 2000, 'Development and conservation of Philippine mangroves: institutional issues', *Ecological Economics*, vol. 35, no. 1, pp. 91-106.

Primavera, JH & Esteban, J 2008, 'A review of mangrove rehabilitation in the Philippines: successes, failures and future prospects', *Wetlands Ecology and Management*, vol. 16, no. 5, pp. 345-58.

Proisy, C, Couteron, P & Fromard, F 2007, 'Predicting and mapping mangrove biomass from canopy grain analysis using Fourier-based textural ordination of IKONOS images', *Remote Sensing of Environment*, vol. 109, no. 3, pp. 379-92.

Proisy, C, Mitchell, A, Lucas, R, Fromard, F & Mougin, E 2003, 'Estimation of Mangrove Biomass using Multifrequency Radar Data: Application to Mangroves of French Guiana and Northern Australia', Mangrove 2003 Conference, Bahia, Brazil.

PSA 2016, *2015 Census of Population*, Philippine Statistics Authority, viewed February 25, 2017, <http://psa.gov.ph/content/highlights-philippine-population-2015-census-population>.

Pumpanen, J, Kolari, P, Ilvesniemi, H, Minkkinen, K, Vesala, T, Niinistö, S, Lohila, A, Larmola, T, Morero, M, Pihlatie, M, Janssens, I, Yuste, JC, Grünzweig, JM, Reth, S, Subke, J-A, Savage, K, Kutsch, W, Østreng, G, Ziegler, W, Anthoni, P, Lindroth, A & Hari, P 2004, 'Comparison of different chamber techniques for measuring soil CO2 efflux', *Agricultural and Forest Meteorology*, vol. 123, no. 3–4, pp. 159-76.

Purvaja, R & Ramesh, R 2001, 'Natural and Anthropogenic Methane Emission from Coastal Wetlands of South India', *Environmental Management*, vol. 27, no. 4, pp. 547-57.

Richards, DR & Friess, DA 2016, 'Rates and drivers of mangrove deforestation in Southeast Asia, 2000–2012', *Proceedings of the National Academy of Sciences*, vol. 113, no. 2, pp. 344-9.

Saatchi, SS, Houghton, RA, Dos Santos AlvalÁ, RC, Soares, JV & Yu, Y 2007, 'Distribution of aboveground live biomass in the Amazon basin', *Global Change Biology*, vol. 13, no. 4, pp. 816-37.

Salmo, S, III, Lovelock, C & Duke, N 2013, 'Vegetation and soil characteristics as indicators of restoration trajectories in restored mangroves', *Hydrobiologia*, vol. 720, no. 1, pp. 1-18.

Samalca, IK 2007, 'Estimation of forest biomass and its error: A case in Kalimantan, Indonesia', *Unpublished MSc. Thesis, ITC the Netherlands, Enschede*.

Sentinel-1_Team 2013, *Sentinel-1 User Handbook*, European Space Agency.

Sentinel-2_Team 2015, *Sentinel-2 User Handbook*, European Space Agency.

Sibanda, M, Mutanga, O & Rouget, M 2015, 'Examining the potential of Sentinel-2 MSI spectral resolution in quantifying above ground biomass across different

fertilizer treatments', *ISPRS Journal of Photogrammetry and Remote Sensing*, vol. 110, pp. 55-65.

Sidik, F & Lovelock, CE 2013, 'CO₂ Efflux from Shrimp Ponds in Indonesia', *PLoS ONE*, vol. 8, no. 6, p. e66329.

Siikamäki, J, Sanchirico, JN & Jardine, SL 2012, 'Global economic potential for reducing carbon dioxide emissions from mangrove loss', *Proceedings of the National Academy of Sciences*, vol. 109, no. 36, pp. 14369-74.

Simard, M, Zhang, K, Rivera-Monroy, VH, Ross, MS, Ruiz, PL, Castañeda-Moya, E, Twilley, RR & Rodriguez, E 2006, 'Mapping Height and Biomass of Mangrove Forests in Everglades National Park with SRTM Elevation Data', *Photogrammetric Engineering & Remote Sensing*, vol. 72, no. 3, pp. 299-311.

Sinha, S, Jeganathan, C, Sharma, LK & Nathawat, MS 2015, 'A review of radar remote sensing for biomass estimation', *International Journal of Environmental Science and Technology*, vol. 12, no. 5, pp. 1779-92.

Sitoe, A, Mandlate, L & Guedes, B 2014, 'Biomass and Carbon Stocks of Sofala Bay Mangrove Forests', *Forests*, vol. 5, no. 8, p. 1967.

SNAP 2016, *Sentinels Application Platform software ver. 4.0.0*, European Space Agency.

Spalding, M, Kainuma, M & Collins, L 2010, *World Atlas of Mangroves*, Earthscan.

Stringer, CE, Trettin, CC, Zarnoch, SJ & Tang, W 2015, 'Carbon stocks of mangroves within the Zambezi River Delta, Mozambique', *Forest Ecology and Management*, vol. 354, pp. 139-48.

Thapa, RB, Watanabe, M, Motohka, T & Shimada, M 2015, 'Potential of high-resolution ALOS–PALSAR mosaic texture for aboveground forest carbon tracking in tropical region', *Remote Sensing of Environment*, vol. 160, pp. 122-33.

Thompson, BS, Clubbe, CP, Primavera, JH, Curnick, D & Koldewey, HJ 2014, 'Locally assessing the economic viability of blue carbon: A case study from Panay Island, the Philippines', *Ecosystem Services*, vol. 8, pp. 128-40.

Tue, NT, Dung, LV, Nhuan, MT & Omori, K 2014, 'Carbon storage of a tropical mangrove forest in Mui Ca Mau National Park, Vietnam', *CATENA*, vol. 121, no. 0, pp. 119-26.

Umali, BP, Oliver, DP, Forrester, S, Chittleborough, DJ, Hutson, JL, Kookana, RS & Ostendorf, B 2012, 'The effect of terrain and management on the spatial variability of soil properties in an apple orchard', *CATENA*, vol. 93, pp. 38-48.

USGS 2016, *EarthExplorer*, United States Geological Service, viewed August 1, 2016, <https://earthexplorer.usgs.gov/>.

Veci, L 2015, *Sentinel-1 Toolbox: SAR Basics Tutorial*, ARRAY Systems Computing, Inc. and European Space Agency.

Vien, N, Sasmito, SD, Murdiyarso, D, Purbopuspito, J & MacKenzie, RA 2016, 'Carbon stocks in artificially and naturally regenerated mangrove ecosystems in the Mekong Delta', *Wetlands Ecology and Management*, vol. 24, no. 2, pp. 231-44.

Wang, G, Guan, D, Zhang, Q, Peart, MR, Chen, Y, Peng, Y & Ling, X 2014, 'Spatial patterns of biomass and soil attributes in an estuarine mangrove forest (Yingluo Bay, South China)', *European Journal of Forest Research*, vol. 133, no. 6, pp. 993-1005.

Warner, DL, Villarreal, S, McWilliams, K, Inamdar, S & Vargas, R 2017, 'Carbon Dioxide and Methane Fluxes From Tree Stems, Coarse Woody Debris, and Soils in an Upland Temperate Forest', *Ecosystems*, pp. 1-12.

Wicaksono, P, Danoedoro, P, Hartono & Nehren, U 2016, 'Mangrove biomass carbon stock mapping of the Karimunjawa Islands using multispectral remote sensing', *International Journal of Remote Sensing*, vol. 37, no. 1, pp. 26-52.

Zaiontz, C 2015, *Real Statistics using Excel*, viewed December 2015, <http://www.real-statistics.com/one-way-analysis-of-variance-anova/kruskal-wallis-test/>.

Zamora, DS 1999, 'Carbon dioxide (CO2) storage potential of multistorey agroforestry systems in Mt. Makiling [Philippines]', Master of Science thesis, University of the Philippines Los Baños.

Ziegler, AD, Phelps, J, Yuen, JQI, Webb, EL, Lawrence, D, Fox, JM, Bruun, TB, Leisz, SJ, Ryan, CM, Dressler, W, Mertz, O, Pascual, U, Padoch, C & Koh, LP 2012, 'Carbon outcomes of major land-cover transitions in SE Asia: great uncertainties and REDD+ policy implications', *Global Change Biology*, vol. 18, no. 10, pp. 3087-99.

APPENDICES

Appendix 1 Coordinates of sampling plots in all land uses under study in Honda Bay

Land use	Transect	Plot	Longitude	Latitude	Plot ID
Mangrove forest	Closed 1a	1	118.7292333	9.89776667	1
	Closed 1a	2	118.7294	9.89818333	2
	Closed 1a	3	118.72935	9.89866667	3
	Closed 1b	1	118.7347833	9.89350000	4
	Closed 1b	2	118.7346667	9.89391667	5
	Closed 1b	3	118.7347667	9.89445	6
	Closed 1c	1	118.7437667	9.903	7
	Closed 1c	2	118.7433167	9.9028	8
	Closed 1c	3	118.74325	9.9024	9
	Closed 2a	1	118.7548167	9.93988333	10
	Closed 2a	2	118.7553167	9.93981667	11
	Closed 2a	3	118.7558	9.93976667	12
	Closed 2b	1	118.7575833	9.93631667	13
	Closed 2b	2	118.7578	9.93615	14
	Closed 2b	3	118.7583	9.93588333	15
	Closed 2c	1	118.7551333	9.93048333	16
	Closed 2c	2	118.7552167	9.931	17
	Closed 2c	3	118.7552333	9.93143333	18
	Closed 3a	1	118.78475	9.95895	19
	Closed 3a	2	118.7847167	9.95846667	20
	Closed 3a	3	118.7847333	9.95798333	21
	Closed 3b	1	118.7906	9.95035	22
	Closed 3b	2	118.7907167	9.95076667	23
	Closed 3b	3	118.7906167	9.95125	24
	Closed 3c	1	118.8002	9.93953333	25
	Closed 3c	2	118.8006667	9.93965	26
	Closed 3c	3	118.8009833	9.9399	27
	Open 1a	1	118.7482	9.82968333	28
	Open 1a	2	118.7478833	9.83003333	29
	Open 1a	3	118.7477	9.83041667	30
	Open 1b	1	118.7502833	9.82861667	31
	Open 1b	2	118.7500667	9.82903333	32
	Open 1b	3	118.7497667	9.82943333	33
	Open 1c	1	118.7506	9.82878333	34
	Open 1c	2	118.7503333	9.82923333	35
	Open 1c	3	118.7501	9.82965	36
	Open 2a	1	118.7428833	9.86536667	37

Appendix 1 continued

Land use	Transect	Plot	Longitude	Latitude	Plot ID
Mangrove forest	Open 2a	2	118.7429167	9.86588333	38
	Open 2a	3	118.7429167	9.86631667	39
	Open 2c	1	118.7436833	9.86483333	40
	Open 2c	2	118.7439333	9.86455	41
	Open 2c	3	118.7442167	9.8642	42
	Open 3a	1	118.7693667	9.80828333	43
	Open 3a	2	118.7696667	9.80791667	44
	Open 3a	3	118.77	9.80756667	45
	Open 3b	1	118.7687	9.80775	46
	Open 3b	2	118.7689167	9.80735	47
	Open 3b	3	118.7689333	9.80693333	48
	Open 3c	1	118.7659833	9.80556667	49
	Open 3c	2	118.76605	9.80515	50
	Open 3c	3	118.7658333	9.80476667	51
Abandoned aquaculture pond	Aqua 1a	1	118.7561667	9.80635	52
	Aqua 1a	2	118.7559833	9.8064	53
	Aqua 1a	3	118.7557167	9.80643333	54
	Aqua 1b	1	118.7561833	9.80615	55
	Aqua 1b	2	118.75575	9.80615	56
	Aqua 1b	3	118.7554833	9.8062	57
	Aqua 2a	1	118.7493833	9.81296667	58
	Aqua 2a	2	118.7497167	9.81263333	59
	Aqua 2a	3	118.74985	9.81213333	60
	Aqua 2b	1	118.7484	9.81306667	61
	Aqua 2b	2	118.74855	9.81263333	62
	Aqua 2b	3	118.7487833	9.81221667	63
	Aqua 3a	1	118.7404333	9.8365	64
	Aqua 3a	2	118.74035	9.83698333	65
	Aqua 3a	3	118.7402667	9.83738333	66
	Aqua 3b	1	118.7399333	9.83628333	67
	Aqua 3b	2	118.73975	9.83675	68
	Aqua 3b	3	118.7396667	9.83723333	69
Coconut plantation	Coco 1a	1	118.7456167	9.81473333	70
	Coco 1a	2	118.74575	9.81448333	71
	Coco 1a	3	118.74585	9.81433333	72
	Coco 1b	1	118.7453833	9.81446667	73
	Coco 1b	2	118.7454333	9.8143	74
	Coco 1b	3	118.7454167	9.81405	75
Abandoned salt pond	Salt 1a	1	118.7387833	9.83536667	76
	Salt 1a	2	118.7389667	9.8349	77
	Salt 1a	3	118.7394333	9.83445	78
	Salt 1b	1	118.7391667	9.83461667	79

Appendix 1 continued

Land use	Transect	Plot	Longitude	Latitude	Plot ID
Abandoned salt pond	Salt 1b	2	118.7394167	9.83513333	80
	Salt 1b	3	118.73925	9.8355	81
	Salt 1c	1	118.7399833	9.8352	82
	Salt 1c	2	118.7401167	9.83471667	83
	Salt 1c	3	118.7402667	9.83433333	84
Cleared mangrove	Cleared 1a	1	118.7572333	9.8075	85
	Cleared 1a	2	118.7567167	9.80743333	86
	Cleared 1a	3	118.7562333	9.80736667	87
	Cleared 1b	1	118.7572167	9.80821667	88
	Cleared 1b	2	118.7567833	9.80813333	89
	Cleared 1b	3	118.7563833	9.80806667	90

Appendix 2 List of plant species recorded in the study site, arranged by family and indicated as present (y) or absent (n) per land use

Species	MF	AP	SP	CP	CM
Rhizophoraceae					
Bruguiera gymnorrhiza (L.) Lamk.	y	n	n	n	n
Bruguiera parviflora (Roxb.) W. & A. ex Griff	y	n	n	n	n
Bruguiera sexangula (Lour.) Poir.	y	n	n	y	n
Ceriops tagal (Perr.) C.B. Rob.	y	n	n	n	n
Rhizophora apiculata Blume	y	y	n	n	n
Rhizophora mucronata Lamk.	y	n	n	n	n
Rhizophora stylosa Griff.	y	y	n	n	n
Myrsinaceae					
Aegiceras floridum Roem & Schult.	y	n	n	n	n
Meliaceae					
Xylocarpus granatum Koen.	y	n	n	y	n
Xylocarpus moluccensis (Lamk.) M. Roem	y	n	n	n	n
Malvaceae					
Camptostemon philippinense (Vid.) Becc.	y	n	n	n	n
Heritiera littoralis Dryand ex. W. Ait	y	n	n	n	n
Lythraceae					
Sonneratia alba (L.) Smith	y	n	n	n	n
Combretaceae					
Lumnitzera racemosa Willd.	y	n	n	y	n
Arecaceae					
Cocos nucifera L.	n	n	n	y	n

MF = Mangrove Forest AP = Aquaculture Pond SP = Salt Pond
CP = Coconut Plantation CM = Cleared mangrove

Appendix 3 Area (ha) of land uses that replaced mangroves in the Philippines for the period 2000-2012

Year	Aquaculture	Recent deforestation	Oil palm	Rice	Erosion	Urban
2001	9.72	27.9	0.63	1.17	NA	NA
2002	36.54	49.23	3.15	NA	1.17	1.44
2003	64.26	12.42	4.68	NA	2.34	1.08
2004	84.06	32.04	3.69	NA	NA	0.72
2005	37.62	18.81	11.25	NA	0.99	NA
2006	71.1	28.98	23.67	2.52	NA	2.43
2007	44.73	44.82	9.81	2.34	NA	1.53
2008	40.05	46.26	7.02	NA	0.54	1.26
2009	45.81	81.9	15.93	3.06	1.08	5.4
2010	41.31	39.06	26.82	0.63	6.03	21.51
2011	26.37	22.41	9.54	1.89	NA	NA
2012	21.24	60.93	41.31	0.81	NA	2.7
sum	522.81	464.76	157.5	12.42	12.15	38.07

Deforested mangrove patches greater than 0.5 hectare in extent

Source: Richards and Friess (2016)

Appendix 4 Sample of computed plot-level aboveground biomass (AGB), belowground biomass (BGB) and downed woody debris biomass (DWB) C stocks in Mg C ha^{-1}

Land use	Transect	Plot ID	AGB C stock	BGB C stock	DWB C stock
Mangrove forest	closed 1a	1	34.50	13.69	2.60
	closed 1a	2	36.78	16.75	7.10
	closed 1a	3	76.34	28.36	4.73
	closed 1b	4	63.03	22.55	0.77
	closed 1b	5	116.15	55.75	20.76
	closed 1b	6	59.14	21.96	3.12
	closed 1c	7	27.15	11.64	1.75
	closed 3c	26	10.43	4.83	12.15
	closed 3c	27	43.98	15.94	8.19
	open 1a	28	2.08	1.00	0.20
	open 1a	29	0.82	0.42	0.20
	open 1a	30	2.67	1.26	0.22
	open 1b	31	9.39	3.87	0.72
	open 3b	46	21.17	7.54	9.62
	open 3b	47	34.91	18.75	0.70
	open 3b	48	19.02	9.48	2.59
	open 3c	49	9.62	4.21	0.40
	open 3c	50	10.52	3.56	1.19
	open 3c	51	1.23	0.50	0.00
Abandoned aquaculture pond	aqua 1a	53	0.00	0.00	0.00
	aqua 2b	63	0.00	0.00	0.00
	aqua 3a	64	0.00	0.00	0.00
	aqua 3a	65	0.13	0.08	0.11
	aqua 3a	66	0.19	0.10	0.11
	aqua 3b	67	0.00	0.00	0.00
	aqua 3b	68	0.00	0.00	0.00
	aqua 3b	69	0.00	0.00	0.00
Coconut plantation	coco 1a	70	3.87	0.23	0.00
	coco 1a	71	8.83	0.40	0.00
	coco 1b	75	0.10	0.10	0.00
Abandoned salt pond	salt 1a	76	0.00	0.00	0.00
	salt 1a	77	0.00	0.00	0.00
	salt 1b	80	0.00	0.00	0.00
Cleared mangrove	cleared 1a	85	0.00	0.00	0.00
	cleared 1a	86	0.00	0.00	0.00
	cleared 1b	90	0.00	0.00	0.00

Appendix 5 Photo-documentation of some of the recorded mangrove species and wildlife encountered while sampling the study site

Rhizophora apiculata

Rhizophora mucronata

Lumnitzera racemosa

Lumnitzera racemosa

Bruguiera gymnorhiza

Aegiceras floridum

Yellow-banded snake in a closed canopy mangrove forest site

King fishers perching in an abandoned pond site

Appendix 6 Field form used for collecting site's metadata

Site Meta Data

Date:_____

Land use:_____ Barangay/Name of area sampled:_____

Site Replicate No. _____

Crew members:_____

Sketch of transects and Plots Location/Direction

GPS Coordinates

Plot	Latitude, N	Longitude, E	Elevation, masl	Dominant sp.
T1 Plot 1				
T1 Plot 2				
T1 Plot 3				
T2 Plot 1				
T2 Plot 2				
T2 Plot 3				
T3 Plot 1				
T3 Plot 2				
T3 Plot 3				

Topography: _____

Landscape position: _____

Disturbance: _____

Additional notes: _____

Appendix 7 Field form used for vegetation biomass sampling

Date:_______
Land use :_____
Transect Number: __________
Tidal position: ___________
Crew members: __________________

Site Replicate No. ______________
Direction of transect:___
Brgy./Name of area sampled:__________

Plot	Species	DBH	Height	Remarks	Plot	Species	DBH	Height	Remarks
No.		cm	m		No.		cm	m	

Data Entry: Name ______________Date:__________ Checked by:____________Date:__________

Appendix 8 Field form used for soil C sampling

Site Soil Carbon

Date: _____ Land use: _____

Brgy/Name of Area sampled: _____ Site Replicate No. _____

Crew members: _____

Plot	Layer	Depth (cm)	Bag. No	Sample actual depth range (cm)		Soil depth 3 readings	Remarks
T1.1	1	0-15					
	2	15-30					
	3	30-50					
	4	50-100					
	5	100-200					
	6	200-300					
T1.2	1	0-15					
	2	15-30					
	3	30-50					
	4	50-100					
	5	100-200					
	6	200-300					
T1.3	1	0-15					
	2	15-30					
	3	30-50					
	4	50-100					
	5	100-200					
	6	200-300					
T2.1	1	0-15					
	2	15-30					
	3	30-50					
	4	50-100					
	5	100-300					
	6	200-300					
T2.2	1	0-15					
	2	15-30					
	3	30-50					
	4	50-100					
	5	100-200					
	6	200-300					
T2.3	1	0-15					
	2	15-30					
	3	30-50					
	4	50-100					
	5	100-200					
	6	200-300					

Appendix 9 Field form used for sampling the soil GHG fluxes

Site Soil GHG fluxes

Date: _____ Land use _____

Brgy/Name of Area sampled: _____ Site Replicate No. _____

Crew members: _ _____

Plot	CO2 flux *in situ*	Time Elapsed, min	Vial No.	Soil temp. 3 readings	Soil ORP 3 readings
T1.1		0			
		1			
		2			
		3			
T1.2		0			
		1			
		2			
		3			
T1.3		0			
		1			
		2			
		3			
T2.1		0			
		1			
		2			
		3			
T2.2		0			
		1			
		2			
		3			
T2.3		0			
		1			
		2			
		3			

Data Entry Name: _____

Checked by: _____

Notes: _____

_____

_____

Appendix 10 Photo-documentation of some of the field work activities


L to R: The author (left most), his Principal Supervisor (3rd from left) and his field survey crew